Cyprus University of Technology

Faculty of Geotechnical Sciences and Environmental Management

Doctoral Dissertation

Anaerobic digestion of cheese whey using acclimatized granular sludge at moderately low pH and zero-valent iron addition

Panagiotis Charalambous

Limassol, July 2024

CYPRUS UNIVERSITY OF TECHNOLOGY

FACULTY OF GEOTECHNICAL SCIENCES AND ENVIRONMENTAL MANAGEMENT

DEPARTMENT OF CHEMICAL ENGINEERING

Doctoral Dissertation

ANAEROBIC DIGESTION OF CHEESE WHEY USING ACCLIMATIZED GRANULAR SLUDGE AT MODERATELY LOW PH AND ZERO-VALENT IRON ADDITION

Panagiotis Charalambous

Limassol, July 2024

Approval Form

Doctoral Dissertation

ANAEROBIC DIGESTION OF CHEESE WHEY USING ACCLIMATIZED GRANULAR SLUDGE AT MODERATELY LOW PH AND ZERO-VALENT IRON ADDITION

Presented by

Panagiotis Charalambous

PhD advisor of Mr Charalambous : Dr. Ioannis Vyrides, Associate Professor,

Department of Chemical Engineering,

Faculty of Geotechnical Sciences and Environmental Management,

Cyprus University of Technology

Signature _____

Committee Chair: Dr. Photis Papademas, Associate Professor,

Department of Agricultural Sciences, Biotechnology and Food Science,

Faculty of Geotechnical Sciences and Environmental Management,

Cyprus University of Technology

Signature _____

External committee member: Dr Gerasimos Lyberatos, Professor,

School of Chemical Engineering,

National Technical University of Athens, Athens, Greece.

Signature _____

Cyprus University of Technology

Limassol, July 2024

Copyrights

Acknowledgements

My deepest appreciation extends to everyone who played a pivotal role in the completion of this doctoral dissertation. The steadfast mentorship, advice, and motivation I have received have been crucial in shaping my scholarly path as well as my development on a personal level.

First and foremost, I would like to express my sincere gratitude to my supervisor, Dr. Ioannis Vyrides, for his unwavering support of my Ph.D. studies, his motivation, patience, and insightful guidance throughout all the stages of my research and thesis writing

My heartfelt thanks go to my fellow lab mates, Charis, Despina,Yiota and Maria, for the stimulating discussions, the countless hours we spent working together, and all the fun we have shared over the last seven years.

Last but not least, I wish to thank my mother, Chrystalla, who has been with me from the beginning to the end of this project, supporting me at every step. I dedicate this thesis to the memory of my father.

ABSTRACT

Cheese whey (CW), a major by-product of cheese manufacturing, is ideal for anaerobic degradation and bioenergy production due to its high biodegradability and significant carbohydrate content, which makes up over 70% of its organic matter. Aligned with the circular economy concept, anaerobic digestion (AD) is a sustainable technology that can exploit the high organic matter (50–102 g/L COD) of CW and generate value-added products, such as biogas and fertilizer. However, its rapid acidification due to volatile fatty acids (VFAs) accumulation coupled with an inherent lack of natural alkalinity (<0.22 $gCaCO_3/L$) resulted in a pH drop, which negatively affects methanogenesis and the process's stability. To date, various methods have been proposed to handle the problematic AD of CW targeting to mitigate VFAs accumulation and improve the process stability. Dosing alkaline agents (NaOH or $NaHCO_3$), co-digestion of CW with rich alkaline substrates, or the two-stage anaerobic digestion process, have been proposed to overcome acid inhibition and to ensure a stable monitoring of the process. However, most of these technologies are cost-effective in terms of operation and chemical additives. Therefore, alternative, cost-efficient technologies to enhance the anaerobic digestion of CW are needed. This research study proposes two alternative strategies to alleviate acid inhibition and improve the performance of AD of CW.

The initial approach explores the use of an acid-tolerant methanogenic culture adapted to operate effectively at lower pH levels (5-6). This culture was developed through a 7-month acclimatization period using anaerobic granular sludge from a full-scale internal circulation (IC) bioreactor treating dairy wastewater, gradually enriched with an acetic acid solution. Experiments conducted under batch conditions with CW at this lower pH demonstrated that reactors employing the acclimatized sludge exhibited higher CH_4 production than reactors using non-acclimatized sludge. The increased abundance of *Methanolinea* under these conditions indicates that a significant portion of CH_4 was generated through the hydrogenotrophic pathway. Furthermore, the lower concentration of acetic acid and the higher abundance of *Clostridium sensu stricto* suggest the involvement of the syntrophic acetate oxidation-hydrogenotrophic methanogenesis (SAO-HM) pathway as the main pathway for CH_4 production. A significant economic benefit was also observed, with a potential reduction in NaOH usage of approximately

68%, substantially lowering operational costs. However, this approach produces 53% less kWh/d than anaerobic digestion at neutral pH.

The second approach investigates the impact of zero-valent iron (ZVI) in two forms (powder and scrap metal) on the AD of CW. It was found that the addition of 25 g/L powder ZVI (PZVI) and 50 g/L scrap ZVI (SZVI) not only enhanced CH_4 production but also lowered VFAs concentrations and reduced the necessity for external pH adjustments. Notably, reactors supplemented with ZVI achieved higher CH_4 yields and demonstrated superior biogas quality, with over 95% CH_4 purity observed in the initial two feeding cycles. Further experiments in semi-continuous and batch operation modes evaluated the performance of 25 g/L PZVI and 50 g/L SZVI. In semi-continuous mode, reactors with 25 g/L PZVI showed superior CH_4 yields and SCOD removal efficiency, indicating effective acid management and process stability. Furthermore, it maintained the lower VFA/ALK ratio. Batch operation further emphasized the potential for biogas upgrading (> 95% CH_4 content) in reactors with 25 g/L PZVI. The reactor with 25 g/L PZVI demonstrated the most efficient VFA reduction, achieving the lowest total VFA level and showing substantial acetate, propionate, and butyrate degradation. In contrast, reactors with 50 g/L SZVI and the control reactors exhibited higher VFA levels and less effective degradation, indicating lower methanogenic activity. Moreover, it was observed that 25 g/L PZVI significantly influenced the processes of methanogenesis and acidogenesis but did not have a pronounced effect on solubilization or hydrolysis. Finally, the study assesses the effects of H_2 supply, either supplied externally (ex-situ) or generated in-situ from the anaerobic oxidation of 25 g/L PZVI. Results show that in-situ H_2 supply significantly enhances CH_4 production, reaching 90% CH_4 content in biogas while also maintaining system alkalinity. However, the end product (digestate) from the in-situ reactor demonstrated inhibitory effects on plant growth, likely due to its high iron content. In contrast, the digestate from the ex-situ reactor showed positive effects on seed germination and growth in phytotoxicity trials with *Sinapis alba* seeds, indicating its potential use as a soil conditioner.

Keywords: Acclimatized granular sludge at pH 5-6, Anaerobic digestion, Biogas upgrading, Cheese whey, VFA degradation, Zero-valent iron

TABLE OF CONTENTS

LIST OF TABLES

LIST OF FIGURES

LIST OF ABBREVIATIONS

ABR	Anaerobic Baffled Reactor
AC	Activated Carbon
AcoD	Anaerobic Co-Digestion
AD	Anaerobic Digestion
AFBR	Anaerobic Fluidized Bed Reactor
AnGrSL	Anaerobic Granular Sludge
AnMBR	Anaerobic Membrane Bioreactor
AnSBBR	Anaerobic Sequencing Batch Biofilm Reactor
BES	2-bromoethanesulfonate
BMP	Biochemical Methane Potential
BOD5	Biochemical Oxygen Demand
BSA	Bovine Serum Albumin
C/N	Carbon to Nitrogen ratio
CE	Circular Economy
CHP	Combined heat and power system
COD	Chemical Oxygen Demand
CSTR	Continuous Stirred Tank Reactor
CW	Cheese Whey
DF	Dark Fermentation
DIET	Direct Interspecies Electron Transfer
DWW	Dairy Wastewater
DWWTP	Dairy Wastewater Treatment Plant
EGSB	Expanded Granular Sludge Bed Reactor
EPS	Extracellular Polymeric Substances

ES	Ensiled sorghum
GAC	Granular Activated Carbon
GHG	Greenhouse gas
GMP	Glycomacropeptide
HR	Hybrid Reactor
HRTs	Hydraulic Retention Times
IC	Internal Circulation Reactor
Igs	Immunoglobulins
IHT	Interspecies Hydrogen Transfer
LCFA	Long Chain Fatty Acids
mZVI	Micro Zero-Valent Iron
nZVI	Nano Zero-Valent Iron
OLRs	Organic Loading Rates
PABR	Periodic Anaerobic Baffled Reactor
PFR	Plug Flow Reactor
PHAs	Polyhydroxyalkanoates
PHB	Hydroxybutyric acid
PLA	Polylactic Acid
POR	Pyruvate-ferredoxin oxidoreductase
PZVI	Powder Zero-Valent Iron
SAOB	Syntrophic acetate-oxidizing bacteria
SBR	Sequencing Batch Reactor
SZVI	Scrap Zero-Valent Iron
TKN	Total Kjeldahl Nitrogen
TP	Total Phosphorus

TSS	Total Suspended Solids
UAF	Upflow Anaerobic Filter Reactor
UAFB	Upflow Anaerobic Fixed-Bed Reactor
UASB	Upflow Anaerobic Blanket Reactor
VFAs	Volatile Fatty Acids
WPC	Whey Protein Concentrate
WPI	Whey Protein Isolate
WSP	Wheat Straw Particle Biochar
ZVI	Zero-Valent Iron
α-La	α-lactalbumin
β-Lg	β-lactoglobulin

1 Introduction

The dairy industry is a major contributor to wastewater generation in the food sector. Milk, a critical human nourishment, predominantly contains water and is extensively used in dairy production processes (Ye and Li, 2023). The Food and Agricultural Organization of the United Nations reported that global milk production in 2023 reached approximately 950 million tonnes, a 1.3% increase from the previous year (FAO, 2023). This rise is attributed to the growing global population and the corresponding surge in demand for dairy products, leading to an expansion of dairy industries (Chokshi et al., 2016). Despite the rising popularity of plant-based dairy alternatives, traditional milk production is expected to grow annually by 1.6%, thanks to improvements in production systems and livestock husbandry (OECD/FAO, 2020).

Dairy industries not only use significant amounts of water (1-10 m^3 per m^3 of processed milk) for creating various milk products (e.g., cheese, butter, cream yogurt, and fresh milk) but also engage in additional operations such as sanitation, cooling of products, and cleaning of equipment, leading to the production of highly contaminated wastewater (Asunis et al., 2020). Stasinakis et al. (2022) reported that the EU-27 generates 192.5 million tonnes of dairy wastewater (DWW) annually. Cheese manufacturing contributes to 49% of this total, while the production of drinking milk, acidified milk products, and butterfat accounts for 19%, 18%, and 13%, respectively. Germany, France, Italy, Poland, Spain, and the Netherlands are responsible for over 73% of the total DWW production, with Germany and France leading in DWW production at 43.6 and 34.7 million tonnes, respectively. Italy, Poland, Spain, and the Netherlands produce between 13.0 and 18.9 million tonnes each (**Fig. 1-1**).

Kim et al. (2022) highlight that global cheese production is projected to increase by up to 14% by 2029, a trend driven mainly by rising dairy consumption in regions like India, Pakistan, and Africa. This trend results in higher production of cheese whey (CW), a liquid by-product of cheese manufacturing (Valdez Castillo et al., 2020). With an annual global production of approximately 190 million tonnes, CW stands as the dairy industry's most contaminated effluent owing to its high

organic content (50-80 g/L COD, 30-40 g/L BOD) and substantial volumetric generation (9-10 L) per kg of cheese produced (Lappa et al., 2019). Its direct discharge into the environment without adequate treatment leads to significant ecological damage. It impairs soil quality, reducing crop yields, and when entering water bodies, it adversely affects aquatic life by causing eutrophication (Valdez Castillo et al., 2020). However, CW presents a valuable opportunity for energy resource utilization due to its high organic content and the presence of biodegradable components (Ahmad et al., 2019).

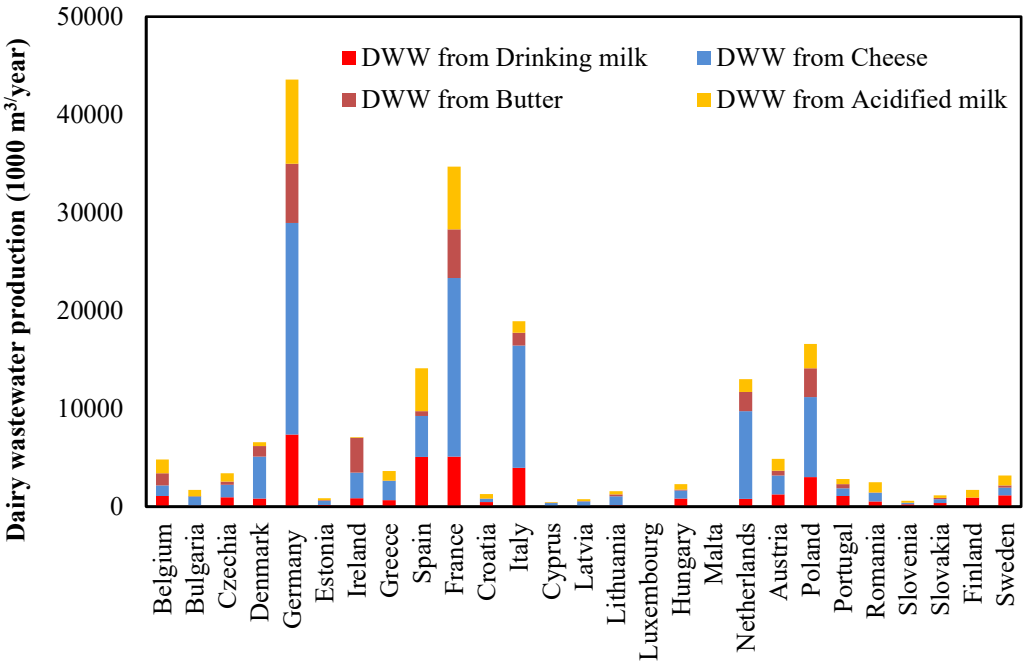

Figure 1-1. Estimated DWW production in different EU-27 countries for 2019. (Stasinakis et al., 2022).

In recent years, the surge in energy demand and escalating costs of traditional fossil fuels have heightened interest in alternative energy sources. Over 80% of the global primary energy supply is currently met by fossil fuels, including coal, oil, and natural gas (Asunis et al., 2020). These energy sources and industrial activities contribute to approximately 65% of worldwide greenhouse gas (GHG) emissions. Many countries, especially Europe, are transitioning to more sustainable and renewable energy options to address these environmental concerns, focusing on solar, wind, geothermal, and bioenergy (An et al., 2024).

Aligned with the circular economy (CE) concept, anaerobic digestion (AD) presents an effective technology that can exploit CW's high organic content and generate value-added products, such as biogas and fertilizer. However, challenges arise due to the high lactose levels in CW, which rapidly convert to volatile fatty acids (VFAs). This conversion, coupled with low alkalinity (<0.22 g/L $CaCO_3$), reduces pH, adversely affecting methanogenesis and the stability of the process (Escalante et al., 2018; Charalambous and Vyrides 2021).

Several studies have focused on addressing the challenges in AD of CW, particularly in mitigating the accumulation of VFAs and optimizing alkalinity. Adding alkaline agents like NaOH or $NaHCO_3$ can prevent process instability, but this increases operational costs and may lead to a high salt content in the digestate (Alavi-Borazjani et al., 2020). As an alternative option, the anaerobic co-digestion (AcoD) of CW with other buffering substrates (e.g. cattle slurry, livestock manure, food wastes etc.) has been explored as a cost-effective method to enhance process stability and carbon/nitrogen (C/N) balance. However, the safety of using the digestate as fertilizer is questionable due to potential pathogen content (Imeni et al., 2019). Moreover, determining the optimum mixing ratio of co-substrates and identifying available substrates could pose challenges. Additionally, a two-stage AD process, where hydrolysis-acetogenesis and methanogenesis occur in separate reactors, has been suggested (Antonopoulou et al., 2008). While this approach allows for lower hydraulic retention times (HRTs) in the methanogenic reactor compared to conventional single-stage AD, it is challenged by high capital costs and possible disruptions in microbial community dynamics (Asunis et al., 2020).

Given the above considerations, this research study explores two approaches aimed at reducing the need for alkaline addition due to the accumulation of VFAs and improving the AD of CW. Specifically, this study investigates two novel approaches to overcome this problem: (a) the anaerobic treatment of CW using an acclimatized methanogenic culture (anaerobic granular sludge) at a moderately low pH of 5.0-6.0, and (b) the effect of zero-valent iron (ZVI) addition in AD of CW

1.1 Production, characteristics and utilization of cheese whey

1.1.1 Cheese manufacturing process

The cheese-making process is a sequential procedure with several essential steps: acidification, coagulation, separating curds and whey, salting, shaping, and ripening (**Fig. 1-2**). These steps begin with four basic ingredients: milk, microorganisms (usually starter cultures of lactic acid bacteria), rennet, and salt (Beresford et al., 2001). Raw milk collected from farms is initially transported to the cheese factory in large containers. After undergoing quality testing, the milk is stored in large tanks at 4-6 °C. Before cheese production, milk is often standardized to optimize the protein-to-fat ratio, ensuring the production of high-quality cheese with a high yield. The next step is pasteurization (optional), which is performed by applying high temperatures for a short time (72-75 °C for 15 sec or 61.5 °C for 30 min) to eliminate pathogenic microbes (Legg et al., 2017; Zheng et al., 2021).

The first step in making cheese is acidification, where a starter culture is added to milk that will change lactose into lactic acid. During this process, the milk's pH level drops, and the cheese flavor develops. The next step is coagulation, where rennet, a mixture of enzymes containing the protease chymosin, is added and acts on the milk proteins (casein) to form a coagulated lump called curd (Dragone et al., 2009; Zheng et al., 2021). After adding the rennet, the curd is left alone for roughly 30 min to let it become a firm coagulum. The curd undergoes fermentation until it reaches a pH level of 6.4. Subsequently, it is sliced into small chunks using cheese knives. This step aids in the separation of whey from the curd. Next, the coagulum fractions are warmed (cooked) to 38°C to facilitate further processing. Stirring the whey-curd mixture during cooking is essential for achieving a dense coagulum. This action is particularly crucial for managing the moisture level (Legg et al., 2017).

Once the cooking step is complete, the whey is drained away, leaving the curd to develop into cheese. Salt is added for flavor and also acts as a stabilizer, thereby increasing the cheese's shelf life. The next step is shaping, where the salted curd pieces are placed in cheese hoops and pressed into blocks to form the cheese. Finally, the cheese is stored in a cool and dry place until the desired age (ripening).

Depending on the variety, cheese can be aged from several months to several years (Bandler 2023).

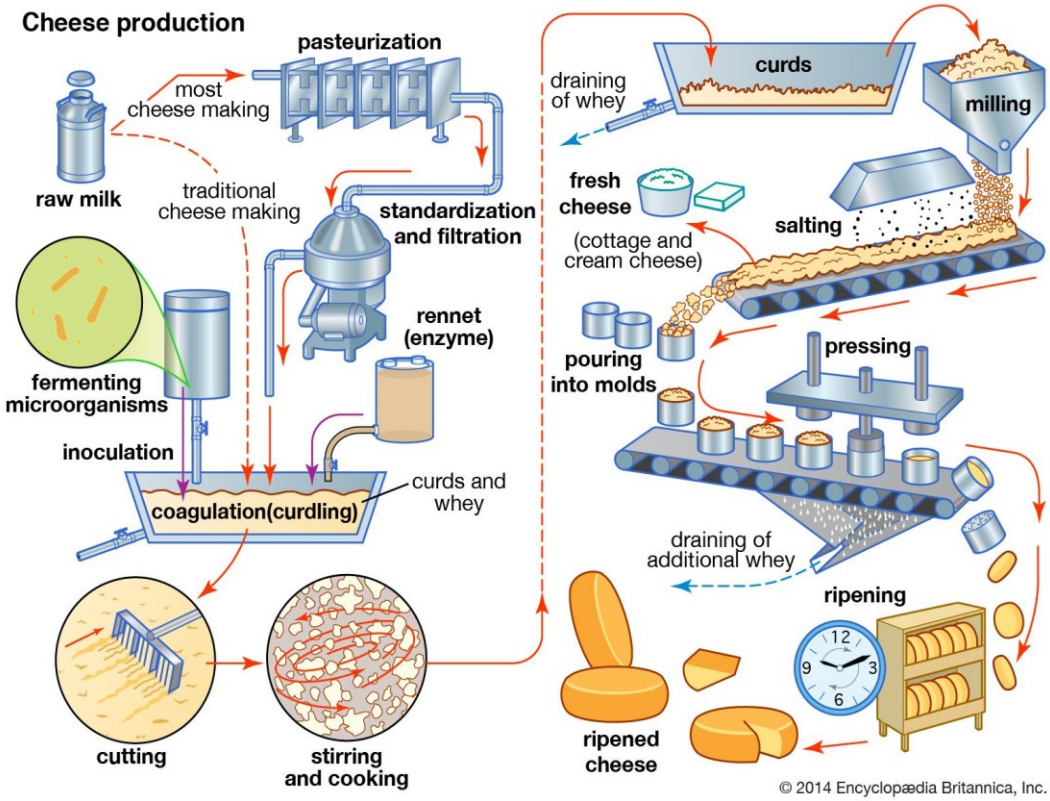

Figure 1-2. Schematic representation of cheese-making process (Bandler 2023)

1.1.2 Characteristics and composition of CW

CW is a liquid by-product remaining after milk casein is precipitated and removed during cheese production. It constitutes 85-95% of the total milk volume and contains approximately 55% of the milk's nutrients. Around 20% of the milk's overall protein content is preserved in the CW (Carvalho et al., 2013; Ryan and Walsh, 2016). Its yellow-green color is attributed to the presence of riboflavin (vitamin B2). CW is primarily composed of water (93-94% of its volume), lactose (4.5-6.0% w/v), soluble proteins (0.6-1.1% w/v), mineral salts (0.8-1.0% w/v), lactic acid (0.05-0.9% w/v) and fats (0.06-0.5% w/v) (Prazeres et al., 2012). Mineral salts are primarily NaCl and KCl (> 50%), along with calcium salts (mainly phosphates), and trace amounts of metals such as zinc and copper (Tsermoula et al., 2021). Additionally, minor constituents such as urea, uric acid, citric acid, and B-complex vitamins are also found within the composition of CW (Ryan and Walsh,

2016). The composition of CW varies depending on factors such as the type of milk used (sheep, goat, cow, or buffalo), the method employed to remove casein (enzymatic or acid coagulation), and various factors influencing milk composition such as animal breed, seasonal cycles, feed, and lactation phase (Pires et al., 2021).

CW is classified into sweet and acid whey depending on the milk protein coagulation method. Sweet whey is produced by adding rennet, typically occurring at pH 6.5, leading to the coagulation of milk casein and the formation of curd. Then the curd is strained from the remaining liquid (Panesar et al., 2012). In contrast, acid whey results from the action of *lactobacilli* or the addition of organic (lactic acid) or mineral acids like HCl or H_2SO_4, causing coagulation at around the isoelectric point of casein (pH 4.6) (Ryan and Walsh, 2016).

Sweet whey is commonly a by-product of hard cheese production such as cheddar, while acid whey is generated during the production of fresh acid cheeses like ricotta or cottage cheese. The main constituents of both types are presented in Table 1-1. Both types differ primarily in mineral content, pH, and whey protein fraction composition. Acid whey typically exhibits higher ash content but lower protein levels compared to sweet whey. Moreover, it contains approximately twice the calcium concentration (1.2-1.6 g/L) but less lactose (Carvalho et al., 2013).

Table 1-1. Typical composition (g/l) of sweet and acid whey (Chatzipaschali and Stamatis 2012)

Component	**Sweet whey**	**Acid whey**
Total solids	63-70	63-70
Proteins	6-10	6-8
Lactose	46-52	44-46
pH	5.9-6.4	4.60-4.70
Fat	5.0	0.4
Ash	5.0	8.0
Calcium	0.4-0.6	1.2-1.6
Phosphate	1-3.	2.0-4.5
Lactate	2	6.4
Chloride	1.1	1.1

About 20% of milk's total proteins are whey proteins, with the major fractions being β-lactoglobulin (β-Lg), α-lactalbumin (α-La), bovine serum albumin (BSA), and immunoglobulins (Igs), while the minor fractions include glycomacropeptide (GMP), lactoperoxidase, proteose peptone, and lactoferrin (Lf) (Papademas and Kotsaki, 2019). In recent years, several studies, highlight the significant nutritional and physiological benefits of whey proteins, including immune support (antimicrobial, antiviral), cardiovascular health (antithrombotic, antihypertensive), and improved digestion and cholesterol levels (Papademas and Kotsaki, 2019; Lappa et al., 2019; Zhao et al., 2022) (**Table 1-2**).

Table 1-2. Major whey proteins and their functions (Ryan and Walsh, 2016)

Protein	**Whey content (%)**	**Nutritional and functional benefits**
β-Lactoglobulin	48-58	Has excellent gelling, emulsifying and foaming properties, Lower blood pressure, Appetite enhancer
α-Lactoglobulin	13-25	Increase serum levels of tryptophan to improve sleep quality, Used in infant formula
Immunoglobulins	8-15	Help protect against illness such as oral or intestinal microbial infections
Bovine Serum Albumin	5-10	Prevention of cancer, Appetite suppressant
Lactoferrin	1-2	Anti-microbial and anti-viral properties, Bone growth promoter
Lactoperoxidase	0.5	Possesses antibacterial activity, Prevention of dental caries
Glycomacropeptide	10-20	Anti-thrombotic activities, Nutritional additive in infant formula
Lysozyme	0.0002	Antimicrobial activity

CW exhibits a high organic concentration with biochemical oxygen demand (BOD_5) and chemical oxygen demand (COD) values ranging between 40-60 g/L and 50-102 g/L, respectively (Chatzipaschali and Stamatis, 2012). Lactose predominantly contributes to the elevated BOD_5 and COD levels, accounting for over 90% of the whey's BOD_5. CW is considered readily biodegradable as a substrate, often indicated by a BOD_5/COD ratio exceeding 0.5 (Carvalho et al., 2013). Table 1-3 presents the primary physicochemical characteristics of CW according to various literature studies. Discharging untreated CW directly into water bodies or onto land causes serious environmental pollution problems. Its nitrogen content ranges from 0.2-1.76 kg/m³ and phosphorus content ranges from 0.124-0.54 kg/m³, posing a high risk of water eutrophication (Prazeres et al., 2012). A notable incident in Ohio (USA) in 2008 exemplifies this impact, where an acid whey spill killed approximately 5400 wildlife, predominantly fish, by reducing dissolved oxygen levels and leading to eutrophication (Papademas and Kotsaki, 2019). Additionally, disposing of CW on land can damage crops due to oxygen depletion from decomposing milk sugars and proteins, potentially reducing soil redox potential, increasing soil salinity, and thereby lowering crop yields (Ghaly et al., 2007).

Therefore, the above factors underscore the necessity to develop sustainable and cost-effective strategies for CW management. Sustainable development has become a global priority, focusing worldwide on sustainability challenges across various sectors, including the milk industry, as highlighted in the UN Agenda 2030 for sustainable development goals (United Nations, 2015). The utilization of CW through various technologies and diverse products is vital to advancing sustainability across multiple dimensions, such as environmental, economic, and social.

Table 1-3. The main physicochemical characteristics of CW according to different studies

pH	TCOD (g/L)	BOD_5 (g/L)	BOD_5/ COD	TS (g/L)	TSS (g/L)	TN (g/L)	TKN (g/L)	TP (g/L)	Fat and oils (g/L)	Lactose (g/L)	Reference
6-6.5	50-70	27-36	0.51-0.54	55-56	10-15		0.01-0.02			50-60	Ebrahimi et al., (2010)
4.46	60 ± 10	40 ± 2.55	0.67	59 ± 0.5	1.5 ± 0.23				0.9 ± 0.5		Gannoun et al., (2008)
5.8	73.4	29.5	0.4		7.2				0.99		Janczukowicz et al., (2008)
6.0 ± 0.1	61 ± 1.5				6.77 ± 0.5		0.826	0.24 ± 0.02	1.0 ± 0.1		Antonopoulou et al., (2008)
6.23 ± 0.1	60.5 ± 2.8				8.69 ± 1.34		0.37 ± 0.05	0.289	1.0 ± 0.1		Venetsaneas et al., (2009)
4.5-5.0	73-86				20-22	0.9-1.2		0.42-0.54			Farizoglou et al., (2004)
4.9 ± 0.3	68.6 ± 3.3	37.7 ± 2.8	0.55	5.93±0.38	1.35 ± 0.06		1.12-0.01		9.44 ± 1.14	45.9 ± 0.88	Saddoud et al., (2017)
4.9	74.2			66.83	22.15		1.49			50	Ghaly and Kamal (2004)
3.92	74.5 ± 0.4				9.4 ± 0.5		0.146	0.124			Erguder et al., (2001)
4.2	102.1			70.9		1.76				49.2	Ferchichi et al., (2005)
3.30	77.5 ± 0.53			59.76 ± 0.05			1.48 ± 0.09				Treu et al., (2019)
5.41 ± 0.01	67.1 ± 0.42			7.87 ± 1.02			11.5 ± 0.16				Kassongo et al., (2020)
3.8-6.3	60.3-66.7	35.5-46.0			4.1-10.0						Blonskaja and Vaalu (2006)

1.1.3 Utilization of CW

In light of the circular economy (CE) principles, the utilization of CW offers a multifaceted solution to managing this by-product, rendering it a valuable resource for creating value-added products owing to its rich components (Lappa et al., 2019; Buchanan et al., 2023). Traditionally, methods such as discharging CW into natural water bodies or municipal sewage systems have posed environmental and economic challenges for cheese manufacturers (Pires et al., 2021). However, the perception of CW as a valuable resource, rather than mere waste, has led to innovative management approaches. Approximately half of the global CW production is transformed into various value-added products, a trend expected to increase with evolving legislation and continuous research (Lappa et al., 2019).

Direct utilization of CW as animal feed for pigs, sheep, and cattle or as an ingredient in foods or beverages, either in its whole form or after deproteinization, represents one of the primary methods for its application (Pires et al., 2021). Furthermore, the stabilization of solid components from CW through physicochemical processes (including membrane filtration technologies, crystallization, drying, evaporation, and centrifugation) facilitates the production of derivatives such as whey powder, whey protein isolate (WPI), whey protein concentrate (WPC), lactose, and minerals (Tsermoula et al., 2021; Soumati et al., 2023). Whey powder is predominantly used for feeding animals, yet a lesser portion finds its application in human consumption products including ice cream, bakery items, pastries, condiments, and various dairy-based products (Pires et al., 2021). WPC and WPI are extensively utilized in the food industry due to their rich protein profile, essential amino acids, and low-calorie and minimal-fat characteristics. Their emulsification, foaming, and gel formation capabilities further enhance their desirability for various food applications (Lappa et al., 2019). Another significant strategy is the bioconversion of lactose, or residual whey permeate into various value-added products through microbial activity.

According to the literature, a variety of physicochemical, biological, or a combination of two or more processes (also known as bioprocess integration) can be employed to exploit CW for the production of industrially significant valuable

products, thus advancing towards a zero-waste dairy industry (Buchanan et al., 2023). Such products include functional foods and beverages, enzymes (e.g., β-galactosidase and polygalactorunase) bioproteins (single-cell protein-SCP), biopolymers (e.g., polylactic acid (PLA), polyhydroxyalkanoates (PHAs)), organic acids (e.g., acetic, lactic, succinic, propionic acids), biofuels (e.g., biohydrogen, biomethane, bioethanol), etc. (**Table 1-4**) (Asunis et al., 2020; Buchanan et al., 2023).

The production of whey-based beverages is an area ripe for research, offering economic and environmental advantages. Several studies have highlighted the nutritional and functional properties of CW, positioning it as an ideal ingredient for high-quality beverages (Papademas and Kotsaki, 2019; Lawton et al., 2021). These beverages range from sports drinks that enhance athlete performance to dairy-type whey beverages with probiotic benefits, alcoholic whey beverages offering unique flavors and sustainability, and carbonated whey beverages as a refreshing option (Lawton et al., 2021) (**Table 1-4**). Moreover, recovering whey proteins and lactose is a crucial aspect of CW valorization, converting these components into high-value products. Techniques such as ultrafiltration, nano-filtration, and ion exchange chromatography have been optimized to recover proteins and lactose efficiently. The recovered proteins are applied in various sectors, including food, pharmaceuticals, and nutraceuticals (Buchanan et al., 2023). Similarly, lactose recovery allows its use in confectionery, bakery products, and as a fermentation substrate, broadening the valorization scope of CW (Bonnaillie and Tomasula, 2008). Microbial fermentation processes, utilizing specific bacterial strains, open new avenues for CW valorization, producing bioenergy and biochemicals (Asunis et al., 2020).

In recent years, integrating biorefining processes for resource recovery has addressed environmental issues associated with CW disposal while contributing to the CE by generating energy and valuable chemicals from waste. For example, recent innovative research has focused on producing bioplastics and edible films, notably polylactic acid (PLA) and polyhydroxyalkanoates (PHAs), from CW, marking a significant step towards sustainable material production (Soumati et al., 2023). The fermentation products of CW, primarily VFAs, serve as precursors for

biopolymer synthesis, with various microorganisms (*Thermus thermophilus, Pseudomonas hydrogenovora, Bacillus megaterium*) demonstrating the capability to convert these substrates into high-value biodegradable plastics (Asunis et al., 2020). Developing these biodegradable polymers offers a promising alternative to conventional petroleum-based plastics, aligning with global efforts to reduce plastic waste and carbon footprint (Chalermthai et al., 2021).

Eco-friendly biofuels such as biomethane, bioethanol, biodiesel, and biohydrogen provide sustainable alternatives to fossil fuels (Buchanan et al., 2023) (Table 1-4). The production of biohydrogen and VFAs from CW through dark fermentation (DF) shows particular promise. Specific microorganisms, like *Lactobacillus* for lactate conversion and *Clostridium* species for hydrogen production, can convert lactose in CW into valuable products. Biohydrogen, known for its minimal emissions, high energy density, and negligible impact on GHG accumulation, highlights its potential as an environmentally friendly energy source (Asunis et al., 2020). Additionally, CW fermentation for bioethanol production by strains such as *Kluyveromyces marxianus* and *Saccharomyces cerevisiae*, which are adept at lactose hydrolysis and ethanol fermentation, is especially suitable for this application (Asunis et al., 2020).

Biomethane production through AD offers a sustainable approach for managing dairy waste with a high organic content, such as CW, transforming it into a valuable renewable energy source (Bella and Rao, 2021). This biochemical process capitalizes on the specialized metabolic functions of a diverse consortium of anaerobic microorganisms, which proficiently convert lactose-rich CW into methane and carbon dioxide. Beyond the significant reduction of waste, AD plays a crucial role in energy recovery, decreasing reliance on fossil fuels and lowering GHG emissions associated with traditional waste disposal practices (Choudhary et., 2021). Additionally, the AD process produces a nutrient-rich by-product, known as digestate, which acts as an efficient biofertilizer to improve soil health and decrease the demand for synthetic fertilizers. Therefore, the AD of CW not only addresses environmental concerns but also advances the principles of the CE by transforming waste into a spectrum of valuable resources (Wainaina et al., 2020).

Table 1-4. Various products result from the utilization of CW through physicochemical and biotechnological processes

Utilization	Products	Example techniques	References
Whey protein-based beverages	Sport drinks, Probiotic beverages, Alcoholic beverages, Fruit-flavoured beverages	Fermentation of whey by-products or whey-derived lactose	Papademas and Kotsaki (2019); Lawton et al. (2021)
Whey protein and lactose recovery	Extraction of specific fractions, such as proteins (i.e., β-Lg, α-La, BSA, Ig, Lf) or lactose, with high purity	Membrane filtration (MF, UF, NF, RO), Ion exchange chromatography,	Bonnaillie and Tomasula (2008)
Whey fermentation by-products	Ethanol, Biohydrogen and Volatile fatty acids (VFAs)	Fermentation and distillation, Dark fermentation	Asunis et al. (2020); Lovato et al. (2021)
Food and Ingredients	Whey powders, Whey protein isolate (WPI), Whey protein concentrate (WPC)	Evaporation, crystallisation, spray drying, Membrane technologies	Lappa et al. (2019) Buchanan et al., (2023)
Chemicals and preservatives	Food preservation, Acetate (98% purity), Production of hydrogen, acetate, butyrate, propionate, valerate, lactate, succinic acid	Hydrolysis or fermentation of whey to release bioactive compounds, Enzymatic and microbial catalysed hydrolysis and fermentation	Buchanan et al., (2023)
Biopolymers	Polyhydroxyalkanoates (PHAs), Poly-3-hydroxybutyric acid (PHB), Edible films	Whey fermentation, Dehydration of protein polysaccharide/ antimicrobial agent biofilms,	Asunis et al. (2021); Lappa et al. (2019)
Biofuels and biochemicals	Biohydrogen, Methane, Bioethanol, VFAs	Anaerobic digestion, Fermentation	Asunis et al. (2021)

1.2 Anaerobic digestion (AD) process

Anaerobic digestion (AD) is an established technology in the waste-to-energy sector that proficiently converts organic matter, in the absence of oxygen, into biogas and a semi-stabilized material known as digestate (Bella and Rao, 2021). The biogas primarily consists of CH_4 (60-70%) and CO_2 (30-40%) which can be inserted into a combined heat and power (CHP) system for electricity and heat production, or used in a boiler for heat generation. Moreover, the by-product, digestate, can be directly applied in agriculture providing essential nutrients such as nitrogen and phosphorus that enhance soil characteristics (Atelge et al., 2020). The AD process can be divided into four distinct stages: hydrolysis, acidogenesis, acetogenesis, and methanogenesis (**Fig. 1-3**).

The first stage of AD is hydrolysis, in which complex organic compounds are broken down into smaller, water-soluble particles, enabling microbial metabolism. Hydrolytic bacteria transform carbohydrates, proteins, and lipids into biodegradable organics such as monosaccharides, amino acids, higher fatty acids, and alcohols using extracellular enzymes like amylase, cellulase, lipase, protease, and pectinase (Harirchi et al., 2022). Hydrolysis often exhibits its highest efficiency in a temperature range of 30-50 °C and a pH range of 5-7 (Westerholm and Schnürer, 2019). In acidogenesis stage these smaller molecules undergoing fermentation, producing short-chain volatile fatty acids (VFAs) like formic, acetic, propionic, butyric, lactic acids, and other products such as alcohols (methanol, ethanol), CO_2, and H_2. Acidogenesis usually progresses more rapidly than hydrolysis, often completing in under 36 hours. Excessive acidification due to the accumulation of VFAs can lower the pH, adversely affecting the next methanogenesis stage (Meegoda et al., 2018).

Methanogens could directly use some products of the acidogenic phase, including acetic acid, H_2, and CO_2, to produce CH_4. However, other higher VFAs, such as propionic and butyric acids, need further degradation to be made accessible for methanogenesis (Laiq Ur Rehman et al., 2019). Syntrophic acetogenesis refers to the process by which these intermediate substances undergo additional biotransformation to produce acetate, H_2, and CO_2. Under thermodynamic standard

conditions, syntrophic acetogenesis is favorable only if the H_2 partial pressure is below 10^{-4} atm. Hydrogenotrophic methanogens and other H_2-utilizers, such as homoacetogens, consume H_2 released, making acetogenesis thermodynamically feasible (Harirchi et al., 2022). In acetogenesis, acidogenic intermediate products are further decomposed into acetic acid, CO_2, and H_2.

In the final stage, methanogenesis, CO_2/H_2, acetic acid, and methylated compounds are reduced to CH_4 by methanogenic archaea. Aceticlastic methanogens convert acetate into a methyl group and CO_2 and subsequently, the methyl group is reduced into CH_4 (Ventorino et al., 2018). In addition, hydrogenotrophic methanogens generate CH_4 by reducing CO_2 as a carbon source and using H_2 as an energy source. Around 70% of CH_4 is derived from acetate conversion and alcohol fermentation, with the remaining 30% coming from CO_2 reduction. The AD process is known for its straightforward operation, cost-efficiency, lower energy consumption, and minimal space requirements compared to aerobic systems (Bella and Rao 2021)

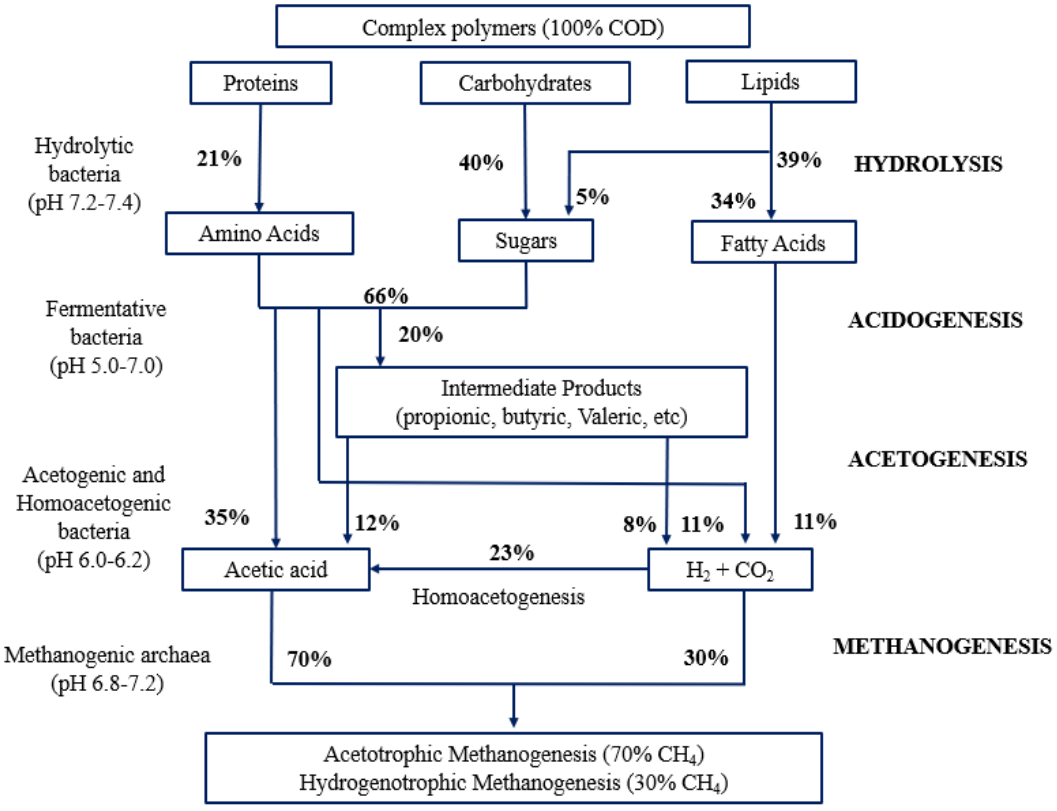

Figure 1-3. Flow diagram of AD process (Casallas-Ojeda et al., 2021)

1.2.1 Microbiology insights into AD process

Indeed, AD is a complex, multi-phased biological process involving various synergistic bacteria and archaea. Each phase of the AD process plays a distinct role in decomposing multiple compounds, and it is crucial to keep the reaction rates balanced among these groups of microorganisms to guarantee efficient and stable digestion (Harirchi et al., 2022). **Table 1-5**. presents some examples of various microorganisms involved in the different stages of the AD process.

Hydrolytic bacteria exhibit significant phylogenetic diversity. Nonetheless, the majority of recognized species predominantly belong to two phyla: *Bacteroidetes* and *Firmicutes* (Peng et al., 2018a; Luo et al., 2018). Additionally, some anaerobic fungi, such as *Neocalimastix*, *Piromyces*, and *Orpinomyces* have been reported to play an essential role in the hydrolysis of cellulosic material (Akyol et al., 2019). Compared to methanogens, hydrolytic bacteria tend to grow more rapidly and show greater resilience to environmental changes, such as fluctuations in pH and temperature. In acidogenesis, the monomers from hydrolysis are converted by different facultative and obligatorily anaerobic bacteria to VFAs and other products such as alcohols, lactate, CO_2, and H_2 (Ventorino et al., 2018). The phyla *Bacteroidetes*, *Chloroflexi*, *Firmicutes*, and *Proteobacteria* includes the majority of identified species of acidogenic bacteria. The ability of acidogenic bacteria to form spores allows them to endure extreme conditions and environments such as low pH, high temperature, and high organic loading rates (OLRs) (Cai et al., 2019).

Acetogens belong to various bacterial genera and convert products from the acidogenic phase into acetic acid, CO_2, and H_2. These strictly anaerobic microorganisms are sensitive to environmental changes and are categorized into two groups: those that produce H_2 and acetate from organic acids, and the homoacetogens, who consume H_2 and CO_2 to produce acetate (Venkiteshwaran et al., 2015).The acetate production by the first group leads to significant H_2 release, causing a decrease in pH within the reactor. This H_2 can be utilized in CH_4 production or during the formation of butyric and propionic acids (Laiq Ur Rehman et al., 2019).

Under standard thermodynamic conditions, anaerobic degradation of propionate ($\Delta G°= +76.1$ kJ/mol) and butyrate ($\Delta G°= +48.1$ kJ/mol) to acetate is endergonic, requiring a reduction in H_2 partial pressure to below 32.04 Pa and 40.34 Pa, respectively (Amani et al., 2010). In this context, the syntrophic relationship between acetogens and methanogens stabilizes the system by supplying the primary substrates (acetate and H_2) for CH_4 generation (Harirchi et al., 2022).This relationship, facilitated by mechanisms like interspecies H_2 transfer (IHT), keeps H_2 partial pressure under 10^{-3} atm, aiding acetogens survival in low H_2 conditions (Kumar et al., 2021), with hydrogenotrophic methanogens, sulfate-reducing bacteria (SRB), and homoacetogens efficiently removing H_2. The degradation of propionate is primarily facilitated by syntrophic acetogens from genera such as *Pelotomaculum, Smithella*, and *Syntrophobacter*, while the oxidation of butyrate is facilated by acetogens from the genera *Syntrophus* and *Syntrophomonas* (Venkiteshwaran et., 2015).

Interspecies H_2 transfer occurs between two cells that lack the ability to independently oxidize organic molecules; consequently, they engage in electron exchange using H_2 to break down organic substances (Harirchi et al., 2022). Hydrogen, a molecule with a high diffusion rate but limited solubility, restricts the distance for H_2 transfer to approximately 10 μm. This limitation significantly influences the choice of electron carriers among microorganisms. Specifically, when the separation between microbial cells is less than 10 μm, H_2 becomes the preferred medium for electron exchange (Wang et al., 2021). In contrast, when the distance exceeds 10 μm, interspecies formate transfer becomes crucial in the syntrophic relationship between acetogens and methanogens. Additionally, certain microorganisms are capable of direct interspecies electron transfer (DIET) via electrically conductive pili. This mechanism enables direct electron transfer from species like *Geobacter* to *Methanosaeta*, facilitating a rapid electron exchange process (Summers et al., 2010). Nevertheless, further research is essential to fully understand these mechanisms and determine how they can be enhanced in engineered systems and in mix microbial communities such as anaerobic biomass

The final phase of the AD process includes three methanogenic pathways: hydrogenotrophic, methylotrophic, and acetoclastic. Generally, methanogens

belong to the domain Archaea, the kingdom of Euryarchaeota, and are typically divided into 5 orders: *Methanobacteriales, Methanococcales, Methanomicrobiales, Methanosarcinales,* and *Methanopyrales*. On the other hand, acetoclastic methanogens are divided into two main genera: *Methanosaeta* and *Methanosarcina*. *Methanosaeta*, known as obligate acetoclastic methanogens, solely uses acetate. Their slower growth rate is offset by a high affinity for acetate, leading to their predominance in environments with low acetate levels (Harirchi et al., 2022).

In contrast, *Methanosarcina*, as a facultative acetoclastic methanogen, can metabolize not only acetate but also H_2/CO_2 and C-1 compounds. Phenotypically, within the genus *Methanosarcina*, the spherical cells cluster together in substantial packets, creating a sarcina-like formation, while *Methanosaeta* is characterized by its rod-shaped cells (Zhao et al., 2018). While methanogens are often considered to be slow-growing microorganisms in AD, the presence of hydrogenotrophic methanogens plays a crucial role in maintaining a low H_2 partial pressure during AD (Wang et al., 2019). *Methanobacterium, Methanobrevibacter, Methanoculleus, Methanospirillum*, and *Methanothermobacter* are the most frequently hydrogenotrophic methanogens. Hydrogenotrophic methanogens exhibit greater resilience to environmental challenges compared to acetoclastic methanogens.

Syntrophic acetate-oxidizing (SAOB) bacteria offer an alternative pathway for CH_4 production. This process involves converting acetate into H_2 and CO_2 by specific bacteria, which then gets transformed into CH_4 by hydrogenotrophic methanogens (Kim et al., 2018). Notably, only a limited number of microorganisms, such as *Clostridium ultunense, Thermacetogenium phaeum, Tepidanaerobacter acetatoxydans, Thermotoga lettingae,* and *Syntrophaceticus schinkii*, are capable of this syntrophic acetate oxidation in partnership with H_2-consuming methanogens. This pathway, however, is not typically dominant in AD for CH_4, as acetoclastic methanogens usually outperform SAOB. Nonetheless, further research is needed to understand its role in AD systems (Venkiteshwaran et al, 2015).

Table 1-5. Microorganisms involved in the various stages of the AD process (modified from Deepanraj et al., 2104; Harirchi et al., 2022)

Reactions for each stage	ΔG°' [kJ/mol]	Microorganisms involved
Stage I: Hydrolysis		*Clostridium, Proteus vulgaris, Vibrio, Bacillus Peptococcus, Bacteriodes, Clostridium, Escherichia, Staphylococcus, Micrococcus, Peptococcus*
$(C_6H_{10}O_5)\ n + nH_2O \rightarrow n(C_6H_{12}O_6)$		
Stage I: Acidogenesis		*Lactobacillus, Escherichia, Bacillus, Staphylococcus, Pseudomonas, Sarcina, Desulfovibrio, Selenomonas, Streptococcus, Veollonella, Desulfobacter, Desulforomonas, Eubacterium limosum*
$C_6H_{12}O_6 + 2H_2O \rightarrow 2CH_3COOH + 4H_2 + CO_2$	(ΔG°'= -206.0 kJ/mol)	
$C_6H_{12}O_6 + 2H_2 \rightarrow 2CH_3CH_2COOH + 2H_2O$	(ΔG°'= -279.4 kJ/mol)	
$C_6H_{12}O6 \rightarrow CH_3CH_2CH_2COOH + 2H_2 + 2CO_2$	(ΔG°'= -254.0 kJ/mol)	
$C_6H_{12}O_6 \rightarrow 2CH_3CH_2OH + 2CO_2$	(ΔG°'= -164.8 kJ/mol)	
$C_6H_{12}O_6 \rightarrow 2CH_3CHOHCOOH$	(ΔG°'=-135.0 kJ/mol)	
Stage III: Acetogenesis		*Syntrophomonas wolfei, Syntrophomonas wolinii, Acetobacterium, Desulfotignum, Eubacterium, Acetoanaerobium, Holophaga, Moorella thermoacetica, Syntophobacter, Desulfovibrio, Pelobacter, Syntrophococcus, Sporomusa, Thermoanaerobacter, Treponema,*
$CH_3CH_2OH + H_2O \rightarrow CH_3COOH + 2H_2$	(ΔG°'= +9.6 kJ/mol)	
$CH_3CH_2COOH + 2H_2O \rightarrow CH_3COOH + 3H_2 + CO_2$	(ΔG°'= +76.1 kJ/mol)	
$CH_3CH_2CH_2COOH + 2H_2O \rightarrow 2CH_3COOH + 2H_2$	(ΔG°'= +48.1 kJ/mol)	
$CH_3CHOHCOOH + H_2O \rightarrow CH_3COOH + CO_2 + 2H_2$	(ΔG°'= -4.2 kJ/mol)	
$4H_2 + 2CO_2 \rightarrow CH_3COOH + 2H_2O$	(ΔG°'= -95.0 kJ/mol)	
Stage IV: Methanogenesis		*Methanococcus, Methanospirillum, Methanothermobacter Methanosaseta, Methanosarcina, Methanobacterium, Methanobrevibacter, Methanomicrobium, Methanothrix soehngenii, Methanobrevibacter smithii*
$CH_3COOH \rightarrow CH_4 + CO_2$	(ΔG°'= -75.7 kJ/ mol)	
$CO_2 + 4H_2 \rightarrow CH_4 + 2H_2O$	(ΔG°'= -131. kJ/mol)	
$2CH_3CH_2OH + CO_2 \rightarrow CH_4 + 2CH_3COOH$	(ΔG°'= -86.6 kJ/mol)	

1.2.2 Anaerobic granular sludge (AnGrSL)

Granule formation is a microbial phenomenon where microorganisms spontaneously organize into dense, structured aggregates known as granules. These form through a seemingly spontaneous process, beginning with the initial inoculation and extending over a prolonged culturing period. Granules are characterized by their rapid settling ability, which facilitates the separation of treated liquid from sludge, a crucial property for the efficient operation of anaerobic reactors (Chong et al., 2012; Show et al., 2020). These granules host diverse bacterial communities that establish syntrophic symbiosis, enabling efficient pollutant breakdown. The size of granules is a commonly monitored attribute, used to evaluate the progress or phase of granulation. Typically, granules vary in size from 0.5 to 4 mm (Trego et al., 2020).

In recent years, reactors designed to leverage AnGrSL have gained prominence due to their operational efficiency and sustainability (Mohan and Swathi, 2022). Notable examples include the Upflow Anaerobic Sludge Blanket (UASB) reactor, Expanded Granular Sludge Bed (EGSB) reactor, Hybrid Reactor (HR), Anaerobic Baffled Reactor (ABR), and Internal Circulation (IC) reactor. These systems are particularly adept at treating high-strength industrial wastewaters from breweries, food processing facilities, and pharmaceutical plants (Van Lier, 2008; Tay et al., 2010; Mohan and Swathi, 2022). Their design promotes the formation and retention of AnGrSL, thus ensuring high pollutant removal efficiency, stable operation under fluctuating load conditions, and resilience to shock loading of waste. Moreover, these reactors are compact, require less space than conventional treatment systems, and produce a low yield of sludge. Despite extensive research, the mechanisms of granule formation remain incompletely understood, with various theories and models proposed to elucidate this phenomenon (Show et al., 2020).

The physicochemical theories emphasize thermodynamic principles, suggesting that interactions like repulsive electrostatic charges, attractive van der Waals forces, and hydration forces are crucial in granulation, guiding microbial cells to cluster and form granules. The inert nuclei model, supported by the work of

Lettinga et al. (1980), posits that bacterial attachment to nuclei or micro-sized biocarriers is an initial step in anaerobic granulation. Experiments have shown that introducing zeolite or hydro-anthracite particles, each about 100 μm in diameter, into inoculated sludge can effectively promote the development of anaerobic granules.

Hulshoff Pol et al. (1988) proposed that granulation is a microbial defense mechanism against external stress, which can be leveraged as a selection pressure to foster granule formation. In UASB reactors, granule development is highly influenced by the balance of hydraulic load and gas generation. Higher selection pressure, achieved by removing lighter sludge, encourages the growth of denser granules and more efficient aggregates, while lower pressure results in a less dense biomass, poor settling, and reduced biogas production. Properly adjusting the upflow liquid velocity and maintaining a shorter HRT are key to enhancing granulation.

Pereboom and Vereijken (1994) suggested a different aspect of granulation, stating that the process begins with microbes detaching from larger granules and adhering to form new ones. While some microbes might be washed out, the main limiting factor for granule size is the removal of excess biomass. Contrary to initial assumptions, external shear forces and internal gas production don't lead to granule disintegration but instead release small particles from the granules. They also noted that the quality of granule size distribution varies with wastewater composition: higher solid concentrations result in poorer distribution, whereas soluble wastewaters yield a more uniform distribution. Moreover, the multi-valence ion-bonding model explains anaerobic granulation through the introduction of multivalent positive ions like Ca, Al, Mg, or Fe. These ions help overcome the repulsive forces among negatively charged bacterial surfaces, promoting cell attachment and initiating granulation (Teo et al., 2000).

In addition to these physicochemical theories, various structural hypotheses that incorporate microbial factors have been proposed. The Cape Town hypothesis, as outlined by Palns et al. (1987), suggests that in environments with high H_2 partial pressure, methanobacteria secrete amino acids excessively, stimulating the formation of extracellular polymeric substances (EPS). These substances trap

Methanobacterium strain AZ and other bacteria, initiating the anaerobic granulation process.

MacLeod et al. (1990) proposed a three-layered structure for anaerobic granules based on electron microscopy studies. They observed a core of acetoclastic methanogens surrounded by a middle layer of H_2- or formate-producing acetogens and H_2- or formate-consuming methanogens, with an outer layer of bacteria responsible for hydrolyzing and acidifying complex organic materials (**Fig. 1-4**).

The Spaghetti theory, as described by Wiegant (1988), suggests that filamentous *Methanothrix* initially attach to precursors and create a three-dimensional network. This structure entraps bacteria like *Methanosarcina,* growing denser and spherical due to cellular multiplication and hydrodynamic shear from upflowing liquid and biogas. The formation of these structured aggregates is a critical step in the overall granulation process.

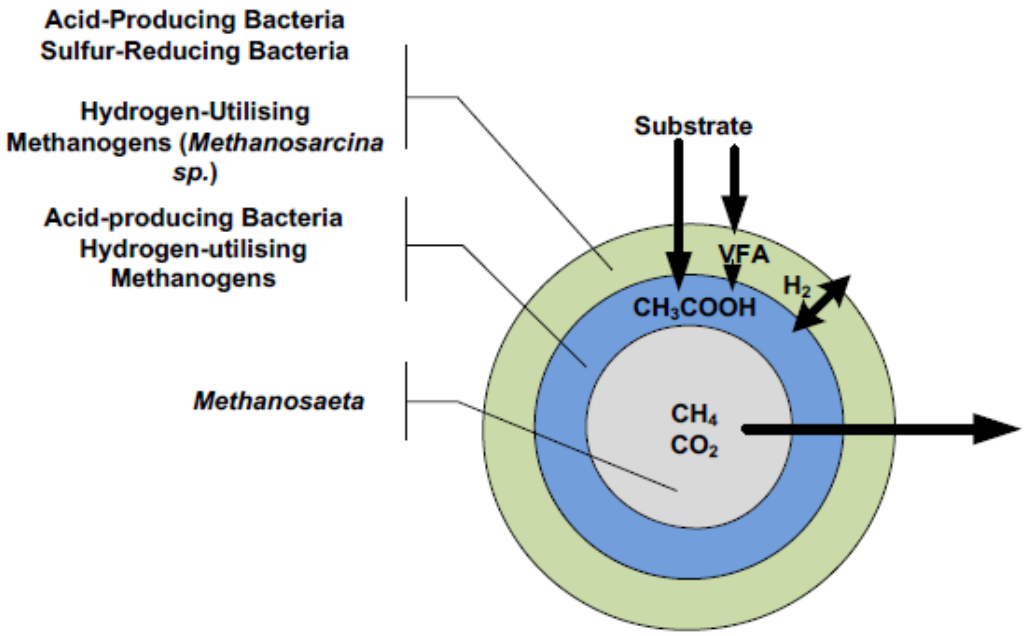

Figure 1-4. Structure of anaerobic granules (Njoya et al., 2019)

1.2.3 Factors affecting the performance of AD process

1.2.3.1 Temperature

AD can operate across a broad temperature spectrum, including psychrophilic (15-25 °C), mesophilic (35-40 °C), and thermophilic (50-60 °C) ranges (Bella and Rao, 2021). Mesophilic AD produces biogas at a slower rate and in lower quantities; however, it ensures a higher diversity of active anaerobic microorganisms, and it remains appealing due to its reduced heating energy requirements compared to thermophilic AD. In contrast, thermophilic AD enables higher organic loading rates (OLRs) and initial substrate hydrolysis, shortens hydraulic retention times (HRTs), and results in increased biogas production yields (Kainthola et al., 2019). Moreover, thermophilic AD enhances pathogen reduction, with Meegoda et al. (2018) observed a 90% reduction in various pathogens in less than an hour at 53°C, compared to several days required to achieve the same reduction in a digester operating at 35°C.

1.2.3.2 Hydraulic Retention Time (HRT)

Hydraulic retention time (HRT) refers to the duration that substrates spend in conjunction with biomass in a reactor or digester. It is calculated by dividing the reactor's volume (V) by the flow rate (Q), using the following formula:

$$HRT=\frac{V}{Q}$$

Where V is the volume of reactor (m^3) and Q is the flow rate in m3/d

In general, longer HRTs allow for more complete degradation of complex organic compounds, leading to higher biogas yields. However, longer HRTs also increase operational costs due to the need for larger digester volumes (Kainthola et al., 2019). On the other hand, too short HRTs may not provide sufficient time for adequate microbial activity, resulting in lower biogas production and incomplete digestion, which could negatively impact the downstream handling of effluents (Bella and Rao, 2021). Typically, HRTs vary depending on the type of digester, the operating temperature, and the characteristics of the feedstock, with typical ranges

being 15-30 days for mesophilic AD and 10-20 days for thermophilic AD (Mao et al., 2015).

1.2.3.3 Organic Loading Rate (OLR)

The OLR is defined as the amount (mass) of organic material introduced into the digester or reactor per unit volume per unit time (Bharati et al., 2017; Sarker et al., 2019). The mass loading can be expressed in terms of Volatile Solids- VS (representing the organic part of the solids applied) or in terms of COD applied on a daily basis to the reactor (Eq. 1).

Eq.1

$$OLR=(\frac{1}{HRT})\ x\ Ci=(\frac{Q}{V})\ x\ Ci$$

Where, OLR is the organic loading rate ($kgVS/m^3/d$), Q is the flow rate (m^3/d), V is the reactor volume (m^3), Ci is the concentration of VS or COD of the influent stream (kg/m^3) and HRT is the hydraulic retention time (d)

The OLR is crucial because it affects both the microbial balance within the digester and the efficiency of biogas production. If the OLR is too high, it can lead to an overload of the system. This overload can cause process imbalances such as acid accumulation, which inhibits methane-producing bacteria, leading to decreased biogas production and potential system failure (Franke-Whittle et al., 2014). In contrast, underloading a reactor/digester with an insufficient quantity of feedstock for the microbes, resulting in inefficient biogas production. Therefore, the optimum range for OLR varies with the type of substrates fed into the reactor/digester, as these substrates determine the level of biodegradation activity that will take place and other operating conditions such as temperature and retention time (Bella and Rao, 2021).

1.2.3.4 Carbon/Nitrogen ratio (C/N)

C/N ratio is a critical factor in the efficiency of the AD process, impacting biogas production and system stability. Optimal C/N ratios vary depending on substrate and operational conditions, with studies suggesting a range of 18 to 35 is ideal for maintaining balance (Fernandes et al., 2014). When the C/N ratio exceeds

35, nitrogen scarcity leads to acidification that impedes methanogenesis, while a ratio below 18 can cause harmful ammonia accumulation affecting bacterial populations. Gómez Romero et al. (2014) investigated the ACoD of CW with fruit vegetable waste using different C/N ratios (7,17,21,31 and 46) for H_2 production. The results indicated that the optimum C/N ratio was 21, which showed a buffer effect that enhanced H_2 generation. In another study, optimal CH_4 production was found at C/N ratios of 25:1 and 35:1 for mesophilic and thermophilic digesters, respectively, during ACoD of dairy and chicken manure with rice straw (Wang et al., 2014).

1.2.3.5 Mixing

Efficient biogas production and stability in AD heavily depend on adequate mixing. Proper agitation ensures the uniform distribution of nutrients, enhances the contact between the substrate and microorganisms, and prevents issues such as scum formation and temperature gradients. However, excessive mixing can disrupt slow-growing microbes and alter critical conditions, including pH and moisture content (Karim et al., 2005). Common methods of mixing include mechanical, manual, and biogas recirculation, each having distinct effects on digester performance. Properly agitating the substrate can increase biogas production by up to 50%, provided that all other operational parameters remain constant. Nevertheless, overly vigorous stirring can adversely affect the microorganisms involved, hence slow mixing is recommended (Singh et al., 2020).

1.2.3.6 Inhibitory Substances

Significant inhibitors of AD include ammonia (NH_3), VFAs, long-chain fatty acids (LCFA), heavy metals, sulfur compounds, antibiotics, etc (Chen et al., 2008). Ammonia plays a crucial role in the AD process for several reasons. It serves primarily as a nutrient source for the anaerobic microbial community and enhances the system's buffer capacity by neutralizing organic acids, thus preventing inhibition by VFAs. Ammonia exists in its free form (NH_3) and ionic form (NH_4^+) in AD. The ionic form is utilized as a nutrient, while the free form is toxic. Nevertheless, high levels of either form can inhibit the activity of methanogenic organisms. Free NH_3 can penetrate cell membranes, leading to an H^+ imbalance or

K^+ deficiency (Astals et al., 2018). The pH level directly influences the dominant form of ammonia in the system; at pH values of 7.2 or lower, the ammonium ion (NH_4^+) prevails. However, at higher pH levels, indicating a lower concentration of H^+ ions, free NH_3 predominates (Westerholm et al., 2016). However, free NH_3 is a significant inhibitor in AD, affecting efficiency at 1 g/L NH_3-N or higher concentrations by impeding the conversion of organic matter to biogas. Excessive NH_3 (TAN ≥ 4 g N/L) not only directly inhibits the process but also leads to the accumulation of intermediate VFAs, such as propionic, butyric, and valeric acids (Riggio et al., 2017; Mirmohamadsadeghi et al., 2019). The microbial community's tolerance to NH_3 varies with substrate composition and operational parameters, with thermophilic systems (55 ºC) capable of handling roughly double the NH_3 levels compared to mesophilic ones (35 ºC) (Rajagopal et al., 2013).

Heavy metals such as copper (Cu), nickel (Ni), chromium (Cr), cadmium (Cd), zinc (Zn), and lead (Pb) can promote the growth of microorganisms involved in biogas production by acting as enzyme cofactors. However, their positive effects become detrimental at higher concentrations due to toxicity (Chen et al., 2008). For example, Hg is highly toxic at concentrations as low as 0.1 mg/L. Pb and Cd inhibit microbial activity at concentrations of 50 mg/L and 10 mg/L, respectively. Cr is toxic at about 5 mg/L, while Cu and zinc become toxic at 50 mg/L and 200-300 mg/L, respectively. Ni shows toxicity at concentrations exceeding 200 mg/L. The primary mechanism behind the toxicity of heavy metals involves altering the structure of enzymes and inhibiting their activity (Kwietniewska and Tys, 2014)

Sulfide (S^{2-}), produced during AD from the reduction of sulfate (SO_4^{2-}) in the feed and the breakdown of proteins, only becomes inhibitory in its soluble form at concentrations above 200 mg/L. The interaction of sulfide with heavy metal cations results in the formation of insoluble precipitates, thereby reducing the toxic effects of the metals. It is estimated that 1 mg/L of sulfide can precipitate about 1.8 mg/L of heavy metals, thus mitigating their inhibitory impact on the AD process (Meegoda et al.,2018).

Long chain fatty acids (LCFAs) such as caprylic, myristic, oleic, lauric, and capric were found to be toxic and disrupt the AD process by dissolving into the cell walls of acetoclastic and hydrogenotrophic methanogens due to their similar

chemical structures of cell wall lipids, inhibiting bacterial function at low concentrations. Concentrations of LCFAs over 500 mg/L in digesters can significantly impair microbial activity, indicating their toxic effect on the anaerobic process (Sarker et al., 2019).

1.2.3.7 pH

The pH value is a critical operational parameter that significantly affects the AD process. It represents the inverse logarithm of the H^+ concentration and influences the process in two primary ways: directly, by altering the activity of enzymes through structural modifications; and indirectly, by affecting the toxicity of specific substances present in the environment of the anaerobic system. Each microorganism requires a different optimal pH for growth (Bharati et al., 2017). For instance, methanogens are very sensitive to pH fluctuations, preferring a pH of 6.5-7.5. In contrast, acidogenic bacteria exhibit remarkable pH resistance, tolerating a broader range of 4.0-8.5. However, the optimal pH range for hydrolysis and acidogenesis is between 5.5-6.5. In general, a pH value within the range of 6.8-7.2 indicates a healthy environment for the digester's microorganisms and is reported as the desired range for biogas production (Bella and Rao, 2021).

1.2.3.8 Alkalinity and Volatile fatty acids (VFAs)

Alkalinity refers to the ability of an aqueous solution to neutralise or buffer acids. Alkalinity in the AD process is primarily presented in the form of bicarbonate and alkalinity of VFAs (Bharati et al., 2017). When organic compounds are decomposed CO_2 is released resulting in the formation of carbonic acid, carbonate alkalinity, and bicarbonate alkalinity. In the AD process, VFAs such as acetate, propionate, butyrate, and valerate are intermediate products that can decrease pH, particularly under high organic loading rates (OLR). Excessive VFA accumulation, especially from easily biodegradable substates, can lead to a sharp pH decline, inhibiting methanogenesis. A drop in pH below the optimal range of 6.5-7.3 due to high VFA accumulation can lower biogas production, resulting in financial losses (Moeller and Zehnsdorf, 2016). Acetic and butyric acids are the primary products at acidic pH levels, while at a pH of around 8.0, the primary products are acetic and propionic acids. Methanogens function optimally with VFA concentrations around

300 mg/L but are inhibited by concentrations between 1500-2000 mg/L. Propionate, notably, is inhibitory at concentrations as low as 30 mM (approximately 2222.7 mg/L). VFAs are managed differently across various anaerobic processes, with levels between 2.2-4.9 g/L causing inhibition (Rajagopal et al., 2017)

The buffering capacity, provided mainly by bicarbonate ions (HCO_3^-) along with other carbonate forms (CO_3^{2-}) and ammonia (NH_3), neutralizes these acids, maintaining a relatively stable pH. When excess hydrogen ions (H^+) are present, bicarbonate (HCO_3^-) reacts with them to form carbonic acid (H_2CO_3), which can then convert to carbon dioxide (CO_2) and water (H_2O) (**Fig. 1-5**). This prevents the accumulation of hydrogen ions, which would otherwise lower the pH drastically.

$$HCO_3^- + H^+ \rightleftharpoons H_2CO_3 \rightleftharpoons CO_2 + H_2O$$

This balance is critical for the process's efficiency and preventing the inhibition of methanogens, which prefer a neutral to slightly alkaline pH range. Typically, alkalinity levels above 2500 mg/L $CaCO_3$ contribute to the formation of a buffering effect in digesters (Bella and Rao, 2021). The system's pH also depends on the dynamic equilibrium between gaseous CO_2 and aqueous HCO_3^-. Continuous CO_2 release from bio digestion of organic compounds may result in higher dissolution in the medium if the system's pH falls excessively. In contrast, a rise in pH can shift CO_2 to carbonic acid, releasing hydrogen ions. At pH 4, CO_2 exists predominantly as free molecules, and at pH 13, as dissolved carbonate, with equilibrium at pH 6.52. Consequently, a rise in pH typically reduces the gaseous CO_2 concentration (Deublein and Steinhauser 2011).

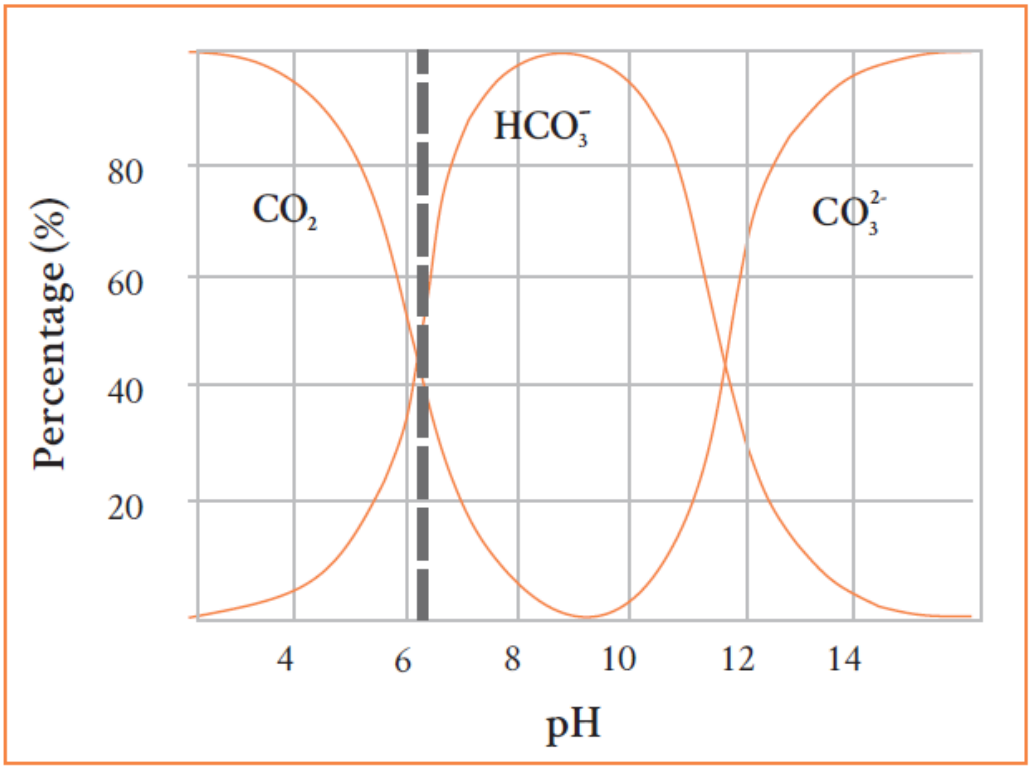

Figure 1-5. Chemical balance between carbon dioxide – bicarbonate ion – carbonate ion (Deublein and Steinhauser 2011).

A key method for managing the buffering system in the AD process and monitoring the production of acids is the intermediate alkalinity to partial alkalinity (VFA/TA) ratio, with the former representing bicarbonate-derived alkalinity and the latter reflecting alkalinity from volatile acids. VFA/TA ratio between 0.1 and 0.35 ensures sufficient alkalinity for methanogens, while exceeding this range (>0.35) indicates potential reactor overloading, suggesting a need to reduce the OLR. One method of preserving the pH value within the desired range is by increasing the system's alkalinity with the addition of external buffering chemicals such as sodium bicarbonate ($NaHCO_3$), lime ($CaCO_3$), sodium hydroxide (NaOH), sodium carbonate (Na_2CO_3), etc (Chen et al., 2015). However, various strategies to overcome excessive acidification in AD have been examined, with key strategies discussed in a subsequent section.

1.3 Strategies for controlling excessive acidification in AD

1.3.1 Alkaline chemicals addition

Alkaline chemicals such as sodium hydroxide (NaOH), sodium bicarbonate ($NaHCO_3$), calcium oxide (CaO), and ammonium bicarbonate (NH_4HCO_3) are widely used to regulate pH levels and neutralize VFAs during AD (Alavi-Borazjani et al., 2020). This method is known for its simplicity and effectiveness in preventing excessive acidification in the digestion process. Many studies have been conducted to evaluate the efficacy of this approach by adding these chemicals directly to the digesters. In a study by Venetsaneas et al. (2009), two-stage AD CW was conducted using 20 g of $NaHCO_3/L_{CW}$ or 2 N NaOH to maintain a pH of 5.2 in the acidogenic reactor. The H_2 yield was 2.9 L/L_{CW} with $NaHCO_3$ and 1.9 L/L_{CW} with NaOH. Processing the effluent through a mesophilic digester resulted in stable operation, with reduced VFAs, CH_4 production of 6.7 L per L of influent, and 95.3% COD removal. A previous study by Agdag and Sponza (2005) showed that alkaline supplementation with $NaHCO_3$ at doses of 3 and 6 g/L/d in AD of organic solid wastes led to lower VFA concentrations, higher pH levels, and increased CH_4 content of 64% and 65%, respectively, compared to 37% in the control reactor without alkaline addition.

On the other hand, some studies have reported adverse effects of alkaline chemicals on AD performance. Anwar et al. (2016) noted a significant reduction in CH_4 yield, with 16 g/L NaCl causing 17-80% inhibition during AD of kitchen waste, due to increased sodium salt concentration leading to VFAs accumulation and decreased volatile solid removal efficiency. The authors recommended keeping sodium salt concentrations below 8 g/L to prevent notable CH_4 production inhibition. Feng et al. (2020) observed that using over 3.5 g/L NaOH for pH adjustment during two-stage AD of food waste decreased CH_4 production due to salt accumulation. Lin et al. (2013) reported that the optimal Na^+ concentration range should be between 3.5-8 g/L. Furthermore, Dai et al. (2013) indicated that excessive reagent use during high acidification degree can cause temperature fluctuations and elevated Ca^{2+} and Na^+ levels, impairing microbial activity in the reactor.

1.3.2 Addition of carbon-based conductive materials

Adding carbon-conductive materials such as graphite, granular activated carbon (GAC), activated carbon (AC), biochar, carbon nanotubes, carbon cloth, felt, and ashes has been proposed to manage excessive acidification (Alavi-Borazjani et al., 2020). These materials enhance AD efficiency due to their high electrical conductivity and strong absorption capacities (Peng et al., 2018). AC, for example, is notably effective because of its porous structure and electrical conductivity, which enhance organic acid adsorption (Alavi-Borazjani et al., 2020). Additionally, the fine pore structure, large surface area, and high porosity of these materials facilitate microbial immobilization and biofilm formation, critical for efficient AD (Ambaye et al., 2021). Their high electrical conductivity also promotes direct interspecies electron transfer (DIET) between oxidizing bacteria and methanogens, optimizing AD processes (Peng et al., 2018).

Several studies have supported the benefits of carbon-based materials in AD. Kaur et al. (2020) found that adding wheat straw particle biochar to the anaerobic co-digestion of food waste sludge reduced VFA accumulation and increased CH4 production by 24%. In a separate study, Sugiarto et al. (2021) reported a 46.9% increase in CH_4 generation when food waste was treated with biochar, attributed to improved system buffering capacity. Similarly, Jang et al. (2018) noted that biochar derived from dairy manure decreased VFA concentration and increased CH_4 production by 24.69% to 35.71%, thanks to the biochar's nutrient content and alkalinity. Furthermore, Wang et al. (2021) demonstrated that biochar could facilitate a rapid recovery in digesters experiencing severe acidification by enhancing VFA oxidation through syntrophic oxidation.

1.3.3 Trace elements supplementation

Trace elements (Fe, Cu, Ni, Co, Mg, Mn, Mo, Se, Zn) play a crucial role in enhancing the efficiency of VFA degradation in AD. They are vital cofactors for enzymes that are involved in microbial growth and the metabolism of methanogens (Garuti et al., 2018). Many researchers have studied the addition of trace elements to accelerate VFA degradation, thus enhancing AD performance. For example, the addition of Fe has been reported to significantly improve the catalytic activity of

pyruvate-ferredoxin oxidoreductase (POR), an essential enzyme in the degradation of propionate (He et al., 2022).

Wei et al. (2014) examined the impact of adding trace elements (Fe, Co, Ni) on the AD of food waste in semi-continuous lab digesters operating at OLRs between 1.0-5.0 g VS L^{-1} d^{-1}. They observed that CH_4 production was hindered at a high VFA concentration of 30,000 mg L^{-1} at an OLR of 4.0 g VS L^{-1} d^{-1} without adding trace elements. However, with the addition of these elements, CH4 production increased from 0.13 to 0.44 L g^{-1} VS added. They concluded that Fe was particularly critical for the stability of the digester. Paulo et al. (2004) investigated the impact of Co addition on the thermophilic AD of methanol. Their study revealed that 0.1 μM of Co effectively boosted methanogen activity without causing excessive acetate accumulation, leading to CH_4 concentrations over 70 mM. In a separate study by Wall et al. (2014), the addition of a mixture of trace elements, including Fe (74.40 mg/L), Co (0.13 mg/L), and Ni (2.48 mg/L), resulted in VFA concentrations remaining below 1000 mg/L and a 12% increase in CH_4 yield during the AD of grass silage.

1.3.4 Enzymes addition

Enzymes have shown to enhance biogas production by effectively breaking down complex organic materials in anaerobic digesters, without causing the souring issue. Their advantages include resilience to toxic substances, adaptability to varying conditions, straightforward application, and improved process control. Notably, enzymes outperform microorganisms in substrate accessibility within AD systems, attributed to their smaller size and higher solubility and mobility (Alavi-Borazjani et al., 2020). Mendes et al., (2006) demonstrated that treating a lipid-rich wastewater from the dairy industry with a low-cost lipase enzyme derived from animal sources (porcine pancreas) at various incubation times (4-24 h) resulted in an enhanced production of biogas within the range of 354-445 mL. The highest biogas production was achieved after 12 h of incubation. Interestingly, under these conditions did not exhibit the development of VFAs.

1.3.5 Bioaugmentation with acclimated acid-tolerant methanogenic culture

In various natural habitats, biogas production has been documented at surprisingly low pH levels within acidic peatlands, with values as low as 5.0 (Bräuer et al., 2006), 3.8 (Duval and Goodwin, 2000), and even 3.0 (Williams and Crawford, 1983). Although low pH environments are generally adverse for methanogens in AD systems, certain studies have demonstrated their potential to adapt and effectively produce CH_4 under these conditions. For instance, Taconi et al. (2007, 2008) and Jain and Mattiasson (1998) observed that methanogenic cultures could be acclimatized to operate effectively at pH values down to 4.5 and 4.0 by gradually reducing the pH from 7.0 in 0.5 increments. Specifically, Jain and Mattiasson (1998) reported that methanogenesis was less affected by a gradual pH reduction compared to a sudden drop, with an 85-day operation using pulp industrial wastewater as a substrate showing a 12% increase in CH_4 yield by acclimatized cultures at lower pH values compared to non-acclimatized cultures.

Building on these findings, Wang et al. (2020) enriched an acid-tolerant methanogenic culture using sodium propionate as the sole carbon source, which thrived at pH 5.0. Their method involved a stepwise pH decrease of 0.5 and extended operation times at each pH level, fostering a microbial culture dominated by acetoclastic *Methanothrix* and hydrogenotrophic *Methanolinea.* However, rapid pH reductions were found to decrease *Methanothrix* populations, enriching hydrogenotrophic methanogens instead. Similarly, Li et al. (2018) enriched an acid-tolerant methanogenic propionate degradation culture from AD system treating crops, noting a microbial shift from acetoclastic to hydrogenotrophic methanogens as pH decreased. Additionally, Ali et al. (2019) successfully acclimated a methanogenic culture to a pH as low as 3.5 over five months using acetic acid as the sole carbon source, finding *Methanothrix soehngenii* to be particularly tolerant of low pH conditions. The potential for acclimatization to acidic conditions is further supported by Taconi et al. (2007) observations, of a 30% higher CH_4 yield at pH 4.5 compared to pH 7.0 using a synthetic acetic acid solution in a batch reactor system. Furthermore, their subsequent study under semi-continuous conditions with acetic acid solution at pH 4.0-5.3 demonstrated enhanced CH_4 production compared to neutral conditions (Taconi et al., 2008).

Several previous studies have suggested that bioaugmentation with enriched acid-tolerant methanogenic consortia, such as propionate-utilizing cultures (Tale et al., 2015), VFA-degrading enrichments (Acharya et al., 2015), and acetate-utilizing consortia (Town and Dumonceaux, 2016), could significantly reduce VFA accumulation and enhance AD process stability. Li et al. (2018) indicated that bioaugmentation of an acid-tolerant methanogenic culture in AD systems overloaded with artificial food waste markedly improved digester performance by reducing VFAs and increasing pH levels, unlike control reactors. Moreover, they observed a significant increase in the populations of *Methanothrix* and *Methanolinea* following bioaugmentation, which likely played a crucial role in boosting CH_4 production. In a different study, the same authors (Li et al. 2022) reported that bioaugmentation of an acclimated propionate-degrading methanogenic culture to semi-continuous AD of chicken manure expedited VFA degradation and increased CH_4 yield by 15-18% under high ammonia levels (5.0-8.4 g NH_4^+-N/L). The results pointed out that bioaugmentation crucially reconstructed the microbial community within the digester, notably enhancing the presence of hydrogenotrophic *Methanobacterium* and slightly increasing the populations of aceticlastic *Methanothrix* and syntrophic propionate-oxidizing bacteria *Syntrophobacter*, which are highlighted as critical contributors to success in handling high ammonia levels.

A key point to emphasize regarding the bioaugmentation approach is the high probability of introduced microbial strains being washed out during the prolonged continuous operation of AD reactors. Consequently, it is crucial to maintain constant monitoring of the microorganisms added to the AD reactors (Yang et al., 2016).

1.4 Anaerobic digestion of CW

1.4.1 Associated problems in AD of CW

The high organic matter content (50-102 g/L COD) of cheese whey makes it a suitable candidate for AD process, which can help recover energy by producing

biogas (Asunis et al., 2020). Studies have shown that the biochemical methane potential (BMP) values for CW range between 0.32-0.85 mLCH_4/g VS (Labatut et al., 2011; Dreschke et al., 2015). However, CW is considered a problematic substrate for AD due to its high biodegradability (approximately 99%) and low alkalinity (<0.22 g/L $CaCO_3$), which can cause rapid acidification and the accumulation of VFAs (Chatzipaschali and Stamatis, 2012).

Lactose, the primary component of CW, is rapidly fermented, leading to the quick and substantial production of VFAs. This process is further constrained by a drop in pH below the range required for methanogenesis, which causes system instability (Escalante et al., 2018; Fernandez-Rodríguez et al., 2021). pH levels play a crucial role in AD since the degradation process functions most effectively within a neutral pH range of 6.8 to 7.2 (Bella and Rao, 2022). Acid inhibition can cause lower efficiency in COD removal, reduced biogas production, decreased CH_4 yield, and difficulties in granulation, resulting from an imbalance in the rates of acidogenesis and methanogenesis (Chatzipaschali and Stamatis, 2012).

1.4.2 Overview of previous AD studies on CW treatment

According to the literature, studies have been conducted to investigate the AD of CW using various reactor configurations, including the continuous stirred tank reactor (CSTR) (Jung et al., 2016), anaerobic sequencing batch reactor (AnSBR) (Fernández et al., 2015), up-flow anaerobic sludge blanket reactor (UASB) (Diamantis et al., 2014), anaerobic membrane bioreactor (AnMBR) (Dereli et al., 2019), expanded granular sludge blanket (EGSB) (Cruz-Salomón et al., 2020), anaerobic sequencing batch biofilm reactor (AnSBBR) (Batista et al., 2023), etc. (**Table 1-6**). Even though more than 80% COD removal efficiency could be obtained in these systems, the potential of rapid acidification and the lack of alkalinity in CW necessitated the supplementation of buffering chemicals (e.g., $NaHCO_3$, NaOH) or the dilution of CW to sustain stable AD performance (Dereli et al., 2019)

Effluent recirculation is a practical solution for maintaining stable performance in UASB and EGSB reactors. This method effectively dilutes the incoming COD and recycles the alkalinity produced in the acetoclastic

methanogenic pathway, thereby reducing the need for external dosing of alkaline chemicals. For example, Erdirencelebi (2011) observed a significant reduction in alkali requirements and achieved over 97% COD removal efficiency during the AD of raw CW through a three-stage process that included pre-acidification and two UASB reactors in series. In a separate study, Escalante et al. (2017) treated CW in a plug flow reactor (PFR) and found that effluent recirculation combined with fresh manure ensured pH stability within the range of 7.5 to 7.9 and kept the VFA/Alk ratio below 0.4, demonstrating the practicality of this approach.

Several pre-treatment methods have been proposed to enhance the bioavailability of organic matter and biogas production during the AD of CW. For example, Bella et al. (2023) investigated the impact of three different pre-treatment methods (ultrasonic, ozonation, and enzymatic) on reducing the protein complexity in CW and enhancing biogas production during anaerobic co-digestion (AcoD) with sludge septage. Their findings highlighted that enzymatic pre-treatment was the most effective, yielding a maximum CH_4 production of 432.2 mL CH_4/gVS. Similarly, Gannoun et al. (2008) reported a 50% reduction in COD and a 60% reduction in TSS following a biological pre-treatment of CW using *Lactobacillus paracasei* and subsequent neutralization with lime. The pre-treated CW was further digested through an up-flow anaerobic filter (UAF) reactor, achieving an average COD removal of 80-90%.

Anaerobic co-digestion (AcoD) of CW with other buffering substrates (e.g., livestock manure, domestic sludge septage, etc.) and a two-stage AD process, where hydrolysis-acetogenesis and methanogenesis occur in separate reactors, have also been recommended to avoid process instability during the AD of CW (see sections 1.4.2.1 and 1.4.2.2).

Table 1- 6. Performance of different types of anaerobic reactors used CW as the only substrate

Reactor type	Substrate	Inoculum	HRT	Temperature	Methane yield	COD removal efficiency	References
AnMBR	Diluted whey permeate	Granular from EGSB treating lactose-based wastewater	6 d	37 °C	280 L CH_4 $kg^{-1}COD_{feed}$	98%	Dereli et al. (2019)
AnSBR	Whey permeate	Sludge from digester treating urban wastewater	8.3 d	55 °C	320 L CH_4 $kg^{-1}COD_{feed}$	87%	Fernández et al. (2015)
AnSBR + CSTR	Whey Permeate	Sludge from the wastewater treatment plant	1st stage:2.2 d 2nd stage:29 d	37 °C	310 L CH_4 $kg^{-1}COD_{removal}$	88%	Dereli et al. (2015)
CSTR+ UASB	Diluted whey	Granular sludge from a UASB treating dairy wastewater	1st stage:0.4 d 2nd stage:0.5-0.7 d	30 °C	370 L CH_4 $kg^{-1}COD_{removal}$	88%	Diamantis et al. (2014)
CSTR + UAF	Raw whey	Sludge from the digester treating fruit and vegetables waste	1st stage: 0.83d 2nd stage: 1-4 d	32 °C 35 °C	110 L CH_4 $kg^{-1}COD_{removal}$	90%	Gannoun et al. (2008)
EGSB	CW wastewater	Granular sludge from UASB treating soft drinks	6 d	26.6 ± 1.4 °C	334 L CH_4 $kg^{-1}COD_{removal}$	90%	Cruz-Salomón et al. (2020)
AnSBBR	CW wastewater	Granular from UASB treating effluents from a sugar and alcohol plant	0.25 d	55 °C	231 L CH_4 $kg^{-1}COD_{removal}$	96%	Batista et al. (2023)
CSTR + AnMBR	Raw whey	Seed sludge from a full-scale WWTP	1st stage:1 d 2nd stage:4 d	37 °C	300 L CH_4 $kg^{-1}COD_{removal}$	99%	Saddoud et al. (2007)

1.4.2.1 Anaerobic co-digestion (AcoD) of CW

Anaerobic co-digestion (AcoD) involves the simultaneous digestion of two or more substrates in specific ratios to produce biogas. According to the literature, the AcoD of CW has been extensively studied due to the dual benefits of this approach: firstly, it enhances nutrient availability, and secondly, it boosts the system's buffering capacity (Casallas-Ojeda et al., 2021). CW due to its high nitrogen and organic content, aiding in achieving an optimal carbon to nitrogen (C: N) ratio. This balance is crucial for supporting specific microbial populations, thereby enhancing the effectiveness and stability of the biogas production process (Bella and Rao, 2022).

Several studies have explored the AcoD of CW with other substrates, such as cattle slurry (Comino et al., 2012), poultry manure (Abdallah et al., 2022), dairy manure (Kavacik and Topaloglu, 2010), domestic waste sludge-septage (Bella and Rao, 2022), ensiled sorghum (Dareioti and Kornaros, 2015), etc., in order to provide buffering capacity, balanced C/N ratio, and mitigate rapid acidification, thereby improving overall stability (**Table 1-7**). For instance, Comino et al. (2012) investigated the AnCoD of CW with cattle slurry (50%:50% v/v), and reported 82% COD removal efficiency and CH_4 yield of 187 L CH_4 kg^{-1} COD_{feed} in a continuous stirred tank reactor (CSTR), without alkaline addition. Similarly, Rico et al. (2015) obtained a CH_4 yield of 392 L CH_4 $kg^{-1}VS_{feed}$ during the AcoD of CW with the liquid fraction of dairy manure in a CSTR under mesophilic conditions. Bella and Rao (2022) examined the AcoD of CW with domestic waste sludge septage at 37± 2 ◦C for 35 days. The results pointed out a maximum CH_4 production at 60% CW fraction (342.22 L CH_4 $kg^{-1}VS$) at a very short lag time of 0.76 ±0.17days (Table 1-7).

Apart from these, other agro-industrial wastes like sugarcane vinasse (Albuquerque et al., 2019), hemp hurds (Papirio et al., 2020), glycerin (Lovato et al., 2016; Almeida et al.,2022a) and coffee pulp wastes (Gonzalez-Piedra et al., 2021) were employed as a co-substrate with CW. Papirio et al. (2020) investigated the synergistic effect of CW with hemp hurds (HH) when these substrates were co-digested. Notably, blending HH and CW resulted in a 10.7% increase in CH_4

production compared to using HH alone. This approach not only improved CH_4 yield but also demonstrated economic benefits, with net gains increasing to 6124 EUR per hectare, compared to 3929 EUR per hectare when only HH was used in the AD process. Previously, Lovato et al. (2016) examined the AcoD of CW with glycerol in a mesophilic anaerobic sequential batch biofilm reactor (AnSBBR). The results showed a CH_4 yield of 298 L CH_4 kg^{-1} COD, along with an 89% COD removal efficiency at a mixing ratio (v/v) of 75% CW and 25% glycerol.

However, not all studies have shown positive outcomes. For instance, Labatut et al. (2011) found that mixing CW with dairy manure in ratios of 10%:90% or 25%:75% led to reduced CH_4 production compared to mono-digestion of CW. Similarly, Vivekanand et al. (2018) reported a decline in CH_4 production when CW was combined with cattle manure, fish ensilage, or both. In AcoD process, the mixed substrates ratio can influence not only the CH_4 yield but also the overall stability of the process. Gelegenis et al. (2007) studied the AcoD of CW and diluted poultry manure in a CSTR, noting an increase in CH_4 yield with CW concentrations up to 35%. However, the process became unstable when the CW content exceeded 50% based on VS.

AcoD of CW aligns with sustainable waste management and resource use principles, reflecting the ideals of the circular economy. Ongoing research is focused on identifying the best substrate mixing ratio for co-digestion with CW and advancing the technology to enhance the efficiency of biogas production in practical applications. Nevertheless, there are various obstacles that need to be overcome in order to adopt it on a large scale. These include the challenge of managing the rising amount of digestate produced and the higher expenses associated with transportation and maintenance (Gonzalez-Piedra et al.,2021).

Table 1-7. Different agro-industrial residues used as co-substrates with CW in various reactor configurations.

Substrate	Mixing ratio	Reactor type	Methane yield	COD removal efficiency	References
CW+ Cattle slurry	50:50 v/v	CSTR	187 L CH_4 kg^{-1} COD_{feed}	82%	Comino et al. (2012)
CW+ Dairy manure	85:15 v/v	CSTR	392 L CH_4 $kg^{-1}VS_{feed}$	n. a	Rico et al. (2015)
CW+ Glycerin	75:25 w/v on a COD basis	AnSBBR	298 L CH_4 kg^{-1} $COD_{removal}$	89%	Lovato et al. (2016)
CW+ Sea lettuce	75:25 v/v	CSTR	300 L CH_4 kg^{-1} COD_{feed}	68%	Jung et al., (2016)
CW+ Sugarcane vinasse	25:75 v/v	AnSBBR	353 L CH_4 kg^{-1} COD	89%	Sousa et al. (2019)
CW+ Glycerin	75:25 w/v on a COD basis	AnSBBR	342 L CH_4 kg^{-1} $COD_{removal}$	68%	Albuquerque et al. (2020)
CW+ Septage sludge	60:40 v/v	BMP (100ml)	342.22 L CH_4 $kg^{-1}VS$	n.a	Bella and Rao, (2022)
CW+ Glycerin	50:50 w/v on a COD basis	AFBR	284 L CH_4 kg^{-1} $COD_{removal}$	87%	Almeida et al. (2022a)
CW+ poultry manure	25:75 w/v on VS basis	CSTR	395 L CH_4 kg^{-1} COD_{feed}	75%	Abdallah et al. (2022)
CW+ coffee pulp wastes	1 gVS_{whey} gVS_{Coffe}^{-1}	batch digester	71.54 L CH_4 $kg^{-1}VS_{remo}$	n.a	Gonzalez-Piedra et al. (2021)
Ensiled sorghum+ CW+ liquid cow manure	55:40:5, v/v/v	CSTR	310 LCH_4 kg^{-1} COD_{remo}	83%	Dareioti and Kornaros, (2015)

1.4.2.2 Two-stage AD of CW

The development of a two-stage AD process, where hydrolysis-acetogenesis and methanogenesis occur in separate reactors, offers an innovative approach to improve the stability and efficiency of AD. This is particularly advantageous for substrates with an easily biodegradable composition such as CW, which can pose problems due to rapid acidification. According to Rajendran et al. (2020) and Srisowmeya et al. (2020), the main advantages of the two-stage AD process include optimal operating conditions, increased productivity, and enhanced process stability through the recirculation of effluents. Additionally, this method facilitates the high-yield production of H_2 and CH_4, which can be utilized as fuel, either individually or combined into biohythane (Meena et al., 2020). However, challenges such as economic viability, toxicity risks from ammonia buildup, and maintaining microbial balance highlight the complexity of implementing a two-stage system (Rajendran et al., 2020).

Many studies underscore the advantages of the two-stage AD of CW. For instance, Antonopoulou et al. (2008) investigated this approach using a system comprising an acidogenic continuous stirred tank reactor (CSTR) followed by a methanogenic periodic anaerobic baffled reactor (PABR) at 37°C. The acidogenic reactor achieved a H_2 yield of 41 L H_2 kg^{-1}COD removed over a 12-hour HRT, while the methanogenic phase, with an HRT of 4.4 d, yielded 310 L CH_4 kg^{-1} COD $_{removed}$ and achieved a 94% COD removal efficiency. Similarly, Saddoud et al. (2007) reported excellent efficiency in their two-stage system, consisting of an acidogenic CSTR and an anaerobic membrane bioreactor (AnMBR), with 300 L biogas kg^{-1} COD $_{removed}$. This system not only achieved a 98.5% reduction in COD and a 99% reduction in BOD_5 but also completely eliminated TSS. However, they noted challenges such as membrane clogging.

Dareoiti et al. (2021) compared single-phase and two-phase AD of CW in continuously stirred tank reactors (CSTRs) under mesophilic conditions (**Fig. 1-6**). The results indicated that the single-stage AD faced operational challenges due to limited buffering capacity. In contrast, the two-stage process achieved a stable CH_4 production rate of 13.7 L CH_4/L $_{feed}$, a CH_4 yield of 180 L CH_4 kg^{-1} COD $_{feed}$, and a 76% COD removal efficiency

Almeida et al. (2023) evaluated the mesophilic and thermophilic anaerobic AcoD of CW with glycerol in a two-stage process using an anaerobic fluidized bed reactor (AFBR), increasing the organic loading rate (OLR) from 2 to 20 gCOD/L/d. The mesophilic reactor outperformed the thermophilic one, producing 270 LCH_4 $kg^{-1}COD_{removed}$ and achieving 67% CH_4 content. Similarly, Lovato et al. (2020) observed a 23.3% increase in CH_4 yield in a two-stage AcoD of CW and glycerol compared to a single process at mesophilic temperature.

Furthermore, Srisowmeya et al. (2020) highlighted that while single-stage AD is cost-effective and simple to operate, it struggles with longer hydraulic retention times (HRTs) and lower tolerance for high organic loads. Conversely, two-stage AD offers improved stability, higher CH_4 yields, and better handling of high organic loads, making it suitable for lipid-rich wastes. However, this approach also faces challenges such as potential H_2 build-up which can inhibit bacteria, increased technical complexity, and higher initial costs.

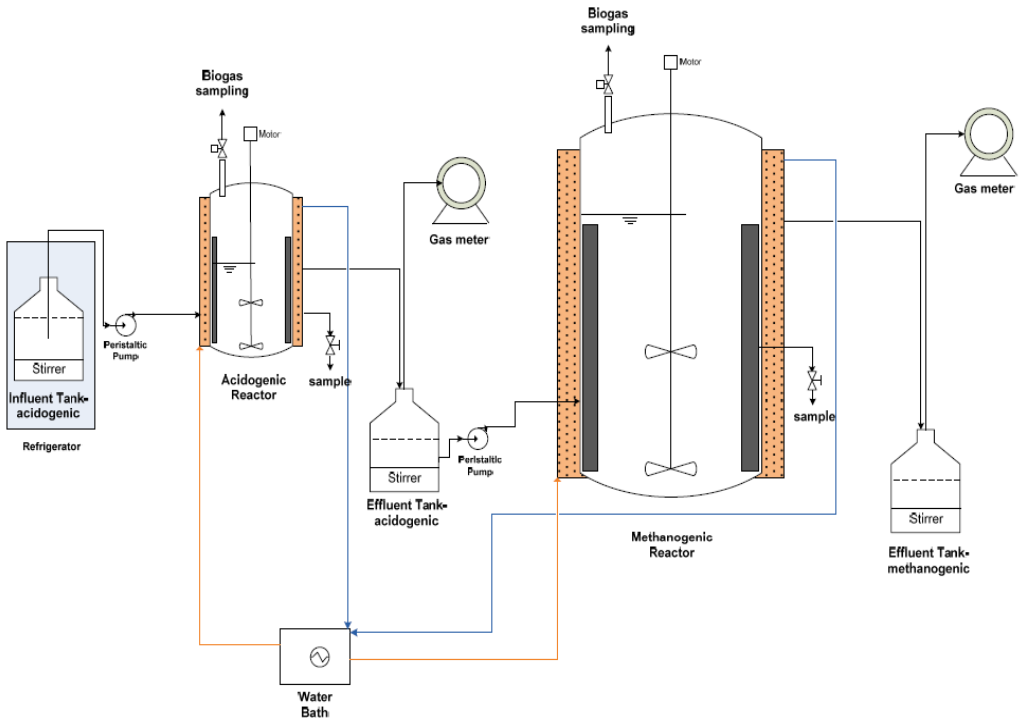

Figure 1-6. Schematic description of the two-stage AD system (Dareoiti et al., 2021)

1.5 Zero-valent iron (ZVI) in AD

Iron, the fourth most abundant element in the Earth's crust, is characterized as an inexpensive, non-toxic metallic material with strong reducibility (E^0 = -440 mV), playing a vital role in both the degradation of organic matter and the removal of contaminants (Ye et al., 2021). ZVI is categorized into various forms, often based on size or surface area. Examples include micro-ZVI (mZVI), nano-ZVI (nZVI), and scrap metal ZVI (Baek et al., 2019). In recent years, ZVI has been added to AD process to enhance the biodegradation of various wastes and wastewaters, including food waste, swine manure, sulfate-rich wastewater, azo dye wastewater, synthetic sucrose wastewater, waste activated sludge etc (Yang et al., 2018; Wang et al., 2019b; Zhou et al., 2020; Kong et al., 2023).

According to the literature (He et al., 2022; Kong et al., 2023), ZVI has been demonstrated to play multifunctional roles in enhancing AD performance. Some of the most important roles of ZVI include the following: (a) optimization of the oxidation-reduction potential (ORP) (Baek et al., 2019), (b) regulation enzyme activities, (c) enhancement of H_2 production, which serves as an electron donor for the metabolism and growth of critical anaerobic microbes involved in AD (Charalambous and Vyrides, 2021); (d) buffering against acid shock caused by rapid acidification and increasing the system's alkalinity (Kong et al., 2023), (e) alteration of the microbial community structure and enhancement of syntrophic-methanogenic associations (He et al., 2022) etc.

1.5.1 Hydrogen production from ZVI and CH_4 production enhancement

Under aquatic anaerobic conditions, ZVI is oxidized to generate H_2, (Eq.1), which can be further used as an electron donor by hydrogenotrophic methanogens and homoacetogens, following the improved biochemical methane potential (BMP) and buffering the pH due to the generation of OH^-(He et al., 2022) (**Fig.1-7**).

$$Fe^0 + 2H_2O \rightarrow Fe^{2+} + H_2 + 2OH^- \qquad (\Delta G^0 = -5.02 \text{ kJ/mol}) \qquad \text{(Eq.1)}$$

However, a recent study by Constantinou et al. (2023) demonstrated that the presence of soluble CO_2 influences H_2 production from ZVI. The study showed that exposing ZVI to aquatic conditions, initially flushed with N_2, led to low H_2

production over time. In contrast, exposure to soluble CO_2 significantly increased H_2 generation, and the medium became alkaline due to the consumption of H^+ (Eq. 2). Under these conditions, as illustrated in Eq. 2, siderite ($FeCO_3$) forms on the outer surface of ZVI over time, which hinders further H_2 release.

$$Fe^0 + HCO_3^- + H^+ \rightarrow FeCO_3 + H_2 \qquad (\Delta G^0 = -79.9\ kJ/mol) \qquad (Eq.2)$$

The Gibbs free energy change ΔG^0 of Eq. 2 in standard conditions (pH 0, all concentrations 1 M and all partial pressures 1 atm) is -79.9 kJ/mol whereas at pH 7 ΔG^0 is -39.9 kJ/mol.

The H_2 generated from the abiotic anaerobic oxidation of ZVI (Eq. 2), along with the available CO_2, can serve as substrates for hydrogenotrophic methanogens (Eq. 3) and homoacetogens (Eq. 4), facilitating the production of CH_4 and acetic acid, respectively (Samanides et al 2020).

$$4H_2 + CO_2 \rightarrow CH_4 + 2H_2O \qquad (\Delta G^0 = -131\ kJ/mol) \qquad (Eq.3)$$

$$4H_2 + 2CO_2 \rightarrow CH_3COO^- + H^+ + 2H_2O \qquad (\Delta G^0 = -95\ kJ/mol) \qquad (Eq.4)$$

Furthermore, acetic acid can be utilized by acetoclastic methanogens for the production of CH_4 and CO_2 (Eq.5).

$$CH_3COO^- + H^+ \rightarrow CH_4 + CO_2 \qquad (\Delta G^0 = -75.7\ kJ/mol) \qquad (Eq.5)$$

In recent years, the use of ZVI for the biological transformation of CO_2 into CH_4 has attracted increasing attention. For instance, Vyrides et al. (2018) investigated the bioconversion of CO_2 to CH_4 utilizing anaerobic granular sludge (AnGrSL) and various concentrations of ZVI. They found that after 18 days, 46 mL of CH_4 was produced with 75 g/L of ZVI, while only 4 mL of CH_4 was created without any ZVI addition. Moreover, the authors stated that CO_2 is mainly converted to CH_4 through hydrogenotrophic methanogenesis. In a different study, Ma et al. (2018) observed a higher CH_4 production rate (61-79 μmol L^{-1} d^{-1}) with ZVI compared to the control (0.6-0.12 μmol L^{-1} d^{-1}) during the CO_2 conversion to CH_4 in petroleum reservoir production waters at 55 °C.

Despite the positive effect of ZVI on the CO_2 conversion to CH_4, $FeCO_3$ formation (Eq. 2) as a passivation layer on the outer surface of ZVI decreases the corrosion rate, thus hindering further oxidation of ZVI. In this regard, several

ligands such as citric, oxalic, ascorbic acids (Constantinou et al., 2023; Wang et al.,2023), ethylenediaminetetraacetic acid (EDTA) (Cai et al., 2019) or even green tea which contains compounds that could form an iron-tannate complex with iron (Menikea et al., 2020) were proposed to improve solubility of ZVI and prevent the $FeCO_3$ formation.

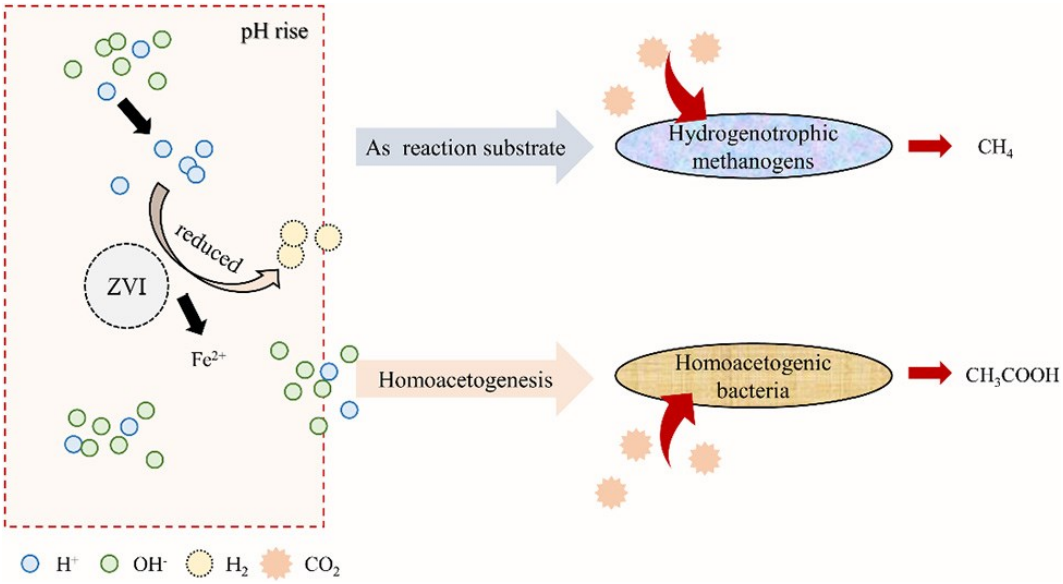

Figure 1-7. The main H_2 consumption pathway induced by ZVI corrosion in AD (He et al., 2022)

1.5.2 Optimization of oxidation-reduction potential (ORP) by ZVI

As a strong reducing agent, ZVI can lower the oxidation-reduction potential (ORP) to below -0.300 mV, thereby creating a more favorable environment for methanogens and other essential anaerobic microbes participating in AD (Baek et al., 2019). The ideal ORP range for acid-producing fermentation is -100 mV to -300 mV (Czatzkowska et al., 2020). Among the three primary fermentation pathways in acidogenesis (butyric type, propionic type, acetic type), propionic-type fermentation predominates at an ORP above -278 mV. In contrast, acetic-type and butyric-type fermentation mainly occur at lower ORP levels. The microorganisms that engage in ethanol and butyric acid fermentation types are strict anaerobes that thrive at low ORP levels, while the species involved in propionic acid-type fermentation are facultative anaerobes and can occur at higher ORP levels (Lizama

et al., 2020). Under anaerobic conditions, converting propionate into acetate and H_2 is thermodynamically unfavorable, as shown in Eq.6

Eq.6

$$CH_3CH_2COO^- + 3H_2O \rightarrow HCO_3^- + CH_3COO^- + H^+ + 3H_2 \quad (\Delta G^0 = +76.1 \text{ kJ/mol})$$

Propionate conversion occurs only through syntrophic oxidation involving interspecies hydrogen transfer (IHT), which is possible only when the H_2 partial pressure is below 10^{-4} atm. Thus, adding ZVI in anaerobic digesters reduces the ORP, shifting fermentation pathways away from propionic acid production and enhancing CH_4 production (Paepatung et al., 2020).

1.5.3 ZVI boosting enzyme activities

Studies have demonstrated that ZVI can enhance the production of soluble organic compounds by enhancing the activities of critical enzymes involved in hydrolysis and acidogenesis. Meng et al. (2013) observed that the addition of ZVI led to increased activities of enzymes such as pyruvate–ferredoxin oxidoreductase (POR), phosphotransacetylase (PTA), and acetate kinase, facilitating a more efficient conversion of propionic acid into acetic acid. This improvement is linked to ZVI's ability to lower the ORP, creating an environment more conducive to enzyme activity. Moreover, Wang et al. (2020) reported that ZVI addition could also enhance the activities of enzymes like coenzyme F_{420} and Methyl-coenzyme M, crucial for methanogenesis. The Fe^{2+} ions generated from ZVI oxidation (Eq. 1) contribute to the formation of Fe-S clusters within enzyme structures, promoting their activity. For instance, Feng et al. (2014) found that adding 20 g/L ZVI to the AD of waste activated sludge increased CH_4 production by 43.5% and enhanced the activities of key hydrolysis-acidification enzymes by 0.6 to 1 time compared to the control.

1.5.4 ZVI buffering pH and mitigating acid inhibition

ZVI significantly impacts pH regulation in AD, serving as an effective acid buffer to mitigate acid inhibition and thus enhancing both the efficiency and stability of the process (Zhang et al., 2020). Through Eq.2, the anaerobic oxidation of ZVI produces H_2, leading to an increase in alkalinity by reducing H^+ ions

(Samanides et al 2020). Consequently, ZVI corrosion helps neutralize acidity by buffering excess VFAs not readily consumed by methanogenic bacteria, maintaining the AD system at a neutral pH condition (pH 6.5-8.0) and avoiding excessive acidification (He et al., 2022).

Several studies, reported that ZVI application positively affects CH_4 yield improvement by rapidly reducing VFAs, particularly from complex substrates such as food waste (FW), that is easier to hydrolyze and acidify due to the presence of abundant biodegradable fractions (Kong et al., 2016; Cao et al., 2019; Shi et al.,2022). For example, Kong et al. (2018) investigated the effect of ZVI to eliminate excessive acidification in AD of the organic fraction of municipal solid waste (OFMSW). Results pointed out a substantial reduction of total VFA (butyric acid decreased from 7200 to 0 mg/L) and an increase of 41.7% in CH_4 production compared to the reactor without ZVI addition. Jing et al. (2022) reported an increase in cumulative CH_4 production by promoting acetic acid (5134.26 mg/L) and significantly reducing propionic acid production with 6 g/L of ZVI on AD of food waste (FW) under different food-to-microorganism (F/M) ratios. Previously, Liu et al. (2012) found that adding 40 g/L ZVI to the AD of artificial wastewater effectively decreased propionic acid production and maintained the neutral pH level (6.5-7.0). Cheng et al. (2020) improved the conversion of propionic acid to acetic acid derived from lactic acid degradation by adding 2 g/L nano-ZVI under batch conditions. Microbial analysis showed an increased abundance of *Candidatus Cloacamonas, Methanomassiliicoccus,* and *Methanosarcina,* which enhanced propionic acid conversion and increased CH_4 yield by 37%.

Kong et al. 2023 assessed the effectiveness of ZVI dosing in reducing excessive acidification and enhancing biogas quality in mesophilic anaerobic digestion (MAD) and thermophilic anaerobic digestion (TAD) reactors under various organic loading rates (OLRs). The findings indicated that, compared to the control reactors that did not receive ZVI and experienced either excessive acidification or low CH_4 content below 70%, the reactors with Fe^0 dosing at an OLR of 35 gVS/L showed significantly improved performance. Specifically, CH_4 yields in the MAD and TAD reactors were 470.88 $mLCH_4$/gVS and 270.40 $mLCH_4$/gVS, respectively. Additionally, these reactors achieved higher CH_4 concentrations,

ranging from 81.32% to 82.23% in MAD reactors and from 83.68% to 88.48% in TAD reactors.

1.5.5 ZVI enhancing syntrophic-methanogenic associations

ZVI is crucial in altering the microbial community structure and enhancing syntrophic-methanogenic associations. For example, Shi et al. (2022) found that ZVI composite carriers in an integrated floating-film and activated sludge (IFFAS) system treating dairy wastewater shifted the fermentation pathway away from the propionic type due to the enhanced syntrophic partnership between the hydrolysis acidification bacteria of *Comamonas* and *Petrimonas* and the acetotrophic methanogens of *Methanosarcina* and *Methanothrix*. Kong et al. (2018) reported that by adding ZVI, excessive acidification in the organic fraction of municipal solid waste (OFMSW) was eliminated due to the improved syntrophic associations between the microbial genera *Syntrophomonas, Clostridium butyricum* and *Methanosarcinales.*

Due to efficient electron transfer, the syntrophic association between methanogens and bacteria crucially enhances CH_4 production during methanogenesis. Interspecies hydrogen transfer (IHT) and direct electron transfer (DIET) are two main mechanisms promoting this process (**Fig. 1-8**) (Zhao et al., 2020; He et al., 2022). During IHT, H_2 serves as an electron mediator between bacteria and methanogens. On the other hand, in DIET, extracellular electrons from electron-donating microbes can be transferred to electron-receiving microbes via conducting pathways. This transfer occurs through one of three mechanisms: (1) electrically conductive pili, (2) cytochromes, or (3) conductive materials (Fig. 1-8).

Several studies in the literature have demonstrated that ZVI lowers H_2 partial pressure by enhancing IHT, facilitating the conversion of propionate and butyrate into acetic acid and thereby boosting CH_4 yield (Zhou et al., 2020; Zheng et al., 2022). Furthermore, studies have shown that hydrogenotrophic methanogens are more enriched in ZVI reactors (Kong et al., 2016; Kong et al., 2018). Vyrides et al. (2018) observed that CO_2 is primarily converted to CH_4 through the hydrogenotrophic pathway in the presence of ZVI.

In contrast, Jia et al. (2017) and Zhu et al. (2020) reported that the particle size and dosage of ZVI not only facilitate electron transfer but also have the potential to promote DIET by stimulating electroactive exoenzymes in extracellular polymeric substances (EPSs) at higher concentrations. However, these studies did not detect any *Geobacter* species; only two related species, *G. metallireducens*, and G. *sulfurreducens,* were confirmed to possess the capability for DIET (Summers et al., 2010). The DIET has been definitely showed only in co-cultures of *Geobacter metallireducens* with *Methanosaeta harundinacea* or *Methanosarcina barkeri* (Rotaru et al., 2014a; Rotaru et al., 2014b). Hence, the mechanisms through which ZVI enhances DIET warrant additional investigation. According to the review study by Wang and Lee (2021), no direct evidence exists that DIET mechanisms enhance AD. Solid proof would require observing the electron flow from syntrophic bacteria to methanogens, coupled with an increased CH_4 production. In addition, most studies on DIET have been conducted using pure cultures. However, in anaerobic digestion, which involves mixed microbial communities, the system is more complex. Therefore, before assuming DIET in the presence of ZVI, other parameters need to be considered, such as hydrogen utilization by bacteria and methanogens.

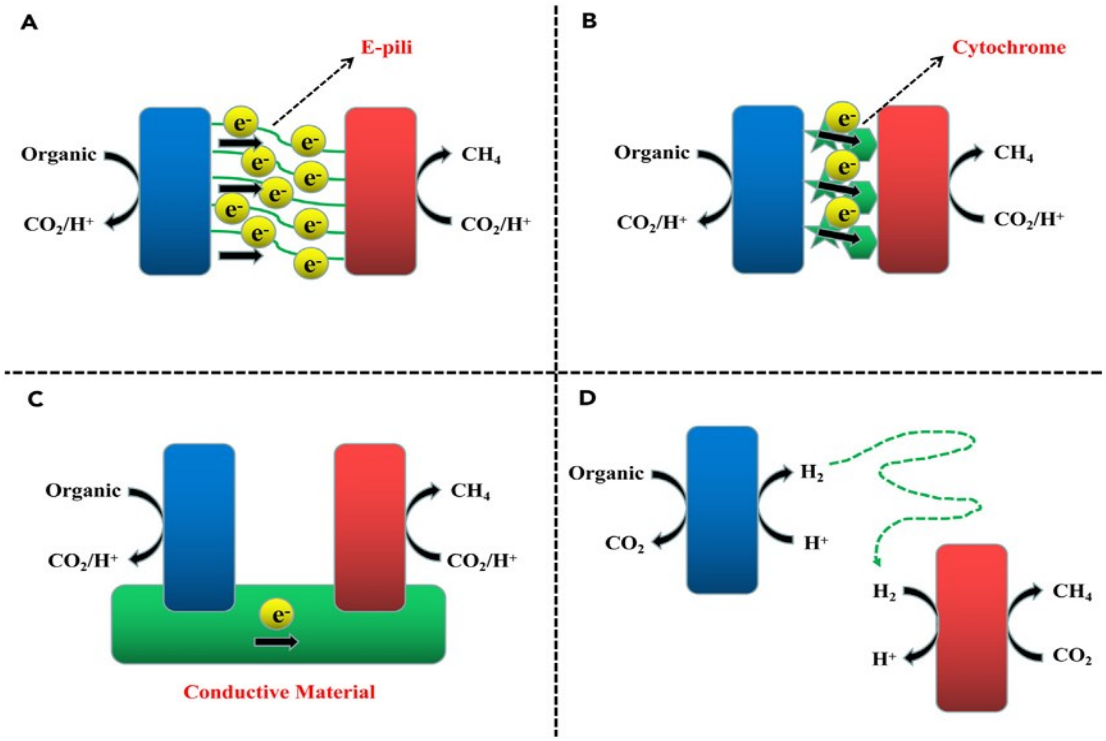

Figure 1- 8. Diagram of Interspecies Electron Transfer (IET) between Electron-donating bacteria (blue) and Electron-accepting methanogens (red): DIET cell-to-cell electron transfer through (A) electrically conductive pili (e-pili); (B) cytochromes associated with outer cell surfaces; (C) conductive material and (D) IHT cell-to-cell electron transfer via diffusive electron carriers, such as H_2 (Zhao et al., 2020)

1.6 Aim and objectives of the study

As mentioned in the previous section (see section 1.4.1), cheese whey is the main by-product of the dairy industry, characterized by high organic matter (50-102 g/L COD and 30–40 g/L BOD_5) and high biodegradability (~ 99%), which makes it suitable for energy recovery through anaerobic digestion (AD). However, its rapid acidification and low alkalinity (<0.22 $gCaCO_3$/L) often lead to VFAs accumulation, which can lower the pH below the optimal range required for methanogenesis (pH 6.8-7.2), causing system instability. To overcome this issue and to ensure efficient performance, various methods and technologies, such as alkaline chemicals (CaO, NaOH, $NaHCO_3$) addition, CW dilution, anaerobic-co-digestion with alkaline-rich substates (dairy manure, poultry waste), and different reactor configurations (two-stage AD, effluent recirculation), have been proposed.

Alternative to the aforementioned methods, this study aims to investigate two new approaches to mitigate acid inhibition from VFAs and enhance the AD performance of CW. The first approach involves using an acclimatized acid-tolerant methanogenic culture to treat CW at pH 5-6. To achieve this, anaerobic granular sludge from a full-scale IC bioreactor treating dairy wastewater was enriched with an acetic acid solution (1.07 g COD/L) for 7 months by gradually decreasing the pH until it reached a pH range of 5-6. After acclimatization, comparative experiments involving both acclimatized and non-acclimatized cultures were conducted under batch conditions with CW at pH 5-6.

The second approach investigates the effect of zero-valent iron (ZVI) in enhancing anaerobic digestion and biogas production from CW. As mentioned in the previous section (see section 1.5), due to its multifaceted roles in AD, many researchers have highlighted that ZVI positively affects CH_4 production from various organic substances (e.g., waste-activated sludge, domestic wastewater, azo-dye, swine manure) and mitigates acid inhibition, particularly from substrates that can easily be acidified, such as food waste. However, to the author's best knowledge, no publication in the literature has examined the effects of ZVI addition on the treatment of real cheese whey. This study is the first of its kind and represents an initial attempt in the area and both the performance of the system and the

mechanisms is studied. Thus, the main objectives of the current study are as follows:

- Exploration of the impacts of adding two district forms of ZVI on the AD of CW under batch conditions. Millimeter-sized ZVI powder and scrap metal shavings were each tested at three different concentrations over four consecutive feeding cycles of CW for 201 d. Following identifying the most effective ZVI type and concentration, the economic viability of integrating ZVI into conventional anaerobic digestion processes for CW was assessed through a desktop scaling-up study using data from a large dairy factory in Cyprus.
- Evaluation of the performance of ZVI addition in AD of CW under semi-continuous and batch operation modes. Herein, building on the previous results, 25 g/L PZVI and 50 g/L SZVI were examined through semi-continuous feeding with CW under different OLRs for 118. The performance between semi-continuous and batch operation modes was evaluated regarding methane production and content, VFA concentration, pH, and SCOD efficiency removal. Secondly, the microbial profile was determined to analyze the differences and similarities in bacterial and archaeal community structures from each reactor. Moreover, the influence of ZVI on the hydrolysis-acidification stages of CW digestion was examined to gain additional insight into the mechanisms of ZVI.
- Determination of the performance of H_2 supply via in-situ ZVI corrosion (in-situ) versus exogenous H_2 supply through abiotic oxidation of ZVI (ex-situ) in AD of CW. Finally, the solid residue (digestate) from each reactor set-up (in-situ and ex-situ) was assessed as a potential soil conditioner through phytotoxicity trials on the growth of *Sinapis alba* seeds.

2 Research Methodology

2.1 Chapter 1: Anaerobic digestion of CW using acclimatized granular sludge at pH 5-6

This chapter explores the anaerobic cheese whey (CW) treatment utilizing an acclimatized methanogenic culture at moderately low pH levels (5-6). Initially, anaerobic granular sludge (AnGrSL) from a full-scale Internal Circulation (IC) bioreactor was gradually acclimatized to a final pH range of 5-6 using acetic acid solution (1.07 g COD/L) over 7 months. After the acclimatization period, batch experiments were conducted to evaluate the anaerobic treatment of CW using both acclimatized and non-acclimatized granular sludge across two consecutive batch cycles lasting 21 and 36 days, respectively.

During the 2nd batch cycle, the microbial profile community was analyzed, and the potential microbial pathways involved in CW biodegradation under these conditions were proposed. Furthermore, an economic analysis was conducted based on the laboratory results obtained from the current experiments and the collected data after a 91-day operational monitoring period of a full-scale IC bioreactor.

2.1.1 Origin and characterization of substrate and inoculum

Cheese whey (CW) was sourced from a local dairy factory (Charalambides Christis Ltd, Limassol, Cyprus) following the precipitation and removal of milk casein during the cheese manufacturing process (**Fig. 2-1**). The CW was collected and stored in a 1-liter plastic container at temperatures below 4 °C to prevent physicochemical alterations prior to experimental use. The average characteristics of the CW utilized in these experiments were determined as follows: pH 6.45 ± 0.2, fat content 0.09% ± 0.01, protein content 0.88% ± 0.01, lactose concentration 42.6 g/L ± 0.15, citric acid concentration 1.51 g/L ± 0.02, total solids 5.58% ± 0.01, and total chemical oxygen demand (COD) 61.87 g/L ± 3.01.

Anaerobic Granular Sludge (AnGrSL), was obtained from a full-scale Internal Circulation (IC) bioreactor located at the same dairy facility. The IC bioreactor treating dairy wastewater (e.g effluents from sanitation, cleaning, and

washing of processing equipment's) excluding CW, under mesophilic conditions (35 °C) at a pH of 7.0-7.5. The total solids (TS) and volatile solids (VS) content of the AnGrSL were measured at 5.7% (on a wet basis) and 85.4% (on a dry basis), respectively. Initially, the AnGrSL was sieved through a 1 mm mesh, washed with distilled water, and then degassed at 35 °C for three days to minimize background methane production before its use as inoculum in the experiments.

Figure 2-1. Anaerobic granular sludge (left) and cheese whey (right)

2.1.2 Low pH adaptation approach: Experimental set-up

Batch experiments were conducted in triplicate using 125 mL glass serum bottles with a working volume of 65 mL over a period of 7 months under mesophilic conditions (35°C). Each serum bottle was initially inoculated with 25 g of Anaerobic Granular Sludge (AnGrSL), and the remaining volume was filled with an acetic acid solution. The bottles were purged with N_2 gas for 2 min to establish anaerobic conditions. The acetic acid solution was prepared by diluting 97% (by weight) glacial acetic acid with distilled water, achieving an initial concentration of 1 g/L (1.07 gCOD/L).

The following nutrients (mg L^{-1}): NH_4Cl (400), $MgSO_4 \cdot 6H_2O$ (250), KCl (400), $CaCl_2 \cdot 2H_2O$ (120), $(NH_4)_2HPO_4$ (80), $FeCl_3 \cdot 6H_2O$ (55) and the trace element salts (i.e. $CoCl_2 \cdot 6H_2O$, $NiCl_2 \cdot 6H_2O$, $MnCl_2 \cdot 4H_2O$, $CuCl_2 \cdot 2H_2O$, $AlCl_3 \cdot 6H_2O$,

$ZnCl_2$, $Na_2WO_4 \cdot 2H_2O$, H_3BO_3, Na_2SeO_3 and $Ma_2MoO_4 \cdot 2H_2O$) (each at 0.5) were added to the acetic acid solution as described by Li et al. (2018).

During the acclimatization phase, 20 mL of the bottle's liquid contents were periodically removed and replaced with the same volume of fresh acetic acid solution to facilitate adaptation. To maintain the desired pH, the pH of the serum bottles was measured daily. Adjustments to the digestate pH were made using either HCl or NaOH (0.1 M) to achieve the target pH values outlined in Table 2-1. To prevent sudden pH shocks, the initial pH of the serum bottles was set at 7.5 and subsequently lowered in a stepwise manner by increasing the acetic acid solution feeding rate during each acclimation period, according to the target pH levels.

Table 2-1. Daily target pH during each period

Acclimation Period (d)	Target pH	OLR (gCOD/Ld)	Num. of acetic acid solution feedings
0-21	7.5-7.2	0.047	3
22-45	7.2-6.8	0.057	4
46-72	6.8-6.5	0.063	5
73-94	6.5-6.2	0.094	6
95-123	6.2-5.5	0.082	7
124-153	5.0-6.0	0.091	8
154-182	5.0-6.0	0.106	9
183-210	5.0-6.0	0.122	10

2.1.3 Batch experiments for CW degradation using acclimatized sludge

Following a 7-month acclimation period, batch experiments were conducted in 125 mL glass serum bottles with a working volume of 65 mL. The primary objective was to compare the anaerobic treatment of CW using acclimatized granular sludge and non-acclimatized sludge pH 5-6. Specifically, 9 g of acclimatized granular sludge (AnGrSL-PE) was mixed with 2 g of fresh anaerobic

granular sludge from the IC bioreactor, and 5 mL of CW were introduced into each serum bottle for 2 consecutive batch cycles lasting 21 and 36 days, respectively. As a control, 11 g of fresh anaerobic granular sludge (F-AnGrSL) from the IC bioreactor, not previously exposed to low pH, was fed with 5 mL of CW under the same conditions. The serum bottles were filled with nutrient medium according to the description provided by Angelidaki et al. (2009), reaching the working volume of 65 mL (**Table 2-2**). Anaerobic conditions were established by purging the bottles with oxygen-free gas (100% N_2) for 2 min and then placing them in a shaking incubator at a constant temperature (33 °C) and shaker speed (100 rpm). To maintain a consistent pH for each serum bottle, pH adjustments were made after every gas and liquid sampling using 2M HCl or 2M NaOH. All experimental conditions were conducted in triplicate.

Table 2-2. Description of anaerobic basic medium (Angelidaki et al., 2009)

Stock solution A (g/L): NH_4Cl, 100; NaCl, 10; $MgCl_2$ $6H_2O$, 10; $CaCl_2$ $2H_2O$, 5
Stock solution B (g/L): K_2HPO_4 $3H_2O$, 200
Stock solution C (g/L): resazurin 0.5
Stock solution D (g/L): Trace-metal and selenite solution: $FeCl_2$ $4H_2O$, 2; H_3BO_3, 0.05; $ZnCl_2$, 0.05; $CuCl_2$ $2H_2O$, 0.038; $MnCl_2$ $4H_2O$, 0.05; $(NH_4)6Mo_7O_{24}$ $4H_2O$, 0.05; $AlCl_3$, 0.05; $CoCl_2$ $6H_2O$, 0.05; $NiCl_2$ $6H_2O$, 0.092; ethylenediaminetetraacetate, 0.5; concentrated HCl, 1ml; $Na_2SeO_3 5H_2O$, 0.1
Stock solution E: Biotin, 2; folic acid, 2; pyridoxine acid, 10; riboflavin, 5; thiamine hydrochloride, 5; cyanocobalamin, 0.1; nicotinic acid, 5; P-aminobenzoic acid, 5; lipoic acid, 5; DL-pantothenic acid.
To 975 ml of distilled water, the following stock solutions should be added **(A)** 10 ml; **(B)** 2ml; **(C)** 1ml; **(D)** 1ml and **(E)** 1ml. The mixture is gassed with 80% N_2 - 20% CO_2 mixture to maintain a neutral pH. Cysteine hydrochloride, 0.5 g and $NaHCO_3$, 2.6 g dissolved in 10 ml distilled water are added and the medium is dispensed to serum vials and autoclaved if necessary. Before inoculation the vials are reduced with Na_2S $9H_2O$ to a final concentration of 0.025%.

2.1.4 Microbial profile characterization

During the 2nd batch cycle, samples were extracted on the 12th day for microbial profile analysis. These samples included: (a) anaerobic granular sludge previously exposed to moderately low pH (AnGrSL-PE), (b) fresh anaerobic granular sludge suddenly exposed to moderately low pH (F-AnGrSL), and (c) anaerobic granular sludge obtained from the IC reactor (AnGrSL-IC) with a pH range of 7-7.5. DNA extraction was conducted using GenElute™ Soil DNA Isolation Kits from Sigma Aldrich, USA, following the manufacturer's instructions.

Sequencing of bacterial 16S rRNA genes and archaeal 16S rRNA genes was performed using the Ion PGM™ System from Life Technologies, in accordance with the manufacturer's protocols. For each DNA sample, the primers BAC518F (5′-CCAGC AGCCG CGGTA ATACG-3′) and BAC805R (5′-GACTA CCAGG GTATC TAATC C-3′) were used to amplify the V4 hypervariable region of the bacterial 16S rRNA genes, and the primers ARC787F (5′-ATTAG ATACC CSBGT AGTCC-3′) and ARC1059R (5′-GCCAT GCACC WCCTC T-3′) were used to amplify the V5-6 hypervariable regions of the archaeal 16S rRNA gene (Yu et al., 2005). The amplicons were labelled with barcodes using the Ion Plus fragment library kit (Life Technologies). For clonal amplification of the library, emulsion PCR was conducted using an Ion PGM™ Hi-Q™ template kit (Life Technologies) and a OneTouch™ 2 instrument (Life Technologies). The template-positive ion sphere particles, enriched by Ion OneTouch™ ES (Life Technologies), were loaded onto a 318™-chip using an Ion PGM™ Hi-Q™ sequencing kit and then sequenced on an Ion PGM™ sequencer (Life Technologies) operated by Torrent Suite™ software (version 5.0). Valid sequences obtained, as verified by Ion Reporter™ software, underwent clustering using UPARSE (usearch version v7.0.1090); reads with ≥ 97% sequence similarity were designated as operational taxonomic units (OTUs). Taxonomic classification of OTUs was performed using the SILVA database version 132.

2.1.5 Economic evaluation of CW treatment under moderately low and neutral pH conditions

An economic analysis was conducted based on the laboratory results of the current experiments. The analysis focused on the potential profits from producing electricity using biogas. It also considered the costs associated with transporting CW and regulating its pH through NaOH consumption in two scenarios.

The first scenario involves treating CW at pH 5-6, and the second involves treating CW at a pH 7.0, both within a full-scale IC bioreactor. To facilitate this assessment, data regarding the operation of a full-scale IC bioreactor at a dairy factory (Charalambides Christis, Limassol, Cyprus) were collected following a 91-day monitoring period in the year 2018 (**Table 2-3**).

The IC bioreactor has an adequate volume of 140 m^3 with a design organic loading rate (OLR) of 2800 kg COD/d and hydraulic retention time (HRT) of 4.6 h. Developed as a high-rate anaerobic treatment system, the IC bioreactor relies on biomass growth in the form of well-settling sludge granules and consists of two compartments stacked on top of each other. The lower compartment, housing the expanded sludge bed, operates under high load, where most biodegradable COD is converted, while the upper compartment is a polishing step (**Fig. 2-2**).

Table 2-3. Operational data collected from a full-scale DWWTP and IC bioreactor following 91-day monitoring period in the year 2018

Parameter	**Value**
Design volume of IC bioreactor	140 m^3
Design organic loading rate (OLR)	2800 kg COD/d
Volume of wastewater treated in IC bioreactor	550 m^3/d
Hydraulic retention time (HRT)	4.6 h
pH in the IC bioreactor	7.0-7.5
NaOH consumption of DWWTP	0.17 kg/m^3 wastewater
Electricity consumption of DWWTP	585 kWh/d
Average influent COD to IC	1820 mg/L
Average effluent COD from IC	309 mg/L
Average COD removal efficiency	79.3 %
Average alkalinity	16 mmol/L
Average biogas production	128.9 m^3/d

The dairy wastewater (550 m^3/d), originating from various processing sections (such as washing and pasteurization waters, detergents, and residual milk from machinery piping), undergoes treatment in IC bioreactor. This treatment occurs at a mesophilic temperature of 35 °C and maintains pH levels between 7.0 and 7.5. The total NaOH consumption required to maintain the desired pH range in the DWWTP is 0.17 kg of NaOH per m^3 of wastewater (**Table 2-3**). It is noteworthy that a substantial volume of cheese whey (81.2 m^3/d) is excluded from processing in the IC bioreactor and is instead directed to another facility for additional treatment with an overall cost of 255 €/d. Currently, the produced biogas (128.9 m^3/d) is directed for combustion in a burner. However, the company is actively exploring the feasibility of installing a combined heat and power (CHP) system to convert the biogas into electricity and heat. Therefore, taking into consideration the

data from the 91 days of monitoring of the full-scale IC bioreactor, the theoretical thermal and electrical energy generation from biogas was calculated according to the following formula:

$$E_{(\text{Thermal or Electrical})} = BG \times EF \times 22\ (MJ/m^3)/3.6\ (MJ/kWh)$$

The following assumptions were made: methane content in biogas is 60%, efficiency of CHP generator is 50% (thermal) and 3 % (electrical), and biogas calorific value is 22 MJ/m^3. Where E (Thermal or Electrical) is the thermal or electrical energy production (kWh), BG is the biogas produced per day (m^3), EF is the thermal or electrical efficiency of the generator (%).

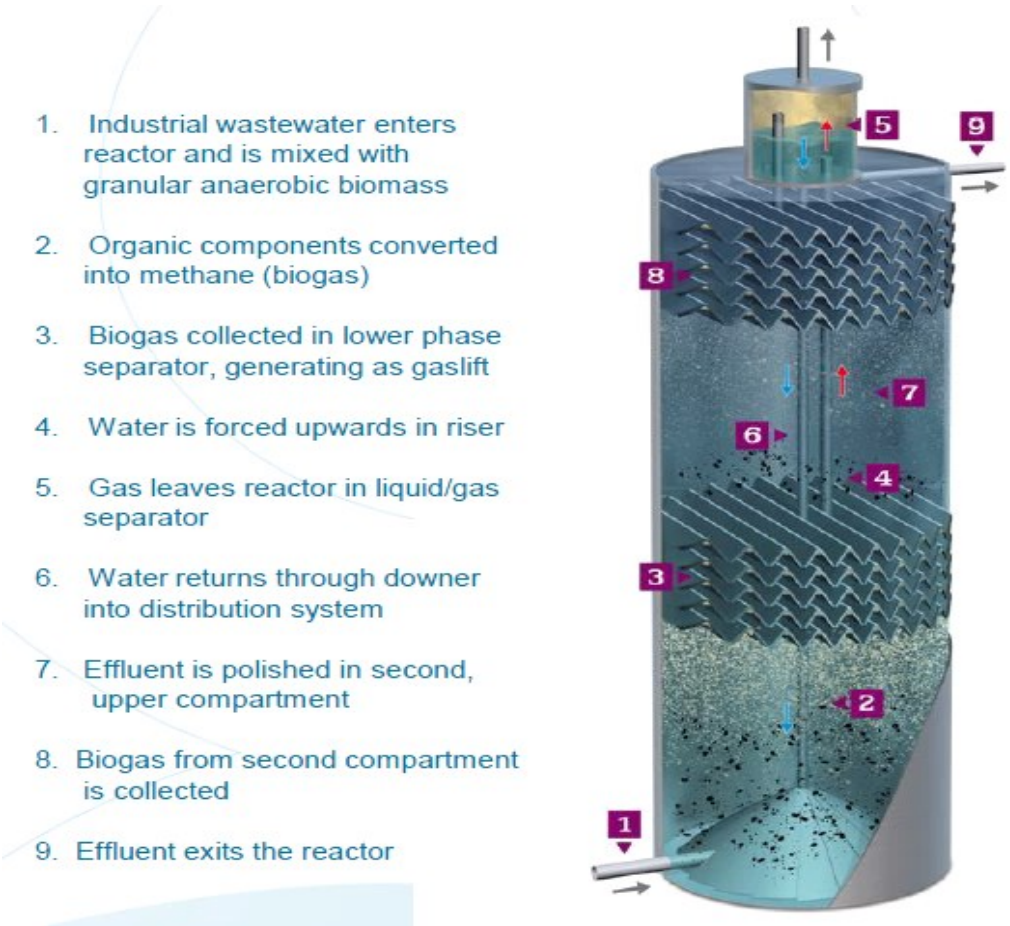

Figure 2-1. On-site full-scale IC bioreactor located at a dairy factory in Cyprus

2.2 Chapter 2: Anaerobic digestion of cheese whey using ZVI addition

In this chapter the effect of zero-valent iron (ZVI) on the AD of CW under batch conditions was investigated. Three concentrations (25 g/L, 50 g/L, and 100 g/L) of both powder zero-valent iron (PZVI) and scrap zero-valent iron (SZVI) shavings were explored using four consecutive volumes of CW feed (18 mL, 30 mL, 50 mL, and 75 mL) for 201 days. Based on the laboratory data an economic analysis was conducted regarding the prospects of this approach in a large industrial cheese factory.

2.2.1 Preparation of inoculum, substrate and additives

The inoculum used in the current experiments consisted of AnGrSL extracted from a full-scale IC bioreactor (Charalambides Christis Ltd, Limassol, Cyprus) that treated dairy wastewater within a pH range of 7.0-7.5. The AnGrSL exhibited total solids (TS) and volatile solids (VS) content of 5.7% (on a wet basis) and 85.4% (on a dry basis), respectively. Prior to utilization, the AnGrSL underwent a series of preparatory steps. Initially, it was subjected to sieving with a 1 mm mesh, followed by thorough washing with distilled water. Subsequently, the AnGrSL was degassed at 35°C for a duration of 2 days to mitigate background methane production. CW was sourced from the same dairy factory after the cheese-making process and exhibited the same physicochemical characteristics as those previously described in section 2.1.1.

Two different sources of zero-valent iron (ZVI) were used in the current experiments: (a) commercial powder ZVI with a particle size of 10 μm and a purity of ≥ 99% (specific surface area ≈1 m^2/g) purchased from Merck KGaA, Germany and (b) scrap zero-valent iron (SZVI) shavings. SZVI shavings were obtained from university machinery (lathe machines), measuring approximately 2.0-4.0 mm in width, 0.2-0.5 mm in thickness, and 20-50 mm in length (Fig. 2-3) (Menikea et al., 2020). The two zero-valent iron (ZVI) types were used without pretreatment.

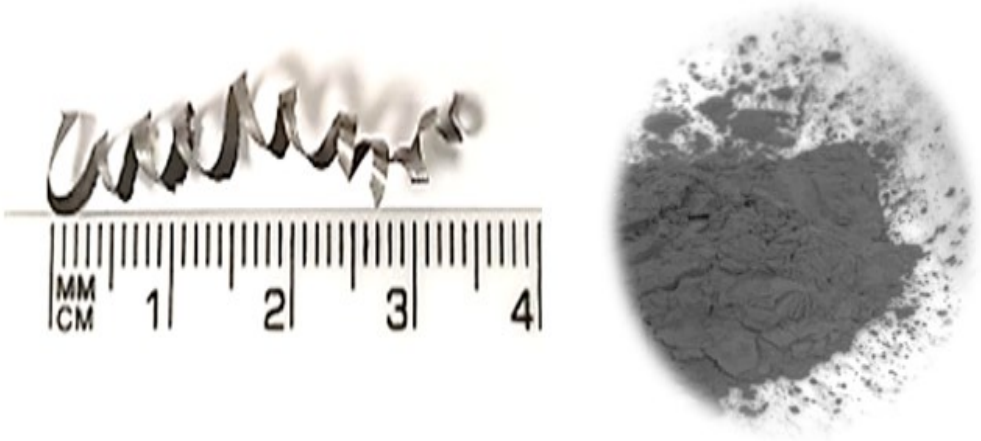

Figure 2-2. Scrap ZVI shavings (left) and commercial ZVI powder 10 μm (right)

2.2.2 Batch experiments

Batch experiments were conducted in 250 mL glass serum bottles with an effective working volume of 100 mL. In each serum bottle, 15 g of AnGrSL and CW at varying concentrations were introduced over 4 consecutive batch cycles. SZVI and PZVI concentrations were added to each serum bottle to investigate the impact of zero-valent iron (ZVI) on the AD of CW. The experimental conditions are given in Table 2-4. The remaining volume was filled with basal media following the protocol described by Angelidaki et al. (2009). The pH was adjusted between 6.8 and 7.3 using 2M HCl or 2M NaOH solutions. Throughout the experimental period, pH was monitored and readjusted to the desired range (6.8 to 7.3) after each liquid and gas sampling, occurring approximately every 2-3 days. Moreover, during the 2nd batch cycle (30 mL CW), a control reactor (AnGrSL and CW only) was set up in parallel without pH regulation (**Table 2-4**). The headspace in each serum bottle was purged with 100% purity N_2 gas for 2 min to eliminate oxygen before sealing with a butyl rubber septum and an aluminum crimp cap to prevent gas leaks. The serum bottles were then incubated in a thermostatic shaker at 33 ± 1 °C and 100 rpm. All the serum bottles were run in duplicate, and the average value is reported; if the absolute difference between the average and each measurement exceeded 25%, the experiment was deemed invalid. Positive control bottles were

prepared for each experimental condition, containing only AnGrSL and CW without any ZVI form.

Table 2-4. Summary of the experimental conditions at anaerobic batch reactors

Batch	Cheese whey	Digestion time	* ZVI type/concentration
1st cycle	18 mL (tCOD: 11.16 g/L)	0-13 d	PZVI/ 25,50,100 g/L SZVI/ 25,50,100 g/L Control (pH reg.)
2nd cycle	30 mL (tCOD: 18.6 g/L)	14-34 d	PZVI/ 25,50,100 g/L SZVI/ 25,50,100 g/L Control (pH reg.)
3rd cycle	50 mL (tCOD: 31 g/L)	35-113 d	PZVI/ 25,50,100 g/L SZVI/ 25,50,100 g/L Control (pH reg.)
4th cycle	75 mL (tCOD: 46.5 g/L)	114-201 d	PZVI/ 25,50 g/L SZVI/ 25,50 g/L Control (pH reg.)

*The concentration of both types of ZVI was added only at the beginning of the 1st batch cycle, and no additional dosage was added until the end of the experimental period.

2.2.3 Abiotic hydrogen production using 25 g/L PZVI and 50 g/L SZVI

Based on the results of the first two batch cycles (total 34 days) (see section 4.3), abiotic tests were carried out to determine the H_2 production using 25 g/L PZVI and 50 g/L SZVI. The assessment of H_2 production involved the use of 25 g/L PZVI and 50 g/L SZVI in 165 mL serum bottles with a working volume of 110 mL. These experiments were performed without AnGrSL, and the CW was initially autoclaved. 16 mL of CW was added to each serum bottle, and then tap water was added to reach the working volume of 110 mL. The serum bottles were capped, sealed with butyl septa and aluminum crimps, and flushed with CO_2 gas for 1-2

minutes to establish anaerobic conditions. Each abiotic test was conducted in triplicate and stirred in an incubator at 100 rpm and 33°C.

2.3 Chapter 3: Anaerobic digestion of CW using ZVI: A comparative analysis of semi-continuous and batch operation modes

In this chapter, semi-continuous and batch reactors were operated to investigate the effect of two distinct types and concentrations of ZVI (25 g/L PZVI and 50 g/L SZVI) on the AD of CW. Furthermore, the influence of ZVI on the solubilization/hydrolysis and acidification phases was examined. At the end of the experimental period, samples were extracted from both semi-continuous and batch reactors for the purpose of characterising the microbial profile.

2.3.1 Selection of ZVI type and feed stream characterization

Based on the results from the previous chapter (see Chapter 4), two distinct types and concentrations of ZVI were selected for the current experiments: 25 g/L PZVI and 50 g/L SZVI. These concentrations had previously shown successful biogas upgrading (CH_4 > 95%) during the batch anaerobic treatment of CW (see section 4.3). Commercial iron powder (10 μm size, 99.9% purity, purchased from Merck KGaA, Germany) and iron shaving scraps (2.0-4.0 mm in width, 0.2-0.5 mm in thickness, and 20-50 mm in length) from lathe machines were utilized as the sources for powder ZVI (PZVI) and scrap ZVI (SZVI), respectively. The CW and AnGrSL were obtained from a local dairy factory (Charalambides Christis Ltd., Limassol, Cyprus), as described in section 2.2.1. The total solids (TS) and volatile solids (VS) of AnGrSL were 9.5% on a wet basis and 85.4% on a dry basis, respectively. The average characteristics of CW in the current experiments are presented in **Table 2-5.**

Table 2-5. Characteristics of CW used in the current experiments

Parameter	Value
pH	6.45 ± 0.2
Electrical Conductivity (μS/cm)	6395 ± 45
Total COD (mg/L)	62765 ± 53
Soluble COD (mg/L)	45164 ± 192
Total suspended solids (mg/L)	2795 ± 55
Total nitrogen (mg/L)	1177 ± 64
Total phosphorus (mg/L)	384 ± 25
Chlorides (mg/L)	1417 ± 22

2.3.2 Semi-continuous operation mode

Semi-continuous experiments were carried out in three 1 L glass reactors (working volume 0.7 L) equipped with three ports, which allowed the biogas collection, the feeding of substrate and the withdrawal of effluent (**Fig. 2-4**). At the beginning of the experiment, 150 g of anaerobic granular sludge and 100 mL of CW (63 g/L COD and pH 6.45) were introduced to each reactor and filled with tap water, reaching the working volume of 0.7 L. 25 g/L of powder ZVI was added to the first reactor (referred to as R25-PZVI), and 50 g/L of scrap ZVI was added to the second reactor (referred to as R50-SZVI). A Control reactor (referred to as R-Control) with no ZVI added was set up in parallel and operated under the same conditions. The addition of 25 g/L powder ZVI and 50 g/L scrap ZVI occurred only once during the start-up phase of operation. Subsequent to the ZVI addition, the reactors were purged with 100% N_2 for 3 minutes to establish anoxic conditions and were placed in a thermostatic water bath at 35 ± 0.2 °C and 80 rpm. Over the 118 days of operation, liquid effluent was withdrawn from the outlet tube of each reactor, while an equivalent volume of CW was fed in semi-continuous mode through the inlet tube using peristaltic pumps (Fisher Scientific CTP100). Four operational phases were implemented with varying average organic loading rates (OLR) (1.6-2.6 gCOD/L.d) during each phase, as outlined in **Table 2-6**. Upon achieving stabilized methane composition and consistent COD removal, the OLR

was incrementally increased. One of the objectives of this experiment was to assess the system's performance under high OLR. The generated biogas from each reactor was collected in 5 L gas sampling bags, and the volume was manually measured using a 100 mL gas-tight glass syringe. Regarding gas composition, 1 mL of gas sample was withdrawn through the septa at the exit of each gas bag and analyzed using a Gas Chromatograph.

Table 2-6. Operational pattern of semi-continuous reactors

Operation phase	**I**	**II**	**III**	**IV**
Period (d)	0-27	27-79	79-104	104-118
OLR (g COD $L^{-1}d^{-1}$)	1.6	1.7	2	2.6
HRT (d)	41	37	31	25
Volume of CW fed (L/d)	0.5	0.1	0.15	0.2

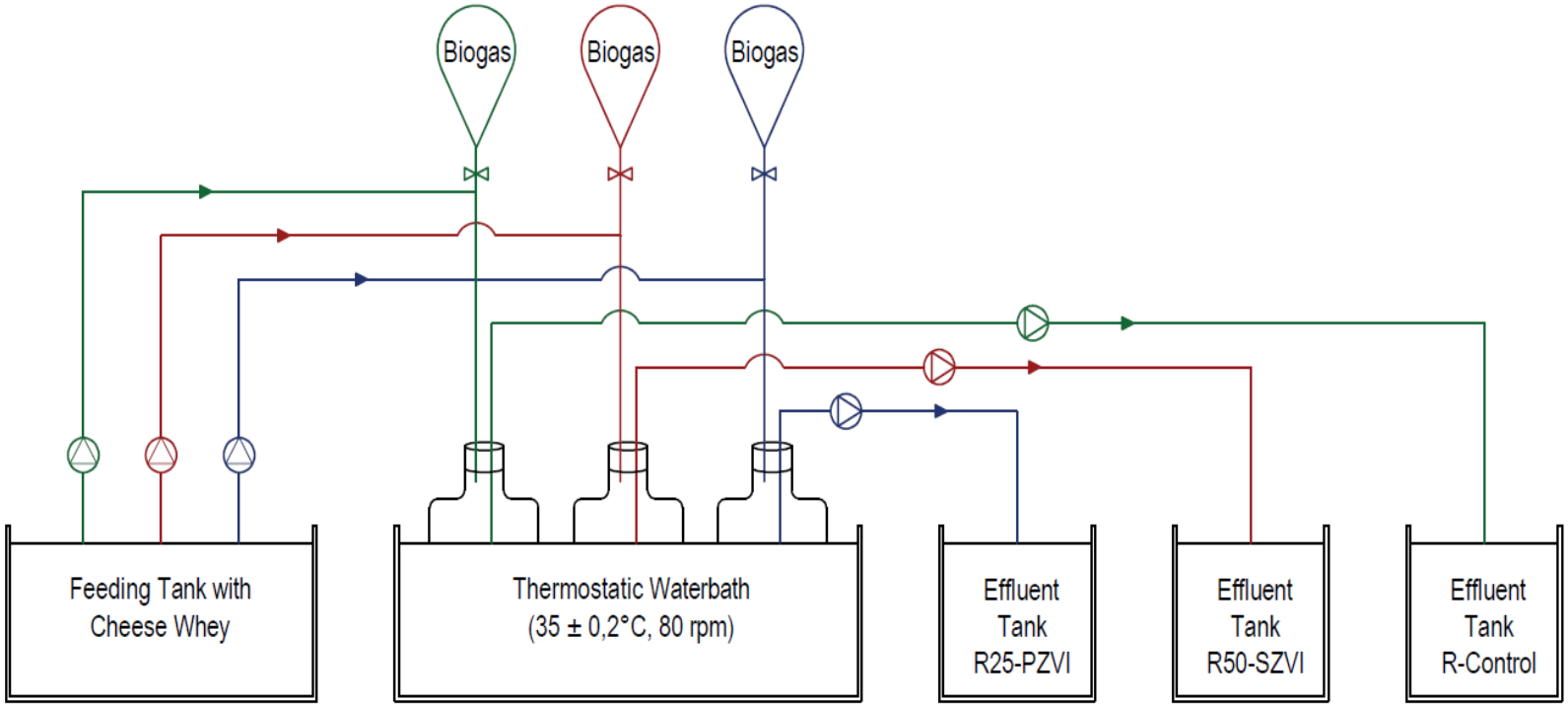

Figure 2-3. Schematic diagram of the laboratory semi-continuous reactors

2.3.3 Batch operation mode

Batch experiments were conducted in 250 mL serum bottles, each with a working volume of 100 mL. The aim was to investigate the effect of zero-valent iron (ZVI) on the anaerobic digestion (AD) of cheese whey (CW) in batch mode. Two different types of ZVI (25 g/L PZVI and 50 g/L SZVI, respectively) were added to each reactor, along with 15 g of anaerobic granular sludge (AnGrSL) and 30 mL of cheese whey (SCOD 45 g/L), over 27 days. A control reactor without ZVI (containing only AnGrSL and CW) underwent the same conditions and procedures. Based on the description by Angelidaki et al. (2009), a nutrient medium was prepared, and each serum bottle was filled with this medium, reaching a working volume of 100 mL. Afterward, the serum bottles were sealed with rubber septa and screw caps, and the headspace was purged with N_2 for 2 minutes to establish anaerobic conditions. The pH of each reactor was adjusted to 7.3 using 1 M NaOH. All experimental conditions were set up in duplicate. The reactors were placed in an incubator at 120 rpm and 33 °C. Routine sampling and monitoring of each reactor were conducted for a predefined set of physicochemical parameters.

2.3.4 Influence of ZVI on solubilization/hydrolysis and acidification of CW

To investigate the influence of ZVI on the solubilization/hydrolysis and acidification processes of CW, a methanogenesis inhibition procedure was performed in the batch anaerobic assays, as mentioned in section 2.3.3. In summary, 15 g of AnGrSL and 30 mL of CW were introduced into serum bottles with 25 g/L PZVI and 50 g/L SZVI, respectively. To prevent the consumption of Volatile Fatty Acids (VFAs), 50 mM of sodium 2-bromoethanesulfonate (BES) was added to each bottle to inhibit methanogenic activity (Zang et al., 2020). Sodium 2-bromoethanesulfonate (BES) mainly inhibits Coenzyme M, a specific cofactor present in all methanogens (not in other bacteria or archaea), and is involved in the final step of methane production. A control reactor (without ZVI) containing only AnGrSL and CW was set up parallel with 50 mM of BES.

Over the experimental period, the degree of hydrolysis was assessed by calculating the Soluble Microbial Products (SMPs). Hydrolysis, associated with the

solubilization of cheese whey, was calculated by subtracting the amount of Volatile Fatty Acids (VFAs), quantified as Chemical Oxygen Demand (COD), from the soluble COD (Stuckey, 2014). Acidification was evaluated based on the accumulation of VFAs over time. Batch experiments were conducted over 27 days at a consistent temperature of 33 °C, with all experimental conditions prepared in duplicate for reliability. Experiments with an absolute difference between the mean and individual measurements exceeding 25% were considered invalid.

2.3.5 DNA extraction and microbial analysis

Wet sludge samples (250-300 mg) were obtained from all the systems at the end of both batch and semi-continuous experiments for DNA extraction. The total genomic DNA was then extracted using the reagents and components included in the QIAGEN DNeasy PowerSoil Pro Kit. Bacterial and archaeal genes targeting the V3-V5 region were amplified with the primer set 341 F (5′-CCTACGGGRSGCAGCAG-3′) and 806 R (5′-GGACTACCAGGGTATCTAAT-3′). The extracted genome was sequenced by Novogene (Beijing, China) using an Ion S5TM XL (Thermo Fisher, USA). PCR amplification followed the procedure reported by Tang et al., 2020. Clean reads were assigned to operational taxonomic units at 97% sequence similarity and classified with the SSUrRNA database using a confidence threshold of 80%.

2.4 Chapter 4: Anaerobic digestion of CW: In situ vs Ex-situ H_2 production via anaerobic oxidation of ZVI

The purpose of this study was to examine the influence of ex-situ and in-situ H_2 supply through the anaerobic oxidation of 25g/L PZVI in two different reactor system configurations (In-situ and Ex-situ). The In-situ Reactor was a single reactor setup, where H_2 was generated and supplied directly through in-situ corrosion of ZVI in the presence of cheese whey (CW) and anaerobic granular sludge (AnGrSL). On the other hand, the Ex-situ reactor system involved two reactors. The first reactor, referred to as the H_2-producer reactor, generated H_2 from abiotic ZVI corrosion using sodium bicarbonate ($NaHCO_3$), and the produced H_2 was then periodically transferred to the second reactor, which contained CW and AnGrSL. (**Fig. 2-5**). At the end of the experimental period (21 d), the remaining solid fraction (digestate) from both the In-situ and Ex-situ reactors was evaluated through phytotoxicity trials using *Sinapis alba* seeds to determine its suitability as a soil conditioner.

2.4.1 Reactors configuration: Experimental setup and operational pattern

Experiments were conducted in triplicate using 250 mL serum bottles, each with a working volume of 120 mL. All reactors were agitated at 100 rpm within an incubator maintained at 33°C. The initial pH in the serum bottles was adjusted between 6.8 -7.3 using 2 M NaOH. Two reactor configurations, termed In-situ and Ex-situ, were used to investigate the influence of ex-situ and in-situ H_2 supply via ZVI oxidation on the AD of CW. The setup for each reactor configuration is described as follows:

1. **In-situ reactor**: 25 g/L of PZVI, 36 mL of CW, and 30 g of AnGrSL, then filled to the working volume with a mineral medium as described by Angelidaki et al. (2009). The bottles were subsequently flushed with N_2 gas for 2 min to establish anoxic conditions (Fig. 2-5)
2. **Ex-situ reactor:** Ex-situ system comprised two separate reactors: (a) H_2-producer reactor (25 g/L PZVI in 120 mL of a 50 g/L $NaHCO_3$ solution, flushed with CO_2 for 2 min); and (b) Ex-situ reactor (36 mL CW, 30 g of

AnGrSL, and flushed with N_2 for 2 min). Throughout the experimental period, this reactor (Ex-situ reactor) was periodically injected with H_2 (2, 4, 7, 11, 14, and 18 d) generated from the first reactor (H_2-producer reactor) (**Fig. 2-5**).

A control set, also prepared in triplicate, contained only AnGrSL (30 g) and CW (36 mL). All reactors were operated concurrently over a 21-day period.

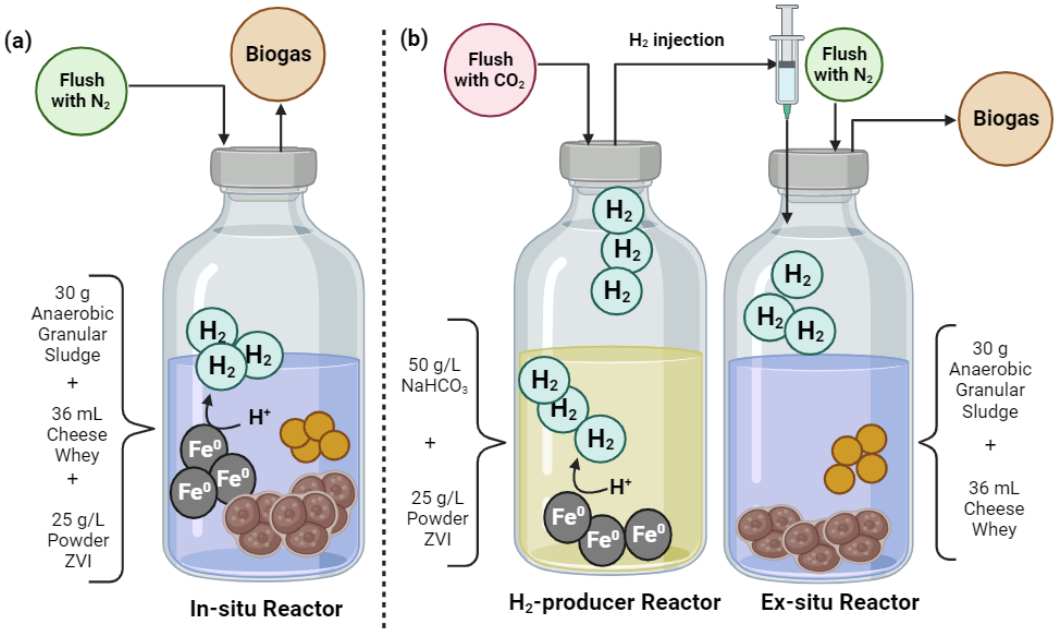

Figure 2-4. System configurations: (a) In-situ Reactor and (b) Ex-situ Reactor

2.4.2 Phytotoxicity assessment

Phytotoxicity is a toxic effect imposed by a compound on plant growth. At the end of the experimental period (day 21), the solid fraction remained after the fermentation period from each reactor set-up (in-situ and ex-situ) was kept for evaluating its potential as a soil supplement through phytotoxicity trials on *Sinapis alba* seeds. The methodology used to evaluate the toxicity of both reactors' end products (digested) on plants was previously mentioned in the study of Photiou and Vyrides (2022). In brief, the end products after the AD process were dried at 105 °C in the oven for 24 h. The final samples were tested using the 2.5 and 3.5% w/w (g of sample per g of control) concentrations on *Sinapis alba* seeds. The samples

were then shaken with deionized water, and the whole portion was transferred to petri dishes. Two layers of absorbent paper and 10 seeds were placed in each petri dish. The petri dishes were sealed with parafilm and place in a dark spot for 3-d at room temperature. Finally, the number of germinated seeds, as well as the length of their roots, were counted. The phytotoxicity was expressed by using the following formulas:

$$\text{Germination Index (GI)} = \frac{(\%\ \text{Seed germination}) * (\%\ \text{Root growth})}{100}$$

Where,

$$\text{Seed germination (\%)} = \frac{\text{No. of germinated seeds in compost}}{\text{No. of germinated seeds in control}} * 100$$

$$\text{Root growth (\%)} = \frac{\text{Mean root length in compost}}{\text{Mean root length in control}} * 100$$

Following this, the phytotoxicity was expressed using the germination index (GI) formula and the length (cm) of the shoot and root of each seed. Higher values of GI indicate a greater rate of germination.

2.5 Analytical Techniques

2.5.1 Determination of Chemical Oxygen Demand (COD)

The chemical oxygen demand (COD) was measured using Spectroquant cell test kits with a measurement range of 500-10,000 mg/L (Merck, Germany), according to the reflux colorimetric method (APHA 2012). Regarding soluble COD measurement, liquid samples underwent centrifugation at 13,500 rpm for 10 minutes and subsequent filtration using a syringe filter pore size of 0.45 mm. Following this, 1 ml of the filtered sample was added to the test kits, securely sealed, thoroughly mixed, and refluxed in a thermoreactor (TR 320, Merck) at 148 °C for

2 hours. After cooling to room temperature, the SCOD was determined using a spectrophotometer (Nova 60, Merck, Germany) at a wavelength of 600 nm.

2.5.2 Determination of biogas composition

The biogas volumes were measured using a wetted 50 ml glass syringe and reported at atmospheric pressure. The volume was discharged after each measurement, allowing the headspace pressure to equilibrate with the atmospheric pressure. The gas composition (H_2, O_2, N_2, CH_4, and CO_2 concentrations) analysis was performed using an Agilent Technologies Gas Chromatographer 7820A connected to a Thermal Conductivity Detector (Wilmington, DE) according to Vardanyan et al. (2018). A sample volume of 1 mL was withdrawn from the headspace and injected in GC-TCD. The separation of the gases was achieved using a ShinCarbon ST packed column (Restek Corporation, Bellefonte, PA, USA) using argon (1 $mLmin^{-1}$) as a carrier gas. The initial column temperature was held for 2 min at 60 °C, then was raised to a final temperature of 160 °C at a rate of 20°C min^{-1} and maintained for 1 min. The injector and detector were maintained at 125 °C and 250 °C, respectively. The coefficient of variation for 10 identical samples was ±2%. The cumulative methane yield was calculated according to Eq. 1 and Eq. 2 as follows:

Eq.1:

$$M_t = CH_{4,t-1} - CH_{4,t}$$

Eq. 2:

$$VCH_{4t} = V_{meas.biogas\,t} \times \frac{(\%CH_{4t})}{100} + V_{head.} \times \frac{(\%CH_{4t} - \%CH_{4t-1})}{100}$$

Where,

Mt is the cumulative methane yield at time t (mL CH_4), VCH_4t is the volume of methane at time t, $V_{meas.\ biogas}\,t$ is the volume of biogas measured at time t, V_{head} is the headspace volume (ml) and CH_4t is the methane content in biogas at time t.

2.5.3 Determination of volatile fatty acids (VFAs)

2.5.3.1 High-Performance Liquid Chromatography (HPLC)

Liquid samples (2 mL) were taken periodically using a sterile syringe to determine the concentration of volatile fatty acids (VFAs). The samples were first centrifuged at 13,500 rpm for 10 min, and the supernatant was filtered through a 0.45 μm syringe filter to remove any remaining solids. VFAs were analyzed by a High-Performance Liquid Chromatography (LC-20AD, Shimadzu, Japan) associated with a Shimadzu SPD20 A UV/VIS detector and a Shimadzu SIL-20 A HT autosampler. Elution was performed isocratically on a Rezex™ ROA-Organic Acid H+ (8%) (150 x 7.8 mm, Phenomenex) with 5 mM H_2SO_4 at 50 °C as described by Vyrides and Stuckey (2009). The injection volume was 1 μL, and the flow rate was 0.7 mL min^{-1}. The UV detector was set at 210 nm during the analysis.

2.5.3.2 Determination of VFA and alkalinity by titration method

Alkalinity and VFA concentration in semi-continuous reactors (see section 5.2) were measured using a titration method according to Kapp. The procedure involved initially filtering the sample through a 0.45μm membrane filter. Then, 20 ml of the filtered sample was placed in a beaker with a magnet to ensure constant mixing with 0.1 N H_2SO_4. An immersed electrode facilitated pH measurement, recording the initial pH value. The sample was titrated slowly with H_2SO_4 (0.1 N) until pH 5.0 was reached, and the volume of the added titrant (A1 (ml)) was recorded. Further acid was incrementally added until pH 4.3 was attained, and the titrant's additional volume (A2 (ml)) was once again noted. This step was iterated until pH 4.0 was achieved, with the volume (A3 (ml)) of the added titrant recorded at each instance. The alkalinity and VFA were calculated according to the Eqs. 1 and 2 as follows:

Eq.1:

$$\text{Alkalinity}\left(\frac{\text{mmol}}{\text{L}}\right)=\frac{\text{A}\times\text{N}\times 1000}{\text{SV}}$$

Eq.2:

$$\text{VFA}\left(\frac{\text{mg}CH_3COOH}{\text{L}}\right) = \frac{131340\times N\times B}{SV} - 3.08\times Alk - 10.9$$

Where,

Alk is the alkalinity (mmol/L), also referred to as TIC (Total Inorganic Carbon), A is the consumption (mL) of H_2SO_4 to titrate sample from initial pH to pH 4.3 [A = A1 + A2], N is the normality of H_2SO_4 (0.1N), SV is the initial sample volume (20 ml), VFA is the concentration of Volatile Fatty Acids (mg/L acetic acid equivalents), and B is the consumption (mL) of H_2SO_4 to titrate sample from pH 5.0 to pH 4.0 due to HCO_3/CO_2 buffer [B = A2 + A3]

A/TIC ratio

The A/TIC Method (German: FOS/TAC) was developed at the Federal Research Institute for Agriculture (FAL) in Braunschweig, Germany. Used as an indicator of the digester's process stability, it expresses the ratio between Volatile Fatty Acids and buffer capacity (alkalinity), or in other words, the amount of Acids (A) compared to Total Inorganic Carbon (TIC).

$$\frac{\text{A}\left(\frac{\text{mg}}{\text{L}}\right)}{\text{TIC}\left(\frac{\text{mg}}{\text{L}}\right)} = \frac{\text{VFA}\left(\frac{\text{mg}}{\text{L}}\right)}{\text{Alkalinity}\left(\frac{\text{mg}}{\text{L}}\right)}$$

Alkalinity needs to be converted to TIC [mg/l $CaCO_3$] by multiplying it with half the molecular weight of $CaCO_3$ (100.084/2=50.042), as each molecule of $CaCO_3$ can take up $2H^+$ ($CaCO_3 + H_2O \rightarrow Ca^{2+} + HCO_3^- + OH^-$).

3 Results and discussion

3.1 Chapter 1: Anaerobic digestion of CW using acclimatized granular sludge at pH 5-6

This study aims to examine the anaerobic digestion of cheese whey using an acclimatized methanogenic culture at moderately low pH levels (pH 5-6). The primary objective is to explore this approach as a potential strategy to reduce the necessity for external alkaline additions typically required to maintain optimal pH conditions. Therefore, batch laboratory experiments were conducted to evaluate the treatment performance of CW using both acclimatized (previously exposed to acetic acid for 7 months) and non-acclimatized methanogenic culture at these pH levels. Additionally, in this chapter, the microbial community structure was characterized, and the potential microbial pathways responsible for the biodegradation of cheese whey under these conditions were proposed. Finally, the possible costs associated with the anaerobic digestion of cheese whey at moderately low pH versus neutral conditions were estimated based on the laboratory findings and data collected from monitoring a full-scale Internal Circulation (IC) bioreactor.

3.1.1 Methane production from CW by acclimatized granular sludge at pH 5-6

Fig. 3-1 and **Fig. 3-2** show the cumulative CH_4 production during AD of CW by acclimatized (AnGrSL-PE) and non-acclimatized (F-AnGrSL) methanogenic cultures over 1st batch and 2nd batch cycles, respectively. As illustrated in **Fig. 3-1**, during the 1st batch cycle (21 days) the acclimatized methanogenic culture (AnGrSL-PE) exhibited a higher CH_4 generation (45 mL) compared to F-AnGrSL, which produced 30 mL of CH_4 upon sudden exposure to these pH conditions. However, the theoretical production was 108 ml CH_4 and the experimental results showed that there is huge potential for improvement. In the initial 5 days, both AnGrSL-PE and F-AnGrSL demonstrated comparable CH_4 production. However, beyond the 5th day, the acclimatized sludge (AnGrSL-PE) displayed a significant increase in its CH_4 production rate compared to F-AnGrSL.

During the 1st batch cycle, CH_4 production rate was 0.033 mL/mL $_{reactor}$ /d for AnGrSL-PE and 0.026 mL/mL$_{reactor}$/d for F-AnGrSL.

This observed trend persisted in the 2nd batch cycle, as depicted in **Fig. 3-2**, indicating the advantageous effects of prior acclimatization of anaerobic granular sludge under moderately low pH conditions (5-6). The lag period observed during the 1st batch cycle for both AnGrSL-PE and F-AnGrSL may be attributed to the time required for adaptation to the cheese whey (CW) under moderately low pH conditions, even though the anaerobic granular sludge previously exposed to acetate and pH 5-6 ultimately exhibited superior performance. Notably, in the 2nd batch cycle, no lag period was observed for both AnGrSL-PE and F-AnGrSL, suggesting the potential of anaerobic granular sludge to acclimatize efficiently under moderately low pH conditions.

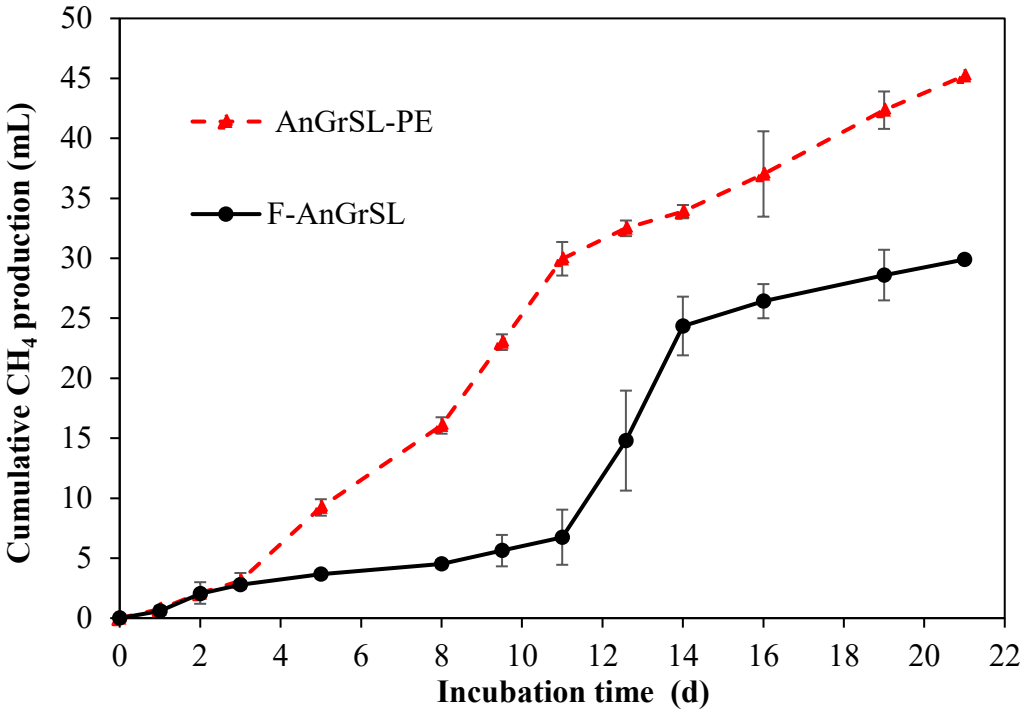

Figure 3-1. Cumulative CH_4 production from CW by acclimatized (AnGrSL-PE) and non-acclimatized (F-AnGrSL) cultures over 21 d of AD at pH 5-6 (1st cycle)

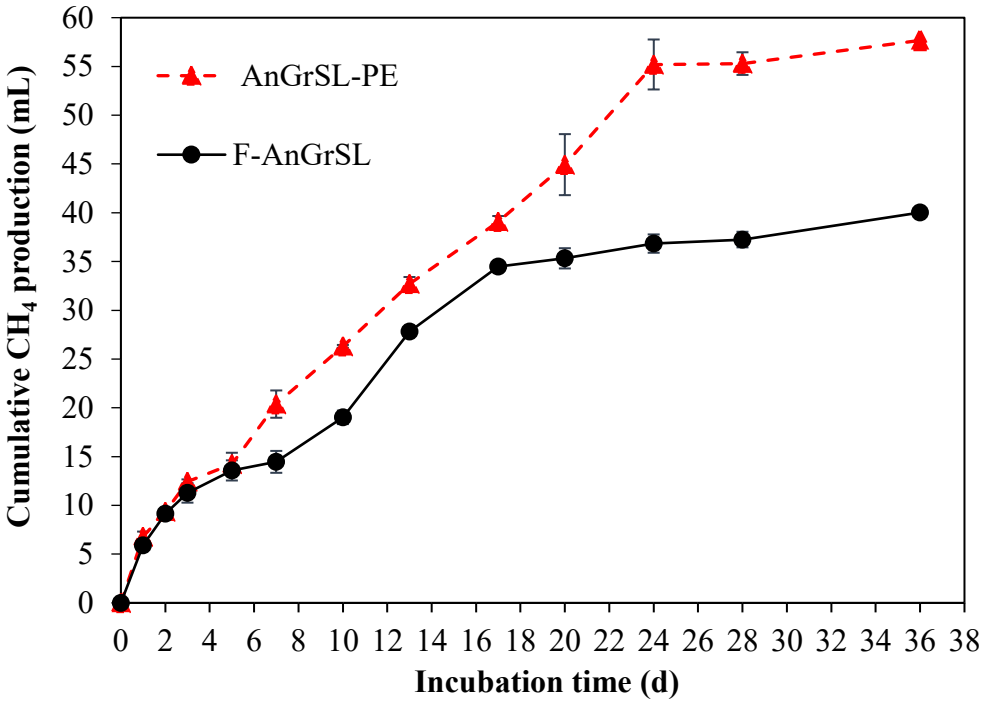

Figure 3-2. Cumulative CH_4 production from CW by acclimatized (AnGrSL-PE) and non-acclimatized (F-AnGrSL) cultures over 36 d of AD at pH 5-6 (2^{nd} cycle)

3.1.2 VFAs production from CW by acclimatized anaerobic granular sludge at pH 5-6

Fig. 3-3 and **Fig. 3-4** illustrate the production of Volatile Fatty Acids (VFAs) resulting from the anaerobic digestion of CW by AnGrSL-PE and F-AnGrSL during the 1^{st} and 2^{nd} batch cycles, respectively. As shown in Fig. 3-3, during the 1^{st} batch cycle (21 days), the acetic acid concentrations for both granular sludges exhibited a consistent pattern, reaching their respective maxima after 3 days before gradually decreasing to 470 mg/L for F-AnGrSL and 140 mg/L for AnGrSL-PE. This pattern persisted even after re-feeding in the 2^{nd} batch cycle, albeit with a marked reduction in the remaining acetic acid after 28 days, measuring approximately 100 mg/L for F-AnGrSL and complete absence for AnGrSL-PE (**Fig. 3-4**). The observed consumption of acetic acid suggests sludge acclimation under these conditions.

A significant difference in propionic acid concentrations between AnGrSL-PE and F-AnGrSL is shown by the findings of VFAs in **Fig. 3-3** and **Fig. 3-4**. During the 1st batch cycle, propionic acid trends reveal a pronounced peak in the F-AnGrSL, reaching the highest concentration of all VFAs at approximately 1962 mg/L on day 8, followed by a sharp decrease. In contrast, on the same day AnGrSL-PE also exhibited an increase in propionic acid concentration (1339 mg/L) but reached a lower peak, followed by a more gradual decline (**Fig. 3-3**). In the 2nd batch cycle, F-AnGrSL exhibited a propionic acid concentration of 3500 mg/L on day 20, whereas AnGrSL-PE recorded 806 mg/L, underlining the distinct responses of the two sludges under these conditions (**Fig. 3-4**). However, propionic acid, being the least biodegradable substrate among the VFAs for both AnGrSL-PE and F-AnGrSL, appears to be the reaction limiting step for cheese whey degradation under these conditions. Notably, butyric acid concentrations were substantially higher for AnGrSL-PE compared to F-AnGrSL (**Fig. 3-3** and **Fig. 3-4**), and this difference was even more obvious during the 1st batch cycle.

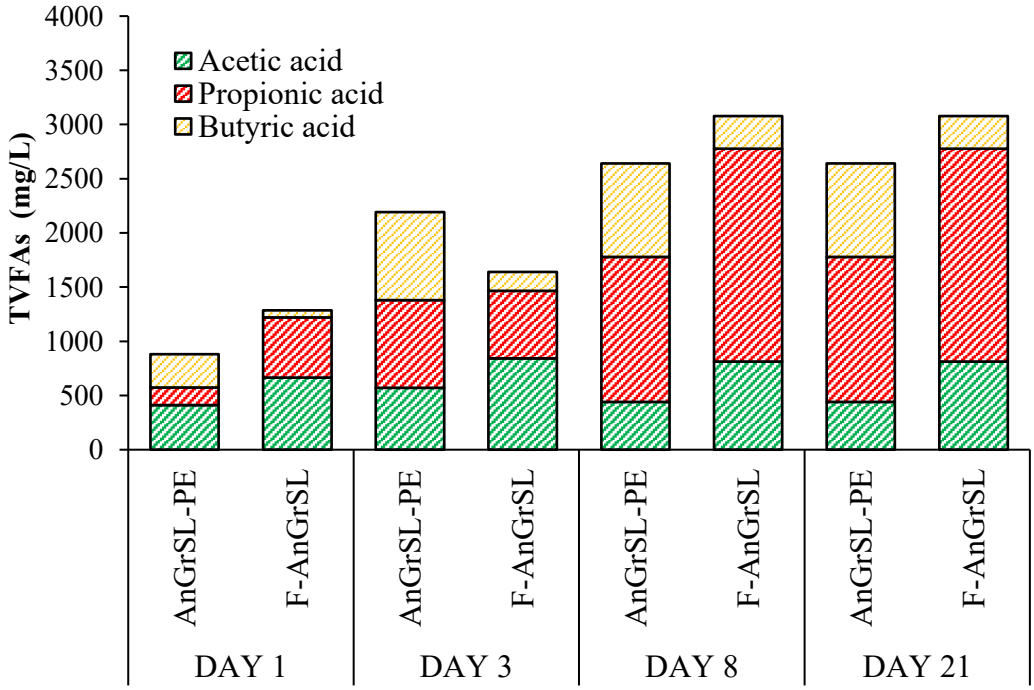

Figure 3-3. VFAs production from CW by acclimatized (AnGrSL-PE) and non-acclimatized (F-AnGrSL) cultures over 21 d of AD at pH 5-6 (1st cycle)

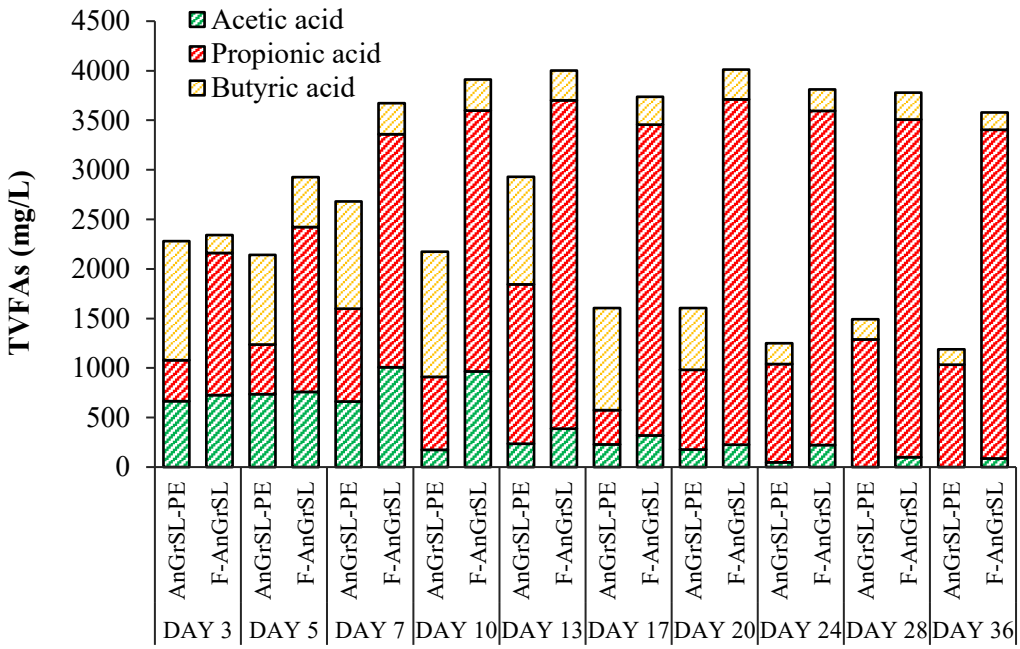

Figure 3-4. VFAs production from CW by acclimatized (AnGrSL-PE) and non-acclimatized (F-AnGrSL) cultures over 36 d of AD at pH 5-6 (2nd cycle)

3.1.3 Microbial community profile

Microbial profile analysis, using next-generation sequencing of the 16S rRNA gene, was conducted on the 12th day of the 2nd batch cycle for the following conditions: (a) anaerobic granular sludge previously exposed to moderately low pH for 7 months and subsequently treated with CW (AnGrSL-PE), (b) fresh anaerobic granular sludge suddenly exposed to moderately low pH and CW (F-AnGRSL), and (c) anaerobic granular sludge obtained from the industrial-scale (IC) bioreactor operating at pH 7-7.5 (AnGrSL-IC). The relative abundance of the archaeal 16S rRNA gene at the genus level is depicted in **Fig. 3-5**. Specifically, *Methanolinea*, a hydrogenotrophic methanogen, was the dominant genus (~53%) for AnGrSL-PE. In contrast, its relative abundance was lower (~42%) for F-AnGrSL, which was exposed to CW at pH 5-6 for around 33 days, and significantly lower (~23%) for AnGrSL-IC obtained from an industrial-scale IC bioreactor operating at pH 7-7.5. These results indicate that the longer anaerobic granular sludge is exposed to lower

pH, the more hydrogenotrophic methanogens evolve compared to acetolactic methanogens. In spite of the fact that a substantial portion (9g out of 11g) from the AnGrSL-PE was previously exposed to acetic acid for 7 months, the abundance of the acetoclastic *Methanosaeta* was significantly lower (~15%) in comparison to the hydrogenotrophic methanogen *Methanolinea* (~53%) (**Fig. 3-5**). These observations indicate that the low pH conditions (5-6) were a significant determinant in shaping the composition of methanogenic communities.

As shown in **Fig. 3-6,** the long exposure of anaerobic granular sludge to pH 5-6 resulted in an increased abundance of *Firmicutes.* Specifically, within AnGrSL-PE, the order *Clostridiales* and the genus *Clostridium sensu stricto* were dominant, comprising ~53.9% and ~51.5%, respectively (**Table 3-1**). In contrast, *Clostridiales* accounted for 28.7% in F-AnGrSL and 6.4% in AnGrSL-IC. Additionally, *Proteobacteria* exhibited a slightly higher abundance in AnGrSL-IC (~27%) compared to AnGrSL-PE (~16%) and F-AnGrSL (~18%), respectively (Fig. 3-6). Other dominant bacteria, including *Prevotella* and *Serratia* were identified in AnGrSL-PE but were absent in AnGrSL-IC. Remarkably, the genus *Treponema*, known for its capability in the homoacetogenic pathway, was present at levels around 2-2.5% for anaerobic granular sludge exposed to pH 5-6 (AnGrSL-PE and F-AnGrSL), whereas it was found at a lower level of only 0.5% for AnGrSL-IC (**Table 3-1**).

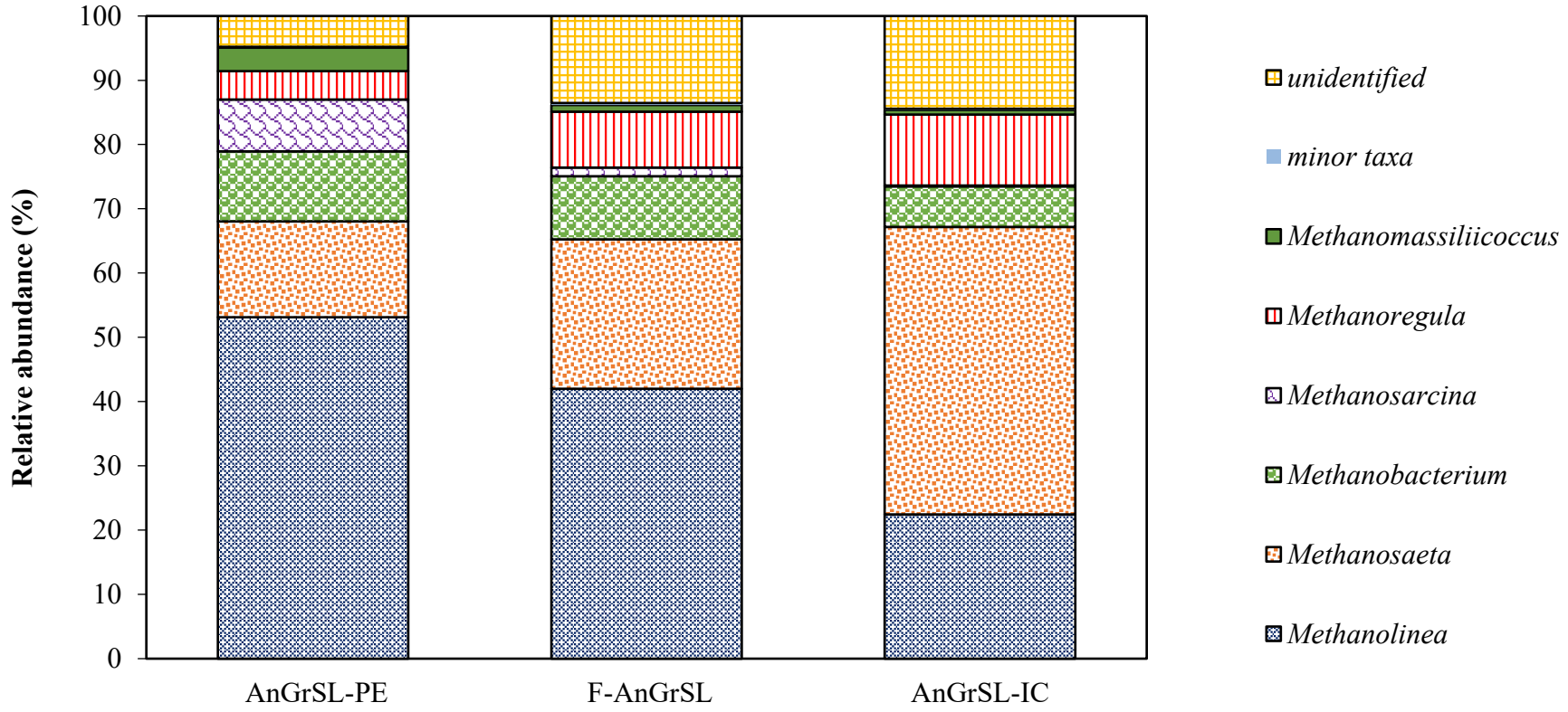

Figure 3-5. Genus level relative abundance of archaea (>0.1% in at least one sample).

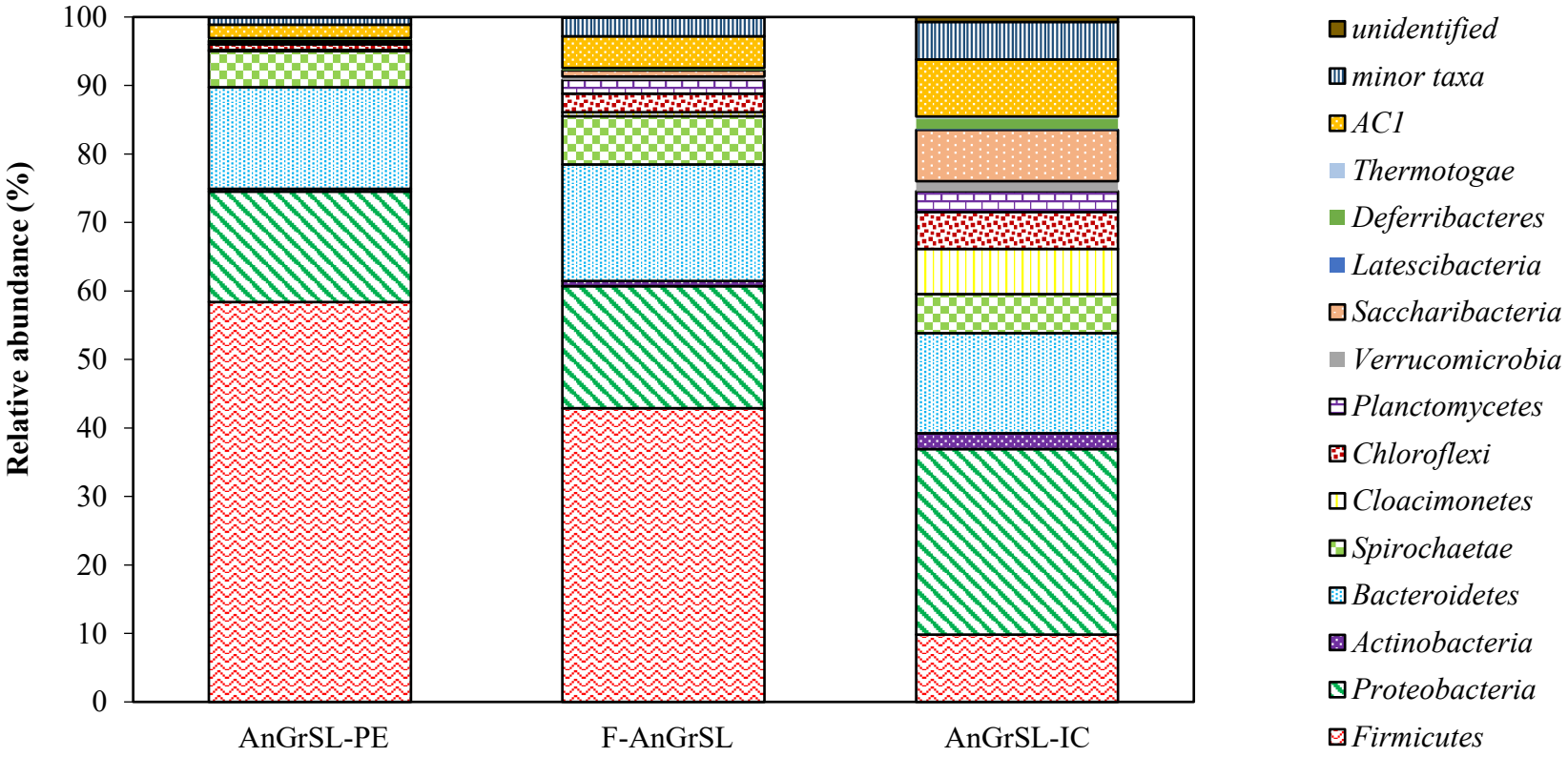

Figure 3-6. Phylum level relative abundance of bacteria (>1% in at least one sample).

Table 3-1. Genera level relative abundance of bacteria. (> 1% in at least one sample)

genus	**AnGrSL-PE**	**F-AnGrSL**	**AnGrSL-IC**
Acinetobacter	0.60	2.6	13.9
Prevotella 7	7.5	3.2	0.1
Serratia	7.1	3.7	0.1
Caldithrix	0.1	0.2	1.5
Blvii28 wastewater-sludge group	0	1.4	4.2
Syntrophorhabdus	0	0.3	1.2
Oscillibacter	0.30	1.9	0.1
Lactococcus	0.2	2.9	0.1
Clostridium sensu stricto 16	0.1	5.1	0.3
Clostridium sensu stricto 14	0.1	1.3	0.0
Clostridium sensu stricto 1	47.6	0.4	0.0
Clostridium sensu stricto 12	1	1.8	0.1
Clostridium sensu stricto 10	1.3	2.7	0.1
Clostridium sensu stricto 7	0.0	1.4	0.1
Clostridium sensu stricto 8	1.4	0.5	0.0
Clostridium sensu stricto 18	0	8.3	0.2
Intestinimonas	0.48	0.8	2.9
Acidaminococcus	0.7	1.3	0.0
Lactobacillus	0.01	0.4	1.0
Treponema 2	2.32	2.4	0.5
Pseudomonas	0.9	0.4	1.3
Selenodonts	1.7	0.0	0.0
Geobacter	0.1	1.0	0.3
Streptococcus	0.2	1.0	1.3
Spirochaeta 2	0.0	0.2	1.0
Enterococcus	0	1.9	0.0
Desulfobulbus	0.6	0.5	0.1
Parabacteroides	0.7	2.4	0.4
U29-B03	0.62	0.00	0.0
bacterium enrichment culture clone JCA3	0.0	0.2	1.1
minor taxa	6.12	16.74	18.21

3.1.4 Proposed microbial degradation pathways for CW by acclimatized granular sludge

Based on the results of the current experiments, a proposed microbial pathway during CW biodegradation by acclimatized methanogenic culture at pH 5-5 is shown in **Fig. 3-7**. Microbial analysis revealed a higher abundance of hydrogenotrophic methanogens over acetoclastic methanogens under these conditions, indicating that hydrogenotrophic methanogenesis is the primary pathway for CH_4 production. In another study, Li et al. (2018) used an acid-tolerant methanogenic culture to address overloading in an anaerobic digester using synthetic food waste (FW). Following bioaugmentation, they observed a significant increase in the populations of both *Methanosaeta* (acetoclastic methanogens) and *Methanolinea* (hydrogenotrophic methanogens). Notably, in a study by Treu et al. (2018), a hydrogenotrophic methanogen *Methanoculleus palmolei M8* was identified in high abundance during the anaerobic digestion of CW, and this was linked to Na^+ in CW, causing more significant inhibition of acetoclastic methanogens compared to hydrogenotrophic methanogens (Vyrides and Stuckey 2017).

In the present study, H_2 and CO_2 can be produced from Eqs. 1, 2, and 3 (**Fig. 3-7**), and subsequently utilized by hydrogenotrophic methanogens, such as *Methanolinea*. Microbial analysis reveals a notably higher abundance of *Clostridium* species in AnGrSL-PE compared to F-AnGrSL and AnGrSL-IC (**Table 3-1**). This suggests that *Clostridium* species are likely the primary biocatalysts for reactions described by Eqs. 1 and 2. This observation aligns with previous studies indicating that *Clostridium* species play a pivotal role in converting cheese whey into H_2, CO_2, acetic acid, and butyric acid. These conversions were demonstrated in mixed cultures predominantly composed of *Clostridium* species (Davila-Vazquez et al. 2009, Moreno et al. 2015) and in studies involving a pure *Clostridium* culture (Ferchichi et al. 2005), specifically under moderately low pH.

Furthermore, the reduction in residual acetic acid levels in AnGrSL-PE can be attributed, in part, to syntrophic acetate oxidation (SAO). This process is facilitated by syntrophic acetate oxidizers and hydrogenotrophic methanogens, as shown in Eqs. 3 and 4 (**Fig. 3-7**). The Eq. 3 is thermodynamically unfavorable under

standard conditions unless hydrogenotrophic methanogenesis (Eq. 4) efficiently utilizes H_2 through interspecies H_2 transfer (Tian et al., 2019). The acetic acid can also undergo biodegradation via acetoclastic methanogenesis (AM) (Eq.5); however the lower relative abundance of acetoclastic methanogens at AnGrSL-PE and F-AnGrSL, compared to hydrogenotrophic methanogens (HM), suggests that the syntrophic acetate oxidation-hydrogenotrophic methanogenesis (SAO-HM) pathway could be also one of a significant microbial pathway for CH_4 generation under these conditions (**Fig 3-7**).

Several studies (Hao et al. (2012), Hao et al. (2013), Lü et al. (2010)) have reported the activation of the syntrophic acetate oxidation-hydrogenotrophic methanogenesis (SAO-HM) pathway under moderately low pH or high concentrations of acetic acid. Specifically, Hao et al. (2013) noted that up to 89% of CH_4 production occurred through the SAO-HM pathway at a high concentration of acetic acid (100 mmol/L), while Lü et al. (2010) found that the SAO-HM pathway can be activated at pH around 5. In another study, Hao et al. (2012) demonstrated that the conversion of 100 mmol/L acetate under thermophilic conditions at pH 5.5 predominantly followed the SAO-HM pathway. Mosbaek et al. (2016) suggested the active involvement of hydrogenotrophic methanogens and five subspecies of *Clostridia* in SAO-HM. In the present study, the high abundance of *Clostridium sensu stricto* (**Table 3-1**) and the rapid decrease in residual acetic acid in AnGrSL-PE indicate a potential and active role of *Clostridium sensu stricto* in SAO-HM (Eqs. 3 and 4) (**Fig. 3-7**).

Additionally, according to Narihiro et al. (2015), hydrogenotrophic methanogen *Methanolinea* demonstrates exclusive prevalence in microbial communities enriched with syntrophic substrates. Consequently, specific methanogens, including *Methanolinea,* may be inclined to selectively facilitate syntrophic partnerships, particularly for H_2 transfer. The same study reported that the majority of *Methanolinea* strains were exclusively isolated from enrichments established under syntrophic conditions. Therefore, the findings of the current study tentatively propose an active involvement of *Methanolinea* species in syntrophic acetate oxidation-hydrogenotrophic methanogenesis (SAO-HM) under moderately low pH. Apart from hydrogenotrophic methanogens, a potential partnership

between homoacetogens and acetoclastic methanogens could utilize part of H_2 and CO_2. The detection of the homoacetogens-related genus *Treponema 2* (**Table 3-1**) exclusively in anaerobic granular sludge exposed to moderately low pH (AnGrSL-PE and F-AnGrSL) supports this possibility.

Under moderately low pH conditions, the substantial accumulation of propionic acid in both AnGRSL-PE and F-AnGRSL (see section 3.2) indicates the presence of propionate producers and a scarcity of propionate utilizers. According to the high relative abundance (Table 3-1) and insights from previous studies (Bundhoo and Mohee 2016, Saady et al. 2013, Sivagurunathan et al. 2014, Castello et al. 2009), species likely involved in propionic acid generation from cheese whey (CW) could include *Clostridium sp., Prevotella sp., and Selenomonas sp*. Microorganisms generating propionic acid can utilize H_2 as an electron donor for propionic acid production from carbohydrates (Bundhoo and Mohee 2016) (Eq. 6). Furthermore, Bundhoo and Mohee (2016) explained that propionate producers such as *Clostridium propionicum* and *Clostridium homopropionicum* generate propionic acid by degrading lactate and consuming NADH in this process (Eq. 7). Saady et al. (2013) also stated that lactate serves as the preferred substrate for propionate-forming bacteria due to its thermodynamically favorable biodegradation (Eq. 7). *Prevotella sp*., recognized for its ability to biodegrade carbohydrates and produce primarily short-chain fatty acids (dos Reis et al., 2015), displayed a considerable abundance in AnGrSL-PE (7.5%), lower in F-AnGrSL (3.2%), and minimal presence at AnGrSL-IC (0.1%). This suggests that the transition from neutral pH to pH 5-6 contributed to the rapid emergence of *Prevotella sp*. Notably, the same genus was prominently detected in an Upflow anaerobic sludge blanket (UASB) reactor treating cheese whey for biohydrogen production (Castelló et al. 2009). *Selenomonas sp.* that was only detected in AnGrSL-PE could also be a potential propionic producer. In a study by Sivagurunathan et al. (2014) propionic acid accumulation was observed in a bioreactor for H_2 production treating beverage wastewater (BW) with *Selenomonas sp.* under conditions of pH 5.5, 37 °C, and hydraulic retention time (HRT) of 8 hours. The high accumulation of propionic acid in both AnGrSL-PE and F-AnGrSL, coupled with the absence of *Syntrophomonas* and *Pelotomaculum* which are involved in syntrophic propionate and butyrate

degradation (Eqs. 8 and 9) (Carballa et al. 2015), points out that the propionic acid is the reaction limiting step for anaerobic granular sludge under these conditions (**Fig. 3-7**).

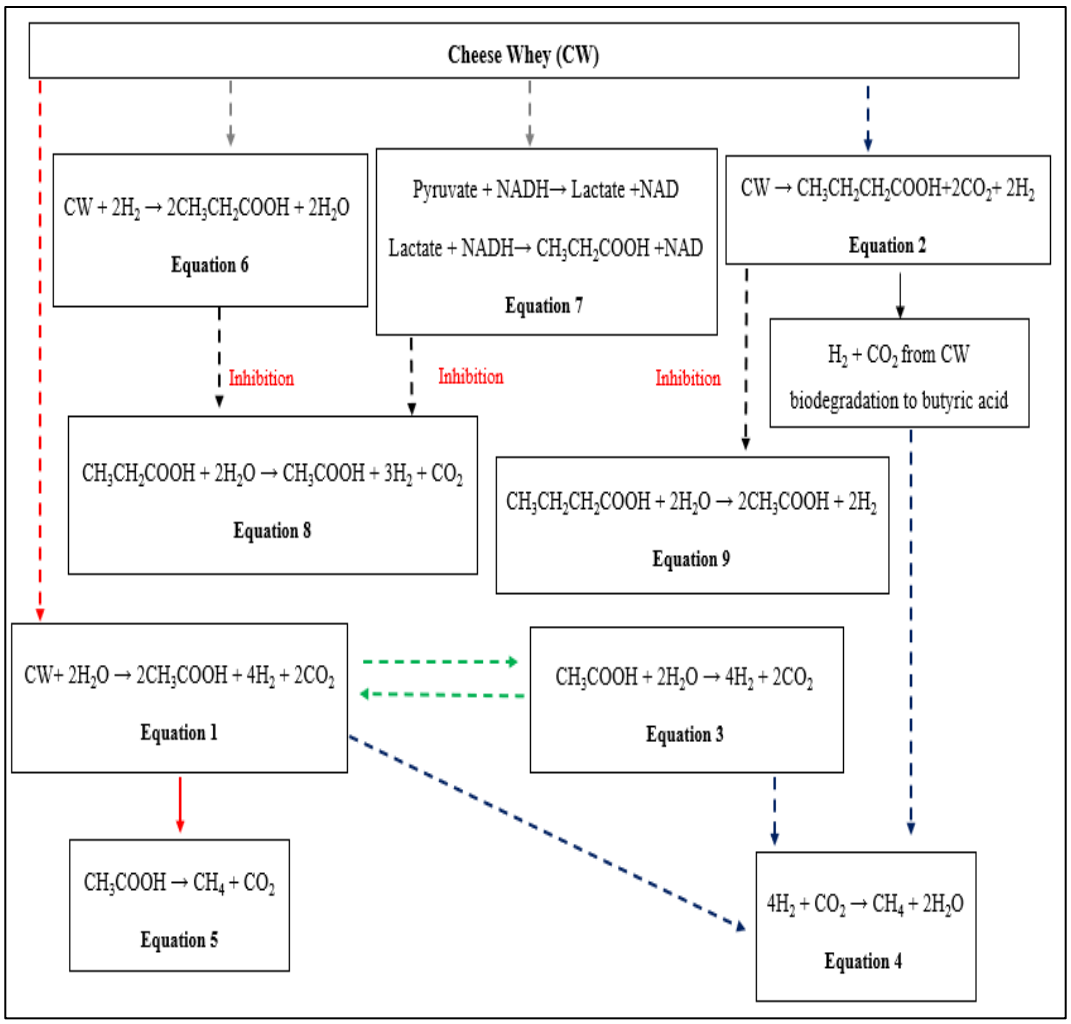

Figure 3-7. Proposed microbial pathways during CW anaerobic biodegradation at moderately acidic pH by AnGrSL-PE and F-AnGrSL

3.1.5 Economic comparison of CW treatment in full-scale IC reactor at pH 5-6 and pH 7

As mentioned in section 2.1.5, an economic analysis was conducted using data from a 91-d operational monitoring period of a full-scale IC bioreactor, supplemented by laboratory results. This analysis aimed to evaluate potential profits from electricity generation through biogas and the associated costs of transporting cheese whey (CW) and pH adjustment using NaOH. The economic assessment focused on the potential treatment of CW in a full-scale bioreactor: (a) at pH 5-6 and (b) at pH 7.

The operational data from the IC bioreactor was initially examined to calculate the potential electricity production from biogas, considering the future installation of a combined heat and power (CHP) system. Currently, the biogas is flared; however, there are plans to utilize it in a CHP system shortly. According to Table 3-2, the biogas generated over the 91-day period averaged 128.9 m^3/day, with the potential to produce an average of 275.7 kWh/day of electrical energy. The DWWTP's daily electricity consumption is 585 kWh, costing 81.4 euros, meaning the expected output from the CHP system could meet about 50% of the plant's energy needs. Additionally, a substantial amount of CW (81.2 m^3/day) produced by a dairy factory is not treated in an IC bioreactor but is instead transported to another facility at a daily cost of 255 euros.

The current study explored the treatment of CW at moderately low pH level (5-6) to potentially reduce operational costs. Small-scale laboratory experiments indicated that the anaerobic digestion of CW at these pH level could theoretically yield an average biogas production of 57.5 m^3/d from 81.2 m^3 of cheese whey (**Table 3-2**). In contrast, anaerobic digestion at a neutral pH (7.0) level could generate an average of 123.6 m^3/d of biogas, about 50% more than at moderately low pH levels. Despite the lower NaOH requirement for the moderately low pH treatment, as shown in **Table 3-2**, this reduction does not lead to an overall decrease in treatment costs because of the reduced biogas production. To improve the feasibility of anaerobic CW treatment at moderately low pH, either a 50% increase in biogas production is necessary, or the retention time must be decreased. It is

important to note that these are preliminary findings from laboratory experiments, and validation through larger-scale operations is essential.

Table 3-2. Economic analysis regarding the treatment of CW in a full-scale IC bioreactor at pH 5-6 and pH 7

Parameter	**Per day**	**Daily cost (€/d)**
Influent wastewater treated in IC bioreactor	550 m^3	
NaOH consumption to maintain the pH (0.17 kg NaOH/m^3 wastewater) *	93.5 kg	46.75 €
Average produced biogas from IC bioreactor	128.9 m^3	
Average electricity consumption of DWWTP *	585 kWh	81.4 €
Potential electricity generation in CHP system	275.7 kWh	38.3 €
Cheese whey volume and transportation cost *	81.2 m^3	255.78 €
Scenario 1: Anaerobic digestion of CW at pH 7		
Potential of biogas generation (retention time 15 d)	123.6 m^3	
Potential of electricity generation	264.3 kWh	36.8 €
NaOH consumption to maintain the pH (0,32 kg NaOH/m^3 wastewater)	25.98 kg	12.99 €
Scenario 2: Anaerobic digestion of CW at pH 5-6		
Potential of biogas generation (retention time 21 d)	57.5 m^3	
Potential electricity generation	123 kWh	17.12 €
NaOH consumption to maintain the pH (0,10 kg NaOH/m^3 wastewater)	8.12 kg	4.06 €

* NaOH (50% w/v) cost: 0.50 €/kg
* Electricity cost in Cyprus for non-households: 0.1392 €/kWh
* Transportation cost of cheese whey: 3.15 €/m^3

Conclusions of Chapter 1

This chapter investigated the anaerobic digestion of cheese whey using an acid-tolerant methanogenic culture maintained at a pH range of 5-6 to counteract acid inhibition caused by the accumulation of volatile fatty acids (VFAs). The results demonstrated that reactors employing acclimatized sludge exhibited 35% and 30% higher CH_4 production over 21 and 36 days of batch operation, compared to reactors with non-acclimatized sludge. VFA analysis identified propionic acid as the least biodegradable VFA, corroborated by microbial analysis indicating the absence of propionate-utilizing bacteria, such as *Syntrophobacter* and *Pelotomaculum*.

Furthermore, microbial analysis showed a higher abundance of hydrogenotrophic methanogens, predominantly *Methanolinea* (~53%), in reactors containing acclimatized methanogenic culture, suggesting that a substantial portion of CH_4 was produced via the hydrogenotrophic pathway under moderately acidic conditions. Despite a 7-month acclimatization to acetic acid, the acetoclastic *Methanosaeta* was considerably less prevalent in acclimatized sludge (~14%) than in non-acclimatized sludge (~ 23%). This difference highlights the enhanced resilience of hydrogenotrophic methanogens to prolonged low pH exposure. Moreover, the observed lower residual acetic acid levels in reactors with acclimatized sludge, combined with a significant presence of *Firmicutes*, particularly within the order *Clostridiales* (53.9%) and genus *Clostridium sensu stricto* (51.5%), suggest as an additional pathway for CH_4 production the involvement of the syntrophic acetate oxidation-hydrogenotrophic methanogenesis (SAO-HM) pathway.

The economic analysis based on laboratory experiments and the data from 91-day monitoring of a full-scale internal circulation (IC) reactor elucidate that operating anaerobic digestion at moderately low pH levels (5-6) with acclimatized granular sludge requires approximately 69% less NaOH (50% v/v) per m^3 of CW compared to neutral pH conditions. However, it is theoretically capable of producing 53.5% less kWh/d, and the overall daily net income is €13.06, compared to €23.8 for anaerobic digestion at neutral pH conditions.

3.2 Chapter 2: Enhancement of AD of CW and in-situ biogas upgrading through zero-valent iron (ZVI) addition

3.2.1 Effect of powder and scrap ZVIs on pH

Fig. 3-8a illustrates the pH profiles during the 1st and 2nd batch cycles over a 34-d incubation period. Despite daily regulation to maintain a pH range of 7.0-7.3, the pH in the control reactors (pH reg.) dropped below 6.0 during the first 3 days. From day 3 to day 13, the pH in the control reactor (pH reg.) fluctuated between 6.12 and 6.8, as shown in **Fig. 3-8a**. In the 2nd batch cycle, 30 mL of CW was added to all reactors. A significant drop in pH was again observed in the control reactors (pH reg.) during the initial days. However, with the addition of NaOH, the pH was regulated to around 7.3 and maintained within a range of 7.3-7.5 until the end of the 2nd batch cycle (day 34).

In contrast, during the first two batch cycles (total 34 days), no NaOH was added to the reactors containing PZVI and SZVI, respectively. As depicted in **Fig. 3-8a**, the pH in these reactors remained within a range of 7.3-8.3 throughout both batch cycles. An exception was noted in the reactors with 25 g/L PZVI; where the pH increased to 8.8 and 8.6 at the end of the 1st and 2nd batch cycles, respectively. The observed elevation in pH levels in the reactors with ZVI and SZVI can be primarily attributed to the consumption of H^+ and the increase in alkalinity from anaerobic $Fe^{(0)}$ corrosion (Eq. 1).

Eq. 1

$$Fe^{(0)} + HCO_3^- + H^+ \rightarrow FeCO_3^- + H_2 \qquad (\Delta G^0 = -79.9\ kJ/mol)$$

The Gibbs free energy change for Eq. 1 under standard conditions (pH 0, all reactant and product concentrations at 1 M, and all partial pressures at 1 atm) is 79.9 kJ/mol, whereas at pH 7 ΔG^0 is −39.9 kJ/mol.

Furthermore, within the pH range of 6.8 to 8.3, conditions were more favorable for acetic acid utilization by acetoclastic methanogens, as compared to the control reactors and the reduction of acetic acid also contributed to pH

increased. Additionally, apart from the conversion of CO_2 to CH_4 by hydrogenotrophic methanogens, a part of the CO_2 may have been absorbed in the alkaline medium, further contributing to the observed reduction of CO_2 in the biogas.

As was previously stated the sudden drop in pH for reactors with ZVI especially for the 2nd, 3rd and 4th cycle was mainly due to the formation and accumulation of VFAs during the CW biodegradation. In the 2nd cycle, the presence of PZVI and SZVI counteracted the low pH and it was raised without any NaOH addition. However, during the 3rd and 4th cycle the buffer capacity of the PZVI and SZVI was lost and therefore NaOH was added on day 44 and on day 188 at the beginning of the 3rd and 4th batch cycle respectively in order to raise the pH (**Fig. 3-8b**). This explained the sudden drop in pH during the 3rd and 4th cycle. It is likely that a passivated layer of $FeCO_3$ forms on the outer surface of ZVI, reducing its activity (Eq. 1) and resulting in fewer protons being consumed in the reaction (Eq. 1). Additionally, the addition of higher CW may contribute to increased VFAs generation, leading to a greater decrease in pH.

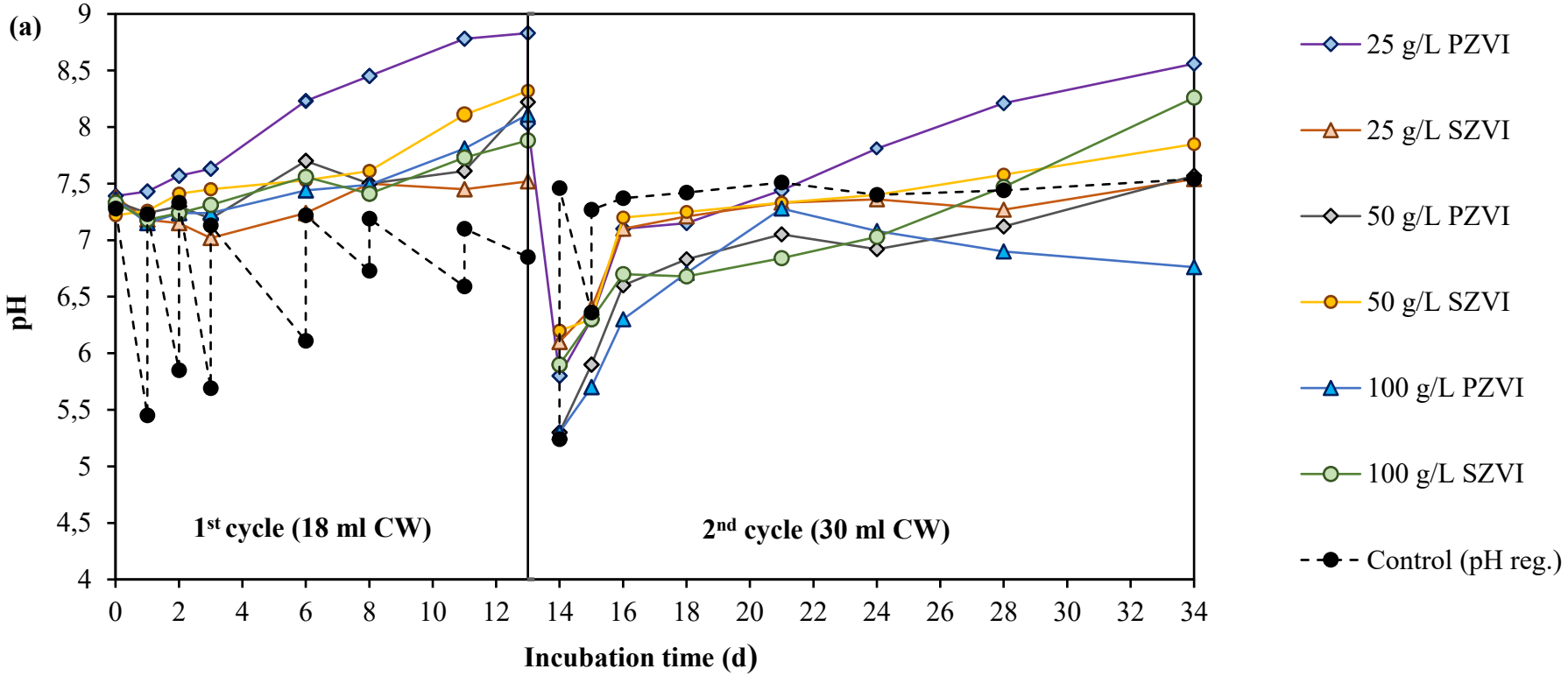
(a)
pH
Incubation time (d)
1st cycle (18 ml CW)
2nd cycle (30 ml CW)
25 g/L PZVI
25 g/L SZVI
50 g/L PZVI
50 g/L SZVI
100 g/L PZVI
100 g/L SZVI
Control (pH reg.)

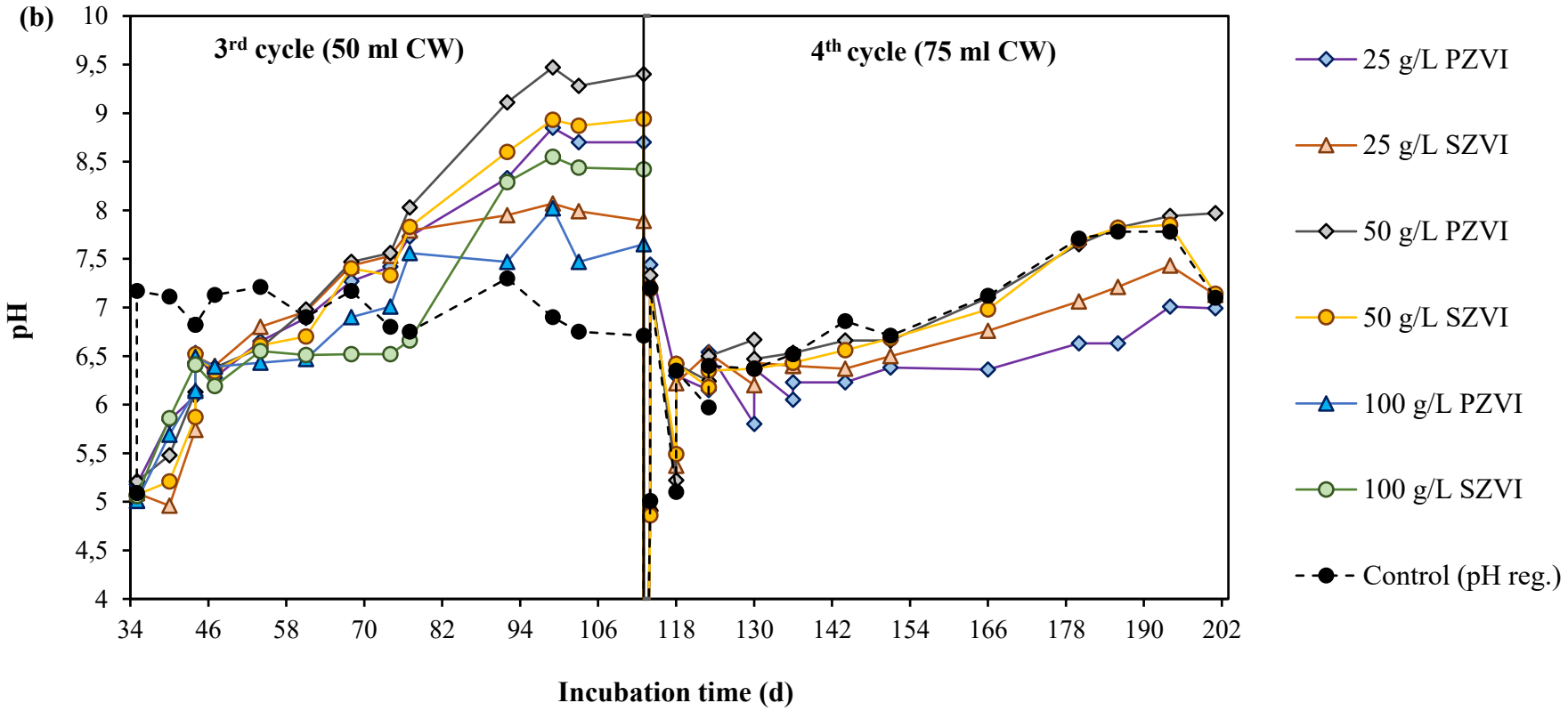

Figure 3-8. pH variations during AD of CW at different concentrations of PZVI and SZVI. (a) 1st cycle (18 mL CW) and 2nd cycle (30 mL CW); (b) 3rd cycle (50 mL CW) and 4th cycle (75 mL CW)

3.2.2 Effect of powder and scrap ZVIs on methane production

The effect of PZVI and SZVI concentrations (25, 50, and 100 g/L, respectively) on CH_4 production from CW under four different consecutive feedings (18, 30, 50, and 75 mL CW, respectively) was investigated for 201 d (operational conditions according to **Table 2-4**).

Fig. 3-9a illustrates the cumulative CH_4 production for three concentrations (25 g/L, 50 g/L, and 100 g/L) of PZVI and SZVI over the initial two batch cycles, lasting 34 days. Specifically, during the 1st cycle (total 13 days), the reactors with 25 g/L PZVI and 50 g/L SZVI exhibited the highest CH_4 production (17.8 mL CH_4/mL CW and 17.9mLCH_4/mL CW, respectively) while the control reactors (ZVI-free) produced the least (7.7 mL CH_4/mL CW)(**Fig. 3-9a**). At 25 g/L and 100 g/L SZVI, cumulative CH_4 production was slightly lower (16.3 mLCH_4/mL CW and 16.6 mLCH_4/mLCW, respectively), compared to 25 g/L PZVI and 50 g/L SZVI. On the other hand, in the reactors with 50 g/L and 100 g/L PZVI, the accumulated CH_4 volume was 11.6 mLCH_4/mLCW and 12.2 mLCH_4/mLCW, respectively, which was lower compared to 25 g/L PZVI (Fig. 4-2a). The theoretical value was 21.7 mL CH_4/mL CW. Only the reactors with the addition of 25 g/L PZVI and 50 g/L SZVI approached this value, achieving 17.8 mL CH_4/mL CW and 17.9 mL CH_4/mL CW, respectively.

After 13 days of incubation, 30 mL of CW (2nd cycle) was fed to all the reactors. The highest CH_4 accumulation was found again at 25 g/L PZVI and 50 g/L SZVI (the same trend as the 1st cycle), followed by control reactors (pH reg.) (**Fig. 3-9a**). The reactor with 100 g/L PZVI mirrored its 1st batch cycle trend, showing lower CH_4 production than other ZVI-containing reactors. Noteworthy, during the 1st and 2nd cycles (total 34 days), no additional NaOH was added to the ZVI-containing reactors for pH to neutralize the pH.

On day 34, 50 mL of new fresh CW (3rd cycle) was fed to all the reactors without adding any PZVI or SZVI (**Fig. 3-9b**). During the initial 13 days of this batch cycle, significant CH_4 production was observed only in the control reactors (pH reg.), while the reactors containing PZVI and SZVI showed limited activity and a drop in pH, as shown in **Fig. 3-9b**.

This is an indication that PZVI and SZVI lost their activity probably due to the formation of outer surface layer such as siderite (Menikea et al., 2020; Puyol et al.,2018) and consequently the non-released of H_2 (see discussion section) as well as the no consumption of H^+ (Eq. 1). For this reason, NaOH (around 5.5 mL 2M NaOH) was added to reactors containing PZVI and SZVI and consequently CH_4 increased. At the end of the 3rd cycle (113 day), the reactors initially received 25 g/L and 50 g/L of PZVI, generated the highest CH_4 (15.9 and 15.8 mLCH_4/mLCW, respectively), whereas the reactors with 25 g/L and 50 g/L SZVI generated 13.3 and 11.7 mLCH_4/mLCW, respectively (**Fig. 3-9b**). The control reactors, with pH regulation, on day 113 produced 13 and 3 mL CH_4/mL CW, respectively. On the other hand, the reactors with 100 g/L SZVI and 100 g/L PZVI demonstrated significantly lower CH_4 production than the other ZVI-containing reactors (see discussion section) and were thus excluded from the 4th batch cycle.

During the 4th batch cycle (75 mL CW), the same trend as in the 3rd cycle was followed, and NaOH was added to all reactors to raise the pH. As shown in **Fig. 3-9b**, the reactor with 50 g/L SZVI exhibited a continuous increase in CH_4 production, reaching 13.9 mL CH_4/mL CW by day 201, while the control reactor (pH reg.) produced 12 mL CH_4/mL CW. In contrast, the reactors with 25 g/L PZVI, 50 g/L PZVI, and 25 g/L SZVI produced less CH_4 than the control.

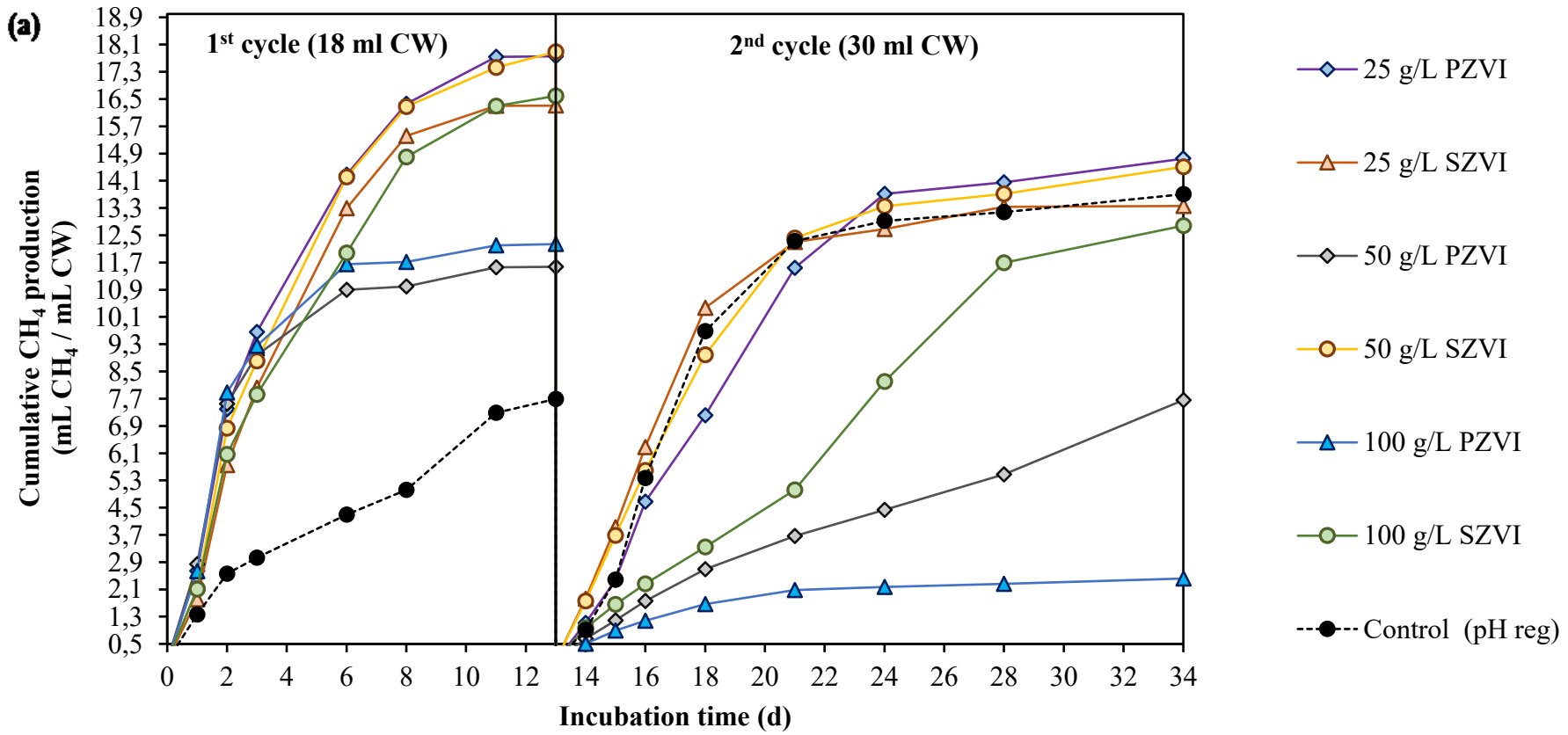
(a)
1st cycle (18 ml CW)
2nd cycle (30 ml CW)
Cumulative CH4 production (mL CH4 / mL CW)
Incubation time (d)
25 g/L PZVI
25 g/L SZVI
50 g/L PZVI
50 g/L SZVI
100 g/L PZVI
100 g/L SZVI
Control (pH reg)

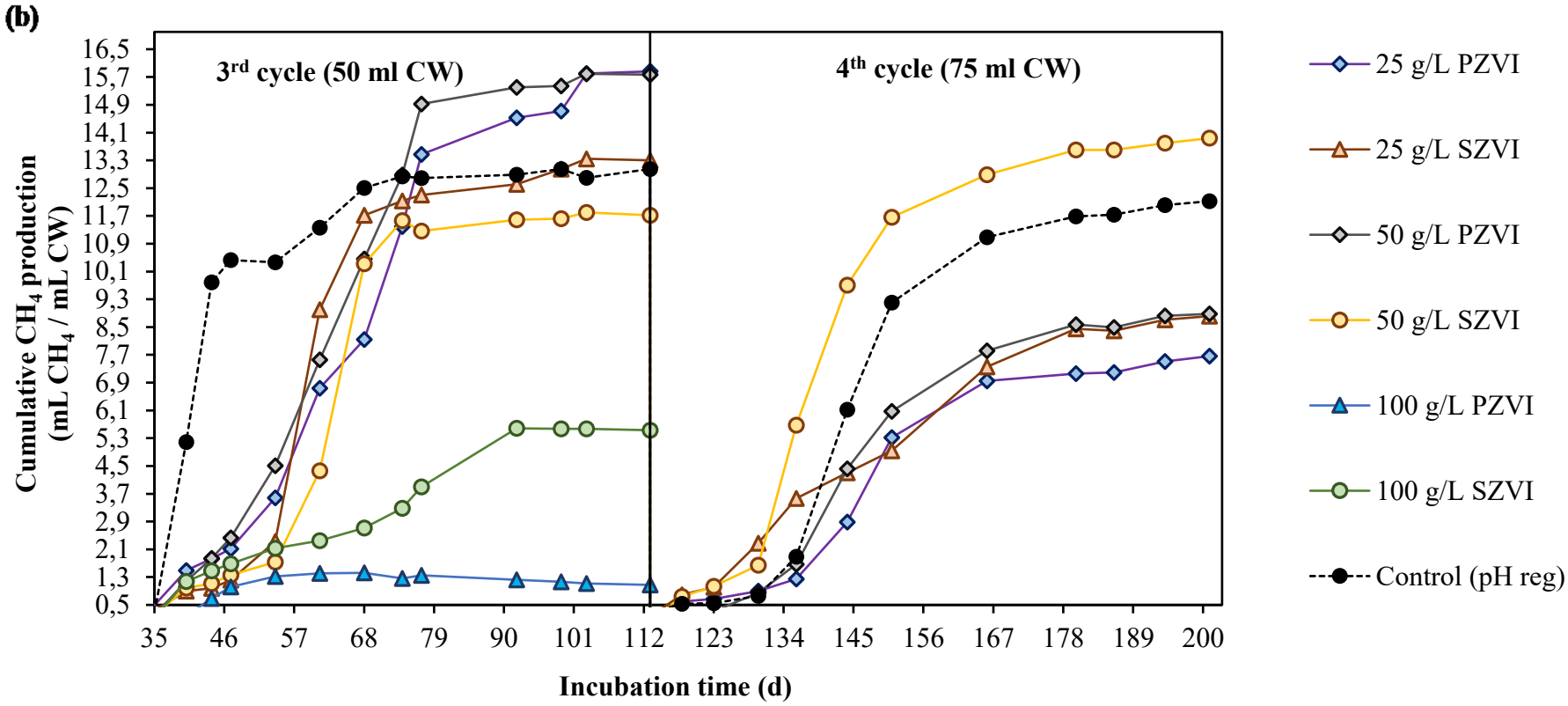

Figure 3-9. Cumulative CH_4 production during AD of CW at different concentrations of PZVI and SZVI. (a) 1st cycle (18 mL CW) and 2nd cycle (30 mL CW); (b) 3rd cycle (50 mL CW) and 4th cycle (75 mL CW)

3.2.3 Effect of powder and scrap ZVIs on methane composition

As shown in **Fig. 3-10a**, the addition of PZVI and SZVI significantly influenced the CH_4 composition in the biogas during the AD of CW. In the first 13 days (18 mL CW), a CH_4 composition higher than 90% was observed in all reactors in which PZVI was added. Particularly, on the 13th day, reactors containing 25 g/L of PZVI demonstrated a CH_4 content of 95.7%. On the same day, reactors that received 25 g/L, 50 g/L, and 100 g/L of SZVI reported CH_4 concentrations of 75.4%, 86.1%, and 92.1%, respectively. In contrast, the control reactors (pH reg.) generated biogas with a CH_4 content of 42.8% (**Fig. 3-10a**)

During the 2nd cycle (30 mL CW), reactors with 25 g/L PZVI demonstrated their superiority by maintaining a stable CH_4 composition, ranging between 95.9%-98.06% from days 24 to 34. In contrast, the reactor with 100 g/L SZVI displayed variable CH_4 composition levels, fluctuating between 85.7% and 97.7%. On day 34, reactors with 50 g/L PZVI and 50 g/L SZVI achieved methane compositions of 95.6% and 95.9%, respectively, as depicted in **Fig 3-10a**. The control reactor (pH reg.) produced biogas with a 74.5% CH_4 content.

Fig. 3-10b illustrates the CH_4 composition in biogas during the 3rd (50 ml CW) and 4th batch (75 ml CW) cycles. As reported in Section 4.1, NaOH was introduced to reactors containing PZVI or SZVI during these cycles to achieve the desired pH levels. In the 3rd cycle, reactors with 25 g/L and 50 g/L PZVI, as well as 50 g/L SZVI, exhibited a gradual increase in CH_4 composition. After day 61, these reactors surpassed a 90% CH_4 composition. From day 61 to day 112, the control reactor (pH reg.) stabilized its CH_4 composition at around 67%. In the 4th cycle (75 mL CW), only the reactor with 50 g/L PZVI generated biogas with a CH_4 content higher than 90%. In contrast, the other reactors exhibited approximately 70% CH_4 composition in the produced biogas, as shown in **Fig. 3-10b.** Interestingly, although the reactor with 50 g/L PZVI demonstrated lower cumulative CH_4 production compared to the reactor with 50 g/L SZVI, as detailed in Section 3.2.2, it maintained a methane composition greater than 90%.

In the reactors containing 25 g/L and 50 g/L of both PZVI and SZVI, as well as a control (pH reg.), a notable pattern in biogas composition was observed during the initial two days of all batch cycles. The H_2 content in the biogas initially surged to approximately 20% and then declined to around 0.5% by the fourth day. This initial increase in H_2 can be attributed to a) the anaerobic degradation of lactose (Charalambous et al., 2020) and b) the anaerobic oxidation of PZVI and SZVI, respectively (Eq. 1). These processes occurred concurrently with the microbial utilization of H_2 and CO_2 according to Eq. 2 and Eq. 3.

Eq.1:

$$Fe^{(0)} + HCO_3^- + H^+ \rightarrow FeCO_3^- + H_2 \qquad (\Delta G^0 = -79.9 \text{ kJ/mol})$$

Eq.2:

$$4H_2 + CO_2 \rightarrow CH_4 + 2H_2O \qquad (\Delta G^0 = -131 \text{ kJ/mol})$$

Eq.3:

$$4H_2 + 2CO_2 \rightarrow CH_3COO^- + H^+ + 2H_2O \qquad (\Delta G^0 = -95 \text{ kJ/mol})$$

On the other hand, reactors containing higher concentrations of ZVI, such as 100 g/L PZVI and 100 g/L SZVI, exhibited different dynamics. These were characterized by a significant initial increase in H_2, which likely hindered methanogenesis. This observation is supported by the results on total CH_4 production in the previous section (see Section 3.2.1) and the significant accumulation of volatile fatty acids (VFAs) (see Section 3.2.4).

Overall, the reactors that received 25 g/L and 50 g/L of PZVI or SZVI, respectively, on day 1 demonstrated significantly higher performance compared to the control reactors during the first two batch cycles (34 days), with the CH_4 composition in the produced biogas exceeding 85%. Moreover, no additional NaOH was added to these reactors during the first two cycles. However, NaOH was introduced to all ZVI reactors in the 3rd cycle (50 ml CW), indicating a decline in ZVI activity after the 2nd cycle. Following the addition of NaOH, the reactors with 50 g/L PZVI exhibited superior performance in terms of total CH_4 production and CH_4 composition compared to the control reactors. In contrast, during the 4th cycle,

only the reactors with 50 g/L SZVI showed higher total CH_4 production than the control reactor (pH reg.) (**Fig. 3-10b**).

In summary, the reactors containing 25 g/L PZVI and 50 g/L SZVI significantly outperformed the control reactors (pH reg.) in terms of total CH_4 production, CH_4 composition, and maintaining a pH above 6.7 without the addition of an alkaline buffer (NaOH) during the1st and 2^{nd} batch cycles (total 34 days), respectively. For this reason, the composition of volatile fatty acids (VFAs) and the techno-economic analysis are presented for these two cycles in Sections 3.2.4 and 3.2.5

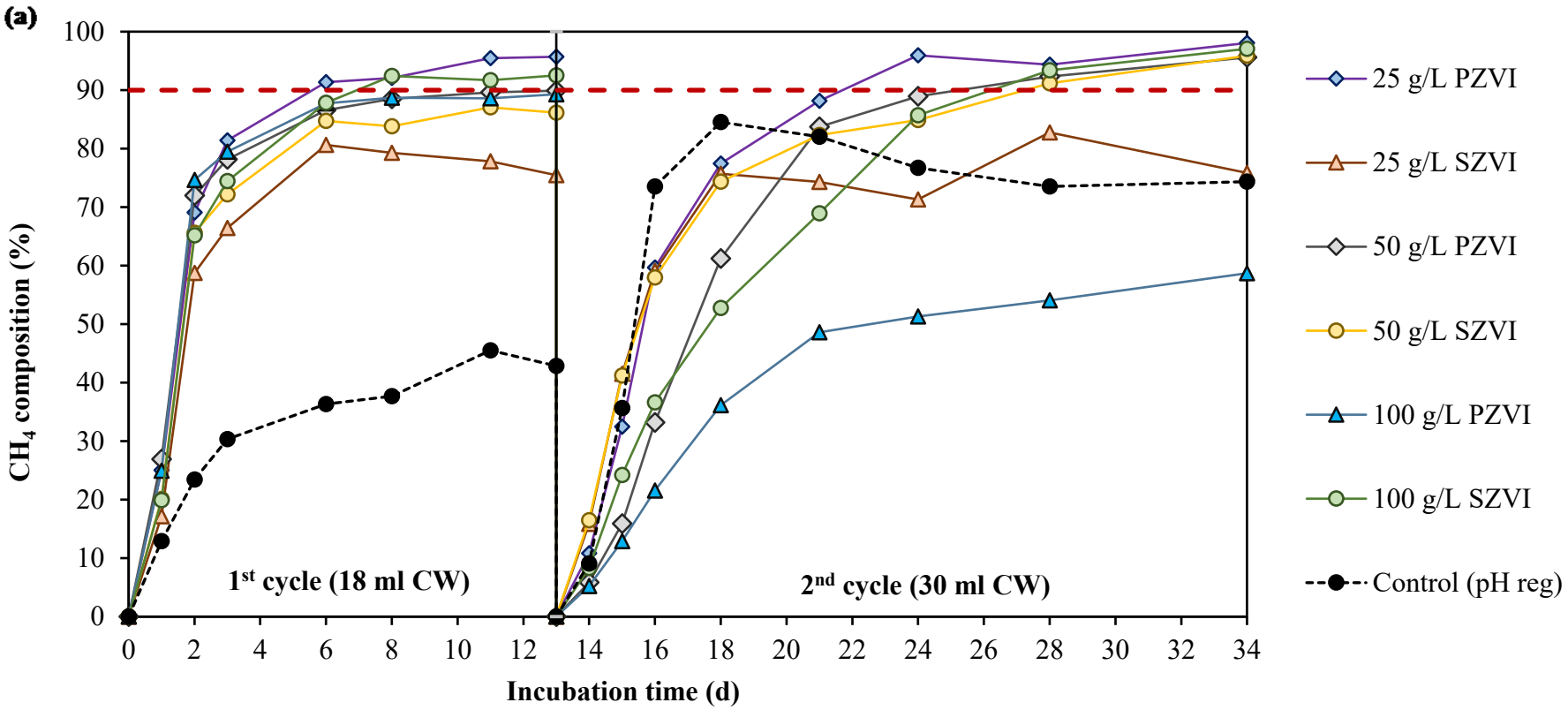
(a)
CH4 composition (%)
Incubation time (d)
1st cycle (18 ml CW)
2nd cycle (30 ml CW)
25 g/L PZVI
25 g/L SZVI
50 g/L PZVI
50 g/L SZVI
100 g/L PZVI
100 g/L SZVI
Control (pH reg)

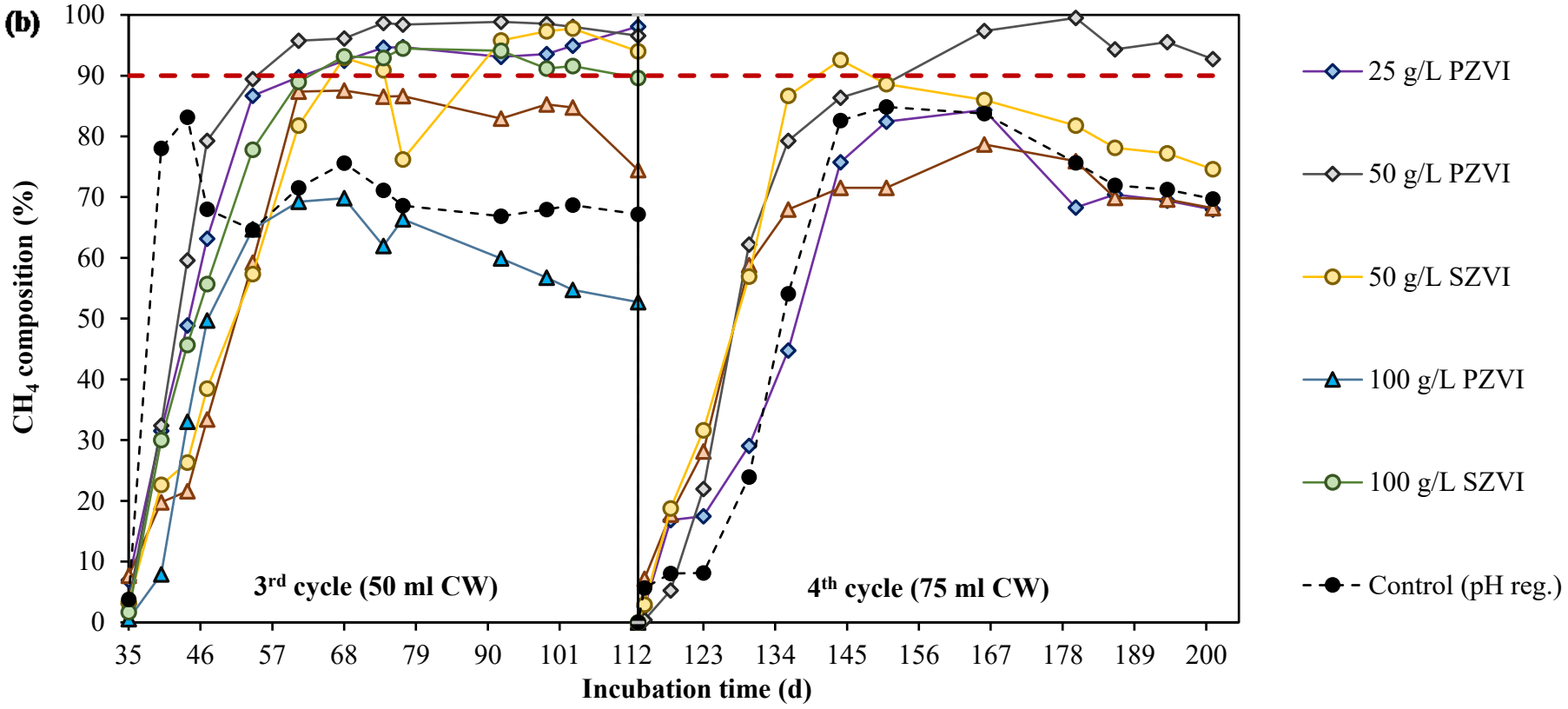

Figure 3-10. Methane composition in produced biogas during AD of CW at different concentrations of PZVI and SZVI (a) 1st cycle (18 mL CW) and 2nd cycle (30 mL CW); (b) 3rd cycle (50 mL CW) and 4th cycle (75 mL CW)

3.2.4 Effect of powder and scrap ZVIs on VFA composition

Fig. 3-11 and **Fig. 3-12** illustrate the changes in volatile fatty acids (VFAs) content during the1st (18 mL CW) and 2nd (30 mL CW) cycles, respectively, under various concentrations of PZVI and SZVI. During the 1st cycle, the control reactor (pH reg.) recorded a VFA concentration of 1196 mg/L on day 2, which decreased to 904 mg/L by day 13. However, among the reactors treated with PZVI, only the reactor containing 25 g/L PZVI exhibited a significant reduction in VFAs, from 964 mg/L on day 2 to 27 mg/L on day 13 (**Fig. 3-11a**). This finding underscores the potential of PZVI in VFA reduction. Similarly, during the same period (from day 2 to day 13), all reactors with SZVI addition demonstrated a significant decrease in VFA concentrations (**Fig. 3-11b**).

A similar trend was observed during the 2nd cycle (30 mL CW); the anaerobic reactors with 25 g/L PZVI demonstrated the most effective performance among those treated with PZVI (**Fig. 3-11a**). The control reactor (pH reg.) exhibited a high initial concentration of volatile fatty acids (VFAs), measuring 4599 mg/L on day 6, which then decreased gradually to 1055 mg/L by day 23. In the same cycle, reactors treated with SZVI showed a substantial reduction in VFAs, with concentrations dropping from 2400-3300 mg/L on day 2 to less than 100 mg/L by day 23 (**Fig. 3-11b**).

During the initial days of each cycle, all reactors showed a significant buildup of propionic acid. This accumulation is typically seen as a negative sign in the performance of the AD process. The conversion of propionic acid to acetate and H_2 is considered thermodynamically unfavorable (Eq. 4), and a low H_2 partial pressure below 10.1 Pa is necessary for its biodegradation (Zhen et al., 2015).

Eq. 4

$$CH_3CH_2COO^- + 3H_2O \rightarrow HCO_3^- + CH_3COO^- + H^+ + 3H_2 \qquad (\Delta G^0 = +76.1 \text{ kJ/mol})$$

However, as shown in Fig. 4-4a and Fig. 4-4b, in reactors where 25 g/L PZVI, 25 g/L SZVI, 50 g/L SZVI and 100 g/L SZVI were added, propionic biodegradation was feasible probably through H_2 utilization. The H_2 released

through the ZVI oxidation (Eq. 1) could have enriched the hydrogenotrophic methanogens (Eq. 2), and homoacetogens (Eq. 3), and these microorganisms could have rapidly utilized the H_2, creating favorable conditions for propionic bioconversion. In a previous study, Meng et al. (2013) found that the propionate conversion rate was increased from 43-77 % to 67-89 % by adding 5 g/L of powder ZVI in an acidogenic reactor with propionate as the sole carbon source. Importantly, no significant reduction in propionic acid was detected in reactors containing 50 and 100 g/L PZVI, respectively (**Fig. 3-11a**). It is likely that at these concentrations, the rate of H_2 production from the anaerobic oxidation of ZVI (Eq.1) exceeded the rate at which hydrogenotrophic methanogens or homoacetogens could utilize it. Consequently, this imbalance did not facilitate the bioconversion of propionate.

During the 2nd cycle (30 ml CW), a higher concentration of butyric acid was observed compared to the 1st cycle (18 mL CW). This increase in butyric acid could be attributed to the lower pH values during the 2nd cycle. At lower pH values, butyrate, and acetate are the main fermentation products during CW anaerobic biodegradation (Charalambous et al., 2020; Lagoa-Costa et al., 2020). However, in the reactors with 25 g/L PZVI, 25 g/L SZVI, 50 g/L SZVI, and 100 g/L SZVI, a significant reduction in the concentrations of butyric, propionic, and acetic acids was observed at the end of the 2nd cycle (30 mL CW) (**Fig. 3-12a** and **Fig. 3-12b**). On the other hand, the reactors with 50 and 100 g/L PZVI respectively showed the same trend as in the 1st cycle, with a slight reduction in the level of VFAs. Kong et al. (2016) found that the addition of scrap metal ZVI to acidogenic reactors decreased the fractional content of butyric acid from 30-40% to 0%.

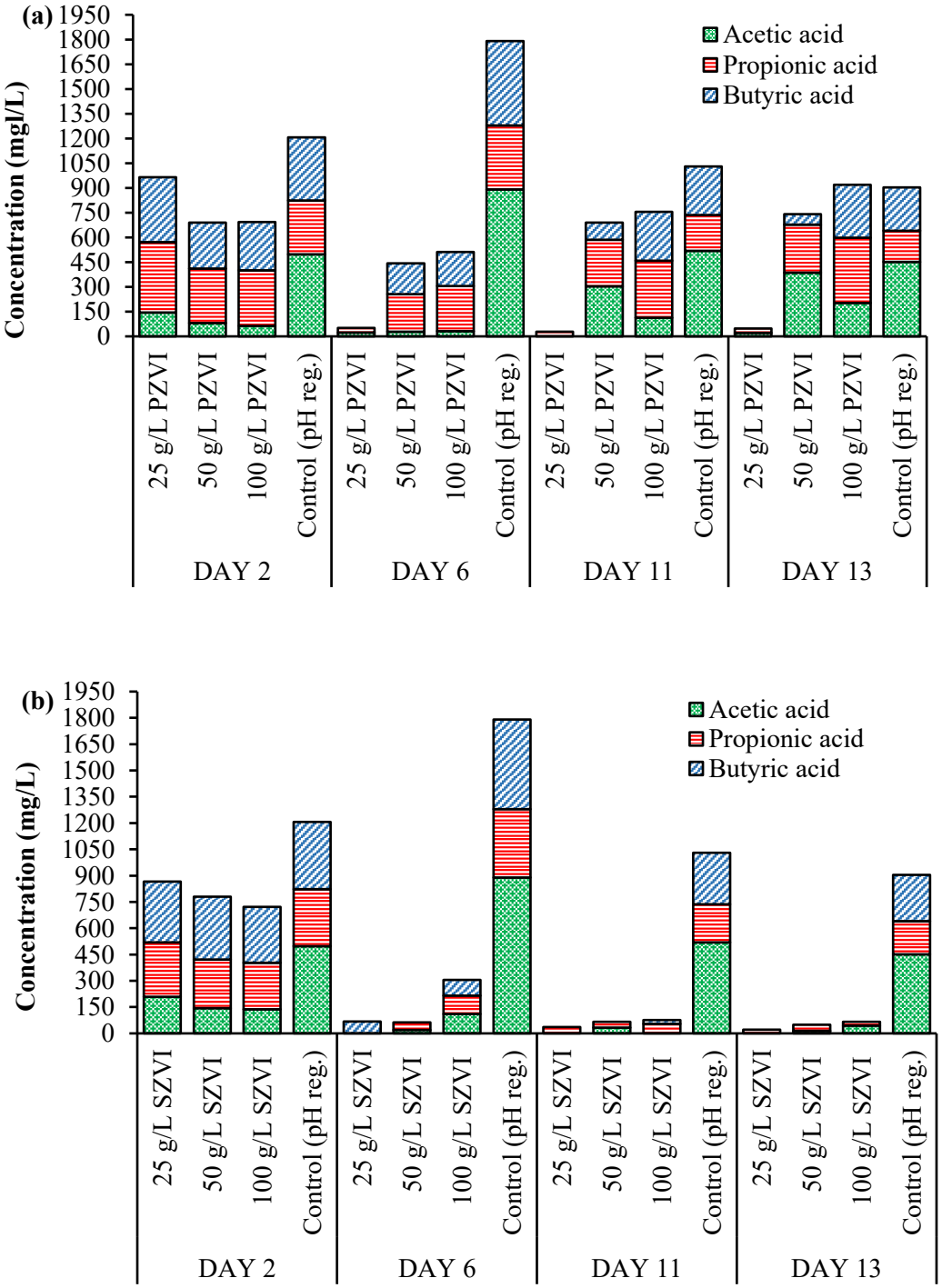

Figure 3-11. Variations in VFA composition during the 1st batch cycle (18 mL CW) of digestion process with different SZVI and PZVI concentrations. (a) variations in the VFA composition at various PZVI concentrations; (b) variations in the VFA composition at various SZVI concentrations.

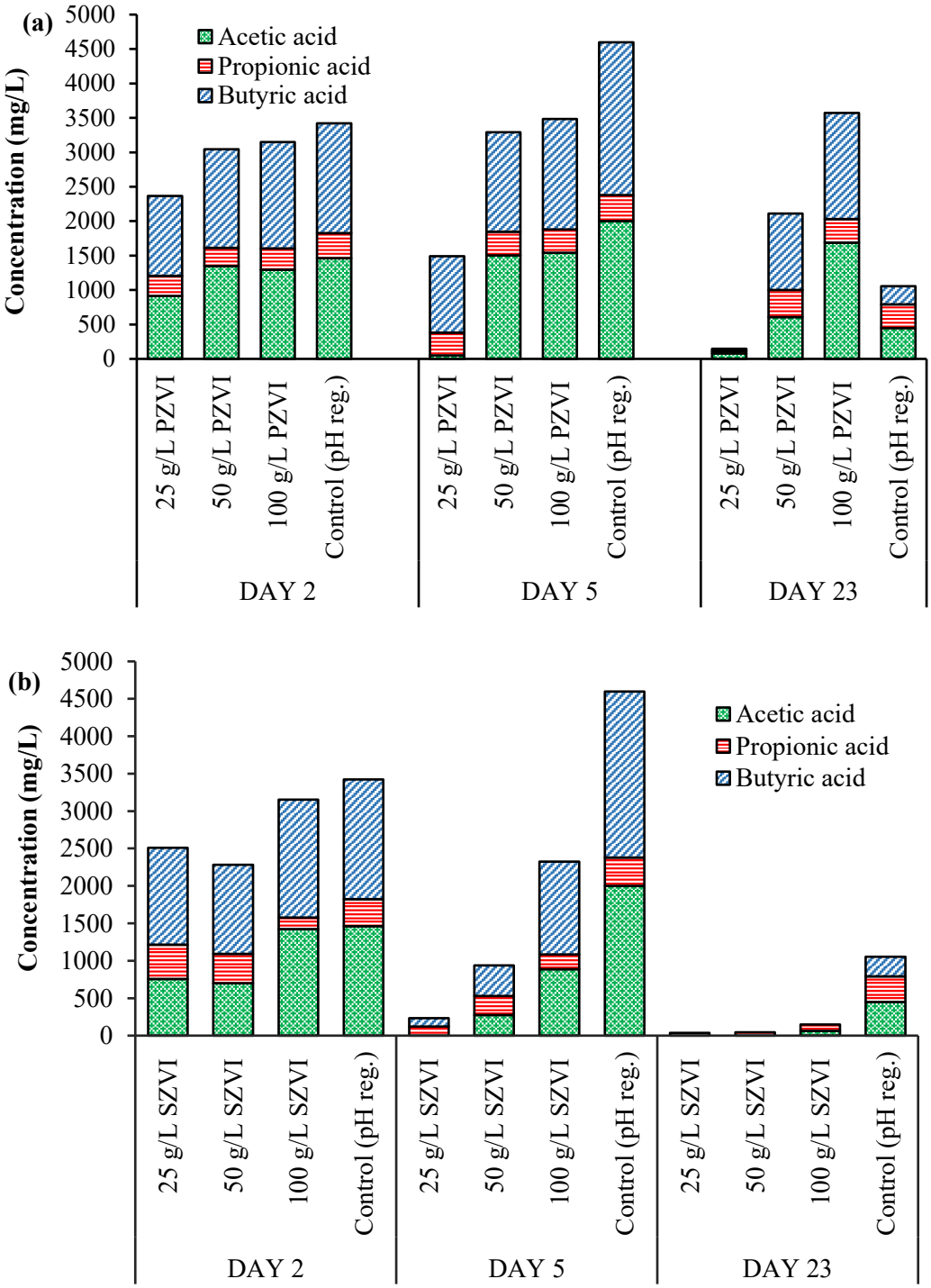

Figure 3-12. Variations in VFA compositions during the 2nd batch cycle (30 mL CW) of digestion process with different SZVI and PZVI concentrations. (a) variations in the VFA composition at various PZVI concentrations; (b) variations in the VFA composition at various SZVI concentrations.

3.2.5 Hydrogen production with 25 g/L PZVI and 50 g/L SZVI under abiotic conditions

Fig. 3-13 presents the evolution of H_2 under abiotic batch conditions with concentrations of 25 g/L PZVI and 50 g/L SZVI in the presence of CW and initially flushed with CO_2. 25 g/L powder ZVI produced H_2 at a faster rate compared to 50 g/L scrap -ZVI. After 7 days, 25 g/L PZVI generated 14.8 ml H_2 per g of ZVI (98.9% H_2), while 50 g/L SZVI produced only 2.1 ml H_2 per g of ZVI (28.5% H_2). Therefore, the superior performance of anaerobic granular sludge when exposed to 25 g/L PZVI is likely attributable to PZVI's higher H_2 production compared to 50 g/L SZVI. However, even in the presence of anaerobic granular sludge and 25 g/L PZVI, the levels of H_2 remain relatively low (less than 1%). This suggests that the H_2 produced by 25 g/L PZVI is rapidly consumed by homoacetogens and methanogens, keeping the H_2 levels low in the system.

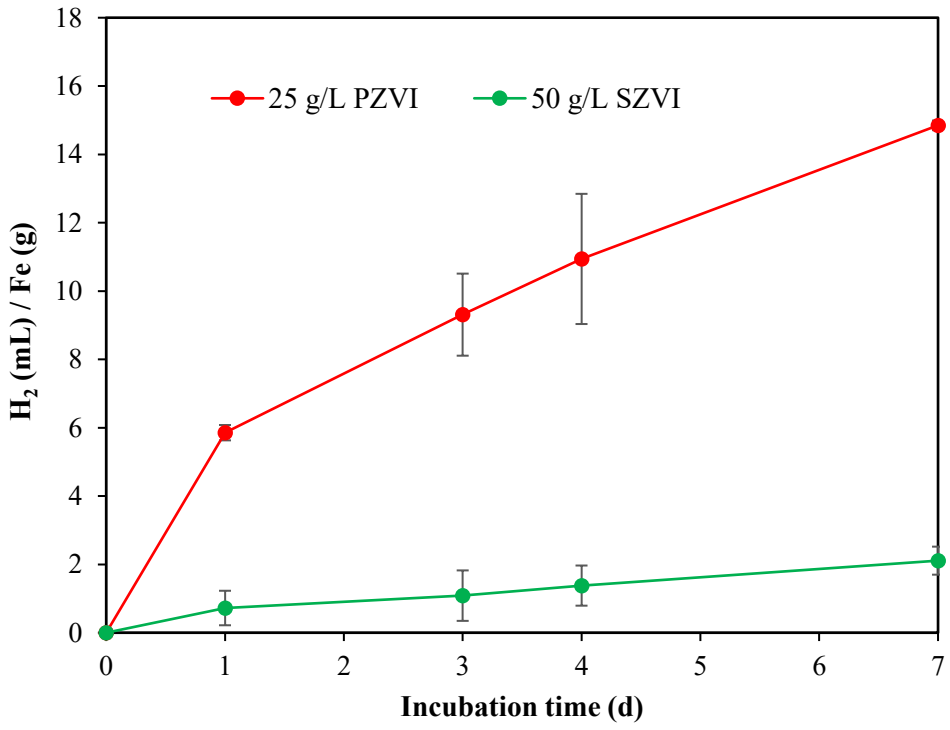

Figure 3-13. Hydrogen production in the presence of 25 g/L PZVI and 50 g/L SZVI under abiotic conditions with CW and initially flushed with CO_2

3.2.6 Economic comparison of CW treatment with 25 g/L PZVI and 50 g/L SZVI

In this study, across the initial 2 cycles (total 34 days-1st cycle tCOD: 11.6 g/L and 2nd cycle tCOD 18.6 g/L), the addition of 25 g/L PZVI and 50 g/L SZVI to anaerobic reactors significantly increased CH_4 production from CW and reduced CO_2 in the produced biogas. Notably, throughout this period (total 34 days), the addition of 25 g/L PZVI and 50 g/L SZVI stabilized the pH without the need for NaOH.

A desktop scaling-up study was conducted to evaluate the economic potential of conventional AD of CW with 25 g/L PZVI and 50 g/L SZVI, using data from the large dairy factory in Cyprus, Charalambides Christis Ltd (Charalambous et al., 2020). These ZVI concentrations were chosen because they showed the best performance in terms CH_4 production and CH_4 composition among the other concentrations of PZVI and SZVI, respectively. The data from the 2nd cycle (30 mL CW) were selected for scaling up. During the 1st cycle (18 mL CW), the control reactor showed lower performance, likely due to the acclimatization phase. Furthermore, in the 3rd (50 mL CW) and 4th cycles (75 mL CW), the activity of PZVI and SZVI decreased, necessitating the addition of NaOH to maintain neutral pH conditions. Based on the laboratory results three scenarios were examined:

1. Treatment of CW without ZVI addition
2. Treatment of CW with 25 g/L PZVI addition
3. Treatment of CW with 50 g/L SZVI addition

The desktop scaling study aimed to compare these scenarios, considering the benefits from electricity generation via biogas, the costs of NaOH addition, the costs of ZVI addition, and the costs for CW transportation and disposal. It was assumed that the capital costs, including reactor and other equipment costs, as well as labor and maintenance costs, were similar across all scenarios. The costs and benefits of adding PZVI or SZVI were estimated and summarized in **Table 3-3**. The large dairy factory produces 29,638 m^3 of CW annually, and another company's annual cost for transportation and treatment is 93,360 euros. It was assumed that the excess sludge from anaerobic digestion of CW would be 10% of this volume

and its associated costs (**Table 3-3**).The generated biogas was presumed to be combusted in a cogeneration plant for the simultaneous production of electricity and heat, with efficiencies of 40% and 50%, respectively (Liu et al., 2015).

Based on the experimental data, the analysis indicated that the most profitable scenario involves the addition of 50 g/L SZVI to the anaerobic digestion every 34 days, potentially yielding an annual profit of 28,376 euros. Conversely, despite its high laboratory performance in the first two cycles, the addition of 25 g/L PZVI is less economically viable due to its high cost, resulting in an annual loss of 221,525 euros (**Table 3-3**). The scenario without ZVI addition yielded a modest annual profit of 808 euros, primarily due to the costs associated with NaOH consumption for pH buffering. Future studies should consider that, apart from powder ZVI, nano-ZVI was used at even higher costs in other studies (Wei et al., 2018). Puyol et al. (2018) also found that while the addition of ZVI to the anaerobic digestion of domestic waste sludge improved methane production, it did not compensate for the costs of ZVI purchase.

Table 3-3. Cost/benefit analysis of CW treatment based on the 2nd batch cycle (total 21 days): (A) without ZVI addition, with 25g/L PZVI, and with 50g/L SZVI

General parameter	**Values**
Production of CW by a large dairy factory in Cyprus	29,638 m^3/y
Transportation and disposal cost of CW	3.15 €/m^3
Current practice-Annual cost of CW transportation and disposal	**-93,360 €/y**
Assumption for Anaerobic digestion	
Initial Total solids (%)	4.02
Initial Volatile solids (%TS)	18.4
SRT in the anaerobic digester (day)	134 d
HRT in the anaerobic digester (day)	21 d
Standard values	
Methane calorific value	35.3 MJ/m^3CH_4
Cost of electricity in Cyprus for non-households	0.1392 €/kWh
Conversion efficiency of methane to heat	50%[b]
Conversion efficiency of methane to power	40%[b]
Cost of NaOH	0.5 €/kg
CW without ZVI (30% CW, 21 d HRT)	
Annual methane production	406,040 m^3/y
Annual electricity through CHP system	1,591,679 kWh/y
Annual income based on the generated electricity	221,561 €/y
Annual NaOH consumption to maintain the pH	442.835 kg/y
Annual cost of NaOH	-211,417 €/y
Annual cost of sludge transportation and disposal	-9336 €/y
Annual Cost or Profit	**+ 808 €/y**
CW with 25 g/L PZVI (30% CW, 21 d HRT)	
Annual methane production	436,567 m^3/y
Annual electricity through CHP system	1,711,345 kWh/y
Annual income based on the generated electricity	238,219 €/y
Annual consumption of PZVI -25g/L PZVI, 21d HRT	2,468,845 kg/y
Annual cost of PZVI based on 190 € PZVI/ton	-469,080 €/y
Annual cost of sludge transportation and disposal	-9,336 €/y
Annual Cost or Profit	**-221,525 €/y**
CW with 50 g/L SZVI (30% CW, 21 d HRT)	
Annual methane production	429,751 m^3/y
Annual electricity through CHP system	1,684,623 kWh/y
Annual income based on the generated electricity	234,499 €/y
Annual consumption of SZVI -50g/L SZVI, 21d HRT	4,919.9 kg/y
Annual cost of SZVI based on 40 € SZVI/ton	-196,796 €/y
Annual cost of sludge transportation and disposal	-9336 €/y
Annual Cost or Profit	**+ 28,376 €/y**

3.2.7 Discussion

Recently, Menikea et al., (2020) and Samanides et al., (2020) pointed out that ZVI and SZVI are anaerobically oxidized to siderite producing H_2 according to Eq. 1. At the same concentrations of ZVI and SZVI the rate of H_2 production by ZVI was 4-5 times higher compared to SZVI (Menikea et al., 2020) probably due to its higher surface area and smaller particles size. Also, it is known that at a higher concentration of PZVI, the rate of H_2 production increased over time (Vyrides et al., 2018). The findings of the current study are on line with the aforementioned studies (Menikea et al., 2020, Samanides et al., 2020, Vyrides et al., 2018) since the optimum dosage of PZVI was 25 g/L whereas for SZVI was 50 g/L. The generated H_2 from anaerobic oxidation of ZVI (Eq. 1) along with the available CO_2 can be used as substrates for hydrogenotrophic methanogens (Eq. 2) and homoacetogens (Eq. 3) for the generation of CH_4 and acetic acid, respectively (Vyrides et al., 2018). The microbial utilization of H_2 create favorable conditions for Eq. 1 and this contributes to further H_2 released until the formation of an outer surface siderite ($FeCO_3$) on ZVI that prevents the released of H_2. Zhao et al., (2018) also found that ZVI positively contribute to AD of activated sludge through the activity increase of hydrogenotrophic and syntrophic methanogenesis.

The current study found that the PZVI and SZVI had a positive effect only during the first 2 batch cycles (34 days) and not in the 3rd and 4th batch cycles; this could be due to the gradual formation of siderite layer in the outer surface for PZVI and SZVI, respectively which it could block the furthered released of H_2 and the consumption of H^+ according to Eq.1 (Menikea et al., 2020).

On the other hand, at higher concentrations of PZVI (100 g/L) and SZVI (100g/L) a fast H_2 production and accumulation was detected; the high partial pressures of H_2 can be inhibitory for acetoclastic methanogenesis and can make fermentation/acidogenesis thermodynamically unfavorable, potentially disrupting the syntrophic relationship between bacteria and methanogens in AD (Yang et al. 2013). Furthermore, at these concentrations (100 g/L PZVI), there is a rapid release of highly soluble ferrous ions. In addition to the reaction Eq.1, these ions may also combine with phosphate to create stable complexes (Hu et al., 2015; Puyol et al., 2018). The lack of available phosphate could potentially inhibit methanogens since

phosphorous is one of the key nutrients for methanogens metabolism (Puyol et al., 2018, Yang et al., 2013). It is also possible for ferrous iron to induce the co-precipitation of other micronutrients necessary for anaerobic sludge.

Several studies (Abdelsalam et al. 2017, Kato et al. 2016, Zhang et al. 2014) stated that ZVI could directly serve as an electron donor for reducing CO_2 into CH_4 through autotrophic methanogenesis. However, the direct extracellular electron uptake mechanisms remain controversial (Kato et al., 2016). In a recent review, Van Steendam et al. (2019) proposed being skeptical of the direct interspecies electron transfer theory in the AD process since several studies proposed these based only on indirect evidence rather than a complex set of methods. In addition, Philips et al. (2018) reported that the main mechanisms of ZVI biocorrosion under microbial anaerobic conditions is H_2 depended and could be due to extracellular components (possibly hydrogenase enzymes) (Deutzmann et al., 2015) or the maintenance of low H_2 concentrations due to utilization (Eq. 2 and 3) by attached cells on ZVI (Menikea et al., 2020).

In the current study, the concentration of 25 g/L PZVI and 50 g/L SZVI were relatively higher compared to other studies (Table 4-2) and this was the key element for the biogas upgrading. In other studies, pointed out a strong indication that the addition of ZVI can increase the CH_4 content (%) in biogas, however the main focused on those studies was the increase in cumulative CH_4 and not the CH_4 composition in biogas. For instance, Xu et al. (2019) reported 99.2 % and 93.4 % CH4 content in AD of blackwater by adding 10 g/L nZVI and 10 g/L mZVI, respectively, compared to the control reactor, which was 80 %. However, at nano-ZVI the biochemical methane potential (BMP) was reduced by 75-81 % relative to the iron-free digester. On the other hand, the anaerobic sludge that received 10 g/L mZVI had the same methane potential as the iron-free digester (**Table 3-4**).

Table 3- 4. Anaerobic digestion of several substrates by addition of ZVI with focus on CH_4 composition in biogas.

Substrate	Type of ZVI and concentration	Performance	CH_4 composition (%) in biogas	Study
Manure	Nano ZVI (0.02 g/L)	159 increment in CH_4 (%) yield	72% CH_4 compared to 60% CH_4 for the control reactor	Abdelsalam et al. (2017)
Excess sludge	Nano ZVI (16.6 g/L)	1304 increment in CH_4 (%) yield	80% CH_4 compared to 52% CH_4 for the control reactor	Hu et al. (2015)
Excess sludge	Nano ZVI (33.3 g/L)	25.3 increment in CH_4 (%) yield	74% CH_4 compared to 52% CH_4 for the control reactor	Hu et al. (2015)
Food waste	Powder ZVI (0.4 g ZVI/g VS $_{\text{of food waste added}}$)	Control operated at around pH 5.3 so not a direct comparison can be done	75% CH_4 compared to 20-30% CH_4 for the control reactor	Kong et al. (2016)
Waste activated sludge	Rusty scrap ZVI (10 g/L)	CH_4 yield increase by 29.5 % by rusty scrap ZVI in anaerobic sludge compared to sludge free of iron	62.9% CH_4 compared to 57.7% CH_4 for the control reactor	Zhang et al. (2014)
Excess sludge	Scrap iron (2.385 g/L)	38.3 increment in CH_4 (%) yield	62-79% CH_4 compared to 62.9-75.5% CH_4 for the control reactor	Zhen et al., (2015)
Food waste	Scrap iron (25 g/L of the mixed organic wastes)	12.2 % Increment in CH_4 (%) yield	72% CH_4 compared to 48% CH_4 for the control reactor	(Cheng et al., 2020)
Blackwater	Nano ZVI (10 g/L)	Decrease of BMP by 75-81%	99.2% CH_4 compared to 80 % CH_4 for the control reactor	Xu et al. (2019)
Blackwater	Micro ZVI (10 g/L)	Similar BMP as the iron free digester	93.4 % CH_4 compared to 80 % CH_4 for the control reactor	(Xu et al. (2019)
Cheese whey	Powder ZVI (25 g/L)	1st cycle: 55% higher total CH_4 (mL) than the control 2nd cycle: 5% higher total CH_4 (mL) than the control	1st cycle: 95.7 % CH_4 compared to 42.8% CH_4 for the control 2nd cycle: 97.1 % CH_4 compared to 74.5% CH_4 for the control	Present study
Cheese whey	Scrap ZVI (50 g/L)	1st cycle: 33.6% higher total CH_4 (mL) than the control 2nd cycle: 5% higher total CH_4 (mL) than the control	1st cycle: 86.1% CH_4 compared to 42.8% for the control reactor 2nd cycle: 97.0% CH_4 compared to 74.5% for the control reactor	Present study

Apart from the use of CH_4 in CHP engine for electricity generation, this study shows the potential of biogas upgrading to CH_4 and its addition to the natural gas grid. Various physicochemical processes are the main technologies used for biogas upgrading, which are highly efficient but expensive, require complex technical equipment and result in methane losses (Muñoz et al., 2015).

In recent years, it was pointed out that biogas upgrading can also be implemented by power-to-gas technology using hydrogenotrophic methanogens that convert the CO_2 and to CH_4. The external H_2 gas is added from a separate electrochemical process unit (electrolysis), which splits water into H_2 gas and O_2 by utilizing surplus renewable electric power (Schiebahn et al., 2015, Angenent et al., 2018). Therefore, this process consisted of two steps: 1) electrolysis ($4H_2O \rightarrow 4H_2 + 2O_2$); and 2) biomethanation by hydrogenotrophic methanogens (Eq. 2). One of the current drawbacks of this process is the relatively high cost of electrolysis (Schiebahn et al., 2015, Angenent et al., 2018.) and the integration of various systems such as electrolysis process, and H_2 addition to anaerobic digester.

However, in recent reviews (Jiang et al., 2019, Prévoteau et al., 2020), no pilot or full scale microbial electrosynthesis study has been reported to date and one of the main challenges in this process is the cost reduction (Jiang et al., 2019). On the other hand, this study found that the addition of 50 g/L of SZVI in AD treating CW can produce biogas with higher than 90 % CH_4 content without the complicate configuration of electrolysis (electrodes, connection with power supply and proton exchange membrane in case of microbial electrosynthesis) (Angenent et al., 2018).

Conclusions of Chapter 2

The current chapter explores a novel method to mitigate acidification and enhance the anaerobic digestion (AD) performance of cheese whey (CW) through the addition of zero-valent iron (ZVI) in the forms of powder and scrap shavings at concentrations of 25, 50, and 100 g/L, respectively. The experiments were conducted under 4 consecutive CW feeding (18, 30, 50 and 75 ml) for 201 d. The results indicate that reactors supplemented with 25 g/L of powder ZVI (PZVI) and 50 g/L of scrap ZVI (SZVI) demonstrated notably better performance during the first two cycles. These reactors not only produced a higher cumulative CH_4 production compared to control reactors without ZVI but also achieved a CH_4 composition exceeding 95% in the biogas, in contrast to the 74% observed in the reactors without ZVI. Specifically, the reactors with 25 g/L PZVI and 50 g/L SZVI yielded 17.8 mL CH_4/mL CW and 17.9 mL CH_4/mL CW, respectively.

Additionally, during this period, no NaOH was required to adjust pH levels in the reactors containing 25 g/L PZVI and 50 g/L SZVI. After the 2nd batch cycle, volatile fatty acids (VFAs) concentration was markedly lower in these reactors than in those without ZVI. However, no beneficial effects of ZVI as an alkaline buffer were observed during the 3rd and 4th cycles, likely due to the inactivation of the outer surface layer of ZVI and/or due to the higher amount of CW that was added that generated higher amount of VFAs.

From an economic perspective, the AD of CW with 50 g/L SZVI proved more cost-effective, yielding an annual profit of €28,376, compared to an annual cost of €221,525 for the treatment with 25 g/L PZVI and a modest profit of €808 for the process without any ZVI addition. This study provides a compelling proof of concept for in-situ biogas upgrading and the alleviation of acidification through the strategic addition of 50 g/L SZVI or 25 g/L PZVI during the anaerobic digestion of cheese whey. This approach not only underscores the operational benefits but also emphasizes the financial viability of incorporating ZVI in biogas production systems.

3.3 Chapter 3: Enhancing biogas production from CW using ZVI: A comparative analysis of batch and semi-continuous operation modes

In the previous chapter (see Chapter 2), we investigated the impact of two forms of ZVI (powder and scrap) at three concentrations (25 g/L, 50 g/L, and 100 g/L) on the anaerobic treatment of cheese whey (CW) under batch conditions. The results demonstrated that 25 g/L PZVI and 50 g/L SZVI significantly enhanced CH_4 production and upgraded biogas quality, achieving more than 95% CH_4 content. This improvement was accompanied by a substantial reduction in volatile fatty acid (VFA) concentrations compared to the control reactor. In contrast, the control reactor showed lower CH_4 production and required substantial additions of NaOH to balance pH levels. However, the effects of ZVI in semi-continuous CW feeding and its impact across various stages of anaerobic digestion, such as solubilization/hydrolysis, acidogenesis, and methanogenesis, remain to be thoroughly explored.

Building on the previous findings (see Chapter 2), this study examined the impact of 25 g/L PZVI and 50 g/L SZVI on the performance of AD using CW as a feedstock in a semi-continuous operation across various organic loading rates (OLRs). To facilitate a more effective performance comparison, batch reactors were operated in parallel, each employing the same types and concentrations of ZVI. Additionally, the impact of ZVI on the solubilization/hydrolysis and acidification stages of AD was investigated by suppressing methanogenesis with 2-bromoethanesulfonate (50 mM). Finally, the microbial profile, including bacteria and archaea, was analyzed to gain comprehensive insights into microbial interactions and responses in batch and semi-continuous reactors.

3.3.1 Performance efficiency in batch operation mode

After 27 days of operation under batch mode, the SCOD removal efficiency of reactors with 25 g/L PZVI, 50 g/L SZVI, and Control were 93%, 71%, and 64.3%, respectively (**Fig. 3-14a**). Correspondingly, the cumulative CH_4 production during the operation period was higher in the reactor with 25 g/L PZVI (341 mL),

followed by the reactor with 50 g/L SZVI (249 mL) and the Control reactor (130 mL) (**Fig. 3-14b**). The theoretical methane was 651 ml CH_4 and only the reactor with 25 g/L PZVI exhibited higher than 50% of the theoretical. In addition, the reactor with 25 g/L PZVI also exhibited a shorter lag phase in CH_4 production. From the perspective of CH_4 content, the results reflected in **Fig. 3-14c** showed that the 25 g/L PZVI exhibited higher than 92% CH_4 composition after 18 days of operation, and this percentage was consistently increased to obtain a biogas upgrading (CH_4 > 95%) for the remaining fermentation time. As depicted in **Fig. 3-14c**, CO_2 composition in the reactor with 25 g/L PZVI was below 10% after 18 days and reduced to less than 1% by day 27. During the first 4 days, H_2 was less than 1% (data not shown); and after the 7^{th} day, no H_2 was detected. The absence of H_2 could be evidence of the immediate utilization of H_2, produced by ZVI, by hydrogenotrophic methanogens (Menikea et al., 2020). After 27 days of batch operation, CH_4 composition reached 97.6%, 73%, and 60% for the reactors with 25 g/L PZVI, 50 g/L SZVI, and Control, respectively (**Fig. 3-14c**). The results demonstrate that the organic removal and methanogenesis rate was notably higher in the reactor supplemented with 25 g/L PZVI compared to the reactor with 50 g/L SZVI and Control, respectively.

Additionally, after 27 days of operation, it was noted that the pH of the medium in the reactor with 25 g/L PZVI increased markedly to a final pH of around 8.31 (with no NaOH addition). On the contrary, the pH value in the reactor with 50 g/L SZVI and Control reactor was around 7.15 and 6.6, respectively (Fig. 5-1d). The increase in pH values due to H^+ consumption via the anaerobic oxidation of ZVI (Eq.1) resulted in the subsequent dissolution part of CO_2 into the aqueous phase which can further explain the high CH_4 content in the biogas generated from the reactor with 25 g/L PZVI addition (**Fig. 3-14c**). Therefore, under batch conditions, ZVI plays a triple role in CO_2 utilization and biogas upgrading: a) a portion of the soluble CO_2 reacts directly with ZVI as shown in Eq.1; b) it elevates the pH (Eq.1), leading to greater absorption of soluble CO_2 c) it generates H_2, which can be utilized by hydrogenotrophic methanogens (Eq.2) for CH_4 production and homoacetogens (Eq.3)for the production of acetic acid. Subsequently, the acetic acid can be further utilized by acetoclastic methanogens for the generation of CH_4 and CO_2 (Eq. 4).

Eq. 1:

$$Fe^{(0)} + HCO_3^- + H^+ \rightarrow FeCO_3^- + H_2 \qquad (\Delta G^0 = -79.9\ kJ/mol)$$

Eq. 2:

$$4H_2 + CO_2 \rightarrow CH_4 + 2H_2O \qquad (\Delta G^0 = -131\ kJ/mol)$$

Eq. 3:

$$4H_2 + 2CO_2 \rightarrow CH_3COO^- + H^+ + 2H_2O \qquad (\Delta G^0 = -95\ kJ/mol)$$

Eq. 4:

$$CH_3COO^- + H^+ \rightarrow CH_4 + CO_2 \qquad (\Delta G^0 = -75.7\ kJ\ mol^{-1})$$

A similar pattern was also observed in the VFA profiles (**Fig. 3-14e**), after 27 days of batch operation, the reactor with 25 g/L PZVI exhibited the lowest total VFA level (149 mg/L), followed by the reactor with 50 g/L SZVI (2504 mg/L), and the Control reactor (3213 mg/L). As shown in **Fig. 3-14c**, acetate, propionate, and butyrate are the predominant acidogenic products in all reactors during the first 14 days of operation. From day 14 to day 18 a significant acetate degradation rate was achieved in the reactor with 25 g/L PZVI, and this indicates high activity of acetoclastic methanogens. The lowest acetate concertation (54 mg/L on day 18) can also be in part attributed to the biogas upgrading in the reactor with 25 g/L PZVI on the same day. On the other hand, a low rate of acetate consumption was found, especially in the Control reactor (HAc: 3415 mg/L on day 18), which may be an indication that the activity of acetoclastic methanogenesis was not high enough to handle the released acetate in the system effectively (**Fig. 3-14e**). Within 27 days of operation, a significant level of both propionate and butyrate remained undegraded in the reactors with 50 g/L SZVI (HPr:1098 mg/L, HBu:1312 mg/L) and Control (HPr:1328 mg/L, HBu:1840 mg/L), while in the reactor with 25 g/L PZVI was almost completely removed (**Fig. 3-14e**). Due to thermodynamic hindrance, the conversion of propionic acid (ΔG^0 = +76.1 kJ/mol) and butyric acid (ΔG^0 = +48.1 kJ/mol) into acetic acid is not spontaneous under conditions of high H_2 partial pressure and high ORP. Consequently, the addition of 25 g/L PZVI promotes the syntrophic relationship between propionic utilizers and

hydrogenotrophic methanogens, as well as the activities of homoacetogens and acetoclastic methanogens. The results from the batch reactors indicated that the supplementation of 25 g/L PZVI and 50 g/L SZVI can positively improve the acidification process of CW mainly by shifting the fermentation pathway away from the propionic type and enhancing acetate production, which is a direct substrate for acetoclastic methanogens.

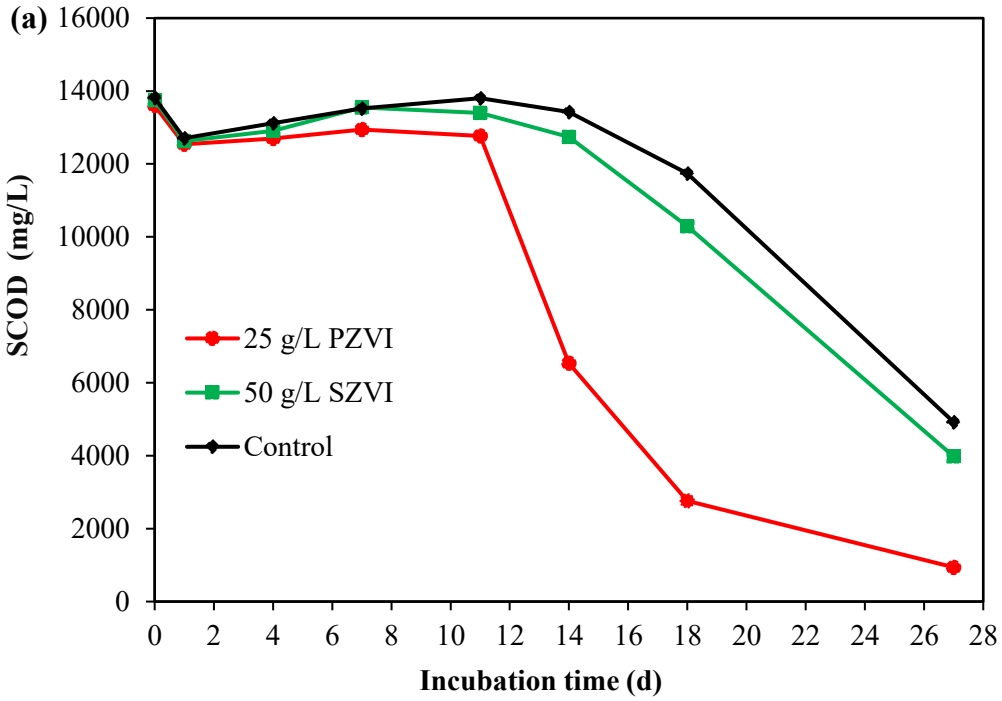

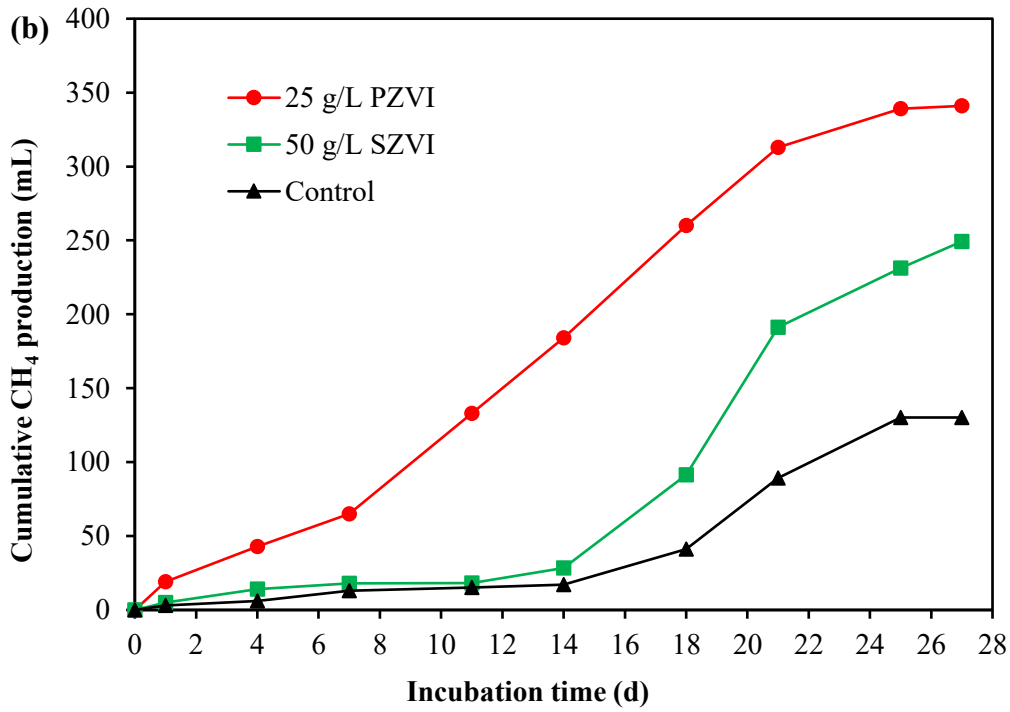
(b)
25 g/L PZVI
50 g/L SZVI
Control
Cumulative CH4 production (mL)
Incubation time (d)

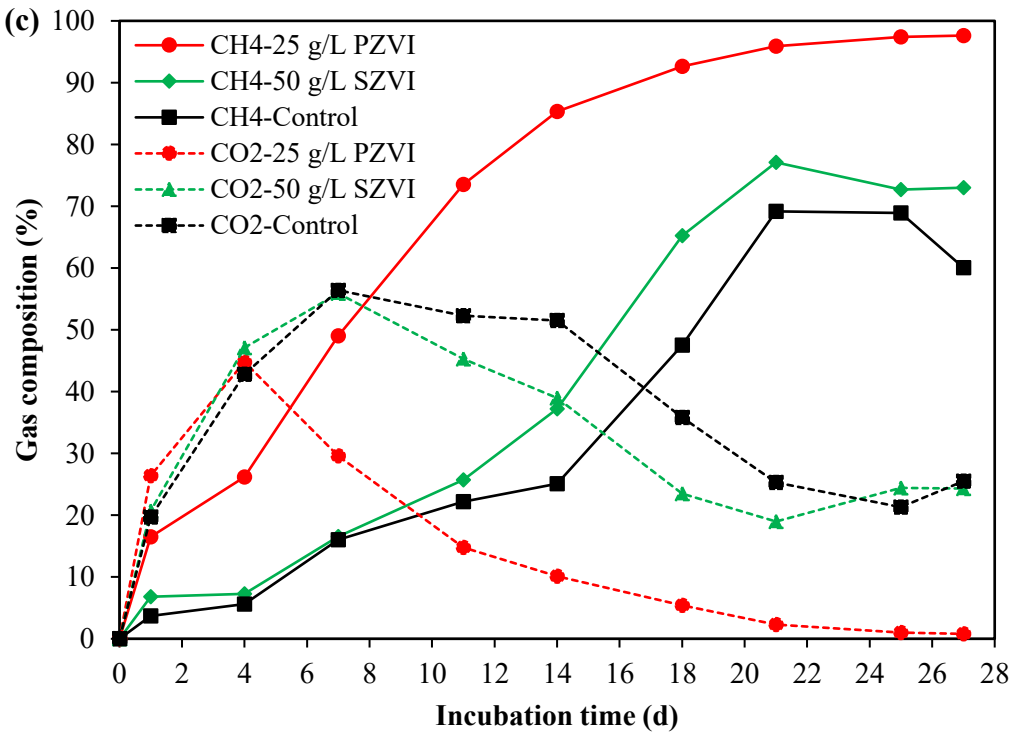
(c)
CH4-25 g/L PZVI
CH4-50 g/L SZVI
CH4-Control
CO2-25 g/L PZVI
CO2-50 g/L SZVI
CO2-Control
Gas composition (%)
Incubation time (d)

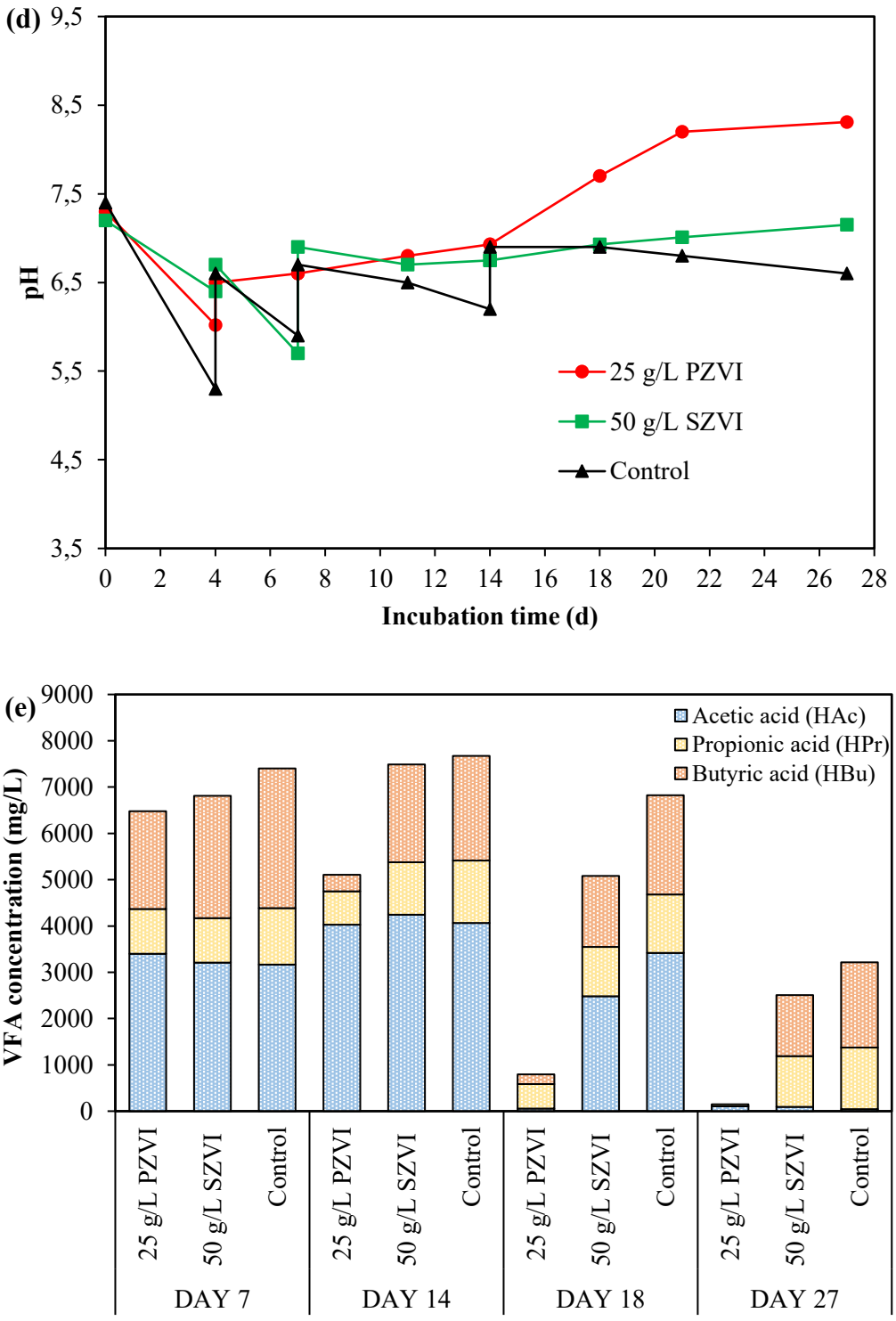

Figure 3-14. Effect of 25 g/L PZVI and 50 g/L SZVI on anaerobic digestion of cheese whey under batch operation mode: (a) SCOD concentration; (b) Cumulative CH_4 production; (c) Gas composition (%); (d) pH and (e) VFA distribution

3.3.2 Performance efficiency in semi-continuous operation mode

3.3.2.1 Effect of ZVI on methane production and composition

The three reactors were fed in a semi-continuous mode with CW under different OLRs for 118 days. As shown in **Fig. 3-15a**, the highest cumulative methane yield (204 $mLCH_4/g\ COD_{added}$) was found in the R25-PZVI reactor, followed by R50-SZVI reactor (177 $mLCH_4/g\ COD_{added}$), and R-Control reactor (161 $mLCH_4/g\ COD_{added}$) (Fig. 5-2a). During operational phase I (0-27 days, OLR 1.6 g COD $L^{-1}d^{-1}$), cumulative methane yield for the R-25 PZVI and R50-SZVI reactors was approximately 31% and 23% higher, respectively, than that for the R-Control reactor. In phase II (27-79 days) at an OLR of 1.7 g COD $L^{-1}d^{-1}$, the R25-PZVI reactor consistently demonstrated a higher CH_4 yield compared to both the R50-SZVI and R-Control reactors. This trend in methane production persisted into phase III (79-104 days, OLR 2 g COD $L^{-1}d^{-1}$), where the cumulative methane yield reached 173 $mLCH_4/g\ COD_{added}$ in the R25-PZVI reactor and 140 $mLCH_4/g\ COD_{added}$ in the R50-SZVI reactor, while the R-Control reactor yielded 136 $mLCH_4/g\ COD_{added}$ (**Fig. 3-15a**).

On the other hand, no significant differences in methane content observed among the three reactors, as the methane content remained relatively stable throughout the 118 days of semi-continuous operation. Specifically, the average CH_4 content in the biogas was 53%, 54%, and 52% for the R25-PZVI, R50-SZVI, and R-Control reactors, respectively (**Fig. 3-15b**). The results suggest that both ZVI types positively affected CH_4 production from cheese whey during semi-continuous operation but had no obvious effect on CH_4 content. Compared to the two ZVI types, 25 g/L powder ZVI showed better performance on CH_4 production than 50 g/L scrap ZVI. Due to its smaller particle size and larger specific surface area, powder ZVI has higher reaction activity than scrap ZVI, leading to rapid H_2 production through surface ZVI oxidation (Eq. 1).

Recently, Constantinou et al. (2022) pointed out that soluble CO_2 acts as a reactant (Eq. 1) with ZVI and produces H_2 and siderite ($FeCO_3$). In our system, CO_2 is produced during the biodegradation of CW and is likely used as a reactant with ZVI. The released H_2 during ZVI oxidation (Eq. 1) can serve as the electron donor

for methanogens, activating the hydrogenotrophic metabolic pathway (Eq. 2). In addition, homoacetogenic bacteria can also utilize H_2 and CO_2, for the production of acetic acid (Eq. 3), which might then be utilized through acetoclastic methanogenesis for CH_4 production (Eq. 4).

Despite the high cumulative methane yield (204 $mLCH_4/g\ COD_{added}$) of R25-PZVI compared to the control, CH_4 content has remained consistent (50-60%) over 118 days of semi-continuous operation and no biogas upgrading was achieved (**Fig 3-15b**). In contrast, under batch operation mode (see section 5.1), a biogas upgrading (95% CH_4) was reported when diluted CW exposed to 25 g/L PZVI.

The fact that no biogas upgrading was achieved could be attributed to the incomplete utilization of H_2. As depicted in **Fig. 3-15c** for 25 g/L PZVI, the H_2 content fluctuated between 3-13% in phase I and reduced to a range of 3-7% in the subsequent phases. The observed disparity between batch and semi-continuous operation modes may likely be due to the differing solubility rates of H_2 and CO_2 under these operational modes. Under batch operation mode, a higher headspace pressure is present, which supports the solubility of H_2 as compared to semi-continuous operation. Similarly, the elevated pH under batch mode (final pH at batch condition being 8.3) promotes enhanced CO_2 solubility. Under alkaline conditions, the conversion of carbonic acid to bicarbonate and to carbonate ions are favourable facilitated more dissolution of CO_2 into the aqueous phase and decreased the concentration of CO_2 in the gas phase (Eq. 5).

Eq. 5:

$$CO_{2(g)} + H_2O_{(aq)} \leftrightarrow H_2CO_3 \leftrightarrow HCO_3^-{}_{(aq)} + H^+_{(aq)} \leftrightarrow CO_2^{-3}{}_{(aq)} + 2H^+_{(aq)}$$

Thus, in batch reactors, the higher CO_2 and H_2 concentration in the aqueous phase resulted in more available substrate for hydrogenotrophic methanogenesis, and therefore, the biogas upgrading (CH_4 >95%) was identified, as discussed in section 3.3.1.

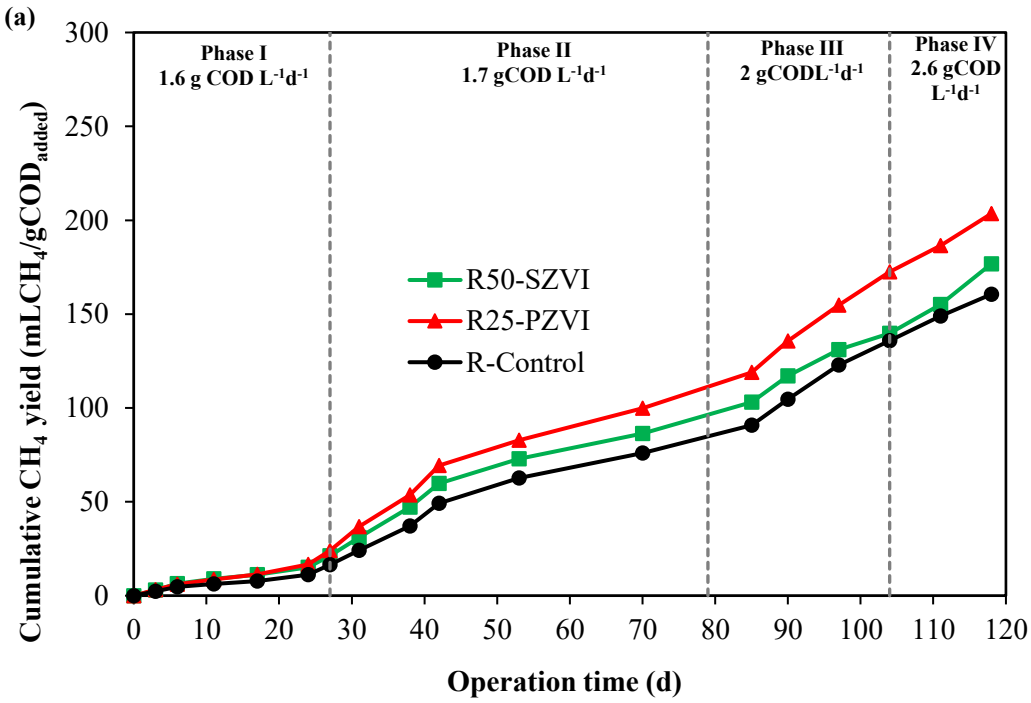
(a)
Phase I
1.6 g COD L-1d-1
Phase II
1.7 gCOD L-1d-1
Phase III
2 gCODL-1d-1
Phase IV
2.6 gCOD
L-1d-1
R50-SZVI
R25-PZVI
R-Control
Cumulative CH4 yield (mLCH4/gCODadded)
Operation time (d)

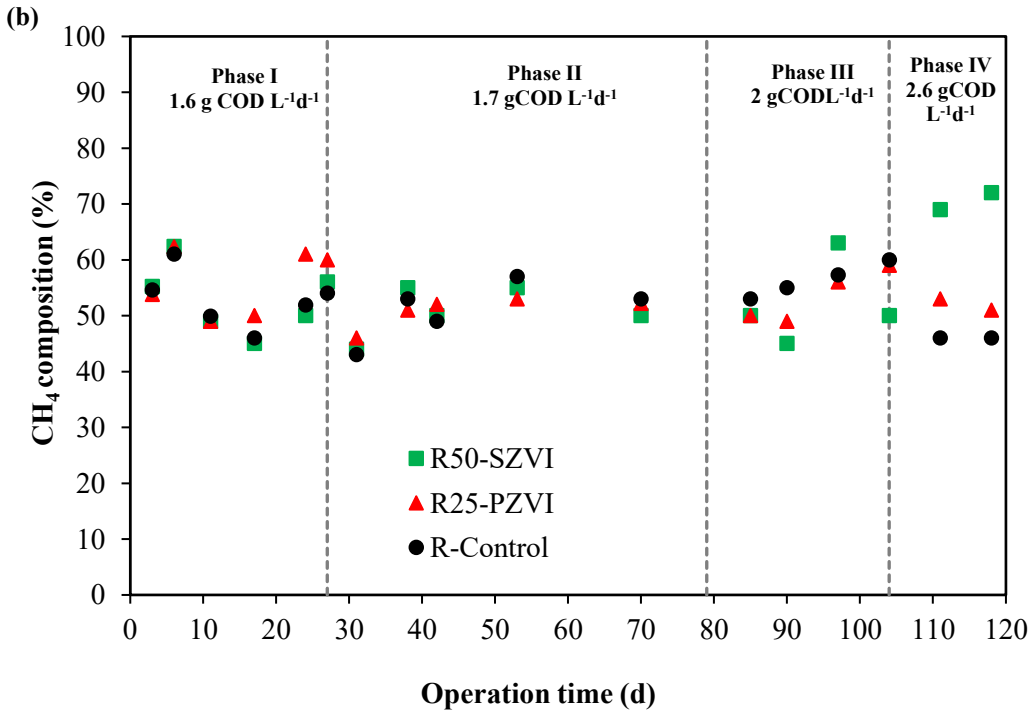
(b)
Phase I
1.6 g COD L-1d-1
Phase II
1.7 gCOD L-1d-1
Phase III
2 gCODL-1d-1
Phase IV
2.6 gCOD
L-1d-1
R50-SZVI
R25-PZVI
R-Control
CH4 composition (%)
Operation time (d)

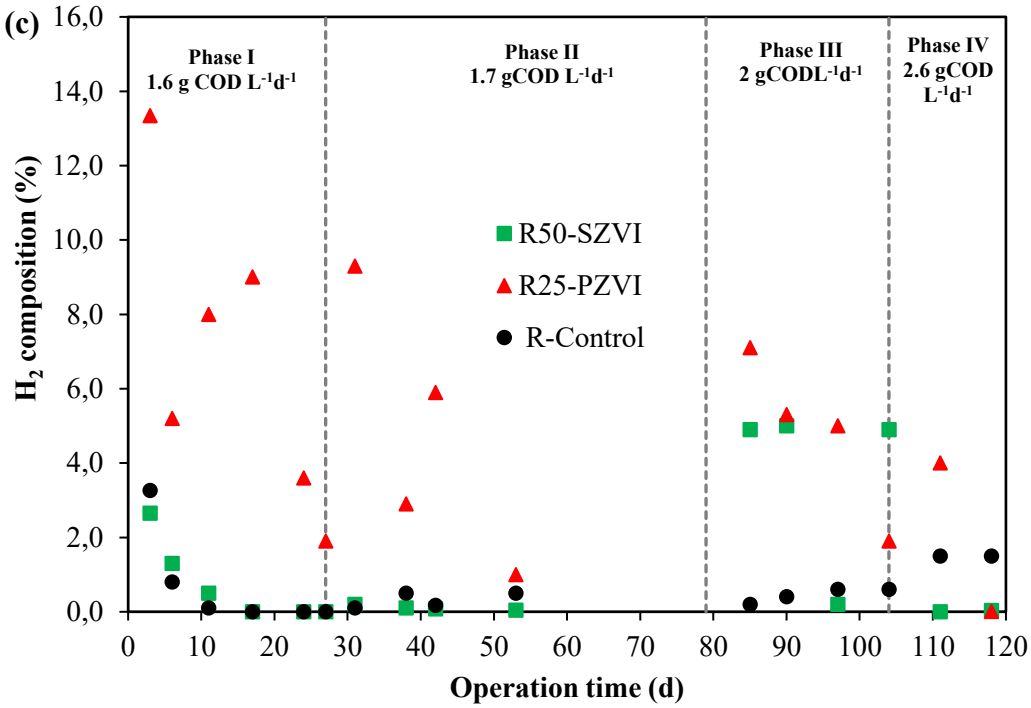

Figure 3-15. Effect of ZVI types on CH_4 production from CW in semi-continuous reactors under different OLRs: (a) cumulative CH_4 yield; (b) CH_4 composition;(c) H_2 composition

3.3.2.2 Effect of ZVI on VFA concentration, VFA/ALK ratio, pH and SCOD

Fig. 3-16a illustrates the difference in total VFA between the three reactors in semi-continuous operation for 118 days. During the first days of phase I (OLR 1.6 g COD $L^{-1}d^{-1}$), total VFA was significantly higher in the R-Control and R25-PZVI reactors than in the R50-SZVI reactor, respectively (**Fig. 3-16a**). As depicted in Fig. 5-2c (see section 3.2.2.1), the H_2 content in the R25-PZVI reactor was remarkably higher than in the R50-SZVI reactor, which is not conducive to the spontaneous thermodynamics of the VFA degradation and contributed to the high VFA accumulation in the R25-PZVI reactor at the begging of operation. The long-term increases in H_2 partial pressure could inhibit the degradation of VFAs due to microbial community imbalances (Feng et al., 2014). Consistent with the high VFA accumulation found in the R-Control reactor as a result of rapid lactose degradation,

the pH decreased to 5.42 (on day 3) and 5.54 (on day 6), suggesting that the reactor was acidified (**Fig. 3-16d**).

The results related to VFA/ALK ratio also confirmed the acid inhibition. As shown in **Fig 3-16b**, the VFA/ALK ratio in R-Control was 0.8 and 0.67 throughout this period (on days 3 and 6, respectively). It is generally known that when the VFA/ALK ratio is higher than 0.4, AD is considered to have a low buffering capacity due to the imbalance in acid-producing bacteria and methanogens (Paepatung et al 2020). To counteract this, the pH was readjusted to 7.16 (on day 3) and 7.14 (on day 6), respectively, using 2 M of NaOH (a total of 11 ml) (**Fig. 3-16d**). In contrast, the average VFA/ALK ratio in R50-SZVI and R25-PZVI reactors was 0.11 and 0.33, respectively, during phase I (0-27 days) (without adding NaOH).

Such differences in the VFA concentration are also reflected in SCOD removal efficiency (**Fig. 3-16c**). During phase I (OLR 1.6 COD $L^{-1}d^{-1}$), R50-SZVI showed better organic removal performance among the three reactors. The average SCOD removal efficiency was 75.2%, 66.9%, and 61.9% for R50-SZVI, R25-PZVI, and R-Control reactors, respectively (**Fig. 3-16c**). As shown in **Fig. 3-16a** from days 27 to 79 at OLR 1.7 g COD $L^{-1}d^{-1}$, VFAs concentration was below 400 mg/L in R25-PZVI while the SCOD removal efficiency fluctuated from 81.2% to 87.1% (**Fig. 3-16c**). On the contrary, average SCOD removal efficiency was 81% and 72% for R50-SZVI and R-Control reactors, respectively, over the same period (**Fig. 3-16c**). The same trend was also found during phases III (79-104 days at OLR 2 g COD $L^{-1}d^{-1}$) and IV (104-118 at OLR 2.6 gCOD $L^{-1}d^{-1}$), respectively, with R25-PZVI consistently resulted in better efficiency in VFAs degradation and organic matter removal than R50-SZVI and R-Control reactors, respectively. In parallel, the average VFA/ALK ratio was 0.13 for the R25-PZVI reactor (**Fig 3-16b**).

Kong et al. (2016) demonstrated that ZVI prevents excessive acidification in food waste AD, maintaining VFA/ALK ratios between 0.01 and 0.02, in contrast to 1.95 for the control reactor. Over the 118 days of semi-continuous operation, the R25-PZVI and R50-SZVI reactors maintained average pH values of 7.56 and 7.35, respectively (**Fig. 3-16d**). In contrast, the R-Control reactor had an average pH value of 6.91, even with NaOH addition. According to Eq 1, the H^+ consumption through the anaerobic corrosion of ZVI increased the pH of the reactor and can

buffer the acids produced by acidogenic bacteria during anaerobic cheese whey (CW) degradation, and this is an addition benefit for using ZVI in anaerobic system.

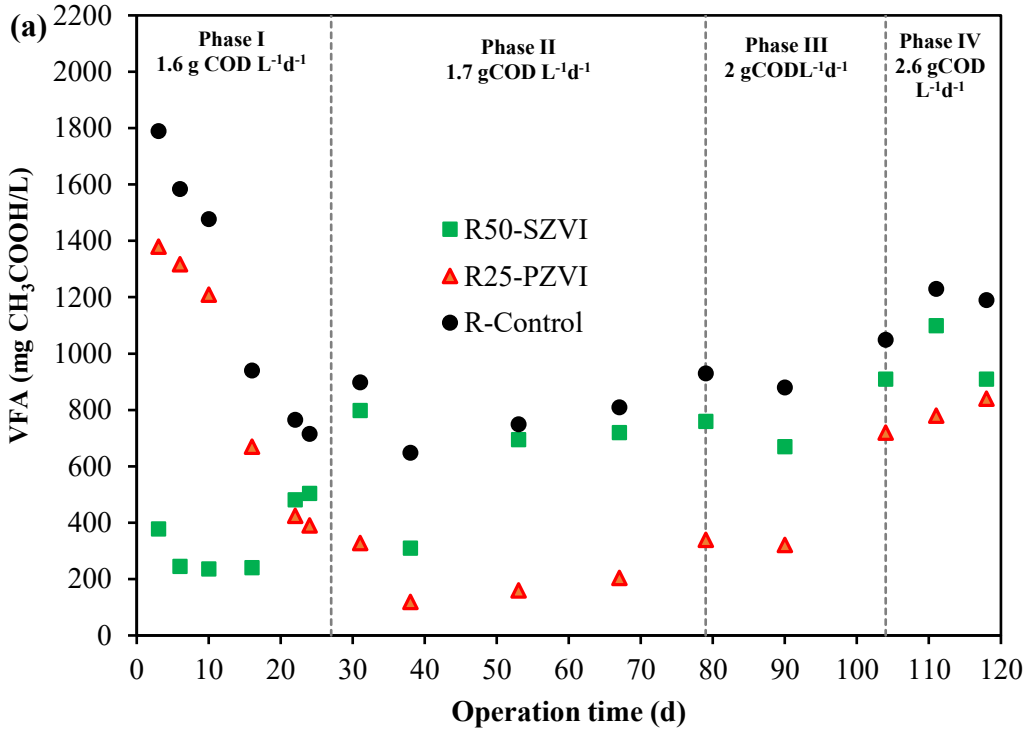

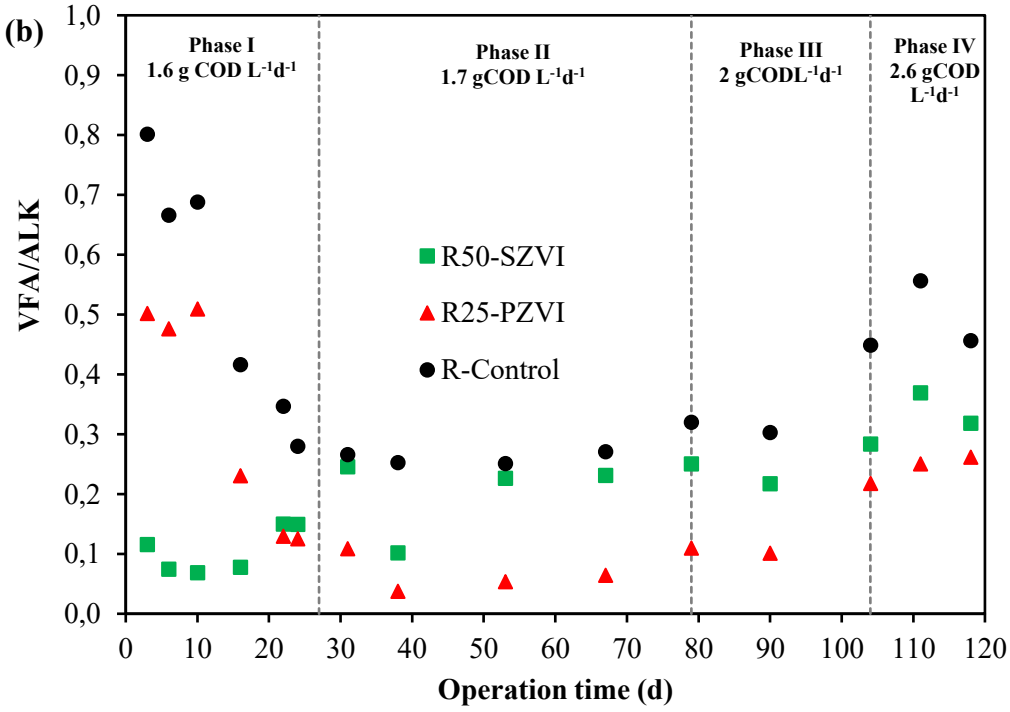

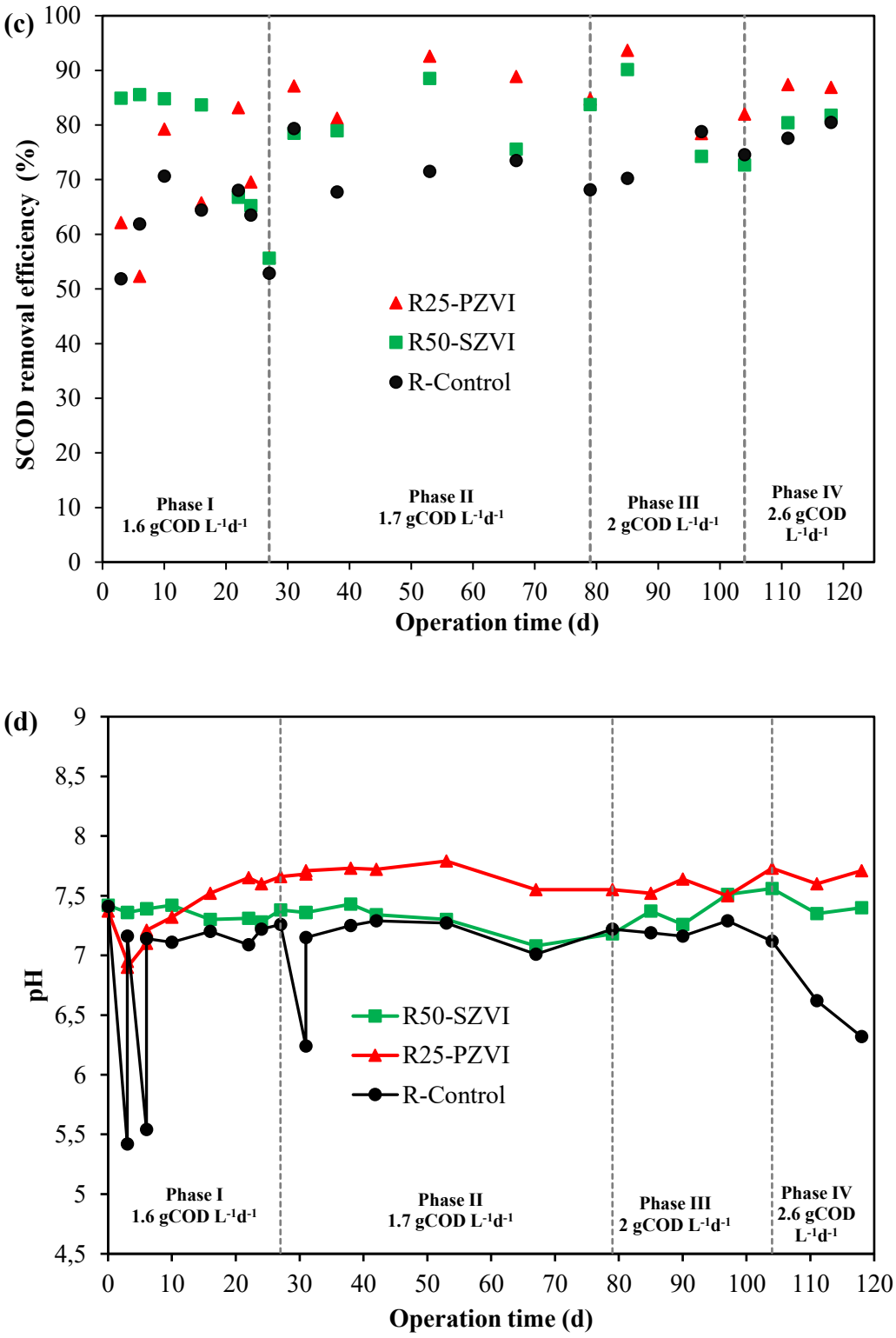

Figure 3-16. Variations in (a) VFA concentration, (b)VFA/ALK ratio, (c) SCOD removal efficiency and (d) pH in the three semi-continuous reactors at varied OLRs

3.3.3 Effect of ZVI on hydrolysis and acidification phase of CW

Particles and complex organic molecules must be solubilized and hydrolyzed into simpler, soluble forms before undergoing acidogenesis to convert to VFAs for methanogenesis (Zhao et al., 2018). As previously reported, 25 g/L of powder ZVI and 50 g/L of Scrap ZVI were selected for this study based on findings related to biogas upgrading at batch conditions. To evaluate the rates of solubilization and hydrolysis at these concentrations, BES was added to inhibit methanogenesis, after which the SMPs were monitored over time. As illustrated in **Fig. 3-17a**, on day 4, the SMPs generated by 50 g/L SZVI and the control exceeded the baseline of 13549 mg COD/L. This indicates that the solubilization/hydrolysis rate surpassed the acidification rate. For 50 g/L SZVI and the control, from day 4 to 18, the SMPs decreased to 690 mg/L and 2560 mg/L, respectively as shown in Fig. 5-4a. However, on day 27, the SMPs increased to 4400 mg/L and 8510 mg/L respectively. In contrast, the anaerobic sludge subjected to 25 g/L PZVI exhibited a continuous decrease in SMPs over time. Similar to this study, Zhao et al. (2018) reported no or minimal effect on hydrolysis of the synthetic wastewater containing bovine serum albumin (5g/L) and dextran (1 g/L) by adding 10 g/L of ZVI. In another study conducted by Xu et al. (2019), micro-ZVI (0.5, 1, and 10 g/L) had a minor effect on hydrolysis of blackwater with slight differences in SCOD production (5158-5258 mg/L) as compared to no ZVI reactor (5124 mg/L).

Fig. 3-17b shows the VFAs distribution in three batch reactors (25 g/L PZVI, 50 g/L SZVI, Control) after inhibition of methanogenic activity. From days 1 to 27, total VFAs in the reactor with 25 g/L of PZVI significantly increased from 3563 mg/L (HAc: 1877 mg/L, HBu: 1012 mg/L) to 10328 mg/L with acetate (4308 mg/L) and butyrate (4837 mg/L) being the major of VFAs. A similar trend in the VFAs concentration was also found in the reactor with 50 g/L SZVI, where acetate (HAc) and butyrate (HBu) increased considerably from 1241 mg/L and 146 mg/L on day 1 to 4578 mg/L and 3877 mg/L on day 27 (**Fig. 3-17b**). On the other hand, total VFAs in the Control reactor (free of ZVI) was below 2000 mg/L on day 1; however, this value increased substantially over time and reached 7526 mg/L on day 27 with propionate (HPr) being the predominant of total VFA (**Fig. 3-17b**).

In contrast, a considerably lower propionate (HPr) concentration was found in reactors with 25 g/L PZVI and 50 g/L SZVI, respectively. It is well recognized that propionic acid conversion to acetic acid is not spontaneous in thermodynamics due to its high Gibbs free energy (Eq. 6), which reflects difficulties for its degradation. To provide favorable thermodynamic conditions for propionic acid conversion, a low level of H_2 partial pressure (lower than 10.1 Pa) is required (Ye et al., 2021). In the test groups containing BES with 25 g/L PZVI and 50 g/L SZVI, the generated H_2 from the anaerobic corrosion of ZVI and the available CO_2 are utilized by homoacetogenic bacteria (Eq. 3), as shown in section 5.2, resulting in less H_2 content, and this unfavorable reaction became feasible and led to an enhancement of the propionate decomposition to acetate.

Eq. 6:

$$CH_3CH_2COO^- + 3H_2O \rightarrow CH_3COO^- + H^+ + HCO_3 + 3H_2 \qquad (\Delta G^0 = +76.0 \text{ kJ/mol})$$

An additional reason was related to the fact that ZVI, as a strong reductive material (E^0= -440 mV), could decrease the oxidation-reduction potential (ORP), which affects the VFAs composition by shifting away from the propionic-type fermentation (Liu et al., 2012). Among the three main fermentation types in acidogenesis (acetic-type, butyric-type, propionic-type), propionic-type fermentation is a facultative anaerobic process and occurs at high ORP (-278 mV), while acetic- and butyric-type fermentation is a strictly anaerobic process and is more beneficial at lower ORP level (Liu et al., 2012). Thus, high acetate (HAc) and butyrate (HBu) detected in reactors with 25 g/L PZVI and 50 g/L SZVI was correlated to the reducibility of ZVI to assist in maintaining a low ORP, which was favorable for acetate and butyrate production.

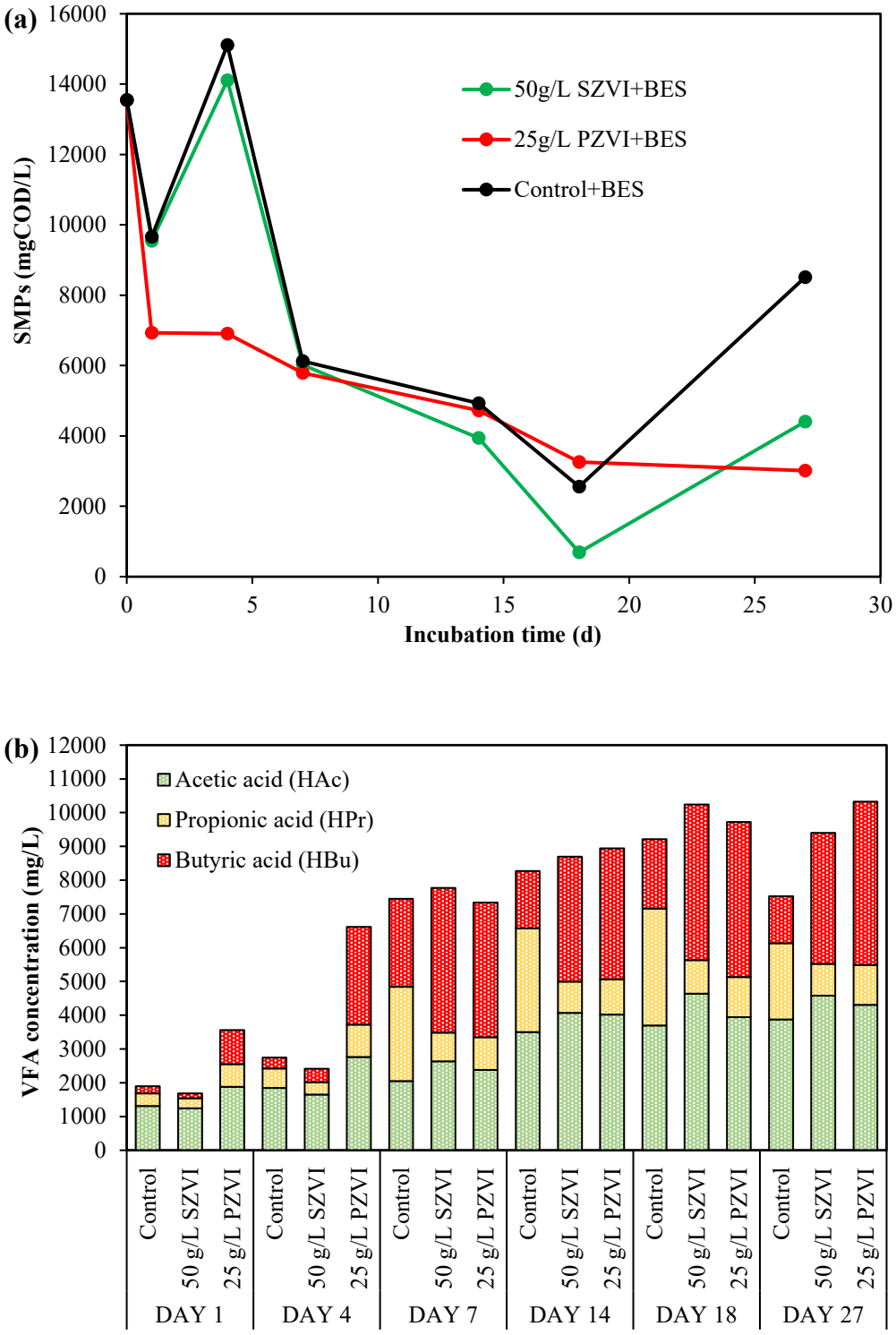

Figure 3-17. Effect of 25 g/L PZVI and 50 g/L SZVI on hydrolysis-acidification stage of CW after inhibition of methanogenesis (50 mM BES): (a) SMPs over time (b) VFA composition

3.3.4 Microbial community structure in semi-continuous and batch operation modes

Fig. 3-18 shows the bacterial microbial profiles from three semi-continuous bioreactors. In all bioreactors, two bacterial phyla, *Firmicutes* and Bacteroidota, were found in high abundance. However, there were notable differences in the reactors that received 25 g/L PZVI and 50 g/L SZVI compared to the control. These differences included an increased presence of the *Synergistota* phylum, mainly the genus JGI-0000079-D21, and the identification of the *Cloacimonadota* phylum, genus W5. *Synergistota* is known for acid formation and is capable of producing short-chain fatty acids, as well as establishing a syntrophic metabolism with hydrogenotrophic methanogens. According to a study by Zhang et al. (2022), an increased abundance of the *Synergistota* phylum was observed in an anaerobic reactor when ZVI and ferrous sulfide (FeS) were added during the co-digestion of food waste and waste-activated sludge. *Cloacimonadota* species, on the other hand, tend to thrive in environments with low H_2 concentrations, suggesting a potential relationship with hydrogenotrophic methanogenesis activities (Palu et al., 2022), and are also involved in the conversion of propionic acid into acetic acid (Cheng et al., 2020).

The *Chloroflexi* phylum was less abundant in the anaerobic reactors with 25 g/L PZVI (5.8%) and 50 g/L SZVI (3.7%) compared to the control (9.85%). Similar trends for this phylum were reported in other studies (Wang et al., 2019) that involved the addition of nano ZVI to anaerobic digesters. *Chloroflexi* contribute to the formation and stabilization of anaerobic granular sludge by developing stratified layers around other microbial constituents within the granule (Bovio et al., 2019). However, the introduction of ZVI and the subsequent production of H_2 appear to alter this symbiotic association, leading to a measurable decline in the abundance of *Chloroflexi* within the granular structure.

Under batch operation mode (**Fig. 3-19**), a similar trend in bacterial microbial profiles was observed. However, in reactors where 25 g/L of PZVI and 50 g/L of SZVI were added, a higher abundance of *Syntrophobacter* species was identified compared to the control. *Syntrophobacter* species often convert

propionate and other organic compounds into acetate and H_2, which methanogens can then use to produce CH_4.

In the samples exposed to BES, a higher relative abundance of *Syntrophobacter* species was also found in the reactors with 25 g/L PZVI and 50 g/L SZVI compared to the control. These may be involved in syntrophic relationships with homoacetogens, but this requires further study. Under these conditions (BES, H_2 generated from 25 g/L PZVI, high alkalinity), a high abundance of the *Anaerolinea* genus was identified in 25 g/L PZVI and 50 g/L SZVI compared to the control (**Fig. 3-19**). This genus is often involved in carbohydrate and protein hydrolysis, favoring cell-cell aggregation, and under these conditions, its presence is favored (Zhu et al., 2023).

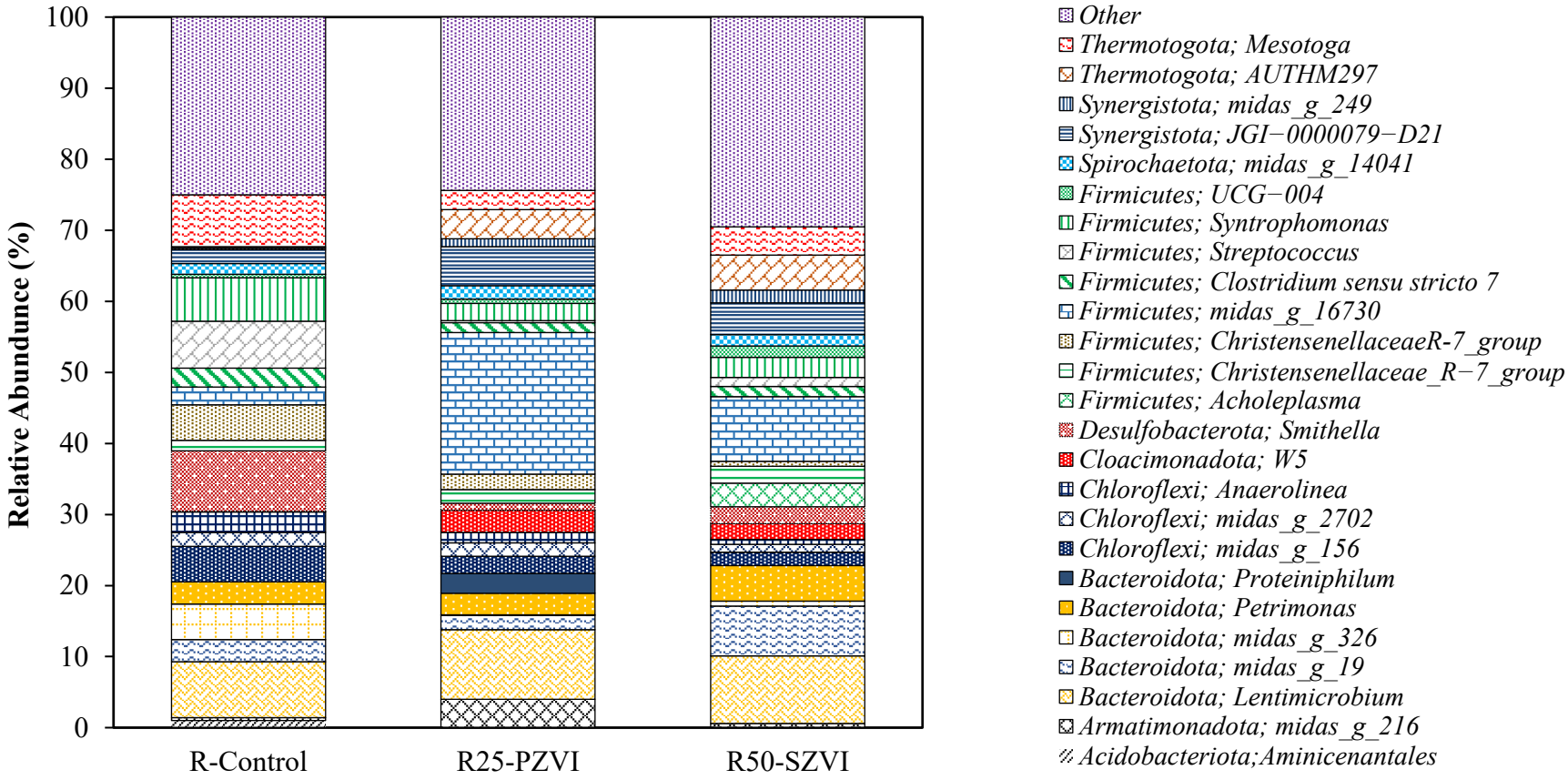

Figure 3- 18. Bacteria relative abundance (%) of semi-continuous reactors at phylum and genera level on day 118

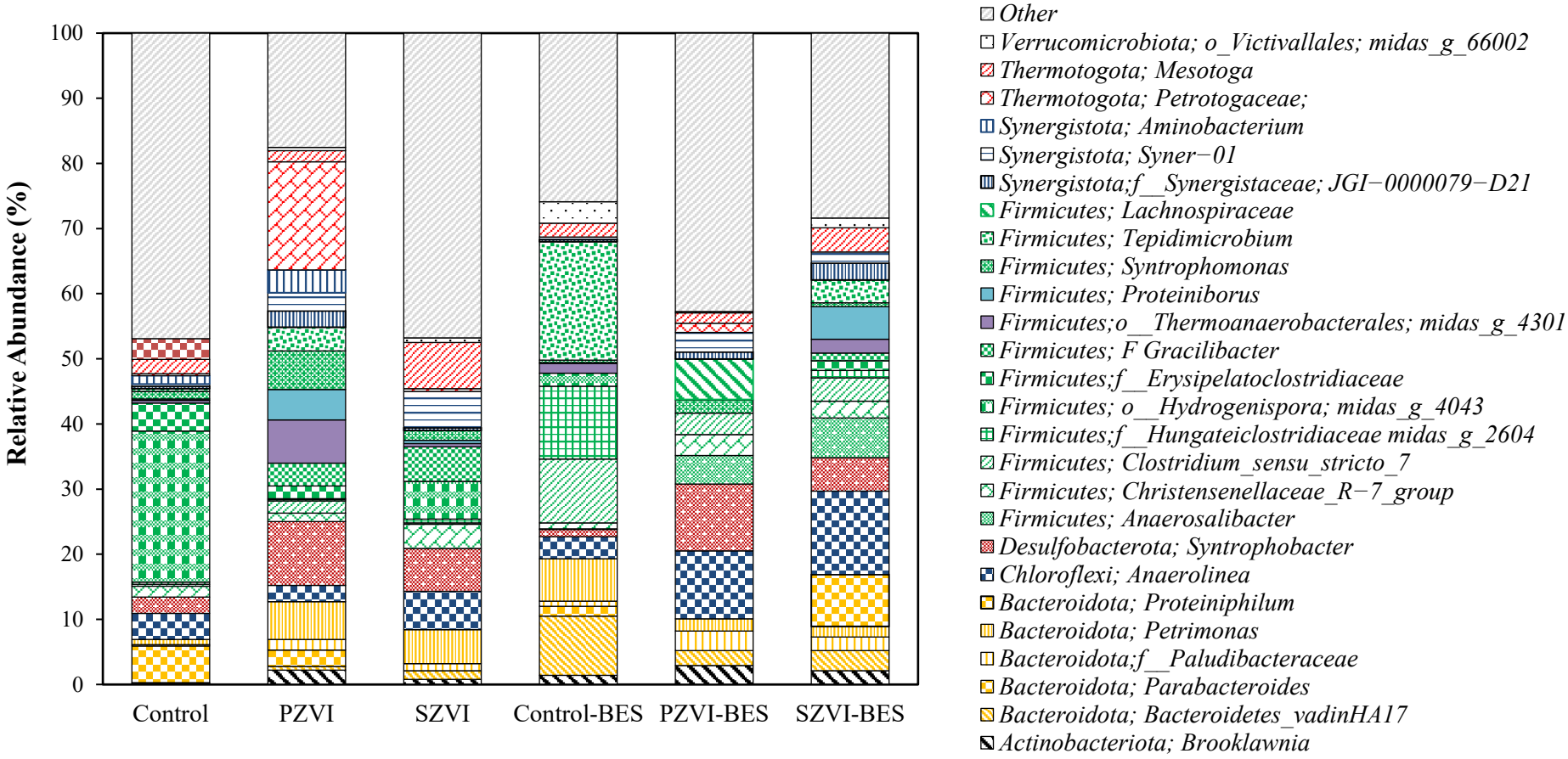

Figure 3-19. Bacteria relative abundance (%) of batch reactors at phylum and genera level on day 27

Fig. 3-20 shows the archaeal microbial profile in semi-continuous operation mode. *Methanobacterium* was the dominant genus among the hydrogenotrophic methanogens in the R-Control, accounting for 54.1%. Conversely, a higher diversity of hydrogenotrophic methanogens was observed in the reactors with 25 g/L PZVI and 50 g/L SZVI. Specifically, the reactors with 25 g/L PZVI reported 22.2%, and those with 50 g/L SZVI had 7.4% of *Methanomassiliicoccus*, compared to just 2.7% in the control. This variation is attributed to changes in the bacterial profile, such as the presence of the *Synergistota* and *Cloacimonadota* phyla, which interact with hydrogenotrophic methanogens to directly convert H_2 generated during propionic acid degradation into CH_4. This interaction prevents H_2 accumulation, which can inhibit the hydrolysis reaction. Similar results were reported by Yang et al. (2019) when ZVI was introduced for swine manure treatment.

Under semi-continuous operation mode, *Methanosarcina* exhibited a high abundance of around 22% in the 25 g/L PZVI and 50 g/L SZVI reactors, compared to the control group. *Methanosarcina's* ability to utilize various substrates and its higher growth rates make it well-suited to semi-continuous conditions. In contrast, the bioreactors where 25 g/L PZVI and 50 g/L SZVI were added had lower abundances of acetoclastic methanogens of the *Methanothrix* genus, showing 11.2% and 11.4% respectively, compared to the control reactor, which had 16.1%.

Under batch operation mode, significant changes were noted in the archaeal profile, particularly in the anaerobic reactors with 25 g/L PZVI. In these reactors, *Methanothrix* emerged as the dominant genus, aligning with its higher acetic acid utilization rate compared to the control and the sludge exposed to 50 g/L SZVI, as shown in Fig. 5-8. Regarding hydrogenotrophic methanogens, *Methanolinea* showed a higher abundance of 25.2% in reactors exposed to 25 g/L PZVI, while *Methanoculleus* was more abundant at 34.2% in the reactor with 50 g/L SZVI. *Methanobacterium* accounted for 30.4% in the control reactor (**Fig. 3-21**).

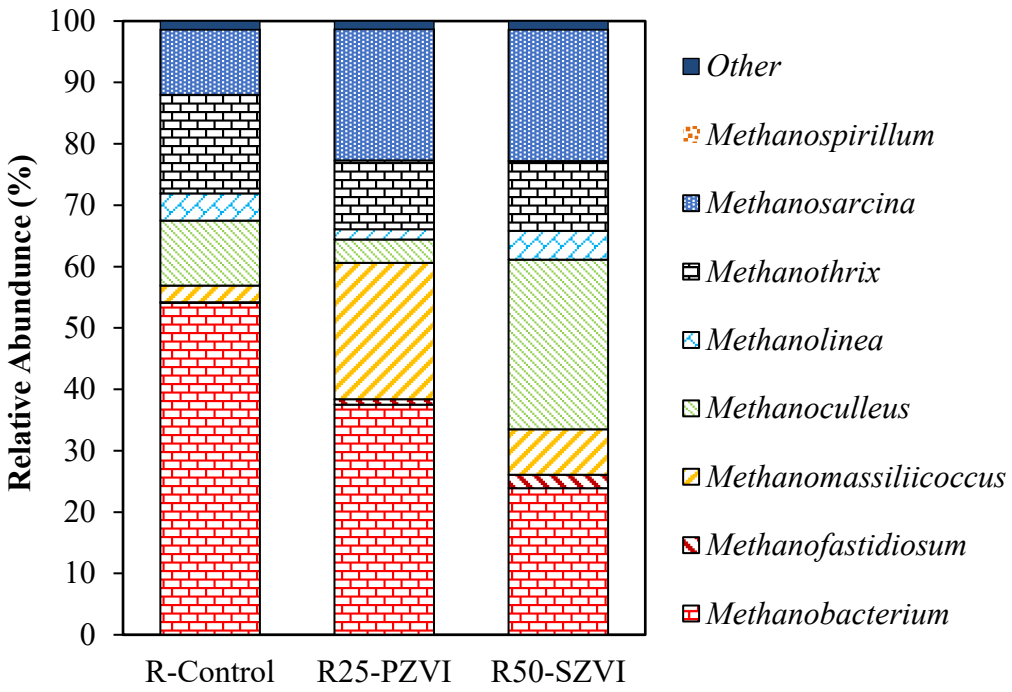

Figure 3-20. Archaea relative abundance (%) of semi-continuous reactors at phylum and genera level on day 118.

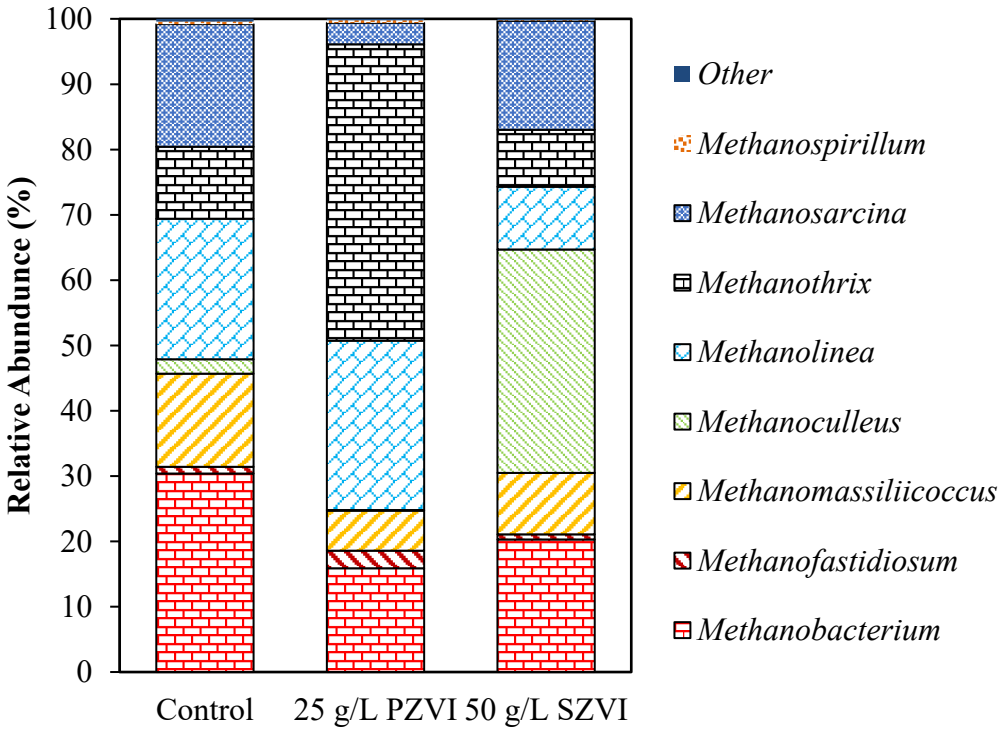

Figure 3-21. Archaea relative abundance (%) of batch reactors at phylum and genera level on day 27

Conclusions of Chapter 3

This chapter explores the effectiveness of 25 g/L PZVI and 50 g/L SZVI in enhancing AD from cheese whey in batch and semi-continuous operation modes, respectively. In semi-continuous mode lab-scale reactors (1L) were operated under four different operational phases (Phase I: 1.6 g COD $L^{-1}d^{-1}$, Phase II: 1.7 g COD $L^{-1}d^{-1}$, Phase III: 2 g COD $L^{-1}d^{-1}$, Phase IV: 2.6 g COD $L^{-1}d^{-1}$) at 35 °C for 118 days. The reactor with added 25 g/L PZVI showed the higher methane yield of 204 mL CH_4/gCOD $_{added}$ and 80% SCOD removal efficiency for 118 d. The reactor with 50 g/L SZVI followed closely, with a methane yield of 177 mL CH_4/gCOD $_{added}$ and a SCOD removal efficiency of 78%. In contrast, the control without added ZVI exhibited a methane yield of 161 mL CH_4/gCOD $_{added}$ and a 61% SCOD removal efficiency. Methane content in the biogas remained stable across all reactors, averaging 53%, 54%, and 52%, respectively. The reactor with added 25 g/L PZVI showed a higher reduction in VFAs over 118 d of semi-continuous operation, and it also maintained a lower volatile fatty acid (VFA) to alkalinity ratios (average 0.21 g CH_3COOH/g $CaCO_3$) as compared to the control reactor (average 0.42 VFA/Alk ratio).

On the other hand, under batch operation mode, after 27 days, the reactor with 25 g/L PZVI exhibited the highest cumulative CH_4 production at 341 mL, significantly outperforming the reactors with 50 g/L SZVI and the control reactor, which produced 249 mL and 130 mL, respectively. SCOD removal efficiency was 93%, 71%, and 64% for the R25-PZVI, R50-SZVI, and control reactors, respectively. Notably, biogas upgrading to over 95% CH_4 was achieved in the reactor with added 25 g/L PZVI due to pressure-induced solubilization of H_2 and CO_2. Moreover, the study noted that 25 g/L PZVI significantly impacted methanogenesis and acidogenesis but had a lesser effect on solubilization or hydrolysis. In the semi-continuous mode, the dominant microbial species in the reactor with added 25 g/L PZVI were *Methanobacterium* and *Methanosarcina*, known for their versatile substrate utilization and rapid growth. Under batch conditions, an increase in *Methanothrix* abundance, associated with enhanced acetic acid utilization, was noted in the reactor with 25 g/L PZVI.

3.4 Chapter 4: Biomethane from CW: Comparison between ex-situ and in-situ H_2 supply through ZVI corrosion

Biological biogas upgrading is becoming increasingly popular due to its gentle operating conditions and minimal requirements for chemicals and energy (Deschamps et al. 2021; Angelidaki et al. 2018). Among the most effective methods is H_2-assisted biogas upgrading, where H_2 is an electron donor for hydrogenotrophic methanogens in the AD process. This process helps to convert CO_2 into CH_4, effectively upgrading biogas in situ (Adnan et al., 2019). For example, research by Mulat et al. (2017) showed that exogenous H_2 supply into an anaerobic reactor could boost the CH_4 composition in biogas to 89%. Thapa et al. (2021) observed that H_2 addition in a trickling filter bed reactor treating thermal post-treated digestate led to a 66.5% increase in CH_4 content and a 67.4% decrease in CO_2. Additionally, Khan et al. (2022) reported that H_2 addition could elevate CH_4 levels to 98.9%. Although these studies confirm the benefits of H_2 addition for biogas upgrading, challenges such as hydrogen's low solubility and mass transfer efficiency must be addressed (Luo et al., 2012).

While H_2-assisted biogas upgrading holds promise, it's crucial to be mindful of the challenges it can pose. Excessive H_2, for instance, can surpass the inhibition partial pressure (10-5 atm), potentially reducing CH_4 purity and hindering microbial activity (Wahid et al., 2019). Moreover, an overabundance of H_2 can disrupt AD systems' buffer capacity and stability. Wahid et al. (2019) observed that an H_2 to CO_2 ratio above 4:1 elevated the pH above 8 and reduced CH_4 production. Tang et al. (2022) found that H_2 generated from nZVI corrosion could raise CH_4 levels to 90.5%, but high concentrations of nZVI impeded CH_4 production. Dong et al. (2019) noted that a ZVI concentration of 12.5 g/L completely converted CO_2, increasing CH_4 production and the prevalence of hydrogenotrophic methanogens, facilitating more efficient H_2 and CO_2 conversion to CH_4.

On the other hand, external H_2 supply has shown significant potential in enhancing the efficiency of in-situ biogas upgrading. Sun et al. (2023) discovered that external H_2 addition notably improved the efficiency of in-situ biogas upgrading. Specifically, 10 g/L coarse ZVI yielded the highest cumulative CH_4

production (286.4 mlCH_4/gVS) and CH_4 composition (95.5%). However, it's worth noting that combining different H_2 sources proved less effective than using a single method of H_2 supply, whether direct or indirect. The estimated H_2 production from ZVI suggested a direct relationship between the amount of H_2 released and the CH_4 yield and content, respectively. In semi-continuous tests, direct external H_2 supply led to a CH_4 production rate of 52.0 mL/gVS/d, whereas indirect supply using 10 g/L cZVI achieved a peak CH_4 concentration of 92.0%.

Tang et al. (2023) evaluated the impact of varying nZVI concentrations (0, 2, 4, 6, 8, and 10 g/L) on the AD of kitchen wastewater using two different buffer systems: 2-[4-(2-hydroxyethyl) piperazin-1-yl] ethane sulfonic acid (HEPES) and sodium hydrogen carbonate ($NaHCO_3$). The introduction of nZVI led to improvements in CH_4 content and the overall stability of the AD process. Specifically, in the HEPES buffer system, CH_4 levels increased across all dosages, reaching a peak of 90.51% with 10 g/L nZVI, a 32.25% increase compared to the control setup. Amen et al. (2017) used various concentrations of nZVI and were subjected to anaerobic-activated municipal sludge to evaluate the effects of nZVI on sludge fermentation, biogas production, and CH_4 enhancement. The findings revealed that adding 250 mg/L of nZVI nanoparticles increased biogas production by 25.23% and elevated the CH_4 content to 94.05% after one week of digestion, compared to a CH_4 content of 62.67% in samples without nZVI addition.

As the aforementioned studies have shown, several methods have achieved CH_4 levels higher than 90% in biogas. Our previous chapters have also demonstrated that adding ZVI to the reactor treating CW under batch mode can result in biogas purity exceeding 95% CH_4. However, a crucial comparison has yet to be made: adding ZVI in situ versus externally supplying the H_2 produced from ZVI to the reactor. The study reported in this chapter aims to fill this gap by comparing two different reactor setups for treating CW: (A) directly adding 25 g/L ZVI to the reactor with CW (in-situ) and (B) external supplying H_2 generated from abiotic oxidation of 25 g/L PZVI to another reactor (ex-situ). This comparison is of utmost importance as it aims to determine which method most effectively enhances the treatment of CW and the upgrading of biogas. The evaluation will focus on the

dynamics of each method, analyzing their impacts on CH_4 production, biogas composition, and pH requirements.

3.4.1 Reactors performance: Ex-situ vs. In-situ H_2 supply via ZVI oxidation

Fig. 3-22. illustrates the performance of three different reactor setups: (A) In-situ reactor where 25 g/L PZVI was directly added, (B) Ex-situ reactor where H_2 was externally supplied on specific days (2, 4, 7, 11, 14, and 18) following the method described in section 2.4.1. This method involved H_2 generation from abiotic oxidation of 25 g/L ZVI exposed to soluble CO_2 (the abiotic H_2 producer reactor contained 50 g/L $NaHCO_3$ + 25 g/L ZVI and was flushed with CO_2 for 2 min) and (C) a Control reactor that received no H_2 or ZVI.

As depicted in **Fig. 3-22a**, the in-situ reactor demonstrated consistently superior CH_4 production performance, with no initial lag phase, achieving approximately 90% CH_4 composition in biogas after 21 days. This suggests that directly incorporating 25 g/L PZVI enhances CH_4 generation, likely due to the sustained release of H_2, which aids the methanogenesis process. On the other hand, the ex-situ reactor, despite the periodic external H_2 supply (on days 2, 4, 7, 11, 14, and 18), faced significant challenges. It exhibited a notable lag phase and showed signs of inhibition under these conditions, with CH_4 content reaching only 31% by day 21 (**Fig. 3-22a**). The composition of H_2 remained above 30% from day 4 to 18, indicating that the added H_2 was not utilized (**Fig. 3-22c**). The non-utilization of H_2 is a key challenge, likely contributed to the low gas-to-liquid phase transfer caused by the low solubility of H_2 (0.0016 g/L). In all gas-liquid fermentation, there is a notable challenge with the effective transfer of gases into the liquid phases where the biological activities occur. The availability of dissolved H_2 is crucial because the microorganisms can only utilize H_2 for their metabolic reactions in this dissolved state (Fu et al., 2020). Without any H_2 or ZVI supplementation, the control reactor exhibited the lowest CH_4 production throughout the experiment, reaching about 21.5% CH_4 content after 21 days. As depicted in **Fig. 3-22c**, the H_2 levels varied between 5-22%, probably due to the rapid biodegradation of the CW, which also caused a drop in pH. Despite attempts to neutralize the pH with NaOH, the pH remained unbalanced, inhibiting the utilization of H_2 by hydrogenotrophic

methanogens (**Fig. 3-22d**). As discussed in the previous chapters, this led to propionic acid accumulation and further system inhibition.

Fig. 3-22b presents the cumulative CH_4 production, confirming that the in-situ addition of ZVI yielded the highest CH_4 production (187.7 mL) from CW. The ex-situ system generated 110.7 mL, while the control reactor produced 99.4 mL after 21 days (theoretical value was 651 ml CH_4). The SCOD levels after 21 days were 2200 mg/L for the in-situ system, 4830 mg/L for the ex-situ system, and 4300 mg/L for the control, corresponding to 82%, 61%, and 64% SCOD removal efficiency, respectively (**Fig. 3-22e**).

The difference in SCOD between the three systems is less pronounced than the variation in CH_4 production because part of the CW was biodegraded into CO_2 and was not utilized in the control and ex-situ reactors. Interestingly, no external NaOH was needed in the in-situ ZVI system (**Fig. 3-22d**), which highlights another advantage of adding ZVI as an alkalinity provider in this system (refer to previous Chapters for more details).

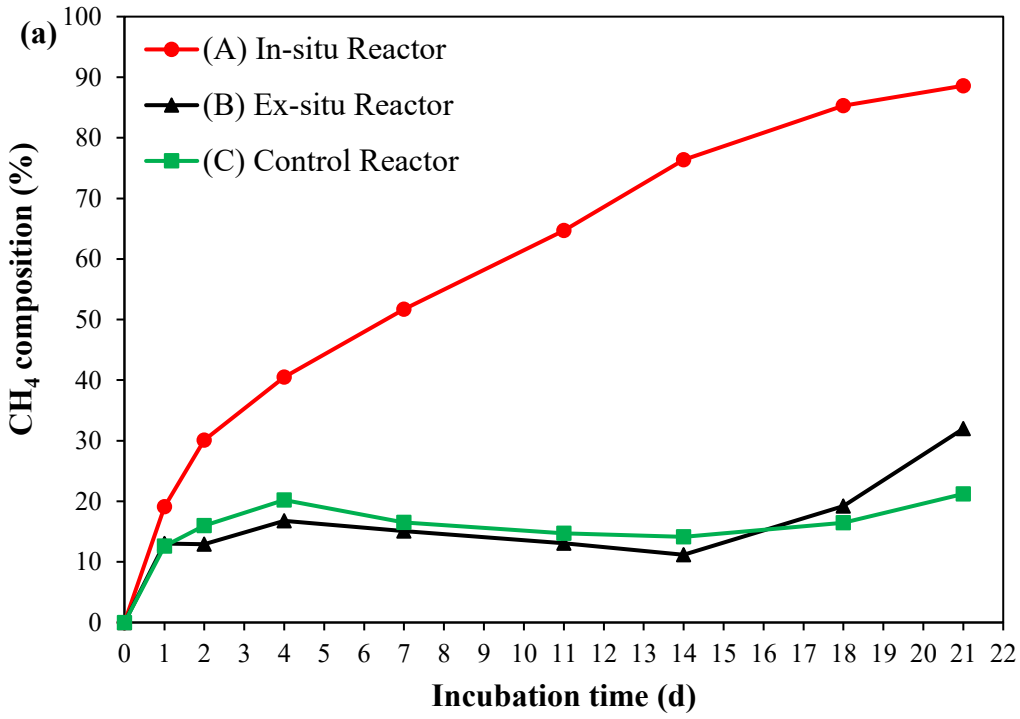

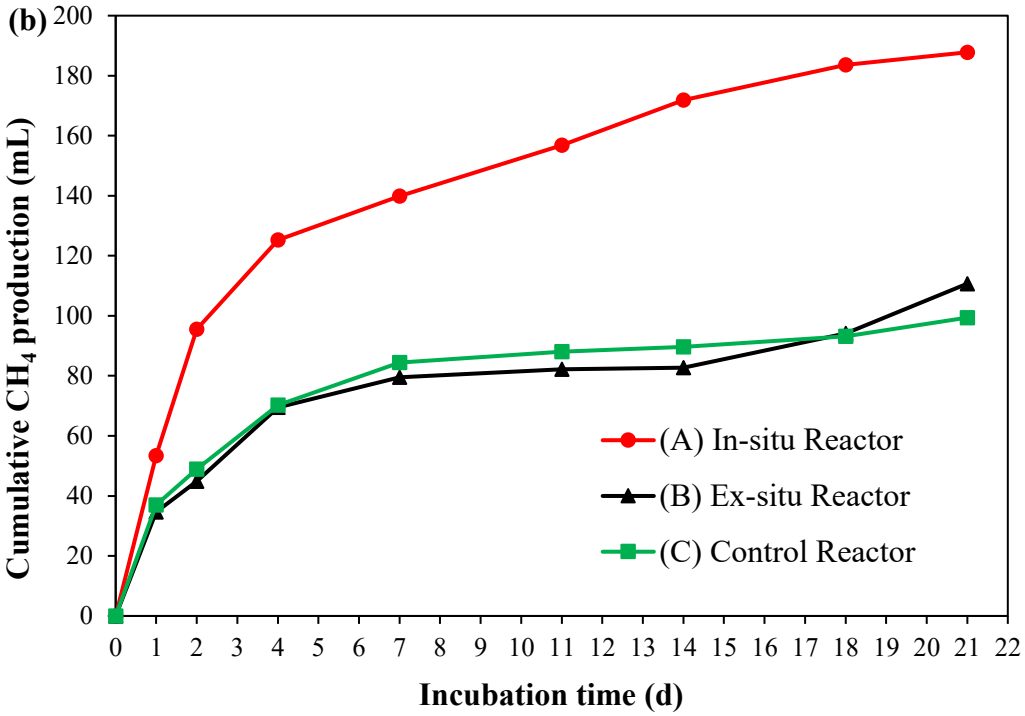
(b)
Cumulative CH4 production (mL)
Incubation time (d)
(A) In-situ Reactor
(B) Ex-situ Reactor
(C) Control Reactor

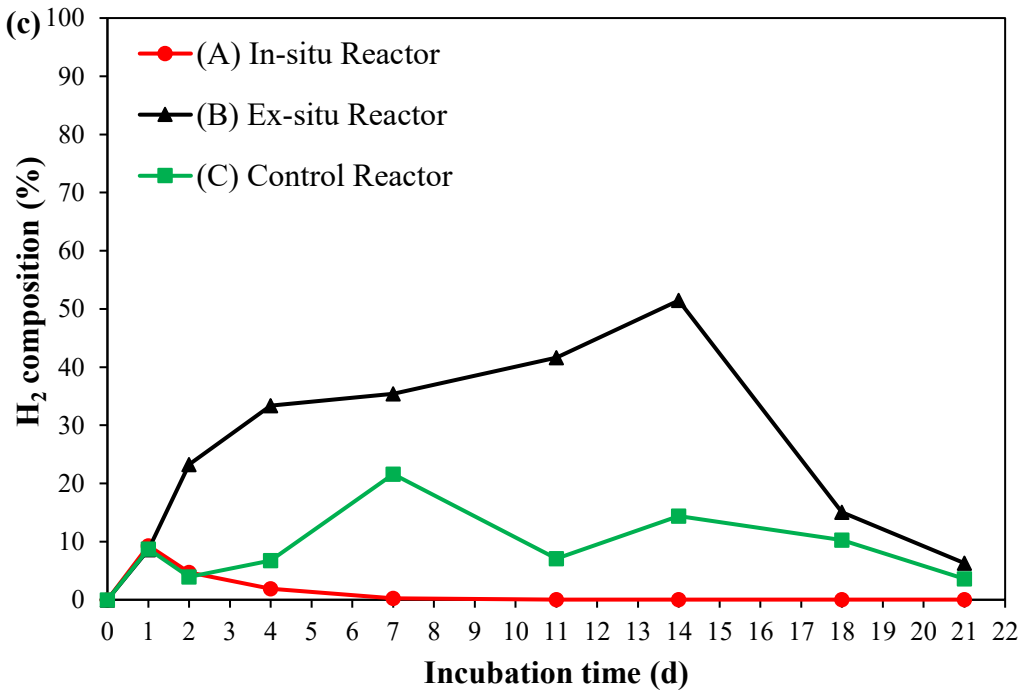
(c)
H2 composition (%)
Incubation time (d)
(A) In-situ Reactor
(B) Ex-situ Reactor
(C) Control Reactor

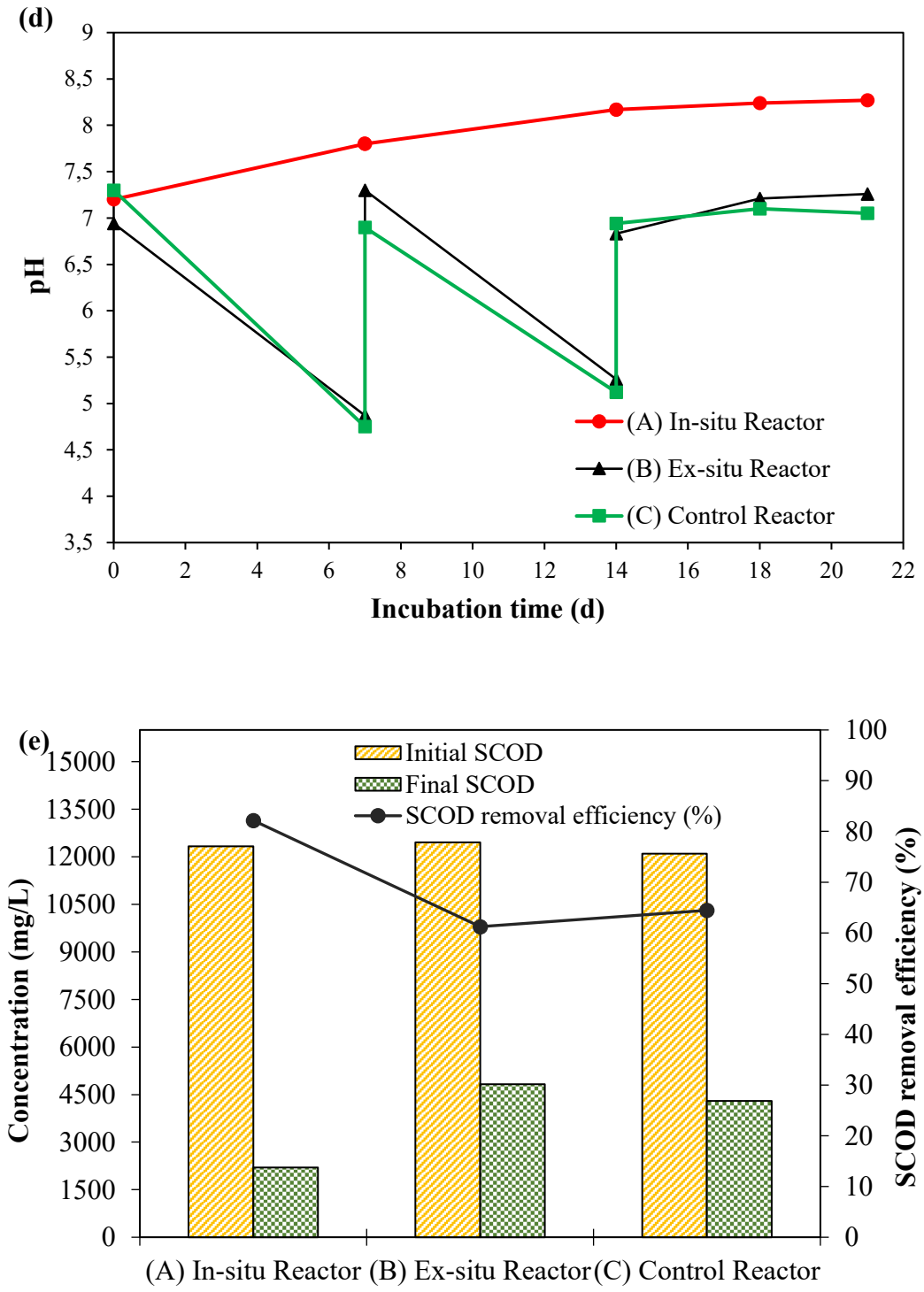

Figure 3- 22. Performance of three reactors set-up (A) In-situ (B) Ex-situ (C) Control on the: (a) CH_4 composition; (b) CH_4 production; (c) H_2 composition; (d) pH and (e) SCOD removal efficiency over 21 d

3.4.2 Assessing the applicability of end-product (digestate) as a soil conditioner

The utilization of the solid fraction (digestate) that remained after the AD process from each reactor (in-situ and ex-situ) was assessed through phytotoxicity trials on *Sinapis alba* seeds. At the end of the experimental period (21 d), both samples were tested by using the 2.5 and 3.5% w/w (g of sample per g of control) concentrations on *Sinapis alba* seeds for their potential toxicity on plant seeds. **Fig. 3-23** illustrates the calculated GI of germinated *Sinapis alba* after applying each end product. The results revealed that the 2.5% w/w concentration was significantly better for the ex-situ (36 mL CW + exogenous H_2 supply) sample, which exhibited higher GI with a percentage (93.7%) compared to the other samples. The increase of the *Sinapis alba* growth observed in the ex-situ sample (2.5% w/w) was statistically proven. Similar results were observed on *Sinapis alba* seeds for both samples when the sample was at 3.5% w/w, with calculated GI ranging between 48.9-51.7%.

According to Aguerre and Gavazzo's 2012 study, it is postulated that when the GI values reach up to 80%, it suggests the absence of phytotoxic substances or their existence in deficient concentrations. In contrast, GI values below 50% strongly indicate the presence of phytotoxic substances, while values ranging from 50% to 80% might suggest a moderate presence of these substances. Generally, a GI under 50% implies waste phytotoxicity. However, the calculated GI value for a 2.5% w/w concentration ex-situ sample is considered non-phytotoxic on plant growth and significantly improves the seed germination of *Sinapis alba* compared to the in-situ sample.

The end product from the in-situ reactor (25 g/L PZVI +36 ml CW) is considered phytotoxic on plant growth for both tested concentrations (2.5 and 3.5% w/w) due to the high concentration of ZVI. Iron is a crucial plant micronutrient, providing advantages at normal levels but becoming toxic at excessive concentrations. This toxicity causes damage to plant cell membranes, decreased growth, disruption of chlorophyll production, and reduced overall plant health. The reported beneficial iron concentration in soil ranges from about 20-300 mg/kg (Zhang et al., 2022).

Several studies have examined the effects of ZVI toxicity on plant growth, reporting that its phytotoxic effects are dose-dependent and vary with plant species. For example, Ma et al. (2013) evaluated the toxicity of nZVI (0-1000 mg/L) on *Typha latifolia* and hybrid poplar (*Populous deltoids* x *Populous nigra*) for four weeks. They found concentrations above 200 mg/L nZVI were phytotoxic, while levels below 50 mg/L promoted plant growth. The authors noted that a black coating formed by high amounts of nZVI on the root surface could block the membrane pores of the root, reducing water and nutrient uptake. Similarly, Guha et al. (2018) reported that 20 mg/L nZVI enhanced the germination and growth of aromatic rice (*Oryza sativa* cv.). El-Temsah and Joner (2012) found that excess nZVI concentrations (2000 mg/L and 5000 mg/L) are detrimental to the germination and growth of ryegrass, barley, and flax. In a study by Libralato et al. (2016), no significant phytotoxicity effects were observed in seed germination of *Lepidium sativum* and *Sinapis alba* at around 300 mg/L nZVI.

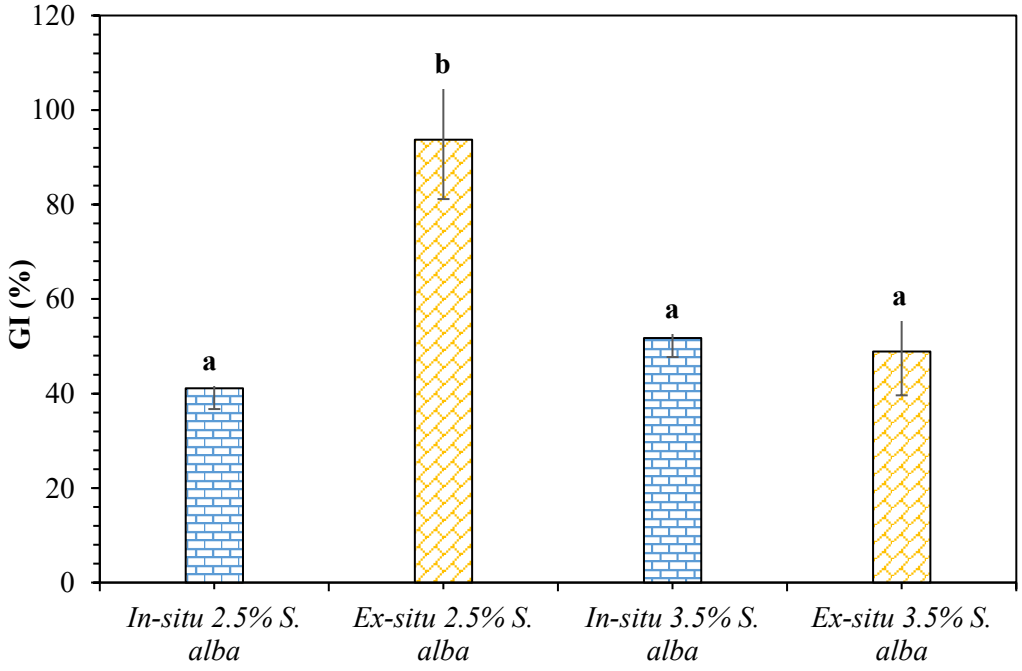

Figure 3-23. Phytotoxicity trials on *Sinapis alba* seeds after a 3-d time period; Germination index (GI (%)) of 2.5 and 3.5% (w/w) concentration of In-situ and Ex-situ samples after 21-d of AD with CW.

Conclusions of Chapter 4

This chapter examined how supplying H_2 externally or in-situ, from the anaerobic oxidation of 25 g/L PZVI, affects the AD of CW in two distinct reactor setups. The results demonstrated that the reactor, supplemented directly with 25 g/L PZVI (in-situ reactor), exhibited significantly enhanced CH_4 production efficiency, achieving approximately 90% CH_4 composition in the biogas within 21 days. This superior performance is attributed to the sustained release of H_2 by 25 g/L PZVI, facilitating methanogenesis without the lag phase observed in other reactor setups. In contrast, the ex-situ reactor, which relied on externally supplied H_2, reflected by a lower CH_4 content of only 31% and unutilized remaining above 30% between days 4 and 18, likely due to inefficiencies in gas-to-liquid phase transfer. These challenges highlight the critical importance of dissolved H_2 availability for effective microbial metabolism.

The control reactor, without any ZVI or H_2 supplementation, showed the lowest performance with a 21.5% CH_4 content. This was hindered by pH imbalances despite neutralization efforts, which likely led to propionic acid accumulation and system inhibition. The in-situ ZVI system, however, eliminated the need for external alkaline adjustments, boosting CH_4 production and maintaining system alkalinity, leading to the most effective removal of SCOD among the tested reactor setups.

Despite the positive impacts of directly adding 25 g/L PZVI on CH_4 production, the digestate assessment revealed phytotoxic effects at 2.5% and 3.5% w/w concentrations. High levels of ZVI contribute to these inhibitory effects, as excessive iron can harm plant health. On the other hand, the digestate from the ex-situ reactor, which used an external H_2 supply, showed promising results as a soil conditioner in phytotoxicity trials with *Sinapis alba* seeds. At a 2.5% w/w concentration, this digestate significantly enhanced seed germination and growth, with a germination index (GI) of 93.7% indicates negligible phytotoxic effects and suggests its safety and efficacy in promoting plant growth.

4 Summary of finding

This research study presents innovative approaches to optimizing the anaerobic digestion (AD) of cheese whey (CW), which addresses the challenges of acidification and methanogenesis inhibition. Cheese whey is a by-product of cheese manufacturing with high organic content and low alkalinity, often leading to rapid acidification and inhibition of methanogenesis in AD. The study introduces and evaluates the effectiveness of two strategies, acid-tolerant methanogenic culture, and zero-valent iron (ZVI) additions, to improve the stability and economic viability of CW AD processes.

The first part of the study investigates the use of acid-tolerant methanogenic culture maintained at a pH of 5-6 to alleviate acid inhibition from volatile fatty acids (VFAs). Acclimatized sludge in AD reactors resulted in a 35% and 30% increase in CH_4 production over 21 and 36 days, respectively, compared to non-acclimatized sludge. Propionic acid was found to be the reaction-limiting step under these conditions. Microbial analysis revealed a higher prevalence of hydrogenotrophic methanogens, particularly *Methanolinea,* suggesting a shift toward hydrogenotrophic pathways under acidic conditions. Furthermore, the lower concentration of acetic acid and the higher abundance of *Clostridium sensu stricto* suggest the involvement of the syntrophic acetate oxidation-hydrogenotrophic methanogenesis (SAO-HM) pathway is the main pathway for CH_4 production. Additionally, economic assessments indicated that using acclimatized sludge could reduce the need for NaOH by 69%, significantly lowering operational costs despite a slight decrease in energy output.

The second part of the study explores the use of zero-valent iron (ZVI) in powder and scrap metal forms to mitigate acidification and enhance methane production in CW AD. Experiments conducted over 201 days under batch conditions demonstrated that reactors with 25 g/L powder ZVI and 50 g/L scrap ZVI outperformed control reactors (no ZVI) in terms of methane yield and achieved over 95% methane purity in the biogas, a significant upgrade compared to control reactors and biogas quality, particularly in the first two cycles (total 34 d) of operation. The presence of ZVI effectively reduced the necessity for external pH

adjustments and lowered VFAs concentrations, highlighting ZVI's potential to improve process stability and reduce reliance on chemical buffers. Economic analysis showed a significant profit increase using 50 g/L scrap ZVI, positioning it as a cost-effective alternative for in-situ biogas upgrading.

Reactors with 25 g/L PZVI and 50 g/L SZVI were selected further to delineate the impact in batch and semi-continuous operation modes. In semi-continuous mode, reactors with 25 g/L PZVI notably outperformed those with 50 g/L SZVI and control reactors, achieving a higher methane yield of 204 mL $CH_4/gCOD_{added}$ and an SCOD removal efficiency of 80%. Additionally, reactors with 25 g/L PZVI demonstrated a lower volatile fatty acid (VFA) to alkalinity ratio, suggesting more efficient acid management and stability in the AD process. However, no biogas upgrading was observed, with methane content across all reactors remaining stable. In contrast, batch operation mode further emphasized the potential for biogas upgrading, with the 25 g/L PZVI reactors achieving over 95% methane purity due to effective pressure-induced solubilization of H_2 and CO_2. It was observed that 25 g/ L PZVI significantly influenced the processes of methanogenesis and acidogenesis but did not have a pronounced effect on solubilization or hydrolysis. The microbial analysis highlighted the predominant presence of *Methanobacterium* and *Methanosarcina* in the semi-continuous mode and *Methanothrix* under batch conditions, enhancing the methanogenesis phase, particularly in acetic acid utilization.

Finally, the effects of H_2 supply, either externally or in-situ from the anaerobic oxidation of 25 g/L PZVI, on the AD of CW were investigated. The results indicate that in-situ H_2 supply from 25 g/L PZVI significantly enhances CH_4 production compared to external H_2 supplementation, achieving a 90% CH_4 content in biogas. Furthermore, it helps maintain system alkalinity and eliminates the need for external pH adjustments. However, the solid residue (digestate) from the in-situ reactor negatively affected plant growth, while the solid residue from the ex-situ reactor positively affected seed germination.

5 Recommendations for future work

Following the completion of the present thesis, the topics presented below could be proposed as future work relevant to the two proposed approaches:

1st Approach: Acid-Tolerant Methanogenic Culture

This research introduced the use of an acid-tolerant methanogenic culture to mitigate VFAs and enhance process stability during the AD of cheese whey at a pH of 5-6. The acid-tolerant methanogenic culture was enriched over 7 months under batch mesophilic conditions using acetic acid as the sole carbon source. While reactors utilizing this acid-tolerant culture demonstrated increased CH_4 production (35% and 30% higher than the non-acclimatized culture for 21 and 36 d, respectively), propionate remained the least decomposed VFA. Microbial analysis confirmed the absence of propionate-degrading acetogens, such as *Syntrophobacter* and *Pelotomaculum*. To further enhance the AD process, the development and introduction of a propionate-utilizing culture highly resistant to low pH are recommended. This culture should ideally incorporate propionate-oxidizing bacteria alongside methanogens to improve both methanogenesis and the breakdown of propionate. Additional recommendations for future research include:

1. Scale-up Experiments: The experiments in this study were conducted using small lab-scale reactors (125 mL serum bottles) under batch conditions for relatively short operational periods (21 and 36 days, respectively). Comprehensive, larger-scale experiments (greater than 1 liter) conducted under various operational modes (such as semi-continuous or continuous) and over extended durations are essential to fully assess the impact of the acid-tolerant methanogenic culture on the AD of CW. These experiments will provide a more complete understanding of the process's scalability and efficiency and validate the findings of this study.
2. Acclimation Strategies: Further research should explore different acclimation strategies, particularly comparing gradual versus sharp pH reductions, to develop an acid-tolerant methanogenic culture and understand microbial community responses to pH variations. This research demonstrated that a step-wise decrease in pH, along with extended

operational periods at each pH level, facilitated the development of a microbial culture where hydrogenotrophic *Methanolinea* (~53%) was the dominant methanogen, in contrast to the lower presence of the acetoclastic methanogen *Methanosaeta* (~15%) compared to reactors with a non-acclimatized culture (~23%). Future experiments may need to determine the optimal duration for maintaining the reactor at each pH level during a gradual pH reduction process.

3. Supporting Materials for Bioaugmentation: Considering the long-term operation of anaerobic reactors, there is a significant likelihood that the introduced acclimatized microbial culture will be washed out. Thus, investigating the addition of supporting materials, such as activated carbon, biochar, carbon nanotubes, etc., can be a promising solution to address this issue. These materials offer a large surface area for microbial attachment and biofilm formation, which can help retain the introduced microbial strains in the reactor for an extended period.
4. Development of Microbial Strains: Future work should focus on identifying and optimizing novel pure microbial strains with enhanced acid tolerance and metabolic capabilities. This can expand the scope and effectiveness of bioaugmentation techniques for acid inhibition in various environmental and industrial settings. Bioaugmentation of acid-tolerant cultures offers a sustainable and cost-effective approach to acid inhibition, presenting a green alternative to traditional chemical treatments. Developing tailored microbial consortia for different acidic environments and optimizing dosing strategies and monitoring techniques to ensure long-term effectiveness should be a priority.

2nd Approach: ZVI Addition in AD of CW

The second approach of this study advocates the use of zero-valent iron (ZVI) as an innovative method to buffer acidification and enhance the performance of AD of cheese whey. Given its multifaceted roles in AD, including improving the hydrogenotrophic pathway, reducing the oxidation-reduction potential (ORP), elevating pH levels, and strengthening syntrophic relationships between bacteria and methanogens, the findings from this research demonstrate the promising

potential for ZVI's application in AD of CW. However, it is imperative to address practical challenges and evaluate performance under real-world conditions to realize potential industrial applications. Future research should include conducting scale-up experiments and pilot studies to assess the feasibility of implementing ZVI on a larger scale.

A key area for future research is the development of efficient and environmentally sustainable methods to dissolve or control the surface inactivation of ZVI, which is often caused by the formation of a siderite layer. This research direction is crucial as it could significantly prolong ZVI's active life and effectiveness in the AD process. As discussed in Chapter 2, applying ZVI over four consecutive CW feedings (18, 30, 50, and 75 mL, respectively) for 201 d under batch conditions showed enhanced CH_4 yield, CH_4 composition, and VFA reduction over 34 days. However, ZVI's efficacy diminished over time, likely due to the formation of a passivation layer of siderite on the ZVI surface, which impeded further H_2 release.

The determination of the optimal dosage and methodology for adding ZVI is a critical aspect. The current research explored higher concentrations of ZVI, 25, 50, and 100 g/L for both PZVI and SZVI, compared to those reported in previous studies which were typically 5-10 g/L. However, these elevated concentrations raise concerns about the economic viability of ZVI for practical engineering applications, particularly considering the cost of powder ZVI which ranges from $0.5 to $20 per kg. On the other hand, scrap metal ZVI is a cost-effective and environmentally friendly option. Our economic evaluation results (see section 4.6) indicated that 50 g/L SZVI was more profitable for large-scale applications than 25 g/L PZVI. Additionally, SZVI minimizes environmental risks associated with dispersal and reversibility compared to powder and nano-ZVI. However, further research is required to evaluate the environmental implications and efficacy of using high ZVI dosages in practical applications. Our findings found that the residual solid fraction in the reactor, containing 25 g/L of powder ZVI, may exhibit phytotoxic effects on plant growth (see section 6.2). Nevertheless, more research is necessary to assess the environmental implications and effectiveness of using high ZVI dosages in practical applications.

Furthermore, identifying the appropriate methodology for ZVI addition is vital. According to the literature, three primary methods have been primarily described for semi-continuous operation mode: (1) adding ZVI at specific intervals through the reactor's feeding port, (2) mixing ZVI with substrates before introduction, and (3) implementing a dedicated ZVI bed within the anaerobic reactor. Each method has its advantages and challenges. A detailed study is necessary to evaluate their effectiveness and practicality for enhancing the AD process on an industrial scale.

Investigating the use of ZVI in conjunction with cheese whey to enhance the production of volatile fatty acids (VFAs) via the carboxylate platform is another promising area for research. According to Chen et al. (2022), VFAs have a significantly higher market value (€1800–€2500 per ton) compared to CH_4 (€1.8/m^3). Recent studies have shown that ZVI can facilitate chain elongation, crucial for producing medium-chain carboxylates such as caproate. These carboxylates are essential precursors for various pharmaceuticals, antimicrobials, and biofuels.

REFERENCES

Abdallah, M., Greige, S., Beyenal, H., Harb, M., Wazne, M., 2022. Investigating microbial dynamics and potential advantages of anaerobic co-digestion of cheese whey and poultry slaughterhouse wastewaters. Sci. Rep. 12, 1–12.

Abdelsalam, E., Samer, M., Attia, Y.A., Abdel-Hadi, M.A., Hassan, H.E. and Badr, Y., 2017. Influence of zero valent iron nanoparticles and magnetic iron oxide nanoparticles on biogas and methane production from anaerobic digestion of manure. Energy, 120, 842-853

Acharya, S.M., Kundu, K., Sreekrishnan, T.R., 2015. Improved stability of anaerobic digestion through the use of selective acidogenic culture. J. Environ. Eng. 141, 04015001

Adnan, A. I., Ong, M. Y., Nomanbhay, S., Chew, K. W., & Show, P. L., 2019. Technologies for biogas upgrading to biomethane: A review. Bioengineering, 6(4), 92.

Agdag, O.N, Sponza, T.D., 2005. Effect of alkalinity on the performance of a simulated landfill bioreactor digesting organic solid wastes, Chemosphere 59, 871–879

Aguerre, Y.S, Gavazzo, G.B., 2012. "Fitotoxicidad de papel reciclado." Proceedings of the ABTCP 2012 + VII CIADICYP. The 45th ABTCP international pulp and paper congress and VII Ibero American Congress on Pulp and Paper Research.

Ahmad, T., Aadil, R.M., Ahmed, H., Ur Rahman, U., Soares, B.C.V., Souza, S.L.Q., Pimentel, T.C., Scudino, H., Guimarães, J.T., Esmerino, E.A., Freitas, M.Q., Almada, R.B., Vendramel, S.M.R., Silva, M.C., Cruz, A.G., 2019. Treatment and utilization of dairy industrial waste: a review. Trends Food Sci. Technol. 88, 361–372.

Akyol Ç, Ince O, Bozan M, et al. Fungal bioaugmentation of anaerobic digesters fed with lignocellulosic biomass: what to expect from anaerobic fungus Orpinomyces sp. Bioresour Technol. 2019;277:1–10.

Alavi-Borazjani, S.A., Capela, I. and Tarelho, L.A., 2020. Over-acidification control strategies for enhanced biogas production from anaerobic digestion: a review. Biomass Bioenergy, 143, 105833.

Albuquerque, J.N., Paulinetti, A.P., Lovato, G., Albanez, R., Ratusznei, S.M., Rodrigues, J.A.D., 2020. Anaerobic sequencing batch reactors Co-digesting whey and glycerin as a possible solution for small and mid-size dairy industries: environmental compliance and methane production. Appl. Biochem. Biotechnol. 192, 979–998.

Almeida, P. de S., de Menezes, C.A., Camargo, F.P., Sakamoto, I.K., Lovato, G., Rodrigues, J.A.D., Varesche, M.B.A., Silva, E.L., 2023. Biomethane recovery through co-digestion of cheese whey and glycerol in a two-stage anaerobic fluidized bed reactor: effect of temperature and organic loading rate on methanogenesis. J. Environ. Manag. 330, 117117

Almeida, P.S., Menezes, C.A., Camargo, F.P., Sakamoto, I.K., Varesche, M.B.A., Silva, E. L., 2022a. Thermophilic anaerobic co-digestion of glycerol and cheese whey – effect of increasing organic loading rate. Process Saf. Environ. Protect. 165, 895–907.

Amani, T., Nosrati, M., Sreekrishnan, T.R., 2010. Anaerobic Digestion from the Viewpoint of Microbiological, Chemical, and Operational Aspects—A Review. Environmental Reviews, 18, 255-278.

Ambaye, T.G., Rene, E.R., Nizami, A.-S., Dupont, C., Vaccari, M., van Hullebusch, E.D., 2021. Beneficial role of biochar addition on the anaerobic digestion of food waste: a systematic and critical review of the operational parameters and mechanisms. J. Environ. Manag. 290, 112537.

Amen, Tareq WM, Osama Eljamal, Ahmed ME Khalil, and Nobuhiro Matsunaga. "Evaluation of nano zero valent iron effects on fermentation of municipal anaerobic sludge and inducing biogas production." In IOP Conference Series: Earth and Environmental Science, vol. 67, no. 1, p. 012004. IOP Publishing, 2017.

An, X., Xu, Y., Dai, X., 2024. Biohythane production from two-stage anaerobic digestion of food waste: A review. J. Environ. Sci. 139, 334-349.

Angelidaki, I., Alves, M., Bolzonella, D., Borzacconi, L., Campos, J.L., Guwy, A.J., Kalyuzhnyi, S., Jenicek, P., Van Lier, J.B., 2009. Defining the biomethane potential (BMP) of solid organic wastes and energy crops: A proposed protocol for batch assays. Water Sci. Technol. 59, 927–934.

Angelidaki, I., Treu, L., Tsapekos, P., Luo, G., Campanaro, S., Wenzel, H., & Kougias, P. G., 2018. Biogas upgrading and utilization: Current status and perspectives. Biotechnology advances, 36(2), 452-466.

Angenent, L.T., Usack, J.G., Xu, J., Hafenbradl, D., Posmanik, R. and Tester, J.W., 2018. Integrating electrochemical, biological, physical, and thermochemical process units to expand the applicability of anaerobic digestion. Bioresour. Technol. 247, 1085-1094.

Antonopoulou, G., Stamatelatou, K., Venetsaneas, N., Kornaros, M., Lyberatos, G., 2008. Biohydrogen and methane production from cheese whey in a two-stage anaerobic process. Ind. Eng. Chem. Res. 47, 5227-5233.

Anwar, N., Wang, W., Zhang, J., Li, Y., Chen, C., Liu, G., Zhang, R., 2016. Effect of sodium salt on anaerobic digestion of kitchen waste. Water Sci. Technol. 73 (8), 1865–1871.

APHA, 2005. Standard Methods for the Examination of Water and Wastewater, 21st ed. American Public Health Association, American Water Works Association, Water Environment Federation, Washington, DC.

APHA. (2012). Standard Methods for the Examination of Water and Wastewater. 1496.

Astals, S., Peces, M., Batstone, D. J., Jensen, P. D., Tait, S., 2018. Characterising and modelling free ammonia and ammonium inhibition in anaerobic systems. Water Research, 143, 127-135.

Asunis, F., De Gioannis, G., Dessì, P., Isipato, M., Lens, P.N., Muntoni, A., Polettini, A., Pomi, R., Rossi, A. and Spiga, D., 2020. The dairy biorefinery: Integrating treatment processes for cheese whey valorisation. J. Environ. Manage. 276, 111240.

Atelge, M., Atabani, A., Banu, J.R., Krisa, D., Kaya, M., Eskicioglu, C., Kumar, G., Lee, C., Yildiz, Y., Unalan, S., 2020. A critical review of pretreatment technologies to enhance anaerobic digestion and energy recovery. Fuel 270, 117494.

Baek, G., Kim, J., & Lee, C., 2019. A review of the effects of iron compounds on methanogenesis in anaerobic environments. Renewable and Sustainable Energy Reviews, 113(July), 109282.

Bandler, D. K., 2023, November cheese making. Encyclopedia Britannica. https://www.britannica.com/topic/cheese-making (Accessed 2 April 2024).

Batista, L.P.P., Paulinetti, A.P., Ferraz Júnior, A.D.N., Albanez, R., Ratusznei, S.M., Etchebehere, C., Lovato, G.L., Rodrigues, J.A.D., 2023. Two-stage thermophilic anaerobic digestion of cheese whey: process optimization, comparison with single- stage, and full-scale estimation. Chemical Engineering and Processing - Process Intensification 183, 109260.

Bella, K., Pilli, S., Venkateswara Rao, P., 2023. A comparison of ultrasonic, ozone, and enzyme pre-treatments on cheese whey degradation for enhancement of anaerobic digestion. J. Environ. Manag. 340, 117960

Bella, K., Rao, P.V., 2021. Anaerobic digestion of dairy wastewater: effect of different parameters and co-digestion options - a review. Biomass Convers. Bioref.

Bella, K., Rao, V. P., 2022. Anaerobic co-digestion of cheese whey and septage: effect of substrate and inoculum on biogas production. J. Environ. Manag. 308, 114581

Beresford, T. P., Fitzsimons, N. A., Brennan, N.L., Cogan, T.M., 200. Recent advances in cheese microbiology. Int Dairy J 11(4–7):259–274.

Bharati, M, Shete, S., Shinkar, N.P., 2017. Anaerobic Digestion of dairy industry waste water-biogas evolution-a review. Int J Appl Environ Sci 12:1117–1130

Blanco, V.M.C., Fuess, L.T., Araujo, M.N., Zaiat, M., 2023. Biodigestion of easily-acidifying cheese whey in a sequential fermentative-methanogenic process:

Strategies for boosting energy production and minimizing alkalinization costs. J. Water Process Eng. 55, 104245.

Blonskaja, V., Vaalu, T., 2006. Investigation of different schemes for anaerobic treatment of food industry wastes in Estonia. Proc Est Acad Sci. 55(1):14–28.

Bonnaillie, L. M., Tomasula, P. M., 2008. Whey protein fractionation. In Whey Processing, Functionality and Health Benefits, Vol. 1, pp. 15-38. Onwulata C I and Huth P J, eds. Hoboken, NJ: Wiley-Blackwell

Bovio, P., Cabezas, A. and Etchebehere, C., 2019. Preliminary analysis of Chloroflexi populations in full-scale UASB methanogenic reactors. Journal of applied microbiology, 126(2), pp.667-683.

Bräuer, S.L., Cadillo-Quiroz, H., Ward, R.J., Yavitt, J.B., Zinder, S.H., 2011. Methanoregula boonei gen. nov., sp. nov., an acidiphilic methanogen isolated from an acidic peat bog. Int. J. Syst. Evol. Microbiol. 61, 45–52.

Bräuer, S.L., Cadillo-Quiroz, H., Yashiro, E., Yavitt, J.B., Zinder, S.H., 2006. Isolation of a novel acidiphilic methanogen from an acidic peat bog. Nature 442, 192–194.

Buchanan, D., Martindale, W., Romeih, E., Hebishy, E., 2023. Recent advances in whey processing and valorisation: Technological and environmental perspectives. International Journal of Dairy Technology 76 1-2.

Buchauer, K., 1998. A comparison of two simple titration procedures to determine volatile fatty acids in influents to waste-water and sludge treatment processes. WATER SA-PRETORIA-, 24, 49-56.

Bundhoo MAZ and Mohee R. Inhibition of dark fermentative bio-hydrogen production: a review Int. J. Hydrogen Energy, 41 (2016), pp. 6713-6733

Cai, G., Zhao, L., Wang, T., Lv, N., Li, J., Ning, J., Pan, X., Zhu, G., 2021. Variation of volatile fatty acid oxidation and methane production during the bioaugmentation of anaerobic digestion system: microbial community analysis revealing the influence of microbial interactions on metabolic pathways. Sci. Total Environ. 754, 142425.

Cai, Y., Hu, K., Zheng, Z., Zhang, Y., Guo, S., Zhao, X., Cui, Z., Wang, X., 2019. Effects of adding EDTA and Fe^{2+} on the performance of reactor and microbial community structure in two simulated phases of anaerobic digestion. Bioresour. Technol. 275, 183-191.

Cao, J., Zhang, Q., Wu, S., Luo, J., Wu, Y., Zhang, L., Feng, Q., Fang, F. and Xue, Z., 2019. Enhancing the anaerobic bioconversion of complex organics in food wastes for volatile fatty acids production by zero-valent iron and persulfate stimulation. Sci. Total Environ. 669, 540-546.

Capson-tojo, R. G., Moscoviz, D., Ruiz, G., Santa-catalina, E., Trably, M., Rouez, M., Crest, J., Steyer, N., Bernet, J., Delgen`es, R. Escudi´e, 2018. Addition of granular activated carbon and trace elements to favor volatile fatty acid consumption during anaerobic digestion of food waste, Bioresour. Technol. 260, 157–168.

Carballa, M., Regueiro, L. and Lema, J.M., 2015. Microbial management of anaerobic digestion: exploiting the microbiome-functionality nexus. Curr Opin Biotechnol, 33, .103-111.

Carvalho, F., Prazeres, A.R., Rivas, J., 2013. Cheese whey wastewater: characterization and treatment. Sci. Total Environ. 445, 385–396.

Casallas-Ojeda M., Torres-Guevara L. E., Caicedo-Concha D. M., Gómez M. F., 2021. Opportunities for waste to energy in the milk production industry: Perspectives for the circular economy. Sustainability, 13(22), 12892.

Castelló, E., y Santos, C.G., Iglesias, T., Paolino, G., Wenzel, J., Borzacconi, L. and Etchebehere, C., 2009. Feasibility of biohydrogen production from cheese whey using a UASB reactor: links between microbial community and reactor performance. Int. J. Hydrog. Energy, 34(14),5674-5682.

Chalermthai, B., Giwa, A., Schmidt, J.E., Taher, H. 2021. Life cycle assessment of bioplastic production from whey protein obtained from dairy residues. Bioresource Technology Reports, 15, 100695.

Charalambous, P. and Vyrides, I., 2021. In situ biogas upgrading and enhancement of anaerobic digestion of cheese whey by addition of scrap or powder zero-valent iron (ZVI). J. Environ. Manage. 280, 111651.

Charalambous, P., Shin, J., Shin, G.S., Vyrides, I., 2020. Anaerobic digestion of industrial dairy wastewater and cheese whey: Performance of internal circulation bioreactor and laboratory batch test at pH 5-6, Renew. Energy 147, 1-10.

Chatzipaschali, A., Stamatis, A., 2012. Biotechnological utilization with a focus on anaerobic treatment of cheese whey: current status and prospects. Energies. 5(9), 3492-3525

Chen, S., Zhang, J., Wang, X., 2015. Effects of alkalinity sources on the stability of anaerobic digestion from food waste. Waste Manag Res 33:1033–1040.

Chen, Y., Cheng, J., Creamer, K., 2008. Inhibition of anaerobic digestion process: a review. Biores Technol 99(10):4044–4064.

Cheng, J., Hua, J., Kang, T., Meng, B., Yue, L., Dong, H., Li, H. and Zhou, J., 2020. Nanoscale zero-valent iron improved lactic acid degradation to produce methane through anaerobic digestion. Bioresour. Technol. 317, 124013.

Cheng, J., Zhu, C., Zhu, J., Jing, X., Kong, F., Zhang, C., 2020. Effects of waste rusted iron shavings on enhancing anaerobic digestion of food wastes and municipal sludge. J Cleaner Production. 242,118195 J. Clean. Prod. 242, 118195.

Chokshi, K., Pancha, I., Ghosh, A., Mishra, S., 2016. Microalgal biomass generation by phycoremediation of dairy industry wastewater: An integrated approach towards sustainable biofuel production. Bioresour Technol 221:455-460.

Chong, S., Sen, T.K., Kayaalp, A., Ang, H.M., 2012. The performance enhancements of upflow anaerobic sludge blanket (UASB) reactors for domestic sludge treatment–a state-of-the art review. Water Res. 46(11), 3434–3470.

Choudhary, M., Joshi, S., Rao, L., Srivastava, N., 2021. Production of biofuel from disposed food and dairy waste in: Bioprospecting of enzymes in industry, healthcare and sustainable environment, Springer, pp. 123-138. Anaerobic digestion (AD) process

Comino, E., Riggio, V.A., Rosso, M., 2012. Biogas production by anaerobic co-digestion of cattle slurry and cheese whey. Bioresour. Technol. 114, 46–53.

Constantinou, D., Samanides, C.G., Koutsokeras, L., Constantinides, G. and Vyrides, I., 2023. Hydrogen generation by soluble CO_2 reaction with zero-valent iron or scrap iron and the role of weak acids for controlling FeCO3 formation. Sustain. Energy Technol. Assessments 56, 103061.

Cruz-Salomón, A., Ríos-Valdovinos, E., Pola-Albores, F., Lagunas-Rivera, S., Cruz-Rodríguez, R. I., Cruz-Salomón, K. D. C., Hernandez-Mendez, J.M.E., Dominguez-Espinola, M.E., 2020. Treatment of cheese whey wastewater using an expanded granular sludge bed (EGSB) bioreactor with biomethane production. PRO 8:931.

Czatzkowska, M., Harnisz, M., Korzcnicwska, E., Koniuszewska, I., 2020. Inhibitors of the methane fermentation process with particular emphasis on the microbiological aspect: a review. Energy Sci. Eng. 8 (5), 1880–1897

Dai, X., Duan, N., Dong, B., Dai, L., 2013. High-solids anaerobic co-digestion of sewage sludge and food waste in comparison with mono digestions: stability and performance. Waste Manage. (Tucson, Ariz.) 33 (2), 308–316.

Dareioti, M.A., Kornaros, M., 2015. Anaerobic mesophilic co-digestion of ensiled sorghum, cheese whey, and liquid cow manure in a two-stage CSTR system:effect of hydraulic retention time. Bioresour. Technol. 175, 553–562.

Dareioti, M.A., Vavouraki, A.I., Tsigkou, K., Kornaros, M., 2021. Assessment of Single- vs. two-stage process for the anaerobic digestion of liquid cow manure and cheese whey. Energies 14 (17), 5423.

Davila-Vazquez, G., Cota-Navarro, C. B., Rosales-Colunga, L. M., de León-Rodríguez, A., & Razo-Flores, E. 2009. Continuous biohydrogen production

using cheese whey: improving the hydrogen production rate. Int. J. Hydrog. Energy, 34(10), 4296-4304.

Deepanraj, B., Sivasubramanian, V., Jayaraj, S., 2014. Biogas generation through anaerobic digestion process-an overview. Res. J. Chem. Environ. 18(5), 80-93.

Demirel, B., Scherer, P., 2008. The roles of acetotrophic and hydrogenotrophic methanogens during anaerobic conversion of biomass to methane: A review. Rev. Environ. Sci. Biotechnol. 7, 173–190.

Dereli, R.K., van der Zee, F.P., Ozturk, I., van Lier, J.B. 2019. Treatment of cheese whey by a cross-flow anaerobic membrane bioreactor: Biological and filtration performance. Environ. Res. 168, 109–117.

Deschamps, L., Imatoukene, N., Lemaire, J., Mounkaila, M., Filali, R., Lopez, M., & Theoleyre, M. A., 2021. In-situ biogas upgrading by bio-methanation with an innovative membrane bioreactor combining sludge filtration and H_2 injection. Bioresource Technology, 337, 125444.

Deutzmann J.S., Sahin M., Spormann A.M., 2015. Extracellular enzymes facilitate electron uptake in biocorrosion and bioelectrosynthesis mBio, 6 (2) p. 15, 10.1128/mBio.00496-15 e00496

Diamantis, V.I., Kapagiannidis, A.G., Ntougias, S., Tataki, V., Melidis, P., Aivasidis, A., 2014. Two-stage CSTR-UASB digestion enables superior and alkali addition-free cheese whey treatment. Biochem. Eng. J. 84, 45–52.

Dong, D., Aleta, P., Zhao, X., Choi, O. K., Kim, S., & Lee, J. W., 2019. Effects of nanoscale zero valent iron (nZVI) concentration on the biochemical conversion of gaseous carbon dioxide (CO2) into methane (CH4). Bioresource technology, 275, 314-320.

Dragone, G., Mussatto, S.I., Oliveira, J.M., Teixeira, J.A. 2009. Characterisation of volatile compounds in an alcoholic beverage produced by whey fermentation, Food Chem., 112, 929–935.

Dreschke, G., Probst, M., Walter, A., Pümpel, T., Walde, J., Insam, H., 2015. Lactic acid and methane: Improved exploitation of biowaste potential. Biores. Technol., 47–55.

Duval, B., Goodwin, S., 2000. Methane production and release from two New England peatlands. Int. Microbiol. 3, 89–95.

Ebrahimi, A., Najafpour GD., Mohammadi M., Hashemiyeh B.,2010. Biological treatment of whey in an UASFF bioreactor following a three-stage RBC. Chem Ind Chem Eng. 16(2):175–82.

El-Temsah, Y.S., Joner, E.J., 2012.Impact of Fe and Ag nano particles on seed germination and differences in bioavailability during exposure in aqueous suspension and soil. Environ.Toxicol.27,42–49.

Erdirencelebi, D., 2011.Treatment of high-fat-containing dairy wastewater in a sequential UASBR system: influence of recycle, J. Chem. Technol. Biotechnol. 86, 525–533

Ergüder, TH., Tezel, U., Güven, E., Demirer, GN., 2001. Anaerobic biotransformation and methane generation potencial of cheese whey in batch and UASB reactors. Waste Manage. 21(7):643–50.

Escalante, H., Castro, L., Amaya, M.P., Jaimes, L., Jaimes-Estevez, J., 2018. Anaerobic digestion of cheese whey: energetic and nutritional potential for the dairy sector in developing countries. Waste Manag. 71, 711-718.

Escalante, H., Castro, L., Besson, V., Jaimes-Estevez, J., 2017. Feasibility of the anaerobic process of Cheese Whey in a plug flow reactor (PFR) under local conditions, Ing., Inv. Techn., 18, 265–277.

FAO, 2023. Dairy Market Review-Emerging trends and outlook in 2023. Rome. Food and Agriculture Organization of the United Nations.

Farizoglu, B., Keskinler, B., Yildiz, E., Nuhoglu, A., 2004. Cheese whey treatment performance of an aerobic jet loop membrane bioreactor. Process Biochem. 39(12):2283–91.

Feng, K., Wang, Q., Li, H., Zhang, Y.Y., Deng, Z., Liu, J.G., Du, X., 2020. Effect of fermentation type regulation using alkaline addition on two-phase anaerobic

digestion of food waste at different organic load rates. Renew. Energ. 154, 385–393

Feng, Y., Zhang, Y., Quan, X. and Chen, S., 2014. Enhanced anaerobic digestion of waste activated sludge digestion by the addition of zero valent iron. Water Res., 52, 242-250.

Ferchichi, M., Crabbe, E., Gil, GH., Hintz, W., Almadidy, A., 2005. Influence of initial pH on hydrogen production from cheese whey. J Biotechnol. 120(4):402–9.

Fernandes, T.V., Keesman, K.J., Zeeman, G., van Lier, J.B., 2014. Effect of ammonia on the anaerobic hydrolysis of cellulose and tributyrin. Biomass Bioenergy. 47, 316-323.

Fernández, C., Cuetos, M., Martínez, E., Gómez, X., 2015. Thermophilic anaerobic digestion of cheese whey: Coupling H_2 and CH_4 production. Biomass Bioenergy, 81, 55–62.

Fernandez-Rodríguez, M.J., Puntano, N.F., Mancilla-Leyt´on, J.M., Borja, R., 2021. Batch mesophilic anaerobic co-digestion of spent goat straw bedding and goat cheese whey: comparison with the mono-digestion of the two sole substrates. J. Environ. Manag. 280

Franke-Whittle, I.H., Walter, A., Ebner, C., Insam, H., 2014. Investigation into the effect of high concentrations of volatile fatty acids in anaerobic digestion on methanogenic communities. Waste Manag. 34, 2080–2089.

Fu, S., Angelidaki, I., Zhang, Y., 2020. In situ biogas upgrading by CO_2-to-CH_4 bioconversion. Trends Biotechnol;39(4):336–47.

Gannoun, H., Khelifi, E., Bouallagui, H., Touhami, Y., Hamdi, M., 2008. Ecological clarification of cheese whey prior to anaerobic digestion in upflow anaerobic filter. Bioresour Technol. 99(14):6105–11.

Garuti, M., Langone, M., Fabbri, C., Piccinini, S., 2018. Methodological approach for trace elements supplementation in anaerobic digestion: experience from full-scale agricultural biogas plants. J. Environ. Manag. 223, 348–357.

Gelegenis, J., Georgakakis, D., Angelidaki, I., Mavris, V., 2007. Optimization of biogas production by co-digesting whey with diluted poultry manure. Renew. Energy 32, 2147–2160.

Ghaly, A.E., Mahmoud, N., Rushton, D., Arab, F., 2007. Potential environmental and health impacts of high land application of cheese whey. American Journal of Agricultural and Biological Sciences, 2, 106-117.

Ghaly, AE., Kamal, MA., 2004. Submerged yeast fermentation of acid cheese whey for protein production and pollution potential reduction. Water Res. 38(3):631–44.

Gomez-Romero, J., Gonzalez-Garcia, A., Chairez, I., Torres, L., García-Peña, E.I., 2014. Selective adaptation of an anaerobic microbial community: Biohydrogen production by co-digestion of cheese whey and vegetables fruit waste. Int. J. Hydrogen Energy, 39, 12541–12550.

Gonzalez-Piedra, S., Hern´ andez-García, H., Perez-Morales, J.M., Acosta-Domínguez, L., Bastidas-Oyanedel, J.R., Hernandez-Martinez, E., 2021. A study on the feasibility of anaerobic co-digestion of raw cheese whey with coffee pulp residues. Energies 14, 1–11.

Guha, T., Ravikumar, K.V.G., Mukherjee, A., Mukherjee, A., Kundu, R., 2018. Nanopriming with zero valent iron (nZVI) enhances germination and growth in aromatic rice cultivar (*Oryza sativa* cv. Gobindabhog L.). Plant Physiol. Biochem. 127, 403-413

Hao, L., Lü, F., Li, L., Wu, Q., Shao, L. and He, P., 2013. Self-adaption of methane-producing communities to pH disturbance at different acetate concentrations by shifting pathways and population interaction. Bioresour. Technol.140, 319-327.

Hao, L.P., Lü, F., Li, L., Shao, L.M. and He, P.J., 2012. Shift of pathways during initiation of thermophilic methanogenesis at different initial pH. Bioresour. Technol.126, 418-424.

Harirchi, S., Wainaina, S., Sar, T., Nojoumi, A., S., Parchami., M., Varjani, S., Khanal, K. S., Wong, J., Awasthi, K. M., Taherzadeh, J. M., 2022.

Microbiological insights into anaerobic digestion for biogas, hydrogen or volatile fatty acids (VFAs): A review. Bioengineered, 13(3): 6521–6557.

He, Z. W., Zou, Z. S., Ren, Y. X., Tang, C. C., Zhou, A. J., Liu, W., Wang, L., Li, Z., Wang, A., 2022. Roles of zero-valent iron in anaerobic digestion: Mechanisms, advances and perspectives. Science of the Total Environment, 852(August), 158420.

Hu, Y., Hao, X., Zhao, D., Fu, K., 2015. Enhancing the CH4 yield of anaerobic digestion via endogenous CO2 fixation by exogenous H2. Chemosphere 140, 34-39.

Imeni, S.M., Pelaz, L., Corchado-Lopo, C., Busquets, A.M., Ponsá, S. and Colón, J., 2019. Techno-economic assessment of anaerobic co-digestion of livestock manure and cheese whey (Cow, Goat & Sheep) at small to medium dairy farms. Bioresour. Technol. 291, 121872.

Jain, S.R., Mattiasson, B., 1998. Acclimatization of methanogenic consortia for low pH biomethanation process. Biotechnol. Lett. 20, 771–775.

Janczukowicz, W., Zielinski, M., Dbowski, M., 2008. Biodegradability evaluation of dairy effluents originated in selected sections of dairy production. Bioresour Technol. 99(10):4199–205.

Jang, H.M., Choi, Y.K., Kan, E., 2018. Effects of dairy manure-derived biochar on psychrophilic, mesophilic and thermophilic anaerobic digestions of dairy manure. Bioresour. Technol. 250, 927–931.

Jiang, Y., May, H.D., Lu, L., Liang, P., Huang, X. and Ren, Z.J., 2019. Carbon dioxide and organic waste valorization by microbial electrosynthesis and electro-fermentation. Water Res. 149, 42-55.

Jing, H., Cui, Y., Ye, M., Yan, X. and Liu, Y., 2022. Effect of zero-valent iron on acidification and methane production using food waste under different food-to-microorganism ratios. Renew. Energy, 198, 131-143.

Jung, H., Kim, J., Lee, C., 2016. Continuous anaerobic co-digestion of *Ulva* biomass and cheese whey at varying substrate mixing ratios: Different

responses in two reactors with different operating regimes. Bioresour. Technol. 221, 366–374.

Kainthola, J., Kalamdhad, A.S., Goud, V.V., 2019. A review on enhanced biogas production from anaerobic digestion of lignocellulosic biomass by different enhancement techniques. Process Biochem. 84, 81–90.

Karim, K., Hoffmann, R., Klasson, K.T., Al-dahhan, M.H., 2005. Anaerobic digestion of animal waste: effect of mode of mixing. Water Res. 39, 3597-3606.

Kassongo, J., Shahsavari, E., Ball, A.S., 2020. Renewable energy from the solid-state anaerobic digestion of grape marc and cheese whey at high treatment capacity. Biomass. Bioenerg. 143, 105880.

Kato, S., 2016. Microbial extracellular electron transfer and its relevance to iron corrosion. Microb. Biotechnol. 9(2), 141-148.

Kaur, G., Johnravindar, D., Wong, J.W.C., 2020. Enhanced volatile fatty acid degradation and methane production efficiency by biochar addition in food waste-sludge co- digestion: a step towards increased organic loading efficiency in co-digestion. Bioresour. Technol. 308, 123250.

Kavacik, B., Topaloglu, B., 2010. Biogas production from co-digestion of a mixture of cheese whey and dairy manure. Biomass Bioenergy 34, 1321–1329.

Khan, A., Akbar, S., Okonkwo, V., Smith, C., Khan, S., Shah, A. A., ... & Badshah, M., 2022. Enrichment of the hydrogenotrophic methanogens for, in-situ biogas up-gradation by recirculation of gases and supply of hydrogen in methanogenic reactor. Bioresource Technology, 345, 126219.

Kim, E., Lee, J., Han, G., Hwang, S., 2018. Comprehensive Analysis of Microbial Communities in Full-Scale Mesophilic and Thermophilic Anaerobic Digesters Treating Food Waste-Recycling Wastewater. Bioresource Technology.

Kim, I.S., Hwang, M.H., Jang, N.J., Hyun, S.H. and Lee, S.T., 2004. Effect of low pH on the activity of hydrogen utilizing methanogen in bio-hydrogen process. Int. J. Hydrog. Energy, 29, (11), .1133-1140.

Kim, N., Jeon, J., Elbert, J., Kim, C., Su, X., 2022. Redox-mediated electrochemical desalination for waste valorization in dairy production. Chemical Engineering Journal, 428, Article 131082.

Kong, X., Li, Q., Zhang, W., Niu, J., Wang, S., Liu, J., Yuan, J., Yue, X., Liu, Y. and Zhang, Y., 2023. Metabolic effects of Fe0 on simultaneously eliminating excessive acidification and upgrading biogas in mesophilic or thermophilic anaerobic reactor. J. Clean. Prod.136079.

Kong, X., Wei, Y., Xu, S., Liu, J., Li, H., Liu, Y. and Yu, S., 2016. Inhibiting excessive acidification using zero-valent iron in anaerobic digestion of food waste at high organic load rates. Bioresour. Technol. 211, 65-71.

Kong, X., Yu, S., Fang, W., Liu, J., Li, H., 2018. Enhancing syntrophic associations among Clostridium butyricum, Syntrophomonas and two types of methanogen by zero valent iron in an anaerobic assay with a high organic loading. Bioresour. Technol. 257, 181–191.

Kong, X., Yu, S., Xu, S., Fang, W., Liu, J. and Li, H., 2018. Effect of Fe0 addition on volatile fatty acids evolution on anaerobic digestion at high organic loading rates. Waste Manag., 71, 719-727.

Kong, X., Yu, S., Xu, S., Fang, W., Liu, J. and Li, H., 2018. Effect of Fe0 addition on volatile fatty acids evolution on anaerobic digestion at high organic loading rates. Waste Manag., 71, 719-727.

Kumar, V., Nabaterega, R., Khoei, S., Eskiocioglu, C., 2021. Insight into interactions between syntrophic bacteria and archaea in anaerobic digestion amended with conductive materials. Renew Sust Energ Rev. 144:110965.

Kunacheva, C. and Stuckey, D.C., 2014. Analytical methods for soluble microbial products (SMP) and extracellular polymers (ECP) in wastewater treatment systems: a review. Water Res. 61, 1-18.

Kwietniewska, E., Tys, J., 2014. Process characteristics, inhibition factors and methane yields of anaerobic digestion process, with particular focus on microalgal biomass fermentation. Renew Sustain Energy Rev 34:491–500.

Labatut, R.A., Angenent, L.T., Scott, N.R., 2011. Biochemical methane potential and biodegradability of complex organic substrates. Biores. Technol., 2255–2264.

Lagoa-Costa, B., Kennes, C. and Veiga, M.C., 2020. Cheese whey fermentation into volatile fatty acids in an anaerobic sequencing batch reactor. Bioresour. Technol. 308, 123226

Laiq Ur Rehman, M., Iqbal, A., Chang, C.C., Li, W., Ju, M., 2019. Anaerobic digestion. Water Environ. Res. 91, 1253-1271.

Lappa, I.K., Papadaki, A., Kachrimanidou, V., Terpou, A., Koulougliotis, D., Eriotou, E., Kopsahelis, N., 2019. Cheese whey processing: integrated biorefinery concepts and emerging food applications. Foods 8(8).

Lawton, M. R., Dana, L. D., Alcaine, S. D., 2021. Lactose utilization by Brettanomyces claussenii expands potential for valorization of dairy by-products to functional beverages through fermentation. Current Opinion in Food Science 42 93–101.

Legg, A. K., Carr, A. J., Bennett, R. J., Johnston, K. A., 2017. General aspects of cheese technology. In P. L. H. McSweeney, P. F. Fox, P. D. Cotter, & D. W. Everett (Eds.), Cheese: Chemistry, physics and microbiology (4th ed., Vol.1, pp. 643-675). San Diego, DA, USA: Academic Press

Lettinga, G., Van Velsen, A.F.M., Hobma, S.W., de Zeeuw, W., Klapwijk, A., 1980. Use of the upflow sludge blanket (USB) reactor concept for biological waste water treatment especially for anaerobic treatment. Biotechnol. Bioeng. 22, 699–734.

Li, S., Cao, Y., Zhao, Z., Zhang, Y., 2019. Regulating secretion of extracellular polymeric substances through dosing magnetite and zerovalent iron nanoparticles to affect anaerobic digestion mode. ACS Sustain. Chem. Eng. 7 (10), 9655–9662

Li, Y., Sun, Y., Li, L. and Yuan, Z., 2018. Acclimation of acid-tolerant methanogenic propionate-utilizing culture and microbial community dissecting. Bioresour. Technol. 250, 117-123

Li, Y., Sun, Y., Li, L., Yuan, Z., 2018. Acclimation of acid-tolerant methanogenic propionate-utilizing culture and microbial community dissecting. Bioresour. Technol. 250, 117−123

Li, Y.; Yang, G.; Li, L.; Sun, Y. 2018. Bioaugmentation for overloaded anaerobic digestion recovery with acid-tolerant methanogenic enrichment. Waste Manag. 79, 744−751.

Libralato, G., Devoti, A.C., Zanella, M., Sabbioni, E., Micetic, I., Manodori, L., Pigozzo, A., Manenti, S., Groppi, F., Ghirardini, A.V., 2016. Phytotoxicity of ionic, micro- and nano-sized iron in three plant species. Ecotoxicol. Environ. Saf. 123, 81-88.

Liu, Y., Wang, Q., Zhang, Y. and Ni, B.J., 2015. Zero valent iron significantly enhances methane production from waste activated sludge by improving biochemical methane potential rather than hydrolysis rate. Scientific reports, 5(1), 1-6.

Liu, Y., Zhang, Y., Quan, X., Li, Y., Zhao, Z., Meng, X. and Chen, S., 2012. Optimization of anaerobic acidogenesis by adding Fe0 powder to enhance anaerobic wastewater treatment. Chemical engineering journal, 192, 179-185.

Lizama, A.C.; Figueiras, C.C.; Pedreguera, A.Z.; Espinoza, J.E.R., 2020. Enhancing the performance and stability of the anaerobic digestion of sewage sludge by zero valent iron nanoparticles dosage. Bioresour. Technol. 2018, 275, 352–359.

Lovato, G., Albanez, R., Ruggero, L.S., Stracieri, L., Ratusznei, S.M., Domingues Rodrigues, J.A., Rodrigues, J.A.D., 2020. Energetic feasibility of a two-stage anaerobic digestion system compared to a single-stage system treating whey and glycerin. Biochem. Eng. J. 161, 107653

Lovato, G., Albanez, R., Triveloni, M., Ratusznei, S.M., Rodrigues, J.A.D., 2019. Methane Production by Co-Digesting Vinasse and Whey in an AnSBBR: Effect of Mixture Ratio and Feed Strategy. Appl. Biochem. Biotechnol.187, 28–46

Lovato, G., Ratusznei, S.M., Rodrigues, J.A.D., Zaiat, M., 2016. Co-digestion of whey with glycerin in an AnSBBR for biomethane production. Appl. Biochem. Biotechnol. 178, 126–143.

Lü, F., Hao, L.P., Shao, L.M., Bouchez, T., He, P.J., 2010. Release from acid crisis by shifting methanogenesis pathway under thermophilic anaerobic digestion. In: Proceedings of Venice 2010, Third International Symposium on Energy from Biomass and Waste, Venice, Italy, November 7–11, 2010.

Luo, G., Johansson, S., Boe, K., Xie, L., Zhou, Q., & Angelidaki, I., 2012. Simultaneous hydrogen utilization and in situ biogas upgrading in an anaerobic reactor. Biotechnology and bioengineering, 109(4), 1088-1094.

Luo, X., Yuan, X., Wang, S., Sun, F., Hou, Z., Hu, Q., Zhai, L., Cui, Z., Zou, Y., 2018. Methane production and characteristics of the microbial community in the codigestion of spent mushroom substrate with dairy manure. Bioresour. Technol. 250, 611-620.

Ma, L., Zhou, L., Mbadinga, S. M., Gu, J. D., & Mu, B. Z., 2018. Accelerated CO_2 reduction to methane for energy by zero valent iron in oil reservoir production waters. Energy, 147, 663–671.

Ma, L., Zhou, L., Ruan, M.Y., Gu, J.D. and Mu, B.Z., 2019. Simultaneous methanogenesis and acetogenesis from the greenhouse carbon dioxide by an enrichment culture supplemented with zero-valent iron. Renew. Energy, 132, .861-870.

Ma, X., Gurung, A., Deng, Y., 2013.Phytotoxicity and uptake of nano scale zero-valent iron (nZVI) by two plant species. Sci.Total. Environ.443,844–849

MacLeod, F.A., Guiot, S.R., Costerton, J.W., 1990. Layered structure of bacterial aggregates produced in an upflow anaerobic sludge bed and filter reactor. Appl. Environ. Microbiol. 56, 1598–1607.

Mao, C., Feng, Y., Wang, X., Ren, G., 2015. Review on research achievements of biogas from anaerobic digestion. Renew. Sustain. Energy Rev. 45, 540–555.

Mariraj Mohan, S., Swathi, T. A., 2022. Review on Upflow Anaerobic Sludge Blanket Reactor: Factors Affecting Performance, Modification of Configuration and Its Derivatives. Water Environ. Res. 94, e1665.

Meegoda, J.N., Li, B., Patel, K., Lily, B., Wang, L.B., 2018. A review of the processes, parameters, and optimization of anaerobic digestion. Int. J. Environ. Res. Public Health, 15, 2224.

Meena, R.A.A., Banu, J.R., Kannah, R.Y., Yogalakshmi, K.N., Kumar, G., 2020. Biohythane production from food processing wastes – challenges and perspectives. Bioresour. Technol. 298, 122449.

Mendes, A.A., Pereira, E., &de Castro, H., 2006.Effect of the enzymatic hydrolysis pretreatment of lipids-rich wastewater on the anaerobic biodigestion. Biochemical EngineeringJournal,32,185–190.

Meng, X., Zhang, Y., Li, Q. and Quan, X., 2013. Adding Fe0 powder to enhance the anaerobic conversion of propionate to acetate. Biochem. Eng. J. 73, 80-85.

Menikea, K.K., Kyprianou, A., Samanides, C.G., Georgiou, S.G., Koutsokeras, L., Constantinides, G. and Vyrides, I., 2020. Anaerobic granular sludge and zero valent scrap iron (ZVSI) pre-treated with green tea as a sustainable system for conversion of CO2 to CH4. Clean. Prod, 268, 121860.

Mirmohamadsadeghi, S., Karimi, S., Tabatabaei, M., Aghbashlof, M., 2019. Biogas production from food wastes: a review on recent developments and future perspectives. Bioresource Technology Reports 7:1–10.

Mockaitis, G., Ratusznei, S.M., Rodrigues, J.A.D., Zaiat, M., Foresti, E., 2006. Anaerobic whey treatment by a stirred sequencing batch reactor (ASBR): Effects of organic loading and supplemented alkalinity. J. Environ. Manage. 79, 198–206.

Moeller, L., Zehnsdorf, A., 2016. Process upsets in a full-scale anaerobic digestion bioreactor: over-acidification and foam formation during biogas production. Energy Sustain. Soc. 6 (1), 30.

Moreno, R., Escapa, A., Cara, J., Carracedo, B. and Gómez, X., 2015. A two-stage process for hydrogen production from cheese whey: Integration of dark

fermentation and biocatalyzed electrolysis. Int. J. Hydrog. Energy, 40(1), 168-175.

Mosbæk, F., Kjeldal, H., Mulat, D.G., Albertsen, M., Ward, A.J., Feilberg, A. and Nielsen, J.L., 2016. Identification of syntrophic acetate-oxidizing bacteria in anaerobic digesters by combined protein-based stable isotope probing and metagenomics. ISME 10, 2405–2418

Moset, V., Poulsen, M., Wahid, R., Højberg, O., Møller, H.B., 2015. Mesophilic versus thermophilic anaerobic digestion of cattle manure: Methane productivity and microbial ecology. Microb. Biotechnol. 8, 787-800.

Mulat, D. G., Mosbæk, F., Ward, A. J., Polag, D., Greule, M., Keppler, F., ... & Feilberg, A., 2017. Exogenous addition of H_2 for an in-situ biogas upgrading through biological reduction of carbon dioxide into methane. Waste Management, 68, 146-156.

Muñoz, R., Meier, L., Diaz, I. and Jeison, D., 2015. A review on the state-of-the-art of physical/chemical and biological technologies for biogas upgrading. Rev Environ Sci Biotechnol. 14, 727-759.

Narihiro, T., Nobu, M.K., Kim, N.K., Kamagata, Y. and Liu, W.T., 2015. The nexus of syntrophy-associated microbiota in anaerobic digestion revealed by long-term enrichment and community survey. Environ. Microbiol., 17, 1707-1720.

Njoya, M., Basitere, M., Ntwampe, S.K.O. 2019. High Rate Anaerobic Treatment of Poultry Slaughterhouse Wastewater (PSW). Nova Science Publishers, Inc.: New York, NY, USA, Volume 38. 173–210.

OECD/FAO, 2020. OECD-FAO Agricultural Outlook 2020-2029. Dairy and Dairy Products.

Paepatung, N., Songkasiri, W., Yasui, H., & Phalakornkule, C. (2020). Enhancing methanogenesis in fed-batch anaerobic digestion of high-strength sulfate-rich wastewater using zero valent scrap iron. J. Environ. Chem. Eng., 8(6), 104508.

Palns, S.S., Loewenthal, R.E., Dold, P.L., Marais, G.R., 1987. Hypothesis for pelletisation in upflow anaerobic sludge blanket reactor. Water SA 13, 69–80.

Palù, M., Peprah, M., Tsapekos, P., Kougias, P., Campanaro, S., Angelidaki, I. and Treu, L., 2022. In-situ biogas upgrading assisted by bioaugmentation with hydrogenotrophic methanogens during mesophilic and thermophilic co-digestion. Bioresour. Technol. 348, 126754.

Panesar, P.S., Kennedy, J.F., 2012. Biotechnological approaches for the value addition of whey. Crit. Rev. Biotechnol. 32 (4), 327–348.

Papademas, P., Kotsaki P., 2019. Technological utilization of whey towards sustainable exploitation. J Adv Dairy Res. 7:231.

Papirio, S., Matassa, S., Pirozzi, F., Esposito, G., 2020. Anaerobic Co-digestion of cheese whey and industrial hemp residues opens new perspectives for the valorization of agri-food waste. Energies 13, 2820.

Patel, G.B., Sprott, G.D., Fein, J.E., 1990. Isolation and Characterization of Methanobacterium espanolae sp . nov . , a Mesophilic , Moderately Acidiphilic Methanogen. Int. J. Syst. Evol. Microbiol. 40, 12–18.

Paulo, L.P., Jiang, B., Cysneiros, D., Stams, A.J.M, Lettinga, G., 2004. Effect of cobalt on the anaerobic thermophilic conversion of methanol, Biotechnol. Bioeng. 85, 434–441.

Peng, H., Zhang, Y., Tan, D., Zhao, Z., Zhao, H., Quan, X., 2018. Roles of magnetite and granular activated carbon in improvement of anaerobic sludge digestion. Bioresour. Technol. 249, 666–672.

Peng, X., Zhang, S.Y., Li, L., Zhao, X., Ma, Y., Shi, D., 2018a. Long-term high-solids anaerobic digestion of food waste: effects of ammonia on process performance and microbial community. Bioresour. Technol. 262, 148-158.

Pereboom, J.H.F., Vereijken, T.L.F.M., 1994. Methanogenic granule development in full scale internal circulation reactors. Water Sci. Technol. 30, 9–21.

Philips, J., 2020. Extracellular electron uptake by acetogenic bacteria: does H_2 consumption favor the H_2 evolution reaction on a cathode or metallic iron? Frontiers in Microbiology, 10, p.483184.

Philips, J., Monballyu, E., Georg, S., De Paepe, K., Prévoteau, A., Rabaey, K. and Arends, J.B., 2019. An Acetobacterium strain isolated with metallic iron as

electron donor enhances iron corrosion by a similar mechanism as Sporomusa sphaeroides. FEMS Microbiol. Ecol., 95, 2, p. fiy222.

Pires, A.F., Marnotes, N.G., Rubio, O.D., Garcia, A.C., Pereira, C.D., 2021. Dairy By- Products: A Review on the Valorization of Whey and Second Cheese Whey. Foods (Basel, Switzerland) 10.

Prazeres, A. R., Carvalho, F., Rivas, J., 2012. Cheese whey management: A review. Journal of Environmental Manag. 110, 48–68.

Prévoteau, A., Carvajal-Arroyo, J.M., Ganigué, R. and Rabaey, K., 2020. Microbial electrosynthesis from CO2: forever a promise? Current opinion in biotechnology, 62, 48-57.

Puyol, D., Flores-Alsina, X., Segura, Y., Molina, R., Padrino, B., Fierro, J.L.G., Gernaey, K.V., Melero, J.A. and Martinez, F., 2018. Exploring the effects of ZVI addition on resource recovery in the anaerobic digestion process. Chem. Eng. J., 335,703-711.

Rajagopal, R., Bellavance, D., and Rahaman, M. S., 2017. Psychrophilic anaerobic digestion of semi-dry mixed municipal food waste: For North American context. Process Safety and Environmental Protection, Institution of Chemical Engineers, 105, 101–108.

Rajagopal, R., Masse, D. I., Singh, G., 2013. A critical review on inhibition of anaerobic digestion process by excess ammonia. Bioresource Technology, 143, 632-641.

Rajendran, K., Mahapatra, D., Venkatraman, A.V., Muthuswamy, S., Pugazhendhi, A., 2020. Advancing anaerobic digestion through two-stage processes: current developments and future trends. Renew. Sustain. Energy Rev. 123, 109746.

Rico, C., Mu˜noz, N., Rico, J.L., 2015. Anaerobic co-digestion of cheese whey and the screened liquid fraction of dairy manure in a single continuously stirred tank reactor process: limits in co-substrate ratios and organic loading rate. Bioresour. Technol. 189, 327–333.

Riggio, S., Torrijos, M., Vives, G., Esposito, G., van Hullebusch, E. D., Steyer, J. P., Escudié, R., 2017. Leachate flush strategies for managing volatile fatty

acids accumulation in leach-bed reactors. Bioresource Technology, 232, 93-102.

Rotaru, A.-E., Shrestha, P.M., Liu, F., Markovaite, B., Chen, S., Nevin, K.P., Lovley, D.R., 2014a. Direct interspecies electron transfer between geobacter metallireducens and methanosarcina barkeri. Appl. Environ. Microbiol. 80, 4599e4605.

Rotaru, A.-E., Shrestha, P.M., Liu, F., Shrestha, M., Shrestha, D., Embree, M., Zengler, K., Wardman, C., Nevin, K.P., Lovley, D.R., 2014b. A new model for electron flow during anaerobic digestion: direct interspecies electron transfer to Methanosaeta for the reduction of carbon dioxide to methane. Energy Environ. Sci. 7, 408e415.

Ryan, M.P., Walsh, G., 2016. The biotechnological potential of whey. Rev. Environ. Sci. Biotechnol. 15 (3), 479–498.

Saady, N.M.C., 2013. Homoacetogenesis during hydrogen production by mixed cultures dark fermentation: unresolved challenge. Int. J. Hydrog. Energy, 38(30),13172-13191

Saddoud, A., Hassaïri, I., Sayadi, S., 2007. Anaerobic membrane reactor with phase separation for the treatment of cheese whey. Bioresour Technol. 98(11):2102–8.

Samanides, C. C., Koutsokeras, L., Constantinides, G., Vyrides, I., 2020. Methanogenesis Inhibition in Anaerobic Granular Sludge for the Generation of Volatile Fatty Acids from CO2 and Zero Valent Iron. Front. Energy Res. 8-37

Samanides, C.G. and Vyrides, I., 2023. CO2 conversion to volatile fatty acids by anaerobic granular sludge and Mg0. Biochem. Eng. J. 191, p.108799.

Sarker, S., Lamb, J.J., Hjelme, D.R., Lien, K.M., 2019. A Review of the Role of Critical Parameters in the Design and Operation of Biogas Production Plants. Appl., 9, 1915.

Savant, D. V., Shouche, Y.S., Prakash, S., Ranade, D.R., 2002. Methanobrevibacter acididurans sp. nov., a novel methanogen from a sour anaerobic digester. Int. J. Syst. Evol. Microbiol. 52, 1081–1087.

Schiebahn, S., Grube, T., Robinius, M., Tietze, V., Kumar, B. and Stolten, D., 2015. Power to gas: Technological overview, systems analysis and economic assessment for a case study in Germany. International Journal of Hydrogen Energy, 40 (12), 4285-4294.

Shi, Y., Liu, T., Chen, S. and Quan, X., 2022. Accelerating anaerobic hydrolysis acidification of dairy wastewater in integrated floating-film and activated sludge (IFFAS) by using zero-valent iron (ZVI) composite carriers. Biochem. Eng. J., 177,108226.

Show, K.-Y., Yan, Y., Yao, H., Guo, H., Li, T., Show, D.-Y., Chang, J.-S., Lee, D.-J., 2020. Anaerobic granulation: A review of granulation hypotheses, bioreactor designs and emerging green applications. Bioresour. Technol. 300, 122751.

Singh, B., Szamosi, Z., Siménfalvi, Z., 2020. Impact of mixing intensity and duration on biogas production in an anaerobic digester: A review. Crit. Rev. Biotechnol. 40, 508-521.

Sivagurunathan, P., Sen, B. and Lin, C.Y., 2014. Overcoming propionic acid inhibition of hydrogen fermentation by temperature shift strategy. Int. J. Hydrog. Energy, 39, (33), .19232-19241

Soumati, B., Atmani, M., Benabderrahmane, A., Benjelloun, M., 2023. Whey valorization- innovative strategies for sustainable development and value-added product creation, J. Ecol. Eng. 24(10) 86-104.

Sousa, S.P., Lovato, G., Albanez, R., Ratusznei, S.M., Rodrigues, J.A.D., 2019. Improvement of Sugarcane Stillage (Vinasse) Anaerobic Digestion with Cheese Whey as its Co-substrate: Achieving High Methane Productivity and Yield. Appl. Biochem. Biotechnol. 189, 987–1006.

Srisowmeya, G., Chakravarthy, M., Nandhini Devi, G., 2020. Critical considerations in two-stage anaerobic digestion of food waste – a review. Renew. Sustain. Energy Rev. 119, 109587.

Stasinakis, A.S., Charalambous, P. and Vyrides, I., 2022. Dairy wastewater management in EU: Produced amounts, existing legislation, applied treatment processes and future challenges. J. Environ. Manage., 303, 114152.

Sugiarto, Y., Sunyoto, N.M.S., Zhu, M., Jones, I., Zhang, D., 2021. Effect of biochar addition on microbial community and methane production during anaerobic digestion of food wastes: the role of minerals in biochar. Bioresour. Technol. 323, 124585.

Summers, Z.M., Fogarty, H.E., Leang, C., Franks, A.E., Malvankar, N.S., Lovley, D.R., 2010. Direct exchange of electrons within aggregates of an evolved syntrophic coculture of anaerobic bacteria. Science. 330(6009):1413–1415.

Sun, Z. F., Zhao, L., Wu, J. T., Wang, Z. H., Wu, K. K., Chen, C., ... & Ren, N. Q., 2023. Exogenous hydrogen supply improves in-situ biogas upgrading of sewage sludge: Performance and mechanisms. Chemical Engineering Journal, 477, 147307

Taconi, K.A., Zappi, M.E., Todd French, W., Brown, L.R., 2007. Feasibility of methanogenic digestion applied to a low pH acetic acid solution. Bioresour. Technol. 98, 1579–1585.

Taconi, K.A., Zappi, M.E., Todd French, W., Brown, L.R., 2008. Methanogenesis under acidic pH conditions in a semi-continuous reactor system. Bioresour. Technol. 99, 8075–8081.

Tale, V.P., Maki, J.S., Zitomer, D.H., 2015. Bioaugmentation of overloaded anaerobic digesters restores function and archaeal community. Water Res. 70, 138–147.

Tang, J., Liu, Z., Zhao, M., Miao, H., Shi, W., Huang, Z., ... & Ruan, W., 2022. Enhanced biogas biological upgrading from kitchen wastewater by in-situ hydrogen supply through nano zero-valent iron corrosion. Journal of Environmental Management, 310, 114774.

Tay, J.H., Show, K.Y., Lee, D.J., Zhang, Z.P., 2010. Anaerobic granulation and granular sludge reactor systems. Chapter 6. Imperial College Press, pp. 113–136

Teo, K.C., Xu, H.L., Tay, J.H., 2000. Molecular mechanism of granulation. II: proton translocating activity. J. Environ. Eng. ASCE 126, 411–418.

Thapa, A., Park, J. G., Yang, H. M., & Jun, H. B., 2021. In-situ biogas upgrading in an anaerobic trickling filter bed reactor treating a thermal post-treated digestate. Journal of Environmental Chemical Engineering, 9(6), 106780.

Tian T., Qiao S., Yu C., Zhou J. (2019) Effects of nano-sized MnO2 on methanogenic propionate and butyrate degradation in anaerobic digestion J. Hazard Mater., 364 (2019), pp. 11-18

Town, J.R., Dumonceaux, T.J., 2016. Laboratory-scale bioaugmentation relieves acetate accumulation and stimulates methane production in stalled anaerobic digesters. Appl. Microbiol. Biotechnol. 100, 1009–1017.

Trego, A.C., Mills, S., Collins, G., 2020. Granular biofilms: function, application, and new trends as model microbial communities. Crit. Rev. Environ. Sci. Technol. 1–24.

Treu, L., Tsapekos, P., Peprah, M., Campanaro, S., Giacomini, A., Corich, V., Kougias, P. G., Angelidaki, I., 2019. Microbial profiling during anaerobic digestion of cheese whey in reactors operated at different conditions. Bioresour. Technol. 275, 375–385.

Tsermoula, P.; Khakimov, B.; Nielsen, J.H.; Engelsen, S.B., 2021. WHEY—The Waste-Stream That Became More Valuable than the Food Product. Trends Food Sci. Technol. 118, 230–241.

UN General Assembly. Transforming our world: the 2030 Agenda for Sustainable Development. New York, USA: United Nations; 2015. Available from:

Valdez Castillo, M., Laxman Pachapur, V., Brar, S.K., Naghdi, M., Arriaga, S., ´ Avalos Ramirez, A., 2020. Yeast-driven whey biorefining to produce value-added aroma, flavor, and antioxidant compounds: technologies, challenges, and alternatives. Crit. Rev. Biotechnol. 930-950.

Van Lier, J.B., 2008. High-rate anaerobic wastewater treatment: diversifying from end-of-the-pipe treatment to resource-oriented conversion techniques. Water Sci. Technol. 57, 1137–1148.

Van Steendam, C., Smets, I., Skerlos, S. and Raskin, L., 2019. Improving anaerobic digestion via direct interspecies electron transfer requires development of suitable characterization methods. Curr. Opin. Biotechnol. 57, 183-190.

Venetsaneas, N., Antonopoulou, G., Stamatelatou, K., Kornaros, M., Lyberatos, G., 2009. Using cheese whey for hydrogen and methane generation in a two-stage continuous process with alternative pH controlling approaches. Bioresour. Technol, 100, 3713-3717

Venkiteshwaran, K., Bocher, B., Maki, J., Zitomer, D., 2015. Relating anaerobic digestion microbial community and process function: supplementary issue: water microbiology. Microbiol Insights.

Ventorino, V., Romano, I., Pagliano, G., Robertiello, A., Pepe, O., 2018. Pre-treatment and inoculum affect the microbial community structure and enhance the biogas reactor performance in a pilot-scale bio digestion of municipal solid waste. Waste Manag. 73, 69-77.

Vivekanand, V., Mulat, D.G., Eijsink, V.G.H., Horn, S.J., 2018. Synergistic effects of anaerobic co-digestion of whey, manure and fish ensilage. Bioresour. Technol. 249, 35–41.

Vyrides I, Andronikou M., Kyprianou A., Modic A., Filippeti A., Yiakoumis C.,. Samanides CG.2018. CO2 conversion to CH4 using Zero Valent Iron (ZVI) and anaerobic granular sludge: optimum batch conditions and microbial pathways J. CO2. Util., 27, 415-422

Vyrides, I. and Stuckey, D.C., 2017. Compatible solute addition to biological systems treating waste/wastewater to counteract osmotic and other environmental stresses: a review. Crit. Rev. Biotechnol., 37(7), 865-879.

Wahid, R., Mulat, D. G., Gaby, J. C., & Horn, S. J., 2019. Effects of H_2: CO_2 ratio and H_2 supply fluctuation on methane content and microbial community

composition during in-situ biological biogas upgrading. Biotechnology for Biofuels, 12, 1-15.

Wainaina, S., Awasthi, M., Sarsaiya, S., Chen, H., Singh, E., Kumar, A., Ravindran, B., Awasthi, S., Liu, T., Duan, Y., Kumar, S., Zhang, Z., Taherzadeh, M., 2020. Resource recovery and circular economy from organic solid waste using aerobic and anaerobic digestion technologies. Bioresour. Technol. 301, 122778

Wang, F., Zou, Z., He, Z., Tang, C., & Zhou, A., 2023. Revealing methane production potential from waste activated sludge through citric acid-assisted hydrogen corrosion of zero valent iron. Chemical Engineering Journal, 145195.

Wang, G., Li, Q., Yuwen, C., Gong, K., Sheng, L., Li, Y., Xing, Y., Chen, R., 2021a. Biochar triggers methanogenesis recovery of a severely acidified anaerobic digestion system via hydrogen-based syntrophic pathway inhibition. Int. J. Hydrogen Energy 46 (15), 9666–9677.

Wang, N.X., Lu, X.Y., Tsang, Y.F., Mao, Y., Tsang, C.W., Yueng, V.A, 2019. A comprehensive review of anaerobic digestion of organic solid wastes in relation to microbial community and enhancement process. J Sci Food Agric. 99(2):507–516.

Wang, P., Chen, X., Liang, X. Cheng, M. and Ren, L., 2019. Effects of nanoscale zero-valent iron on the performance and the fate of antibiotic resistance genes during thermophilic and mesophilic anaerobic digestion of food waste. Bioresour. Technol. 293,122092

Wang, Q., Feng, K., Li, H., 2020. Nano iron materials enhance food waste fermentation. Bioresour. Technol. 315, 123804

Wang, W., Lee, D.-J., 2021. Direct interspecies electron transfer mechanism in enhanced methanogenesis: A mini-review. Bioresour. Technol. 330, 124980.

Wang, X., Yang, G., Feng, Y., Ren, G., Han, X., 2012. Optimizing feeding composition and carbon-nitrogen ratios for improved methane yield during

anaerobic co-digestion of dairy, chicken manure and wheat straw. Bioresour. Technol. 120, 78-83.

Wang, Z., Wang, T., Si, B., Watson, J., Zhang, Y., 2021b. Accelerating anaerobic digestion for methane production: potential role of direct interspecies electron transfer. Renew Sust Energ Rev. 145:111069.

Wei, J., Hao, X., Loosdrecht, M.C.M.V., Li, J., 2018. Feasibility analysis of anaerobic digestion of excess sludge enhanced by iron: A review. Renew. Sustain. Energy Rev. 89, 16–26.

Wei, Q., Zhang, W., Guo, J., Wu, S., Tan, T., Wang, F., Dong, R., 2014. Performance and kinetic evaluation of a semi-continuously fed anaerobic digester treating food waste: effect of trace elements on the digester recovery and stability. Chemosphere 117 (1), 477–485.

Westerholm, M., Moestedt, J., Schnürer, A., 2016. Biogas production through syntrophic acetate oxidation and deliberate operating strategies for improved digester performance. Applied Energy, 179, 124-135.

Westerholm, M., Schnürer, A., 2019. Microbial responses to different operating practices for biogas production systems. Anaerob. Dig.

Wiegant, W.M., 1988. The Spaghetti theory on anaerobic granular sludge fermentation, or the inevitability of granulation. In: Granular Anaerobic Sludge: Microbiology and Technol., Lettinga, G., Zehnder, A.J.B., Grotenhuis, J.T.C., Hulshoff Pol, L.W. (Eds.), Wageningen, The Netherlands, pp. 146–152.

Williams, R.T., Crawford, R.L., 1983. Microbial diversity of Minnesota peatlands. Microb. Ecol. 9, 201–214.

Xu, R., Xu, S., Zhang, L., Florentino, A.P., Yang, Z. and Liu, Y., 2019. Impact of zero valent iron on blackwater anaerobic digestion. Bioresour. Technol. 285, 121351.

Yang, Y., Guo, J. and Hu, Z., 2013. Impact of nano zero valent iron (NZVI) on methanogenic activity and population dynamics in anaerobic digestion. Water Res. 47(17),.6790-6800

Yang, Y., Wang, J. and Zhou, Y., 2019. Enhanced anaerobic digestion of swine manure by the addition of zero-valent iron. Energ. Fuels, 33(12), 12441-12449.

Yang, Y., Yang, F., Huang, W.W., Huang, W.L., Li, F., Lei, Z.F., Zhang, Z.Y., 2018. Enhanced anaerobic digestion of ammonia-rich swine manure by zero-valent iron: with special focus on the enhancement effect on hydrogenotrophic methanogenesis activity. Biresour. Technol. 270, 172–179.

Yang, Z. R. Guo, X. Xu, L. Wang, M. Dai, Enhanced methane production via repeated batch bioaugmentation pattern of enriched microbial consortia, Bioresour. Technol. 216 (2016) 471–477.

Ye, M., Li, Y.Y., 2023. Methanogenic treatment of dairy wastewater: A review of current obstacles and new technological perspectives. Sci. Total Environ. 866, 161447

Ye, W., Lu, J., Ye, J., & Zhou, Y., 2021. The effects and mechanisms of zero-valent iron on anaerobic digestion of solid waste: A mini-review. J. Clean. Prod., 278 (130), 123567.

Yu, Y., Lee, C., Kim, J., Hwang, S., 2005. Group-specific primer and probe sets to detect methanogenic communities using quantitative real-time polymerase chain reaction. Biotechnol. Bioeng. 89, 670-679.

Zang, Y., Yang, Y., Hu, Y., Ngo, H.H., Wang, X.C. and Li, Y.Y., 2020. Zero-valent iron enhanced anaerobic digestion of pre-concentrated domestic wastewater for bioenergy recovery: Characteristics and mechanisms. Bioresour. Technol. 310, 23441.

Zhang, D., Wei, Y., Zhang, M., Wu, S. and Zhou, L., 2022. A collaborative strategy for enhanced anaerobic co-digestion of food waste and waste activated sludge by using zero valent iron and ferrous sulfide. Bioresour. Technol. 347, 126420.

Zhang, J., Qu, Y., Qi, Q., Zhang, P., Zhang, Y., Tong, Y. W. & He, Y. 2020. The bio-chemical cycle of iron and the function induced By ZVI addition in anaerobic digestion: A review. Water Research, 186, 116405.

Zhang, S., Yi, K., Chen, A., Shao, J., Peng, L., Luo, S., 2022. Toxicity of zero-valent iron nanoparticles to soil organisms and the associated defense mechanisms: a review. Ecotoxicology. 31: 873-883

Zhang, Y., Feng, Y., Yu, Q., Xu, Z., Quan, X., 2014. Enhanced high-solids anaerobic digestion of waste activated sludge by the addition of scrap iron. Bioresour. Technol. 159, 297–304.

Zhao, C., Chen, N., Ashaolu, T. J., 2022. Whey proteins and peptides in health-promoting functions–a review. International Dairy Journal, 126, 105269.

Zhao, J., Westerholm, M., Qiao, W., Yin, D., Bi, S., Jiang, M., Dong, R., 2018. Impact of temperature and substrate concentration on degradation rates of acetate, propionate and hydrogen and their links to microbial community structure. Bioresour. Technol. 256, 44e52.

Zhao, Z., Li, Y., Zhang, Y., Lovley, D.R., 2020. Sparking anaerobic digestion: promoting direct interspecies electron transfer to enhance methane production. iScience.

Zhao, Z., Zhang, Y., Li, Y., Quan, X. and Zhao, Z., 2018. Comparing the mechanisms of ZVI and Fe3O4 for promoting waste-activated sludge digestion. Water Res. 144, 126-133.

Zhen, G., Lu, X., Li, Y. Y., Liu, Y., Zhao, Y., 2015. Influence of Zero Valent Scrap Iron (ZVSI) supply on methane production from waste activated sludge. Chem. Eng. J. 263, 461-470.

Zheng, S., Yang, F., Huang, W., Lei, Z., Zhang, Z., Huang, W., 2022. Combined effect of zero valent iron and magnetite on semi-dry anaerobic digestion of swine manure. Bioresour. Technol. 346, 126438

Zheng, X., Shi, X., Wang, B., 2021. A Review on the General Cheese Processing Technology, Flavor Biochemical Pathways and the Influence of Yeasts in Cheese. Front. Microbiol. 12, 703284.

Zhou, J., You, X., Niu, B., Yang, X., Gong, L., Zhou, Y., Wang, J., Zhang, H., 2020. Enhancement of methanogenic activity in anaerobic digestion of high solids sludge by nano zero-valent iron. Sci. Total Environ. 703, 135532

Zhu, D., Wang, Z., Liu, K., Si, B., Yang, G., Tian, C. and Zhang, Y., 2023. Multi-cycle anaerobic digestion of hydrothermal liquefaction aqueous phase: Role of carbon and iron based conductive materials in inhibitory compounds degradation, microbial structure shaping, and interspecies electron transfer regulation. J. Chem. Eng., 454,140019.

Zhu, Y., Zhao, Z., Yang, Y., Zhang, Y., 2020. Dual roles of zero-valent iron in dry anaerobic digestion: enhancing interspecies hydrogen transfer and direct interspecies electron transfer. Waste Manag. 118, 481–490.